

**CHARACTERISATION OF TOPOISOMERASE II $\alpha$   
AMPLIFICATION AND EXPRESSION IN HUMAN  
LUNG CANCER CELL LINES**

**Jacqueline C. Coutts (B.Sc.)**

**Thesis submitted to the University of Glasgow  
for the degree of Doctor of Philosophy**

Department of Medical Oncology,  
University of Glasgow,  
CRC Beatson Laboratories,  
Glasgow.  
G61 1BD

October 1994

ProQuest Number: 11007844

All rights reserved

INFORMATION TO ALL USERS

The quality of this reproduction is dependent upon the quality of the copy submitted.

In the unlikely event that the author did not send a complete manuscript and there are missing pages, these will be noted. Also, if material had to be removed, a note will indicate the deletion.



ProQuest 11007844

Published by ProQuest LLC (2018). Copyright of the Dissertation is held by the Author.

All rights reserved.

This work is protected against unauthorized copying under Title 17, United States Code  
Microform Edition © ProQuest LLC.

ProQuest LLC.  
789 East Eisenhower Parkway  
P.O. Box 1346  
Ann Arbor, MI 48106 – 1346

1161  
10,009  
Copy 1



To Colin,

For all his love, support, understanding and encouragement,  
despite being 250 miles away

and

To Papa Joe,

I know you would have been so proud.

# CONTENTS

	<b>PAGE</b>
List of Figures	i
List of Tables	v
Acknowledgements	vii
Abbreviations	viii
Abstract	x
<b>Chapter 1</b>	<b>General Introduction</b>
	<b>1-14</b>
Topoisomerase I	1
Topoisomerase II	2
The Catalytic Cycle of Topoisomerase II	2
Role of Topoisomerase II in the Cell	5
Phosphorylation of Topoisomerase II	7
Genetic Regulation of Topoisomerase II Expression	8
Drug Interactions with Topoisomerase II	9
Cell Death	10
Multistage Tumorigenesis	11
<b>Chapter 2</b>	<b>Materials &amp; Methods</b>
	<b>15-46</b>
2.1	Materials
2.1.1	Chemicals
2.1.2	Radiochemicals
2.1.3	Restriction Endonucleases and other Enzymes
2.1.4	Size Markers
2.1.5	Media, Solutions and Buffers
2.1.5.1	General Solutions
2.1.5.2	Tissue Culture Solutions
2.1.5.3	Southern and Northern Solutions
2.1.5.4	Fluorescence <i>In Situ</i> Hybridisation Solutions
2.1.5.5	Protein and Western Blotting Solutions

	2.1.5.6	Topoisomerase II Assay Buffers	23
	2.1.5.7	Immunofluorescence Solutions	24
	2.1.5.8	Flow Cytometry Solutions	24
2.2		Methods	
	2.2.1	Cell Lines and Tissue Culture	27
	2.2.2	Southern Analysis	27
	2.2.2.1	DNA Extraction	27
	2.2.2.2	Southern Blotting	28
	2.2.2.3	Chromosome 17 Cosmid Library Filters	29
	2.2.3	Northern Analysis	29
	2.2.4	Hybridisation and Washing of Membranes	30
	2.2.5	Autoradiography	30
	2.2.6	Southern and Northern Probes	30
	2.2.6.1	Probes Used	30
	2.2.6.2	Preparation of probes for labelling	31
	2.2.6.3	Random Labelling of dsDNA	31
	2.2.7	Re-probing of Southern and Northern Membranes	31
	2.2.8	Fluorescence <i>In Situ</i> Hybridisation	32
	2.2.8.1	Preparation of Chromosomes from Lymphocytes	32
	2.2.8.2	Preparation of Chromosomes from Cell Lines	33
	2.2.8.3	Probes Used for FISH	33
	2.2.8.4	Isolation of Cosmids	34
	2.2.8.5	Labelling of Probes for FISH	34
	2.2.8.6	Preparation of Slides for Labelling	35
	2.2.8.7	Hybridisation of Slides	35
	2.2.8.8	Washing and Detection of Probes	36

2.2.9	Protein Analysis	38
2.2.9.1	Preparation of Crude Nuclear Extracts	38
2.2.9.2	Preparation of Whole Cell Extracts	39
2.2.10	Western Analysis	39
2.2.10.1	Gel Running and Electroblothing	39
2.2.10.2	Immunodetection	40
2.2.10.3	Band Depletion Assay	40
2.2.11	Biochemical Assay for Topoisomerase II	41
2.2.12	Immunofluorescence	42
2.2.13	Flow Cytometry	44
2.2.13.1	Cell Cycle Analysis using Bromodeoxyuridine (BrdUrd) and Propidium Iodide (PI)	44
2.2.13.2	FACS for Topoisomerase II $\alpha$	44
2.2.13.3	FACS for P-Glycoprotein and MRP	45
<b>Chapter 3</b>	<b>Characterisation of a 17q Amplicon in the Non-Small Cell Lung Adenocarcinoma Cell Line, CALU-3</b>	<b>47-64</b>
3.1	Introduction	47
3.2	Results	
	Characterisation of the 17q Amplicon by Southern Analysis	54
	Isolation of Cosmid Probes for NM23H1, RAR $\alpha$ TOPO II $\alpha$ , and NF1	55
	Investigation of Gross Genetic Changes to Chromosome 17 in L-DAN, CALU-3 and SK-MES-1 by FISH	56
	Co-hybridisation of Single-Copy Gene Cosmids with Chromosome 17-Specific Centromere Probe in Lymphocytes	57

	Analysis of TOPO II $\alpha$ and ERBB2 Gene Copy Number in L-DAN and SK-MES-1	58
	Further Characterisation of the Chromosome 17 Amplicon in CALU-3 using FISH	59
3.3	Discussion	61
<b>Chapter 4</b>	<b>Chromosome 17q Amplicon: Analysis of Expression</b>	<b>65-82</b>
4.1	Introduction	65
4.2	Results	
	Northern Blot Analysis of TOPO II $\alpha$ Expression	69
	Western Blot and Immunofluorescence Analysis of TOPO II $\alpha$ Expression	70
	Biochemical Assays for Topoisomerase II	70
	Band Depletion Assay	71
	Flow Cytometry	72
	Investigation into the Methylation Status of TOPO II $\alpha$ and TOPO II $\beta$ Genes	74
	Expression of Other Loci on 17q	75
4.3	Discussion	77
<b>Chapter 5</b>	<b>Expression Analysis of Topoisomerase II<math>\beta</math></b>	<b>83-93</b>
5.1	Introduction	83
5.2	Results	
	Dot Blot Analysis for Topoisomerase II $\beta$	87
	Western Blot Analysis for Topoisomerase II $\beta$	87

	Band Depletion Assay	88
	Immunofluorescence Analysis of TOPO II $\beta$ Expression	89
5.3	Discussion	90
<b>Chapter 6</b>	<b>Investigation into the VP16-Resistance of a CALU-3 Clone</b>	<b>94-106</b>
6.1	Introduction	94
6.2	Results	
	Western Blotting Detection of Topoisomerase II $\alpha$	99
	Biochemical Assays for Topoisomerase II	99
	Flow Cytometry	100
	Western Analysis for MRP	101
6.3	Discussion	103
<b>Chapter 7</b>	<b>General Discussion</b>	<b>106-109</b>
	<b>References</b>	<b>110-147</b>

## List of Figures

		<b>PAGE</b>
<b>Figure 1A</b>	The catalytic cycle of topoisomerase II	2
<b>Figure 3A</b>	General uses of fluorescence <i>in situ</i> hybridisation	48
<b>Figure 3B</b>	Basic methodology for FISH	48
<b>Figure 3C</b>	"Onion-skin" model for gene amplification by over-replication	51
<b>Figure 3D</b>	Sister chromatid exchange and bridge/breakage/fusion model of gene amplification	51
<b>Figure 3.1</b>	Southern blot analysis of L-DAN, CALU-3 and SK-MES-1	54
<b>Figure 3.2</b>	Further Southern blot analysis of L-DAN, CALU-3 and SK-MES-1	54
<b>Figure 3.3</b>	Confirmation of identity of ICRF NM23H1 and TOPO II $\alpha$ cosmids by Southern analysis	55
<b>Figure 3.4</b>	Detection of chromosome 17 and chromosome 17 centromere in lymphocytes and lung tumour cell lines by FISH	56
<b>Figure 3.5</b>	Double hybridisation of single-copy gene cosmids and chromosome 17 centromere probe in lymphocytes	57
<b>Figure 3.6</b>	Diagram showing positions of genes on 17q according to mean fractional length measurement (FLM)	58

<b>Figure 3.7</b>	Analysis of TOPO II $\alpha$ and ERBB2 copy number in L-DAN and SK-MES-1 using FISH	58
<b>Figure 3.8</b>	Double hybridisation of single-copy gene cosmids and chromosome 17 centromere probe in CALU-3	59
<b>Figure 3.9</b>	Hybridisation of single-copy gene cosmids in CALU-3	60
<b>Figure 3.10</b>	Double hybridisation of single-copy gene cosmids in CALU-3	60
<b>Figure 3.11</b>	Double hybridisation of single-copy gene cosmids in CALU-3	60
<b>Figure 3E</b>	Extended model of gene amplification for CALU-3	64
<b>Figure 4.1</b>	Detection of topoisomerase RNA levels by Northern blot analysis	69
<b>Figure 4.2</b>	Detection of topoisomerase II $\alpha$ expression by Western bot analysis	70
<b>Figure 4.3</b>	Detection of TOPO II $\alpha$ gene expression by immunofluorescence	70
<b>Figure 4.4</b>	Decatenation of kinetoplast DNA by cellular extracts from (a): L-DAN, (b): CALU-3 and (c): SK-MES-1	70
<b>Figure 4.5</b>	Inhibition of topoisomerase II activity by VP16	71
<b>Figure 4.6</b>	Diagrammatic explanation of the band depletion assay	72
<b>Figure 4.7</b>	Band depletion assay of topoisomerase II using whole cell lyates, analysed by Western blot	72

<b>Figure 4.8</b>	Cell cycle analysis using bromodeoxyuridine incorporation	72
<b>Figure 4.9</b>	Cell cycle regulation of topoisomerase II $\alpha$ expression by FACS	73
<b>Figure 4.10</b>	FACS analysis of nm23H1/H2 expression	73
<b>Figure 4.11</b>	Investigation into the methylation status of TOPO II $\alpha$ and II $\beta$ genes, using Southern analysis	74
<b>Figure 4.12</b>	Detection of ERBB2 gene expression by immunofluorescence	75
<b>Figure 4.13</b>	Detection of retinoic acid receptor alpha (RAR $\alpha$ ) expression by Western blot analysis	75
<b>Figure 4.14</b>	Detection of nm23H1/H2 expression by Western blot analysis	75
<b>Figure 4.15</b>	Detection of NM23H1/H2 gene expression by immunofluorescence	75
<b>Figure 5.1</b>	Detection of topoisomerase II $\beta$ using dot blot analysis	87
<b>Figure 5.2</b>	Detection of topoisomerase II $\beta$ using Western analysis	87
<b>Figure 5.3</b>	Band depletion assay of topoisomerase II $\beta$ using whole cell lysates, analysed by Western blot	88
<b>Figure 5.4</b>	Detection of TOPO II $\beta$ gene expression by immunofluorescence	89
<b>Figure 5.5</b>	Co-localisation of topoisomerase II $\beta$ with a nucleolar control antibody	89

<b>Figure 6.1</b>	Detection of topoisomerase II $\alpha$ in CALU-3 clone 4 and CALU-3/10 <sup>-5</sup> M VP16 using Western analysis	99
<b>Figure 6.2</b>	Decatenation of kinetoplast DNA by cellular extracts from A: CALU-3 clone 4, B: CALU-3/10 <sup>-5</sup> M VP16	99
<b>Figure 6.3</b>	Inhibition of topoisomerase II activity by VP16	100
<b>Figure 6.4</b>	Flow cytometry graphs of P-glycoprotein status in A & B: A2780, C & D: A2780/Adr	100
<b>Figure 6.5</b>	Flow cytometry graphs of P-glycoprotein status in A & B: CALU-3 clone 4 C & D: CALU-3/10 <sup>-5</sup> M VP16	101
<b>Figure 6.6</b>	Detection of MRP (p190) using Western analysis	101

## List of Tables

		<b>PAGE</b>
<b>Section 2.1.6</b>	Table of Primary Antibodies used in Immunofluorescence, Flow Cytometry and Western Blotting	25
<b>Section 2.1.7</b>	Table of Antibodies used for Fluorescence <i>In Situ</i> Hybridisation	26
<b>Table 3.1</b>	Relative hybridisation frequencies of the three TOPO II $\alpha$ cosmids, pC5, ICRFc105H01119 and ICRFc105B041155 on lymphocyte metaphase spreads	57
<b>Table 3.2</b>	Hybridisation frequencies of NF1, NM23H1, RAR $\alpha$ and C05123 cosmids on lymphocyte metaphase spreads	57
<b>Table 3.3</b>	Table showing mean, median and standard deviation of fractional length measurements for all genes studied by FISH	58
<b>Table 3.4</b>	Table showing p-values from Mann-Whitney analysis for all gene-pair combinations	58
<b>Table 3.5</b>	Hybridisation frequencies of TOPO II $\alpha$ , ERBB2, NF1, NM23H1, RAR $\alpha$ and C05123 cosmids on CALU-3 metaphase spreads	60
<b>Table 4.1</b>	Percentage of cells in the different stages of the cell cycle	72
<b>Table 4.2</b>	Number of cells in different stages of the cell cycle in a topoisomerase II $\alpha$ FACS experiment (polyclonal antibody)	73

<b>Table 4.3</b>	Percentage of cells positive for topoisomerase II $\alpha$ expression in G1 and G2/M (polyclonal antibody)	73
<b>Table 4.4</b>	Number of cells in different stages of the cell cycle in a topoisomerase II $\alpha$ FACS experiment (monoclonal antibody)	79
<b>Table 4.5</b>	Percentage of cells positive for topoisomerase II $\alpha$ expression in G1 and G2/M (monoclonal antibody)	79

## Acknowledgements

Firstly, I would like to thank my supervisor, Dr. Nicol Keith for providing me with excellent guidance over the past three years. Not a better supervisor could have been wished for (most of the time!!).

I would also like to thank Dr. Jane Plumb for deriving the CALU-3 resistant cell line, without which a chapter of this thesis would not exist (thanks Jane!!) and Dr. Carol Clugston and Dr. Bob Brown for spending endless hours of fun trying to teach me how to use the FACS machine (unsuccessfully!!).

Lots and lots of "thankyou's" go to Peter, for all his help with the confocal and the colour printer and the computing and the confocal again, not to mention the colour printer and the confocal.....!!

My thanks also extend over the pond to Dr. Susan Cole in Ontario for kindly probing one of my Western blots with her monoclonal antibody against MRP.

Of course, I must not forget the members of the FISH lab, Sharon, Stacey and (last but not least!) Dermot, without whom life would have been so unbearable it would not have been worth continuing with!

Finally, I would like to thank all members of the ex-Goldfish Bowl (now demoted to the Portacabin II crew) for their usually inane chatter, but it was good fun all the same and I'll miss it!!

Almost forgot to thank my Mum and Dad for all their hard work over the last 24 years which has made me the person I am today.

## Abbreviations

APS	ammonium persulphate
ATCC	American Type Culture Collection
ATP	adenosine tri-phosphate
BSA	bovine serum albumin
CAT	chloramphenicol acetyltransferase
CGH	comparative genome hybridisation
dATP	deoxyadenosine-tri-phosphate
dCTP	deoxycytidine-tri-phosphate
DAPI	4, 6-diamidino-2-phenylindole :
DMEM	Dulbeccos modified Eagles medium
DMSO	dimethyl sulphoxide
DNA	deoxyribonucleic acid
dsDNA	double stranded DNA
DTT	dithiothreitol
ECL	enhanced chemiluminescence
EDTA	ethylene diaminetetra-acetic acid (disodium salt)
FACS	fluorescence activated cell sorting
FISH	fluorescence <i>in situ</i> hybridisation
FITC	fluorescein isothiocyanate
G-CSF	granulocyte colony-stimulating factor
GST $\pi$	glutathione-S-synthetase $\pi$
kb	kilobase
kDNA	kinetoplast DNA
M	molar
mA	milliamps
mg	milligramme
min(s)	minute(s)
ml	millilitre
mM	millimolar
$\mu$ l	microlitre
$\mu$ g	microgram
MOPS	4-morpholinepropanesulfonic acid
NF1	neurofibromatosis type 1 gene
PBS	phosphate buffered saline
PCR	polymerase chain reaction
PI	propidium iodide

PIPES	piperazine-N-N-bis(2-ethane-sulphonic acid)
PKC $\alpha$	protein kinase C alpha
PMSF	phenyl methyl sulfonyl fluoride
RAR $\alpha$	retinoic acid receptor alpha
RNA	ribonucleic acid
RNase	ribonuclease
rpm	revolutions per minute
SDS	sodium dodecyl sulphate
SSC	saline sodium citrate
TAE	tris-acetate EDTA
TEMED	N, N, N', N'-tetramethylethylenediamine
TBE	tris-borate EDTA
UV	ultra violet
V	volts
ana	antinuclear antibody
v-ERBB	avian erythroblastosis virus transforming gene
ERBB2	human proto-oncogene closely related to v-ERBB (also called HER2 or NEU)
mAMSA	amsacrine
NM23	putative anti-metastasis gene
TOPO II $\alpha$	topoisomerase II alpha gene
VM26	teniposide
VP16	etoposide

All gene names currently written in capital letters should be in italics

TOPO II $\alpha$  should read *TOP II $\alpha$*   
TOPO I should read *TOP I*  
RAR $\alpha$  should read *RARA*  
NM23H1 should read *NME1*

## ABSTRACT

Work has been undertaken to characterise an amplicon on chromosome 17 in a non-small cell lung carcinoma cell line, CALU-3. There are a number of different genes in this region which have been implicated in tumorigenesis. These include topoisomerase II $\alpha$  (TOPO II $\alpha$ ), ERBB2, NM23H1 and retinoic acid receptor alpha (RAR $\alpha$ ) genes. Topoisomerase II $\alpha$  is also a target for numerous anti-cancer drugs, such as VP16 and doxorubicin. Changes in the expression of topoisomerase II $\alpha$  have been seen to have an effect on the response of cells to such topoisomerase II inhibitors, with overexpression causing sensitivity and reduced expression causing resistance to these agents. Therefore, CALU-3 is of interest as a model to study the genetic changes which have occurred around the topoisomerase II $\alpha$  locus.

Southern hybridisation was initially used to investigate which genes were within the amplicon. From this analysis it was confirmed that the TOPO II $\alpha$  and ERBB2 genes were amplified and discovered that the RAR $\alpha$  and G-CSF genes were also involved in the amplicon. Fluorescence *in situ* hybridisation (FISH) has subsequently been performed with CALU-3 to visualise the extent and structure of amplification for the different genes and to find any other cytogenetic changes which may have occurred to chromosome 17. New cosmid probes for TOPO II $\alpha$ , RAR $\alpha$ , NM23H1 and NF1 genes have been developed from an Imperial Cancer Research Fund Reference Library-Database chromosome 17 library, for use in FISH analysis. By using a flow-sorted whole chromosome 17 paint, seven regions of hybridisation were observed in CALU-3. None of these regions covered an entire chromosome. Five chromosome 17-specific centromere sequences were also detected in CALU-3. It has been discovered that CALU-3 carries three large regions of TOPO II $\alpha$  and ERBB2 gene amplification, residing on three separate chromosomes. The RAR $\alpha$  gene has also been found to be amplified on the same three regions, although not as highly as TOPO II $\alpha$  or ERBB2. Counts of hybridisation signals indicate that CALU-3 has at least eight copies of RAR $\alpha$ . A cosmid containing sequences thought to be in the region of the BRCA1 gene has been used and this appears to be amplified in CALU-3 at a similar level to RAR $\alpha$ . Five copies of both NF1 and NM23H1 genes were also found, each associated with a chromosome 17 centromere sequence. The NM23H1 gene also appears to be inverted since it is seen in close association to the centromere. Therefore, in CALU-3 there appears to have been some gross changes to chromosome 17, including numerous

translocations, as well as the formation of an amplicon involving at least five genes on 17q.

Expression analysis using Western blotting and immunofluorescence has confirmed that amplification of TOPO II $\alpha$  and ERBB2 genes in CALU-3 can be correlated with the high expression of topoisomerase II $\alpha$  and erbB2 proteins. No alterations were found to the expected location of either of these proteins in CALU-3, as shown by immunofluorescence, with topoisomerase II $\alpha$  present in the nucleoplasm and erbB2 detected in the cell membrane. Flow cytometry has shown that the topoisomerase II $\alpha$  protein from CALU-3 still appears to be cell cycle regulated. The topoisomerase II enzyme in CALU-3 is also still sensitive to inhibition, as has been demonstrated by the addition of VP16 to biochemical assays of topoisomerase II activity. More specifically, the topoisomerase II $\alpha$  isozyme is still capable of being stabilised in a drug/enzyme/DNA complex by VP16, as shown by band depletion assay.

CALU-3 is very sensitive to treatment with topoisomerase II inhibitors and it seems likely that this is as a result of amplification and overexpression of the topoisomerase II $\alpha$  gene. There is an obvious clinical interest in this relationship since topoisomerase II inhibitors are commonly used in the treatment of a variety of cancers. However, resistance to these agents is a major problem in tumour treatment. Therefore, a resistant cell line was derived by exposure to VP16, from a sensitive CALU-3 clone (clone 4) and analysed for possible mechanisms of drug resistance. A cell line was subsequently derived which was resistant to  $10^{-5}$ M VP16, as well as being cross-resistant to doxorubicin and vincristine. Western analysis of CALU-3/ $10^{-5}$ M VP16 showed no difference in topoisomerase II $\alpha$  expression when compared to the parental clone. Subsequent biochemical assays also found no difference in catalytic activity between the CALU-3 clone 4 and CALU-3/ $10^{-5}$ M VP16. Flow cytometry was then performed to analyse P-glycoprotein expression levels in the two cell lines. No expression of this drug efflux pump was found in either parental or resistant lines. Expression of the atypical drug resistance associated protein, MRP, was then investigated using a polyclonal antiserum from Dr. Melvin Center. By Western blot analysis it appeared that CALU-3/ $10^{-5}$ M VP16 overexpressed MRP when compared to the parental cell line. This result was confirmed by independent analysis of a Western blot with a monoclonal antibody against MRP by Dr. Susan Cole in Ontario, Canada. Therefore, it appears that MRP may play a role in the mechanism of drug resistance in CALU-3/ $10^{-5}$ M VP16.

# CHAPTER 1

## GENERAL INTRODUCTION

Cell division and gene expression both involve alterations to the topological nature of the DNA helix. For example, during chromosome segregation, recombination products must be resolved through breakage and rejoining of the double helix, thus allowing strand passage. Also, to allow gene expression, sister DNA strands must be separated to create access for transcription machinery. In eukaryotic cells, changes in DNA topology through strand breakage and reunion are regulated by topoisomerase enzymes. Mammalian topoisomerases are classified into two groups, based on their mechanism of action and referred to as type I and type II reviewed in Wang, 1985. Both classes of topoisomerase are also targets for a number of anti-cancer agents (Liu, 1989; Smith, 1990; Takano *et al.*, 1992).

### Topoisomerase I

Topoisomerase I is a 100kD protein, encoded by a gene that has been mapped to chromosome 20q11.2-q13.1 (Kunze *et al.*, 1989). This enzyme only cleaves a single strand of the DNA duplex, without the requirement of ATP, and is thought to be involved in the relaxation of DNA supercoils, such as might occur ahead of replication forks (Wang, 1991). Topoisomerase I has been found associated with the nucleoli of cells (Fleischmann *et al.*, 1984; Muller *et al.*, 1985), which is the site of transcription by RNA polymerase I. Therefore, it has been proposed that topoisomerase I is somehow involved specifically in the transcription of ribosomal RNA genes (Muller *et al.*, 1985). Topoisomerase I has also been found to be associated with active regions of DNA transcription, as observed in heat-shock induced DNA puffs in the giant polytene chromosomes from *Drosophila* salivary glands (Fleischmann *et al.*, 1984). The structure of the promoter of the topoisomerase I gene (TOPO I) has been characterised (Kunze *et al.*, 1990; Kunze *et al.*, 1991). The promoter region is found to be rich in GC content, a feature often associated with housekeeping genes, and lacks TATA and CCAAT elements which are usually present in promoter regions of regulated genes. Binding sites for a number of transcription factors, such as Sp1 and octamer transcription factor 1, have been localised to the 5'-flanking region of the TOPO I gene. In addition to these binding sites, a putative

cAMP-responsive element was also found (Kunze *et al.*, 1990; Kunze *et al.*, 1991). The importance of these regulatory elements was seen in CAT reporter gene assays as most of the *in vitro* transcriptional activity from the TOPO I gene was abolished when the region containing these binding sites was deleted (Kunze *et al.*, 1991). It has also been found that purified topoisomerase I can be activated by protein kinase C phosphorylation (Pommier *et al.*, 1990).

## **Topoisomerase II**

Two forms of topoisomerase II have been reported, alpha ( $\alpha$ ) and beta ( $\beta$ ) (Chung *et al.*, 1989; Drake *et al.*, 1987; Wang, 1985). The two topoisomerase II isoforms are coded for by separate genes, TOPO II $\alpha$  on chromosome 17q (Tsai-Plugfelder *et al.*, 1988) and TOPO II $\beta$  on chromosome 3p (Jenkins *et al.*, 1992; Tan *et al.*, 1992). The TOPO II $\alpha$  gene encodes a 170kD protein, whereas the TOPO II $\beta$  gene encodes a 180kD protein. At the protein level, the isoforms exhibit a 72% homology (Jenkins *et al.*, 1992). More details concerning the expression, cell cycle regulation and the subcellular localisation of the topoisomerase II $\beta$  isozyme are given in Chapter 5. The topoisomerase II $\alpha$  isoform is known to be cell cycle regulated, with an increased expression of the enzyme being observed at the G2/M phase of the normal cell cycle (Kaufmann *et al.*, 1991; Prosperi *et al.*, 1994; Prosperi *et al.*, 1992). The following section on the role, mechanisms of regulation and catalytic cycle of topoisomerase II all refer to the II $\alpha$  form, although this does not necessarily exclude the possibility that the same applies to the beta enzyme.

## **The Catalytic Cycle of Topoisomerase II**

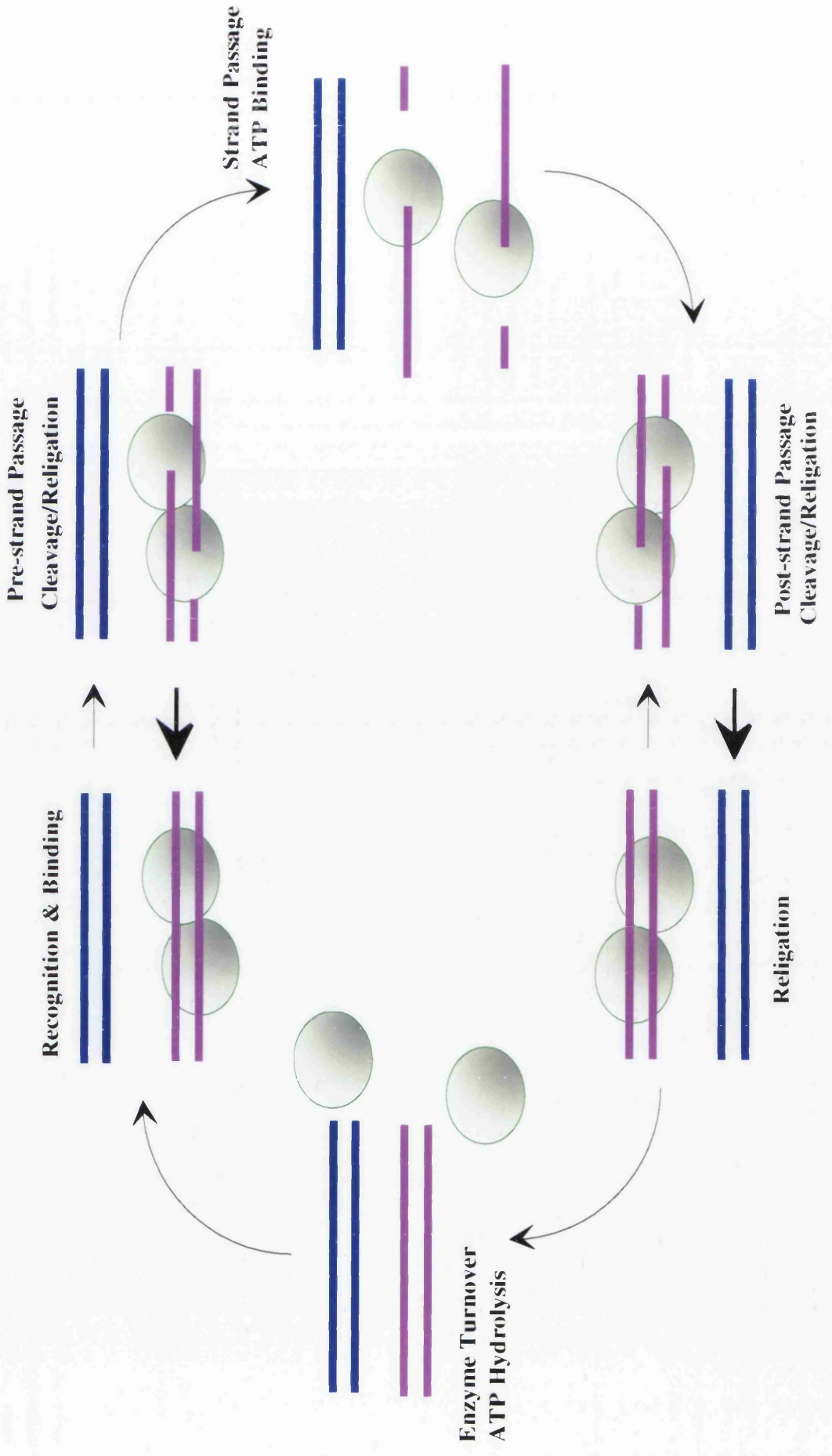
An outline of the topoisomerase II catalytic cycle is shown in Figure 1A. The initial stage of the cycle involves recognition and binding of topoisomerase II molecules to a region of the DNA duplex. Two topoisomerase II molecules bind as a homodimer to supercoiled DNA. The actual binding properties of topoisomerase II are poorly understood, although it has been observed that the enzyme appears to bind preferentially to supercoiled DNA (Zechiedrich & Osheroff, 1990), especially in the region of DNA crossovers. It has also been shown that topoisomerase II recognises specific regions of secondary structure in DNA duplexes (Froelich-Ammon *et al.*, 1994). Using transcriptional footprinting, topoisomerase II was observed to protect a 28 bp region of RNA, with a more strongly protected central 22 bp

## **Figure 1A**

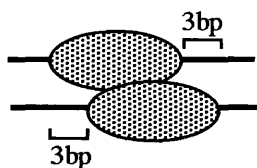
### **The Catalytic Cycle of Topoisomerase II**

This diagram shows the basic steps in the catalytic cycle of topoisomerase II, beginning with recognition and binding of a topoisomerase II homodimer to a region of dsDNA. Topoisomerase II cleaves the DNA (pre-strand passage cleavage/religation) creating a gate through which the sister DNA molecule can pass (strand passage). The gap in the DNA backbone is then sealed by the topoisomerase (religation), following which the enzyme is turned over and is capable of releasing the dsDNA and binding to another region (enzyme turnover).

See text for full details of the catalytic cycle.



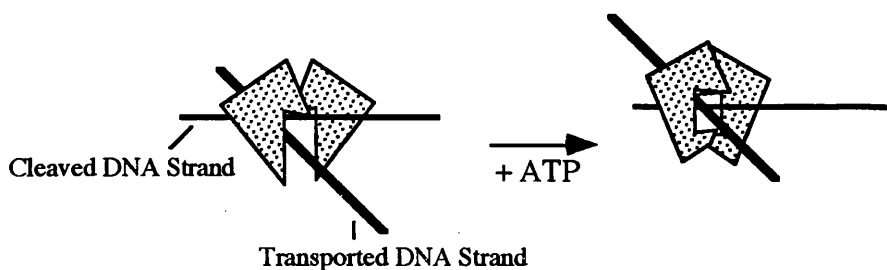
region (Thomsen *et al.*, 1990). It was therefore hypothesised that the two topoisomerase II protein molecules bind to DNA with a 3 bp displacement at either end, as shown:



Following binding of the topoisomerase homodimer to the DNA duplex, an reaction equilibrium is established between cleavage and religation of the DNA. The equilibrium favours the religation reaction. For the pre-strand cleavage stage of the catalytic cycle to occur there is an absolute requirement for a divalent cation, such as magnesium (Osheroff, 1987). This study demonstrated that magnesium ions were required for relaxation and cleavage of DNA by *Drosophila* topoisomerase II, as well as being necessary for ATP hydrolysis with this enzyme. No evidence was found for the involvement of magnesium ions in the initial binding reaction. When the availability of magnesium ions is limited by inclusion of excess EDTA in the reaction, or other divalent ions such as calcium or cobalt are substituted for magnesium, the enzyme is found to only cleave one strand of DNA rather than two (Lee *et al.*, 1989). Therefore, it appears that DNA cleavage involves the topoisomerase II nicking each strand (Zechiedrich *et al.*, 1989) thus creating a staggered double-strand break, with a 5'-end 4 base-pair overhang. The topoisomerase II molecule becomes covalently linked to the 5'-phosphoryl end of the DNA at this stage (Wang, 1985). Observation of topoisomerase II cleaved linear DNA using electron microscopy has shown association of individual topoisomerase II subunits with the ends of DNA molecules (Zechiedrich *et al.*, 1989), thus it was proposed that the individual subunits each create a nick in the duplex thus producing the double-stranded gap for passage of the sister DNA duplex. Numerous experiments have been carried out to investigate consensus sequences for topoisomerase II cleavage (Capranico *et al.*, 1990; Fosse *et al.*, 1991; Freudenreich & Kreuzer, 1993; Pommier *et al.*, 1991; Sander & Hsieh, 1985). From these investigations, cleavage consensus sequences have been suggested, but no one sequence agrees with all the others. These studies did find, however, that there appear to be two types of cleavage site, strong and weak, with the stronger sites showing more homology with the consensus than weak sites. It is notable that all consensus sequences which have been suggested are asymmetric and

would therefore require the topoisomerase enzyme to cleave between different nucleotides on each of the sister strands of the DNA duplex. It also appears that the enzyme can distinguish between the sequences of the two strands (Andersen *et al.*, 1989), with the non-coding strand being preferentially cleaved over the coding strand. It should be pointed out, however, that most of the cleavage studies using mammalian topoisomerase II have been performed in the presence of drug since the actual cleavage reaction is extremely transient. Therefore, it is not known whether the consensus sequences that have proposed would act as such under normal cellular conditions.

Once the topoisomerase II enzyme has created a double-strand gap in the DNA backbone, passage of the sister DNA molecule can occur through this gap. This strand passage event is entirely dependent on the presence of magnesium and ATP, although hydrolysis of ATP does not occur at this stage of the cycle since non-hydrolysable analogues of ATP will allow one cycle of strand passage (Osheroff, 1987; Osheroff *et al.*, 1991). Although it was known that type II topoisomerases required ATP for their action almost from the moment of their discovery (Hsieh & Brutlag, 1980; Liu *et al.*, 1980) it was not known what function the ATP performed, or when it was bound. Recently it has been proposed that the ATP molecule actually causes a conformational change in the topoisomerase homodimer (Lindsley & Wang, 1991). This finding has led to a model suggesting that topoisomerase II acts as an ATP-dependent protein clamp (Roca & Wang, 1992), as depicted below.



from Roca & Wang, 1992

This model was based on the finding that binding of topoisomerase II to a non-hydrolysable analogue of ATP triggers conformational change in the homodimer which limits the enzymes' binding to only linear and not circular DNA forms. Therefore, prior to the binding of ATP, it is proposed that the topoisomerase II molecule exists as an open complex ready to accept a second DNA duplex. On binding of the ATP, however, the molecule closes, trapping the second strand, which can then be passed through the gate in the cleaved

strand. The problem still exists, however, as to how the transported DNA strand escapes from being held by the topoisomerase II. Recent experiments using a non-hydrolysable analogue of ATP, which seals the DNA strand-entry gate because it cannot be hydrolysed, have shown that relaxed DNA can still exit from the topoisomerase II molecule (Roca & Wang, 1994). This suggests that there is a second gate, at the opposite end of the topoisomerase II homodimer to the strand entry gate, through which transported DNA duplexes can be released.

Following strand passage, the post-strand passage religation must occur to seal the gate created in the DNA duplex. Again, an equilibrium exists at this stage between cleavage and religation. This phase of the catalytic cycle has been difficult to study due to the lack of means for isolating intermediates following strand passage and before enzyme turnover. Use of non-hydrolysable ATP analogues, however, which will support strand passage but not enzyme turnover, has enabled some study of this step (Robinson & Osheroff, 1991). The equilibrium at this stage has been found to be slightly more in favour of cleavage, although it is not clear why this should be so. It may be that the stability of the cleaved DNA at this stage allows release of the second DNA duplex prior to religation of the bound DNA duplex.

The final stages of the topoisomerase II catalytic cycle involve hydrolysis of the bound ATP and turnover of the enzyme. Topoisomerase II has intrinsic ATPase activity, but this activity is seen to be stimulated approximately 20-fold by the presence of DNA (Lindsley & Wang, 1993). As has already been hinted at, ATP hydrolysis is required for enzyme turnover. It appears that enzyme turnover regenerates the active conformation of the topoisomerase II molecule, and also allows the enzyme to dissociate from the DNA (Osheroff *et al.*, 1991).

### **Role of Topoisomerase II in the Cell**

Mammalian topoisomerase II was previously identified as a major component in the metaphase chromosome scaffold (Boy de la Tour & Laemmli, 1988; Earnshaw & Heck, 1985; Gasser & Laemmli, 1986), representing 1%-2% of the total mitotic chromosomal protein. In particular, the enzyme was found to be associated at or near the base of chromatin loops (Earnshaw & Heck, 1985; Gasser *et al.*, 1986). The findings of these early experiments pointed to the idea that topoisomerase II may be involved in the organisation of the higher order structure of the chromatin. The base of chromatin loops are thought to be defined by specific sequences, known as

scaffold-associated regions (or SARs). These sequences are found to be A-T rich, and have a high frequency of potential topoisomerase II binding sites (Cockerill & Garrard, 1986; Gasser & Laemmli, 1986). It was subsequently shown *in vitro* that topoisomerase II did bind specifically to these SAR sequences (Adachi *et al.*, 1989). Recently, topoisomerase II cleavage sites have been found in an SAR from the *Drosophila* histone gene repeat (Kas & Laemmli, 1992). This discovery thus strengthened the idea that topoisomerase II plays some kind of structural role in the organisation of mitotic chromosomes. Indeed when decondensed mitotic chromosomes are incubated with anti-topoisomerase II antibodies the scaffold can be clearly seen in a helical array (Boy de la Tour & Laemmli, 1988), with the sister chromatids related by mirror-symmetry. A recent study of metaphase chromosome structure (Saitoh & Laemmli, 1994) also found that staining with anti-topoisomerase II antibodies produced a helical banding pattern which appeared to be localised to A-T rich regions of DNA.

One of the first observed roles for topoisomerase II *in vivo* was that of the segregation of daughter molecules at the end of DNA replication (DiNardo *et al.*, 1984). This was discovered by using a temperature-sensitive budding yeast mutant which was defective in topoisomerase II activity when grown at 37°C. At this temperature, the mutant yeast cells were observed to arrest during nuclear division. The nucleus in the arrested cells was seen to be located in the neck between the parent cell and the daughter bud. This arrest at cell division pointed to the requirement of topoisomerase II for separation of the newly synthesised daughter DNA molecules. Further experiments using temperature sensitive topoisomerase II yeast mutants have confirmed this hypothesis (Holm *et al.*, 1989) and have also suggested a role for topoisomerase II in preventing the breakage and nondisjunction of chromosomes.

Experiments involving the reconstitution of nuclei *in vitro* showed that topoisomerase II appeared to be involved in the condensation of DNA (Newport, 1987). In this study, cytoplasmic nuclear reformation extracts were prepared from *Xenopus* oocytes. Deproteinised lambda DNA added to these extracts were seen to be packaged into replica eukaryotic nuclei, which were subsequently capable of replication. Topoisomerase II inhibitors added to the system prevented the formation of highly condensed chromosome structures. The same result was observed when eukaryotic interphase nuclei were added to the reformation extract (Newport & Spann, 1987). It is not clear, however, if this blockage is due to specific inhibition of topoisomerase II, or a non-specific effect of the drug treatment. The role of

topoisomerase II in chromosome condensation has also been shown in temperature-sensitive yeast mutants (Uemura *et al.*, 1987) with growth at the non-permissive temperature resulting in production of long, entangled chromosomes. Condensation of chromosomes was seen to occur if cells were transferred to the permissive growth temperature. This study also showed the requirement for topoisomerase II at chromosome separation by only allowing the expression of topoisomerase II at certain stages after chromosome condensation. By using a double mutant of spindle formation and topoisomerase II, it was shown that even if spindle formation was allowed and topoisomerase II was inactivated, aberrant chromosomes were still produced (Uemura *et al.*, 1987). Even if topoisomerase II was active in short pulses during chromosome separation, chromosome disjunction was still seen. It has also been shown in chick erythrocyte cells that the degree of condensation of interphase nuclear material correlates with topoisomerase II level (Wood & Earnshaw, 1990). In a different study using *Xenopus* mitotic extract, HeLa cell nuclei and chick erythrocyte nuclei (Adachi *et al.*, 1991), the degree of chromosome condensation was analysed in topoisomerase II-depleted extracts. The chick erythrocyte nuclei, which have a low endogenous level of topoisomerase II, failed to produce condensed chromosomes in the depleted extracts. Chromosome condensation did occur, however, when purified topoisomerase II was added.

Therefore, from data on the role of topoisomerase II *in vivo*, it would appear that this enzyme is involved in the higher structural organisation of chromosomes. There is also good evidence that the processes of chromosomal segregation and condensation require topoisomerase II. It has also been shown that topoisomerase II appears to play a role in illegitimate recombination (Bae *et al.*, 1988; Sperry *et al.*, 1989) and the stability of regions of DNA encoding ribosomal genes (Kim & Wang, 1989). The involvement of topoisomerase II in these processes indicates that intimate topological manipulation of the DNA is required in order for them to occur normally. Thus it is now known that topoisomerase II is vital for certain cellular functions, particularly at cell division.

### **Phosphorylation of Topoisomerase II**

Phosphorylation is one way of post-translational processing of proteins that can be used to regulate enzymatic activity. *In vitro* experiments have shown that topoisomerase II can be phosphorylated by casein kinase II, protein kinase C, Ca<sup>2+</sup>/calmodulin-dependent protein kinase and p34<sup>cdc2</sup>

kinase (Ackerman *et al.*, 1985; Cardenas *et al.*, 1992; Sahyoun *et al.*, 1986). The phosphorylated enzyme was found to have an approximate 3-fold stimulation of relaxation activity compared to dephosphorylated (Ackerman *et al.*, 1985). It was later shown that topoisomerase II existed as a phosphoprotein *in vivo* in phorbol-stimulated dissociated sponge cells (Rottmann *et al.*, 1987) and in *Drosophila* (Ackerman *et al.*, 1988). In *Drosophila* it appeared as if casein kinase II was the main phosphorylating enzyme of topoisomerase II, whereas in *Geodia* cells, protein kinase C appeared to be responsible for the topoisomerase II phosphorylation. In the sponge system, phosphorylated topoisomerase II was found to be 2.5-fold more active in relaxation assays than non-phosphorylated enzyme (Rottmann *et al.*, 1987). It is now thought that casein kinase II is the major kinase responsible for phosphorylation of topoisomerase II *in vivo* since this kinase has been co-purified with yeast topoisomerase II (Bojanowski *et al.*, 1993; Cardenas *et al.*, 1993) and is capable of re-activating dephosphorylated enzyme. Also, yeast mutants which have temperature-sensitive casein kinase II activity show little phosphorylation of topoisomerase II when grown at the nonpermissive temperature (Cardenas *et al.*, 1992). Dephosphorylated yeast topoisomerase II has also been shown to be unable to decatenate kinetoplast DNA (Cardenas *et al.*, 1993). In yeast, it has been demonstrated that casein kinase II sites are more highly modified in metaphase than in G1 (Cardenas *et al.*, 1992). A study of topoisomerase II phosphorylation in mammalian cells has shown that topoisomerase II is phosphorylated maximally at M-phase which was also shown to be the stage at which topoisomerase II had maximal cleavage activity (Burden *et al.*, 1993). It has been proposed that prior to phosphorylation the topoisomerase II homodimer exists in a negative conformation which requires phosphorylation of particular C-terminal residues to possibly alter the conformation of the enzyme thus making it active (Cardenas & Gasser, 1993).

### **Genetic Regulation of Topoisomerase II Expression**

Until recently, little was known about the how the expression of mammalian topoisomerase II genes was regulated. It has now been discovered that the 5'-flanking region of the human TOPO II $\alpha$  gene exhibits promoter activity (Hochhauser *et al.*, 1992). A number of potential transcription factor binding sites were found upstream of the translation start site, including two Sp1 factor binding sites, a consensus site for ATF binding and five inverted CCAAT boxes (Hochhauser *et al.*, 1992). Such sequences

have also been found in the 5' regions of other proliferation-controlled genes, including the gene for thymidine kinase and DNA polymerase  $\alpha$  (Knight *et al.*, 1987; Pearson *et al.*, 1991). The pattern of transcription produced by deletion fragments in CAT assays also indicated that negative regulatory elements are found towards the 5'-end of the isolated promoter fragment (Hochhauser *et al.*, 1992). Recent analysis of the topoisomerase II promoter region has shown that there may be a phorbol regulatory region present (Loflin *et al.*, 1994). Initial evidence for phorbol regulation of topoisomerase II $\alpha$  expression came from the discovery that topoisomerase II $\alpha$  mRNA was down-regulated in a human leukaemia cell line, HL-60 when cells were treated with the phorbol ester phorbol 12-myristate 13-acetate (PMA) (Zwelling *et al.*, 1988). This down-regulation was not observed in a cell line derived from HL-60 which is refractory to differentiation using PMA (Zwelling *et al.*, 1990a). Analysis of the topoisomerase II $\alpha$  promoter in the parent and derived cell line, however, has shown that there are no mutations of this region, but that there is an alteration in methylation pattern of the promoter region between differentiation-sensitive and resistant cells (Loflin *et al.*, 1994). This methylation may be specific to a phorbol-regulatory region and therefore have an effect on topoisomerase II $\alpha$  transcription in the differentiation-resistant cell line.

### **Drug Interactions with Topoisomerase II**

The topoisomerase II enzyme has been identified as the target for a number of commonly used chemotherapeutic agents (Liu, 1989; Smith, 1990; Takano *et al.*, 1992). There are two major types of topoisomerase inhibitors, those that intercalate with DNA and those that do not. Intercalative agents include drugs such as the acridine mAMSA, non-intercalators include the epipodophyllotoxins VP16 and VM26. These three drugs all appear to cause topoisomerase II inhibition by stabilisation of the cleavable complex by forming a nonproductive drug-enzyme-DNA complex. Studies investigating topoisomerase II cleavage in the presence of mAMSA or VM26 show that there are DNA base sequence preferences for the binding of each of these particular drugs (Pommier *et al.*, 1991) which suggests that the drugs may intercalate into the DNA backbone flanking the cleavage site. It is still not clear, however, how the presence of these complexes actually brings about cell death. A new class of inhibitors has also recently been discovered, bis(2,6-dioxopiperazine) derivatives, which appear to inhibit the catalytic activity of

topoisomerase II without forming a stabilised drug-enzyme-DNA complex (Ishida *et al.*, 1991; Tanabe *et al.*, 1991).

Once it was known that anti-tumour agents targeted the topoisomerase II enzyme, people began to investigate whether topoisomerase II levels in cells corresponded to response of those cells to anti-tumour drugs (Davies *et al.*, 1988; Fry *et al.*, 1991; Potmesil *et al.*, 1988; Webb *et al.*, 1991). The take-home message from all these studies was that low levels of topoisomerase II in cells corresponded to resistance to topoisomerase II inhibitors and high levels of topoisomerase II led to increased sensitivity to inhibitors. It could therefore be postulated that, since not all tumours respond to treatment with topoisomerase II inhibitors, some of the resistance to anti-tumour agents seen in the clinic may be due to alterations in topoisomerase II expression in tumours. There have been many studies of *in vitro* derived drug resistant cell lines (Beck *et al.*, 1993a; Beck *et al.*, 1993b; Bugg *et al.*, 1991; de Jong *et al.*, 1993; Friche *et al.*, 1992; Hinds *et al.*, 1991; Long *et al.*, 1991; Ritke *et al.*, 1994) in which both alterations in expression and mutations of the topoisomerase II molecule have been found. Other mechanisms of drug resistance, such as P-glycoprotein and MRP, have also been detected in cell lines which are resistant to topoisomerase II inhibitors (Cole *et al.*, 1992; Kamath *et al.*, 1992). Therefore, resistance to topoisomerase II inhibitors, at least *in vitro*, may be due to a variety of mechanisms.

### **Cell Death**

As mentioned previously, it is not clearly established how the topoisomerase II inhibitors bring about cell death. Recently it has come to light that both topoisomerase I and II inhibitors appear to cause apoptosis in cells (Bertrand *et al.*, 1991; Solary *et al.*, 1993). When cells are treated with topoisomerase II inhibitors, the complex of enzyme-DNA and drug become stably bound to the DNA. This leaves the DNA with many double- or single-strand breaks which obviously appear as DNA damage to the nuclear machinery. Alternatively, it has been suggested that travelling replication forks may collide with topoisomerase/drug complexes which are trapped on the DNA, and thus cause irreversible stalling of the replication fork (Zhang *et al.*, 1990). This may leave exposed regions of single-stranded DNA which could appear as DNA damage. One possible response to DNA damage in the cell is the induction of the p53 protein (Kastan *et al.*, 1991). It has recently been shown that the cytotoxicity of various anti-tumour agents, including etoposide, is modulated by p53 (Lowe *et al.*, 1993). Interestingly, one of the

first indications of apoptosis in cells is the appearance of large fragments of DNA which result from endonuclease activity within the nucleus (Oberhammer *et al.*, 1993). It is thought that these fragments are chromatin loops which have been released from the scaffold. Therefore, since there is strong evidence that topoisomerase II binds to the base of these loops (Cockerill & Garrard, 1986; Gasser & Laemmli, 1986), it would not seem unlikely for there to be some co-operation of topoisomerase II in this pathway of cell death. Recent studies of drug-sensitive and resistant cells show that c-JUN, involved in the response to DNA damage, is activated when drug-sensitive cells are treated with VM-26 (Kim & Beck, 1994). Internucleosomal DNA ladders are also observed in the treated cells. Cells resistant to VM-26, however, showed an attenuation of both c-JUN induction and formation of DNA laddering. Therefore, some features associated with apoptosis are observed following topoisomerase II inhibition.

The apoptotic pathway is extremely complex, involving the collaboration of many genes (Levine *et al.*, 1994; Williams & Smith, 1993). It appears from what has been said above that the inhibition of topoisomerase II by drugs such as VP16, indirectly triggers the DNA damage response in cells and ultimately programmed cell death. Many of the genes involved in apoptosis also participate in the tumorigenic process, by mutation or amplification.

### **Multistage Tumorigenesis**

The development of a tumour is known to be a complex multistep process involving numerous complex changes to the genome (Vogelstein & Kinzler, 1993; Weinberg, 1989). The growth of a normal cell is thought to be balanced by two distinct mechanisms. Firstly, cellular proliferation is promoted by proto-oncogenes. When a proto-oncogene is activated, by mutation or amplification for example, it becomes an oncogene which can drive the growth of a tumour cell. In a number of cases these oncogenes have been shown to encode growth factors, receptor tyrosine kinases and other proteins vital to cell signalling pathways, reviewed in Aaronson, 1991. Secondly, the growth-promoting effects of proto-oncogenes are counter-balanced in normal cellular proliferation by the effects of tumour suppressor genes. These are genes which impose growth constraints on cells, possibly by controlling growth-inhibitory signals between cells (Weinberg, 1991). Inactivation of tumour suppressor genes, which can occur by deletion or mutation, will also result in deregulated cell growth. Therefore, an

alteration in either of these pathways allows a cell to escape from the growth controls which are normally imposed on it. Once such changes have occurred the cell has the potential to become tumorigenic.

Thus in a number of tumour types, mutation, deletion or amplification at specific loci have been observed. For example, inactivation of the retinoblastoma susceptibility gene, RB, by deletion is found in most cases of retinoblastoma (Horowitz *et al.*, 1990) and amplification of the N-MYC gene is seen in a high percentage of aggressive neuroblastomas (Schwab & Amler, 1990). Despite the fact that there are obviously specific gene targets for these alterations, often larger areas around the target genes are found to be deleted or amplified. For example, a large deletion of chromosome 6q is commonly observed in malignant melanoma (Trent *et al.*, 1989), and amplifications involving large regions of chromosome 20q and 11q are commonly observed in breast cancers (Tanigami *et al.*, 1992; Tanner *et al.*, 1994). This leads to the situation where genes unrelated to the target gene become deleted or amplified.

In the case of gene amplification, a number of amplicons have been analysed in tumours where such co-amplified genes may have an effect on the response of the tumour to certain chemotherapeutic agents. One of these regions is the aforementioned amplification of chromosome 11q13, found in up to 18% of breast tumours and 48% of head and neck tumours (Brison, 1993). A number of genes have been mapped to this region including CCND1 (or PRAD1), EMS1, FGF4 (or HSTF1), FGF3 (or INT2), BCL1 and GST $\pi$  (Lammie & Peters, 1991). Expression analyses of the genes within 11q13 have shown that FGF3 and FGF4 are rarely expressed by cells carrying the amplicon (Schuurin *et al.*, 1992) and thus are probably not the target genes of the amplification. It appears that there are two possible oncogene targets within 11q13, these being CCND1 which has been found to encode a D-type cyclin (Motokura *et al.*, 1991; Xiong *et al.*, 1991) and EMS1, the gene product of which is thought to be involved in the invasive potential of cells (Schuurin *et al.*, 1993). Interestingly, co-amplification of the GST $\pi$  gene has also been observed with FGF3 and FGF4 gene amplification in breast tumours (Saint-Ruf *et al.*, 1991). The glutathione-S-transferase enzymes are a family of drug-detoxifying enzymes which have been associated with drug resistance in tumours (Tew, 1994). Specifically, GST $\pi$  expression has been seen to be increased in a number of different tumour types (Moscow *et al.*, 1989) with high expression found in head and neck tumour samples (Moscow *et al.*, 1989) where, as previously mentioned, 11q13 amplification is relatively

common. It is not known, however, if any correlation exists between GST $\pi$  amplification, GST $\pi$  expression and possible drug resistance in these tumours.

Of particular relevance to the work presented in this thesis is the amplification of genes on 17q. Among the genes localised to this region are ERBB2 (Fukushige *et al.*, 1986), RAR $\alpha$  (Mattei *et al.*, 1988), TOPO II $\alpha$  (Tsai-Plugfelder *et al.*, 1988) and NM23H1 (Varesco *et al.*, 1992). These genes are all of interest with respect to the process of carcinogenesis and drug resistance. ERBB2 is found to be amplified in up to 30% of breast and ovarian tumours (Hynes, 1993; Iglehart *et al.*, 1990; Liu *et al.*, 1992; Slamon *et al.*, 1987; Slamon *et al.*, 1989) and expression of this gene has also been correlated with poor prognosis of breast cancer patients (Press *et al.*, 1993; Tetu & Brisson, 1994; Varley *et al.*, 1987; Winstanley *et al.*, 1991). Analysis of genetic changes in acute promyelocytic leukaemia patients has found that there are often changes to the RAR $\alpha$  gene, with it often being found re-arranged and fused to a gene on chromosome 15, PML (Chang *et al.*, 1991; de The *et al.*, 1990). This gene fusion results in the production of a fusion protein which is thought to play a key role in leukaemogenesis. The TOPO II $\alpha$  gene is important with respect to the expression levels of topoisomerase II alpha enzyme in the cell, since it has already been mentioned that the levels of topoisomerase II $\alpha$  within a cell can affect the drug sensitivity of a tumour. The NM23H1 gene is also of interest since the product of this gene is proposed to have an effect on the metastatic potential of tumour cells (Leone *et al.*, 1993a; Leone *et al.*, 1993b; Steeg *et al.*, 1988b; Wang *et al.*, 1993), with loss of the protein associated with greater metastatic ability of cells. In certain cases of amplification of ERBB2 in breast tumours, it has been observed that there is co-amplification of the TOPO II $\alpha$  gene (Keith *et al.*, 1993; Smith *et al.*, 1993). In some of these cases there was also amplification of the RAR $\alpha$  gene (Keith *et al.*, 1993).

The observation of ERBB2 and TOPO II $\alpha$  co-amplification is extremely interesting because of the role that topoisomerase II plays in drug resistance and sensitivity. It is likely that the co-amplification of these genes has arisen due to their proximity on chromosome 17q, of which the same is probably true for the co-amplification of GST $\pi$  with other genes on 11q. Whatever the reason for the co-amplification of TOPO II $\alpha$  and GST $\pi$  genes, the fact remains that any alteration to the expression of these genes may have an effect on the response of the tumour to certain anti-tumour drugs. The finding that genes such as GST $\pi$  and TOPO II $\alpha$  can be affected in this way, and thus perhaps affect tumour response, makes clear the importance of studying the full extent of amplicons in human tumours. In addition to the

role that topoisomerase II plays in drug resistance, this enzyme may also participate in tumour progression. This suggestion has arisen since topoisomerase II has been proposed to mediate illegitimate recombination (Bae *et al.*, 1988; Sperry *et al.*, 1989) and possible binding sites for topoisomerase II have also been detected at the breakpoints of chromosomal translocations (Dong *et al.*, 1993). In addition to this, in patients being treated for tumours with topoisomerase II-targeting agents, secondary myeloid leukaemias involving 11q chromosomal abnormalities have been observed (Pui *et al.*, 1991). Thus it is inferred that targeting topoisomerase II somehow has a knock-on effect to cause instabilities of chromosome 11.

# CHAPTER 2

## MATERIALS & METHODS

### 2.1 Materials

The following section lists all routinely used materials. Less frequently used materials are described within the appropriate Methods' section.

#### 2.1.1 Chemicals

All chemicals were obtained from the following manufacturers unless otherwise stated; BDH Chemicals Ltd., GIBCO BRL, Pharmacia LKB Biotechnology or Sigma Chemicals.

#### 2.1.2 Radiochemicals

The  $\alpha$ -<sup>32</sup>P-dCTP used in random prime labelling reactions of Southern and Northern probes and  $\gamma$ -<sup>32</sup>P-dATP used in 5' end-labelling reactions were obtained from Amersham International plc.

#### 2.1.3 Restriction Endonucleases and other Enzymes

The majority of restriction endonucleases were obtained through the Wolfson Laboratories of Molecular Pathology from GIBCO BRL, Northumbria Biologicals Ltd. or Pharmacia LKB Biotechnology.

Other enzymes were obtained as follows:

Pepsin (P6887)	Sigma Chemicals
RNAse A	Boehringer Mannheim

Restriction digests were run out on 1% agarose/TBE gels containing ethidium bromide, visualised under UV illumination and photographed using either a Polaroid MP4 land camera with Type 57 Kodak film or an Appligene "Imager" CCD camera with supplied software. In the latter case, images were printed on thermal paper or stored on 3 1/2" Verbatim MF2-HD diskettes.

## 2.1.4 Size Markers

### DNA size markers

- (a) *Hind III* digested phage  $\lambda$  IBI Ltd.  
(b) *EcoRI/BamHI* digested Adenovirus IBI Ltd.

### Protein size markers

Prestained protein standards, 15,300-206,450 BRL

## 2.1.5 Media, Solutions and Buffers

### 2.1.5.1 General Solutions

#### 20 x SSC

3M NaCl

0.3M Tri-sodium citrate

Brought to pH 7.0 with NaOH

#### TBE (x 1)

89mM Tris borate

89mM Boric acid

2.5mM EDTA

For TBE with ethidium bromide, use at final concentration of 0.5mg/ml

#### TAE (x 1)

40mM Tris base

2mM EDTA

20mM NaCl

20mM Na Acetate

Brought to pH 8.15 with glacial acetic acid

#### PBS

Per 2 litres distilled water:

20 PBS (Dulbecco 'A') formulated tablets (OXOID, Unipath Ltd.)

For PBST (PBS with 0.05% Tween) add 2mls 25% Tween 20 per litre

## 2.1.5.2 Tissue Culture Solutions

### Medium for CALU-3, L-DAN and SK-MES-1

50:50 Hams' F10 (ICN Biomedicals):Dulbecco's Modified Eagle's  
Medium

0.075% sodium bicarbonate

2mM L-glutamine

10% foetal calf serum (GlobePharm or GIBCO BRL)

in autoclaved distilled water

to pH 7.2-7.4 with 1M NaOH

For the resistant CALU-3 cell line, F10/DMEM medium was supplemented with  $10^{-5}$ M VP-16. Cells were exposed to drug for 24 hours once a month.

### Medium for GLC<sub>4</sub>, GLC<sub>4</sub>/Adr, A2780 and A2780/Adr

RPMI 1640 with:

0.075% sodium bicarbonate

1mM sodium pyruvate

2mM L-glutamine

10% foetal calf serum (as above)

in autoclaved distilled water

to pH 7.2-7.4 with 1M NaOH

For GLC<sub>4</sub>/Adr and A2780/Adr, 400 $\mu$ l of a 40 $\mu$ g/ml doxorubicin solution was added per 25mls of medium.

### Trypsin

0.25% trypsin

1mM EDTA

in autoclaved PBS

### Phosphate Buffered Saline

140mM NaCl

10mM Na<sub>2</sub>HPO<sub>4</sub>

2mM KCl

1mM KH<sub>2</sub>PO<sub>4</sub>

### **2.1.5.3 Southern and Northern solutions**

#### **Northern Gel**

1.2% agarose solution in distilled water  
microwaved to dissolve and cooled to room temp.  
1 x MOPS  
0.5% formaldehyde

#### **MOPS (x 10)**

200mM MOPS  
10mM EDTA  
50mM Na Acetate  
to pH 7 with glacial acetic acid and then autoclaved

#### **RNA Loading Dye**

95% formamide  
20mM EDTA  
0.05% bromophenol blue  
0.05% xylene cyanol  
1/10<sup>th</sup> volume of 50% glycerol

#### **Southern Gel**

0.8% agarose in distilled water

#### **DNA Lysis Buffer**

0.3M sodium acetate, pH 8.0  
0.5% SDS  
5mM EDTA

#### **DNA Loading Dye**

0.25% bromophenol blue  
0.25% xylene cyanol FF  
30% glycerol

#### **20 x Genescreen**

0.5M Na<sub>2</sub>HPO<sub>4</sub>  
0.5M NaH<sub>2</sub>PO<sub>4</sub>

**Denaturation Solution**

2.5M NaOH

7.5M NaCl

**Neutralisation Solution**

1M Tris base (pH 7.4)

1.5M NaCl

**Southern and Northern Hybridisation Buffer**

50mM PIPES

50mM NaH<sub>2</sub>PO<sub>4</sub>·2H<sub>2</sub>O

50mM Na<sub>2</sub>HPO<sub>4</sub>

100mM NaCl

1mM EDTA

5% SDS

Filter sterilised before use

**Southern and Northern Hybridisation Wash Buffer**

1 x SSC

5% SDS

**2.1.5.4 Fluorescence *In Situ* Hybridisation Solutions****70% Hybridisation Solution for Centromeric Probes**

70% formamide

2 x SSC

5% dextran sulphate

500µg/ml salmon sperm DNA

**50% Hybridisation Solution for Single-Copy Probes**

50% formamide

2 x SSC

10% dextran sulphate

500µg/ml salmon sperm DNA

**Hypotonic Solution**

0.075M KCl

**Fix**

3 volumes methanol:1 volume glacial acetic acid

**Post-Fix**

Streck Tissue Fixative (Alpha Labs)

**Denaturation Solution**

70% formamide in 2 x SSC at 70-80°C

**10% Block Solution Stock**

10% Boehringer Mannheim blocking reagent in maleic acid buffer

Microwave until solution becomes yellow and turbid and then autoclave to dissolve.

Used at a concentration of 0.5% in maleic acid buffer/Tween, 4 x SSC-T or PN-T buffer

**4 x SSC-T Wash Solution**

4 x SSC

0.05% Tween 20

**Maleic Acid Buffer**

0.1M maleic acid

0.15M NaCl

0.35M NaOH

pH to 7.5 with NaOH

For maleic acid buffer with 0.05% Tween, add 2 mls of 25% Tween 20 per litre

**PN buffer**

Mix of 0.1M NaH<sub>2</sub>PO<sub>4</sub> and 0.1M Na<sub>2</sub>HPO<sub>4</sub>

(a) 0.1M Na<sub>2</sub>HPO<sub>4</sub>: 35.6g in 2 litres distilled water

(b) 0.1M NaH<sub>2</sub>PO<sub>4</sub>: 13.7g in 1 litre distilled water

Add solution (b) to 2 litres of solution (a) until pH 8.0 is reached

**PN-T Buffer**

PN buffer

0.05% Tween 20

## 2.1.5.5 Protein and Western Blotting Solutions

### **Nucleus Buffer**

1mM KH<sub>2</sub>PO<sub>4</sub>  
5mM MgCl<sub>2</sub>·6H<sub>2</sub>O  
1mM EDTA, pH6.4  
2.5% SDS

Store at 4°C

Immediately prior to use various protease inhibitors were added, to the following final concentrations:

0.2 mM DTT (from 1mM stock kept at -20°C)  
1μM pepstatin  
1mM PMSF

### **Protease Inhibitors (stock concentrations)**

10mM PMSF in isopropanol  
1mg/ml pepstatin in ethanol  
10mg/ml leupeptin in distilled water  
500mM benzamidine in distilled water

### **Sample Lysis Buffer**

2% SDS  
25% spacer gel buffer  
5mM EDTA  
10% glycerol  
2.5% β-mercaptoethanol

Protease inhibitors added before use

### **Running Buffer**

1.5M Tris base  
0.4% SDS  
pH to 8.9 with conc. HCl

### **Spacer Gel Buffer**

0.5M Tris base  
0.4% SDS  
pH to 6.7 with conc. HCl

**5 x Tank Buffer**

0.25M Tris base  
0.5M glycine  
0.5% SDS

**Transfer Buffer**

48mM Tris-base  
39mM glycine  
0.038% SDS

**8% Polyacrylamide Gel**

8ml running buffer  
8.5ml 30% acrylamide, 0.8% bis-acrylamide (Severn Biotech Ltd)  
3.2ml 1% polyacrylamide  
12.2ml distilled water  
120 $\mu$ l 10% APS  
15 $\mu$ l TEMED

**15% Polyacrylamide Gel**

8ml running buffer  
16ml 30% acrylamide, 0.8% bis-acrylamide  
3.2ml 1% polyacrylamide  
4.8ml distilled water  
180 $\mu$ l 10% APS  
15 $\mu$ l TEMED

**4% Spacer Gel**

3ml spacer gel buffer  
1.6ml 30% acrylamide, 0.8% bis-acrylamide  
1.2ml 1% polyacrylamide  
6.2ml distilled water  
250 $\mu$ l 10% APS  
20 $\mu$ l TEMED

**Wash Buffer (PBST)**

PBS  
0.05% Tween 20

**Blocking Solution**

5% Marvel (Premier Beverages) in PBST

**Western Loading Dye**

4% SDS

50% spacer gel buffer

10mM EDTA

20% glycerol

5%  $\beta$ -mercaptoethanol

0.25% bromophenol blue

**Gel Stain**

90% methanol/H<sub>2</sub>O (1:1)

10% glacial acetic acid

0.25% Coomassie Brilliant Blue R250

**Destain**

25% methanol

7% glacial acetic acid

**2.1.5.6 Topoisomerase II Assay Buffers****Assay Buffer**

50mM Tris-HCl, pH8

120mM KCl

10mM MgCl<sub>2</sub>

0.5mM ATP

0.5mM DTT

30 $\mu$ g/ml BSA

**Stop Buffer/Loading Dye**

5% Sarkosyl

0.0025% bromophenol blue

25% glycerol

### **2.1.5.7 Immunofluorescence Solutions**

#### **Blocking Solution**

Same as that for FISH

Used at a concentration of 0.05% in PBS-T

#### **PBS-T Wash Solution**

PBS

0.05% Tween 20

### **2.1.5.8 Flow Cytometry Solutions**

Same as those for immunofluorescence plus:

#### **PBT**

PBS containing 0.5% bovine serum albumin and 0.1% Tween 20

**2.1.6 Table of Primary Antibodies used in Immunofluorescence, Flow Cytometry and Western Blotting**

<b>Antibody</b>	<b>Supplier</b>
Anti-Topoisomerase II $\alpha$ (Polyclonal, IM, FACS)	TopoGEN, U.S.A.
Anti-Topoisomerase II $\alpha$ (Polyclonal, FACS, W)	Cambridge Research Biochemicals
Anti-Topoisomerase II $\beta$ (Monoclonal, IM, W)	Negri et. al.
Anti-ErbB2, NCL-CB11 (Monoclonal, IM, FACS)	Novocastra
Anti-nm23H1/H2 (Polyclonal, IM, FACS, W)	Cambridge Research Biochemicals
Anti-P-glycoprotein, JSB-1 (Monoclonal, FACS)	Monosan (via Bradsure Biologicals Ltd)
Anti-P-glycoprotein, MRK-16 (Monoclonal, FACS)	Tsuruo et al., Cancer Chemotherapy Centre, Tokyo
Anti-Retinoic Acid Receptor Alpha (Polyclonal, W)	Affinity BioReagents
Anti-bromodeoxyuridine (Monoclonal, FACS)	DAKO
Anti-Human Nucleolar Control (Polyclonal, IM)	ImmunoConcepts (via Alpha Labs)

FACS:      Used in flow cytometry  
IM:         Used in immunofluorescence analysis  
W:         Used in Western analysis

**2.1.7 Table of Antibodies used for Fluorescence *In Situ* Hybridisation**

<b>Antibody</b>	<b>Supplier</b>
Sheep anti-digoxigenin	Boehringer Mannheim
Mouse anti-biotin	Boehringer Mannheim
Donkey anti-sheep-FITC	Jackson ImmunoResearch (via Stratech Scientific)
Goat anti-mouse-FITC	Jackson ImmunoResearch (via Stratech Scientific)
Donkey anti-rabbit-FITC	Jackson ImmunoResearch (via Stratech Scientific)
Donkey anti-sheep-Cy <sup>5</sup>	Jackson ImmunoResearch (via Stratech Scientific)
Goat anti-mouse-Cy <sup>5</sup>	Jackson ImmunoResearch (via Stratech Scientific)
Avidin-FITC DCS	Vector Laboratories
Biotinylated anti-Avidin D	Vector Laboratories

## **2.2 Methods**

### **2.2.1 Cell Lines and Tissue Culture**

*Details of all growth media used in tissue culture are given in Section 2.1.5.2*

The human non-small cell lung carcinoma cell lines CALU-3 and SK-MES-1 were obtained from the American Type Culture Collection (ATCC, Rockville, MD). L-DAN is a squamous lung cancer cell line established in the Department of Medical Oncology in Glasgow. All three cell lines are adherent lines and were tested monthly for mycoplasma contamination. Cells were passaged 1:10 once a week.

A VP16 resistant clone of CALU-3 was derived in the Department of Medical Oncology by Dr. Jane Plumb. A sensitive clone (ID50 for VP16=0.2 $\mu$ M) was selected for derivation of the resistant cell line from the heterogeneous population of CALU-3. Cells were exposed to between 0.1 $\mu$ M and 1 $\mu$ M VP16 for 24 hours following which they were allowed to regrow. Cells which grew through the highest concentration (1 $\mu$ M) were then re-exposed to this concentration of VP16 twice (cells frozen down at this stage, CALU-3/10<sup>-6</sup>M VP16). After six months the cells were tested for sensitivity to VP16 and reselected in between 1 and 10  $\mu$ M of the drug. Cells which survived 9 $\mu$ M drug (CALU-3/9x10<sup>-6</sup>M VP16) were reselected in 10 $\mu$ M VP16 and these cells were then tested for sensitivity to VP16, doxorubicin, vincristine and cisplatin. This cell line, CALU-3/10<sup>-5</sup>M VP16 is the resistant clone which has been studied as part of this work. When culturing this cell line, 10<sup>-5</sup>M VP16 was added to the growth medium.

Human lung cell lines GLC4 and GLC4/Adr were cultured briefly (< 7 days) for use as controls in Western analysis, as were the A2780 and A2780/Adr ovarian cell lines.

### **2.2.2 Southern Analysis**

*Details of solutions used in Southern analysis are given in Section 2.1.5.3*

#### **2.2.2.1 DNA Extraction** (from Keith *et al.*, 1992)

Genomic DNA was harvested independently from the three lung cancer cell lines mentioned above for use in the preparation of Southern blots. Extraction of DNA was achieved by addition of 10 mls of equilibrated

phenol to cells growing in a 75cm<sup>2</sup> tissue culture flask. Cells were scraped from the bottom of the flask using a Costar disposable cell scraper and the mixture left, shaking gently at 37°C for 10 minutes. Ten mls of DNA lysis buffer were then added and the flask again incubated, shaking gently at 37°C for 10 minutes. Once this incubation was complete the contents of the flask were emptied into a 50 ml Falcon "Blue Max" tube (Becton Dickinson) and 10 mls of chloroform/isoamyl alcohol (25:1) was added. The tube was then incubated at 37°C on a rotating rack for 10 minutes. After this time the solution was centrifuged for 15 minutes at 3500 rpm, 22°C, following which the supernatant was removed and the genomic DNA precipitated using an equal volume of isopropyl alcohol. This solution was placed at -20°C for approximately 30 minutes prior to centrifugation, which was performed as detailed above. The DNA pellet was air-dried for approximately 10 minutes and resuspended in 100-200µl of distilled water. All genomic DNA samples were stored at 4°C.

### 2.2.2.2 Southern Blotting

See Sambrook *et al.*, 1989 for review of technique.

Twenty micrograms of genomic DNA were used in digestions for Southern blotting. DNA was digested overnight at 37°C in a 150µl volume with 100U of the required restriction enzyme according to manufacturers instructions. Digested DNA was precipitated using 0.1 volume 3M sodium acetate (pH 8) and 2 volumes absolute alcohol and incubated at -20°C overnight. DNA was pelleted at 13,000 rpm for 25 mins, air-dried for 30 mins and resuspended in 50µl distilled water. Resuspension was carried out at 37°C overnight. Five µl of DNA loading dye was then added and samples were run on a 0.8% agarose/TAE gel overnight at approximately 50V using gel tanks from IBI Ltd., Cambridge.

Following electrophoresis, the digested DNA was <sup>visualised in</sup> stained for 45 mins with ethidium bromide (0.5µg/ml) and then photographed using Kodak Type 57 film under UV illumination with a Polaroid MP4 land camera in order to check levels of DNA loading. DNA on the gel was then denatured by 2 x 15 min washes in denaturation solution and neutralised by 2 x 30 min washes in neutralisation solution. Gels were then blotted overnight onto nylon filters (HyBond Nfp, Amersham, U.K.) using 1 x Genescreen buffer. Filters were then rinsed briefly in Genescreen and dried. DNA was subsequently cross-linked to the filter by a 5 minute exposure to a UV light source.

Hybridisation and washing of filters was carried out as described in Section 2.2.5.

### **2.2.2.3 Chromosome 17 Cosmid Library Filters**

Two duplicate cosmid library filters were obtained from the ICRF, through Dr. Donny Black at the Beatson Institute. The filters consisted of approximately 20000 bacterial clones each having been spotted in 3 x 3 colony grids on the filter. Each of the individual clones contains a cosmid incorporating some sequence from chromosome 17. In order to find a cosmid probe for the RAR $\alpha$  gene for use in FISH, 40mer oligos from part of the RAR $\alpha$  gene were obtained from Oncogene Science, end-labelled using a Promega 5'-end labelling kit (according to manufacturers instructions) and hybridised as detailed in section 2.2.4. An RAR $\alpha$  plasmid, p63, acquired from the ATCC was <sup>32</sup>P-labelled using a Stratagene random prime kit (see section 2.2.6.3) and hybridised independently from the oligo probe to the filters. Following autoradiography, x and y grid co-ordinates of positive colonies were taken, provided the colony was positive on both filters, and these co-ordinates sent back to the ICRF. The requested clones were then kindly supplied in the form of an agar stab.

### **2.2.3 Northern Analysis**

See Sambrook *et al.*, for a review of Northern blotting

*Details of solutions used in Northern analysis are given in Section 2.1.5.3*

RNA was harvested from 75 cm<sup>2</sup> tissue culture flasks of CALU-3, L-DAN and SK-MES-1 cells according to the RNazol 'B' method (Cinna/Biotech Laboratories, Texas, USA). Twenty micrograms of total cellular RNA was used per cell line for Northern analysis. Samples, containing 20  $\mu$ g RNA (made up to 12.5  $\mu$ l with autoclaved, distilled water), 1  $\mu$ l ethidium bromide (1 mg/ml stock), 4.5  $\mu$ l 5 x MOPS, 4.5  $\mu$ l 37% formaldehyde and 22.5  $\mu$ l formamide, were denatured at 55°C for 15 minutes before addition of 5  $\mu$ l RNA loading dye.

Gels were electrophoresed at 50V overnight, in IBI gel tanks, in 1 x MOPS, photographed as for Southern gels and then blotted for 7-8 hours in 0.05M NaOH onto Hybond Nfp nylon membrane (Amersham, U.K.).

Hybridisation and washing of filters were carried out as described in the following section.

## **2.2.4 Hybridisation and Washing of Membranes**

(previously detailed in Keith *et al.*, 1992)

Hybridisation and washing of filters were carried out using the Hybaid rotisserie system and oven set at 65°C. Filters were rolled in 20 x 20cm squares of nylon mesh (Hybaid) and placed in glass hybridisation bottles. Bottles were then incubated in the oven. Filters were prehybridised for 1-2 hrs in approximately 20 mls of hybridisation solution before the addition of radiolabelled probe. Labelled probes were applied to filters in a 10 ml volume of hybridisation buffer and hybridisation was then carried out for 18-24 hours at 65°C in the Hybaid oven. Filters were subsequently washed in 20-30 mls of wash solution for several hours also in the rotisserie oven with repeated changes of solution.

## **2.2.5 Autoradiography**

Probed filters were exposed to Kodak XAR 5, or FUJI RX autoradiography film in sealed film cassettes with fast tungstate intensifying screens at -70°C for varying lengths of time depending on the signal intensity.

## **2.2.6 Southern and Northern probes**

### **2.2.6.1 Probes Used**

The human topoisomerase II $\alpha$  gene probe used was SP1 (Chung *et al.*, 1989). ERBB2 was detected by the probe pCER204, RAR $\alpha$  by the probe p63 and PKC $\alpha$  by pHPKC-alpha 7 (Parker *et al.*, 1986). All these gene probes were obtained from the ATCC. The nm23 gene probe was kindly provided by Dr. Patricia Steeg (N.I.H., Bethesda). pHJi, a genomic clone of the human immunoglobulin heavy chain locus, was used to quantify DNA loading in Southern blots (Erickson *et al.*, 1982). The same probe for topoisomerase II $\alpha$  was used in Northern analysis and the SP12 probe used to detect topoisomerase II $\beta$ . Topoisomerase I was detected by the pScI70 probe (Sunde *et al.*, 1989) and a 7S RNA probe was used as a loading control. The probe for G-CSF was obtained from Dr. I Pragnell, Beatson Institute.

### **2.2.6.2 Preparation of Probes for Labelling**

For SP1 and SP12, inserts were cut from whole plasmids for use as Southern and Northern probes. The appropriate digests were performed with plasmids in order to release inserts. Digested plasmid was run on 1.5% TBE gel so as to obtain well separated bands. The required band was excised from the gel and put into a "Spin-X" column with 100 $\mu$ l distilled water. The gel fragment was mashed using a sealed glass pipette and then spun at 13,000 rpm for 25 mins. Solution pushed through the filter unit was re-applied to the gel remains above, a further 100 $\mu$ l of water was added and the column left at 4 $^{\circ}$ C to elute overnight. The next morning the column was spun again, solution re-applied to filter and left for 30 mins following which the column was re-spun. This process was repeated 6-7 times before a 10 $\mu$ l aliquot was taken and run on a test gel with a known amount of marker to ensure <sup>the</sup> required fragment had been purified and to estimate probe concentration. Purified insert was stored at -20 $^{\circ}$ C.

### **2.2.6.3 Random Labelling of dsDNA**

<sup>32</sup>P-labelled dsDNA probes (used for Southern and Northern) were prepared using the Stratagene "Prime-It" kit and 100ng of template DNA. The labelling protocol was carried out according to manufacturer's instructions. Following labelling, probes were purified using Sephadex-containing NICK columns (Pharmacia) and chemically denatured before being applied to filters in 10 mls of hybridisation buffer.

### **2.2.7 Re-probing of Southern and Northern Membranes**

Filters were re-probed with a number of probes for different genes. In order to remove previous hybridisation signal, filters were placed in boiling 0.1% SDS solution and left until cooled to room temperature.

## **2.2.8 Fluorescence *In Situ* Hybridisation (FISH)**

All protocols listed below are variations from the following published methods: Kallioniemi *et al.*, 1992b, Coutts *et al.*, 1993, Gosden *et al.*, 1992.

*Details of all solutions used in FISH are given in Section 2.1.5.4*

The individual stages of FISH, preparation of chromosomes and slides, hybridisation and post-hybridisation washing, have been separated for ease of understanding.

### **2.2.8.1 Preparation of Chromosomes from Lymphocytes**

Chromosomes were prepared using a small amount of fresh blood from a willing volunteer and "chromosome medium 1A" bought from GIBCO Life Technologies. 200 $\mu$ l of blood was added to each 5ml tube of medium and incubated for 72 hrs at 37 $^{\circ}$ C. Tubes were agitated daily to prevent settling of the contents. Seventy-one hours after the blood had been seeded, colcemid (GIBCO) was added to each tube to a final concentration of 0.1 $\mu$ g./ml. Tubes were then agitated gently and left for 1 hr at 37 $^{\circ}$ C. Following this incubation the blood culture was transferred to 15ml Falcon tubes, spun down (2500 rpm for 5 mins) and the supernatant poured off. Cells were resuspended in the small amount of remaining medium and 10 mls of warmed (37 $^{\circ}$ C) hypotonic solution added slowly. Tubes were incubated at 37 $^{\circ}$ C for 10 mins before being spun, as detailed previously. The hypotonic solution was then poured off, leaving a very small amount remaining above the cell pellet in which the cells were then resuspended. At this stage it is crucial that the cells are well resuspended and not at all clumpy. Ten mls of fix was added to the cell suspension very slowly dropwise, with the tube constantly being agitated by the fingers. Once the fix was all added the cells were left at room temperature for 15 mins to allow penetration of the fix into the cells. Tubes were then spun as before. The fix solution was poured off, leaving a small amount remaining in which cells were resuspended and a second 10mls of fix solution was added. Cells were then spun immediately.

This process of fixing and spinning samples was continued until the resuspended solution became clear and there was no trace of haemoglobin from the lysed red blood cells, usually 5-6 repetitions. A sample of the fixed cells was then dropped onto a slide to check for the presence of metaphase spreads and also for determination of cell density. Final lymphocyte preparations were stored in fix at -20 $^{\circ}$ C.

### 2.2.8.2 Preparation of Chromosomes from Cell Lines

Chromosomes were prepared from 75cm<sup>2</sup> tissue culture flasks of sub-confluent cell lines. Different concentrations of colcemid were used for the three different cell lines with 0.2µg/ml being added to L-DAN and SK-MES-1 cultures and 0.25µg/ml added to CALU-3 cultures. L-DAN and SK-MES-1 were then incubated for 2 hours and CALU-3 for 3 hours at 37°C. Medium was then removed, cells were rinsed with PBS and trypsinised to remove them from the base of the flask. Cells were washed in PBS, spun down ( 2500 rpm for 5 mins) and the PBS poured off leaving a small amount covering the cells. The cell pellet was resuspended in this small amount of PBS and 10 mls of warmed hypotonic solution added, as for the lymphocyte preparation. All cell lines were incubated for 15 mins with hypotonic solution at 37°C and then spun, as before. The chromosome preparation then continued as outlined for lymphocytes with fix and spin cycles being repeated 4-5 times.

### 2.2.8.3 Probes Used for FISH

A number of different probes from chromosome 17 were used, as outlined in the following table:

Probe Name	Region of Chr.17 Detected	Supplied By
Chromosome 17 paint	Whole chromosome	Cambio
17-specific centromere	Centromere only	Home-made via PCR
pC5	TOPO IIα gene	Dr.Ian Hickson, ICRF
ICRFc105B041155	TOPO IIα gene	ICRF RLDB
ICRFc105H01119	TOPO IIα gene	ICRF RLDB
ICRFc105C0861	NF1 gene	ICRF RLDB
ICRFc105H12160	NM23H1 gene	ICRF RLDB
ICRFc105F1255	RARα gene	ICRF RLDB
C05123	BRCA1 region	Dr. Donny Black, CRC
Neu 1	ERBB2 gene	White & Leppert, Utah
Neu 4	ERBB2 gene	White & Leppert, Utah

ICRF RLDB: Imperial Cancer Research Fund Reference Library-DataBase

#### **2.2.8.4 Isolation of Cosmids**

Cosmids were usually supplied in bacterial agar stabs. A sample of the stab was taken using a sterile wire loop and grown in a 10 ml culture of L-broth and the relevant antibiotic (either kanamycin or ampicillin, both used at a final concentration of 20 $\mu$ g/ml) overnight at 37°C in a shaking incubator. This overnight culture was seeded into either 100 or 500 mls of L-broth/antibiotic and grown for a further 24 hours. The cosmid DNA was isolated from these cultures using the Qiagen system (Hybaid).

Following the Qiagen isolation protocol, DNA pellets were resuspended in 100-400 $\mu$ l of distilled water. A 2 $\mu$ l sample of cosmid was digested with *EcoRI* and run on a 0.8% TBE/EtBr gel in order to check cosmid size and 1 and 5 $\mu$ l undigested samples were also run on these gels to check DNA concentration. The remaining cosmid preparation was stored at -20°C.

In order to confirm that cosmids contain inserts from a particular gene, approximately 1 $\mu$ g of cosmid was digested using *EcoRI* and then run on a 0.8% agarose/TAE gel. Gels were stained, photographed and blotted according to Southern blot protocol (section 2.2.2.2) and hybridisations were then performed using the appropriate probe (topoisomerase II alpha, retinoic acid receptor alpha or nm23H1), as described previously.

Occasionally cosmids were received as samples of DNA, in which case it was necessary to package them into bacteria. This was achieved using a GigaPack Gold II packaging kit from Promega and by following the supplied manufacturer's instructions.

#### **2.2.8.5 Labelling of Probes for FISH**

Probes were labelled with either biotin or digoxigenin. In order to label the cosmid probes with biotin a "Bio-Nick" nick translation kit from GIBCO was used. For incorporation of digoxigenin a Boehringer Mannheim nick translation kit was used. For each of these kits, 1 $\mu$ g of cosmid DNA was labelled. The chromosome paint used was purchased already labelled with biotin and the centromere sequence could be labelled with either hapten during the initial PCR reaction.

Nick translation reactions were performed at 16°C for 2-3 hours following which DNA was precipitated by the addition of 1 $\mu$ l glycogen, 1 $\mu$ l 0.5M EDTA, 5 $\mu$ l 3M NaAc, pH8.0, 25-75 $\mu$ l human *CotI* DNA and 300 $\mu$ l ethanol and incubated at -20°C overnight or in a dry ice/ethanol bath for 30

mins. DNA was pelleted by centrifugation at 13,000 rpm for 25 mins, washed in 70% ethanol and then vacuum dried for 15 mins at 56°C in a Howe GyroVap. The DNA pellet was resuspended in 50µl of 50% hybridisation mix (for single-copy gene cosmids) or 70% hybridisation mix (for repetitive probes) and left to resuspend at 37°C for an hour.

#### **2.2.8.6 Preparing Slides for Hybridisation**

The first step in preparing slides for hybridisation was to drop a small quantity of the required chromosome preparation onto a clean glass slide. Slides and coverslips (for final mounting) were kept in 100% ethanol with a few drops of concentrated hydrochloric acid added to it. Chromosomes were dropped from a couple of feet above the slide using a short-form glass pipette. Slides were then rinsed with a pipette-full of fixative and air-dried.

A 1 hour fixation in 3:1 methanol/acetic acid followed, after which slides were rinsed in 2 x SSC and incubated in 100µg/ml RNase in 2 x SSC for 1 hour at 37°C. Slides were rinsed in PBS and then incubated in 0.01% pepsin in 0.01M HCl for 10 mins at 37°C. Following a rinse in 2 x SSC, the post-fix stage was performed using Streck tissue fixative, in which slides were left for 10 mins at room temperature. Slides were then dehydrated by passing twice through 70% ethanol (2 mins each time) and twice through 100% ethanol (2 mins each time).

Denaturation of slides was performed just prior to hybridisation and was achieved by incubation of the slides for 5 mins in 70% formamide at 75°C. The formamide solution was heated to 1°C higher than 75°C for each slide to be denatured. Ice-cold 70% ethanol was then used to rinse the slides at least 5 times (1 min each time) following which dehydration in 100% ethanol was carried out, as detailed above and slides were air-dried.

Slides were then ready to be hybridised with the required probe.

#### **2.2.8.7 Hybridisation of Slides**

Before hybridising, all probes were denatured to single-stranded DNA by incubation at 70°C for 5 mins (unless otherwise instructed by the manufacturers) followed by an hours' incubation at 37°C to enable competing out of any repetitive sequences in the probe by the CotI DNA. Ten microlitres of denatured probe was then added to slides, as prepared above, covered with a coverslip and sealed round the edges of the coverslip with Cow Gum, rubber adhesive using a 1 or 2 ml syringe. Slides were then incubated

in a humidified chamber overnight at 37°C. Where double hybridisations were performed using a centromere probe and a single-copy gene probe, 3µl of the centromere probe was mixed with 9µl of single-copy probe after both had been denatured. This entire mixture was then applied to the slide. For doubles with two single-copy probes, 5µl of each was taken, mixed and applied to the slide.

### **2.2.8.8 Washing and Detection of Probes**

The washing procedure was always the same, irrespective of which detection method was used. The Cow Gum sealant was removed carefully from the slides by dipping slides in 2 x SSC and peeling off using a pair of curved, pointed forceps. The coverslips were then gently prised off by holding a corner of the coverslip. Slides were then washed twice in 50% formamide/1 x SSC at 42°C and twice in 2 x SSC at 42°C in Coplin jars. Blocking and detection then proceeded according to one of the following protocols. All antibodies were diluted in block solution with 100µl of diluted antibody being applied per slide. Parafilm coverslips were then placed over the antibody on the slide to ensure even coverage of the area previously hybridised.

Different detection methods were used dependent on which hapten the probe was labelled with and which fluorochrome one wished to use to detect that hapten.

#### **Version I, for Biotin or Digoxigenin labelled probes**

- (i) Rinse slides briefly in maleic acid/Tween buffer
- (ii) Block for 30 mins at 37°C in 0.5% block solution in maleic acid/Tween buffer
- (iii) Incubate with first antibody for 1 hour at 37°C in a humidified box.

Either mouse anti-biotin (for biotin probes) or sheep anti-digoxigenin (for digoxigenin probes). Both antibodies were used at 1:200 dilution in 0.5% blocking solution.

- (iv) Rinse slides for 10 mins in large glass slide holder on stirrer with maleic acid/Tween buffer.
- (v) Incubate with second antibody for 30 mins at 37°C in a humidified box.

Either goat anti-mouse-FITC or donkey anti-sheep-FITC, both at 1:500 dilution in block solution.

- (vi) Rinse slides for 30 mins in large glass slide holder on stirrer with maleic acid/Tween buffer.
- (vii) Dehydrate, as detailed in Section 2.2.5.5, Version I

**Version II, for Biotin labelled probes**

- (i) Rinse slides briefly in 4 x SSC-T buffer
- (ii) Block for 10 mins at room temperature in 4 x SSC-T/0.5% block (4 x SSC-TB).
- (iii) Incubate with FITC-Avidin DCS at 1:200 dilution in 4 x SSC-TB for 45 mins in humidified box at room temperature.
- (iv) Rinse slides for 10 mins, in large stirrer in 4 x SSC-T {keep for use again in steps (vi) and (viii)}.
- (v) Incubate with Biotinylated anti-avidin D at 1:100 dilution in 4 x SSC-TB for 45 mins in humidified box at room temperature.
- (vi) Rinse slides, as above.
- (vii) Incubate again with FITC-Avidin DCS 4 x SSC-TB, as above {Step (iii)}
- (viii) Rinse slides in 4 x SSC-T for 20 mins in large stirrer.
- (ix) Dehydrate, as detailed in Section 2.2.5.5, Version I

**Version III, for double hybridisations with biotin and digoxigenin probes**

- (i) Rinse slides briefly in 4 x SSC-T
- (ii) Block for 10 mins at room temperature in 4 x SSC-T/0.5% block.
- (iii) Incubate with FITC-Avidin DCS at 1:200 dilution in 4 x SSC-TB for 45 mins in humidified box at room temperature.
- (iv) Wash slides in 4 x SSC-T in large glass stirrer for 10 mins at room temperature.
- (v) Transfer slides to PN-T buffer for 2 mins.
- (vi) Block slides for 10 mins in PN-T buffer/0.5% block at room temperature.
- (vii) Incubate with biotinylated anti-avidin D at 1:100 and sheep anti-digoxigenin at 1:200, both in PN-T buffer/0.5% block solution for 45 mins at room temp in a humidified box.
- (viii) Wash in PN-T buffer for 10 mins in large glass stirrer at room temp (keep for later use).
- (ix) Incubate slides with FITC-Avidin DCS at 1:200 and anti-sheep Cy<sup>5</sup> at 1:400 in PN-T buffer/0.5% block for 45 mins at room temp.

(x) Wash slides in PN-T buffer for 20 mins in large glass stirrer.

(xi) Dehydrate, as detailed in Section 2.2.5.5, Version I.

Following dehydration slides were mounted in 10 $\mu$ l of Vectashield anti-fade mountant H-1000 (Vector Labs) with propidium iodide (1:5000 dilution) and DAPI (1:2000 dilution) added as counterstains. Clean coverslips were then applied and sealed with clear nail varnish. Slides were stored in darkness at 4°C.

Analysis of slides was performed on a Bio-Rad MRC-600 laser scanning confocal microscope equipped with a krypton/argon ion laser. For FITC and PI, 488/568 nm line excitation and dual channel 522 and 585 nm emission filters were used. For Cy<sup>5</sup>, 647 nm line excitation and a 680 EF-32 emission filter were used. Image analysis was performed using Bio-Rad software.

## **2.2.9 Protein Analysis**

*Details of solutions used for the isolation of proteins are given in Section 2.1.5.5*

### **2.2.9.1 Preparation of Crude Nuclear Extracts**

(from van der Zee *et al.*, 1991)

Subconfluent flasks of cells were washed with approximately 10 mls of ice-cold phosphate buffered saline solution (PBS) and cells scraped off the base of the flask using a disposable cell scraper. This solution was centrifuged at 2500rpm for 10 minutes. The resulting cell pellet was resuspended in 200 $\mu$ l of nucleus buffer in a 1.5ml eppendorf tube and freeze-thawed twice in a dry ice/ethanol bath. One-tenth volume of 3.5M NaCl was then added to give a final concentration of 0.35M NaCl. The cell solution was vortexed briefly and incubated on ice for 1 hour, mixing after 30 mins. Cells were then spun at 15000 rpm for 20 mins at 4°C.

The resulting supernatant was removed and split three ways; (i) 20  $\mu$ l for protein estimation, (ii) 50 $\mu$ l for activity assays (diluted with an equal volume of 87% glycerol), (iii) remainder used for Western blotting (diluted with an equal volume of Western loading dye). Protein estimation was performed using Bio-Rad protein assay dye and doubling dilutions of the unknown extract. The standard curve was produced using 1mg/ml BSA

solution. Readings were taken using a Perkin Elmer Lambda 2 spectrophotometer.

### **2.2.9.2 Preparation of Whole Cell Extracts**

For adherent cell lines, cells were counted using a Coulter counter and seeded at a concentration of  $1 \times 10^5$  per well in 6-well plates and left at 37°C, 2% CO<sub>2</sub> for approximately 24 hours. Medium was then removed and cells were washed briefly with PBS before being lysed by the addition of 100µl of protein loading dye (with added protease inhibitors). Non-adherent cells were counted and diluted to a concentration of  $1 \times 10^5$  cells per ml. One ml aliquots of cells were then spun down (3000 rpm, 5 minutes), washed with PBS and resuspended in 100µl loading dye. Samples were stored at -20°C, unless used immediately.

### **2.2.10 Western Analysis (as shown in Keith *et al.*, 1993)**

*Details of solutions used in Western analysis are given in Section 2.1.5.5*

#### **2.2.10.1 Gel Running and Electroblothing**

Samples containing either 50µg of protein or  $1 \times 10^5$  cells were run using the Bio-Rad Protean II system on 8% or 15% non-denaturing gels in depending on the size of protein being analysed. Gels were run for 4-6 hours at 35-40mA, or at 10mA overnight.

Dot-blotting was also performed on a couple of occasions using a dot-blot manifold from BRL. For this technique, 50µg of protein was used in the first column from which seven doubling dilutions were made stepwise down the filter. Each sample was applied in triplicate to the dot-blot manifold.

Proteins were transferred to membranes using a Millipore semi-dry electroblotter. Millipore Immobilon-P membrane was used, which required pre-wetting in methanol, then water and finally transfer buffer before being used. Six sheets of 3MM Whatman filter paper were sandwiched between the anode and cathode of the blotter with the gel and filter layered in the middle. Transfer was performed at 200mA for 45 mins following which the gel was stained with Coomassie Brilliant Blue dye. The filter was rinsed in methanol, water and finally PBS-T before detection was performed.

### **2.2.10.2 Immunodetection**

All steps were carried out at room temperature unless otherwise stated. Filters were blocked at for at least 1 hour in 5% Marvel before application of any antibodies. All antibody dilutions were performed in this block solution. Filters were incubated with primary antibodies overnight on a rocking table at room temperature sealed in plastic files. Anti-topoisomerase II $\alpha$  antibody was used at 1:1000 dilution, anti-topoisomerase II $\beta$  at 1:50, anti-retinoic acid receptor alpha (RAR $\alpha$ ) antibody at 1:500 and anti-nm23H1/H2 antibody also used at 1:500. Blocking peptides for nm23H1/H2 and RAR $\alpha$  antibodies were used to try and prevent antigen binding. Four microlitres of RAR $\alpha$  primary antibody and 4 $\mu$ l of its' blocking peptide (Affinity Bioreagents) were incubated overnight at 4 $^{\circ}$ C in a 20 $\mu$ l volume and made up to 2 mls with 5% Marvel prior to use. For nm23H1/H2 blocking, 4 $\mu$ l of antibody was incubated with 2 $\mu$ l of blocking peptide (Cambridge Research Biochemicals) under the same conditions as for RAR $\alpha$ . These blocked primary antibodies were then incubated with filters in the same way as normal primary antibodies.

Following exposure to primary antibody, filters were rinsed briefly in PBS-T and then incubated with 10 mls of diluted secondary antibody, protein A-horseradish peroxidase (Amersham) for 30 mins. This antibody was used at 1:5000 dilution in 5% Marvel. Filters were then rinsed for 30 mins in PBS-T with the solution being changed every 5-10 mins.

Signal was detected by chemiluminescence using either Amersham ECL reagents or Boehringer Mannheim reagents (for detection of POD labelled antibodies). Protocols for detection were followed according to the manufacturers' instructions. Filters were exposed to ECL fluid for 1 minute, blotted on Whatman 3MM paper and wrapped in SaranWrap. Stratagene GloGos stickers were used to aid in sizing bands after autoradiography. Films were initially exposed for 1-5 mins with a second film being exposed for longer, as required.

### **2.2.10.3 Band Depletion Assay**

(adapted from Zwelling *et al.*, 1989)

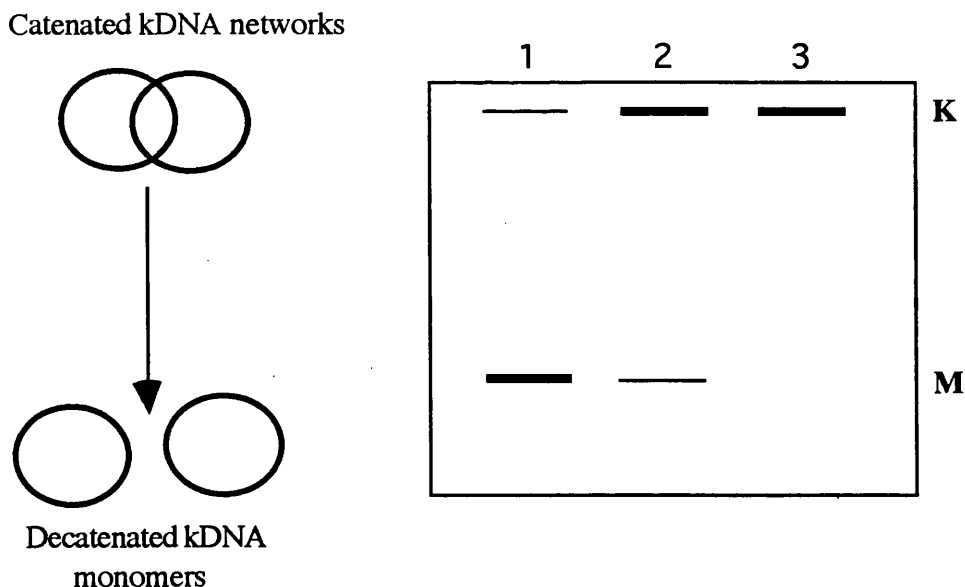
Cells from the three cell lines were seeded at a concentration of 10<sup>5</sup> cells per well in 6-well plates. Plates were allowed to grow in a 2% gassing incubator at 37 $^{\circ}$ C for 24 hours before being treated with VP-16. Concentrations of VP-16 used were 5 x 10<sup>-4</sup>M, 5 x 10<sup>-5</sup>M, 5 x 10<sup>-6</sup>M and 5 x

$10^{-7}M$  in growth medium. One well was kept untreated as a control. Cells were incubated with drug for 2 hours in the incubator following which the medium was removed, cells were washed briefly with PBS and then lysed with western loading buffer. Extracts were then loaded onto an 8% western gel and run and electroblotted as detailed in Section 2.2.10.1. Resultant filters were incubated with anti-topoisomerase II $\alpha$  antibody and horseradish peroxidase conjugated second antibody, as described previously. Detection of signal was achieved as described in Section 2.2.10.2. A more in-depth explanation of this technique will be given in Chapter 4.

## 2.2.11 Biochemical Assay for Topoisomerase II

*Details of solutions used in biochemical assays are given in Section 2.1.5.6*

This assay was performed according to manufacturer's instructions (TopoGEN Inc., Ohio). Activity of topoisomerase II is observed through the enzymes' ability to decatenate kinetoplast DNA (kDNA), as shown below.



Kinetoplast DNA is mitochondrial DNA from Crithidia fasciculata and consists of networks of 2.5kb rings catenated together. Topoisomerase II can monomerise these rings via its catalytic, ATP-dependent cycle of cleavage, strand passage and religation. The amount of topoisomerase II within a cell will therefore determine how much of the

kDNA is decatenated. When reactions are resolved on an agarose gel, the monomeric circles of DNA migrate much faster than catenated circles and therefore move further within the gel. Any remaining networks of kDNA stay in the wells as they are not able to migrate. Three situations may arise in this experiment, which are depicted above. Lane 1 indicates the result if an extract containing high topoisomerase II activity is used. Almost all of the kDNA (K) has been monomerised (M). Low activity of an extract is shown in lane 2, where most of the kDNA remains catenated. An extract containing no activity would give the result seen in lane 3.

The assay involves incubating a known amount of nuclear extract (see Section 2.2.9.1), in doubling dilutions from  $5\mu\text{g}$  down to  $0.0375\mu\text{g}$  of protein, with 300ng of kDNA in assay buffer (see Section 2.1.5.6). Samples are then incubated at  $37^\circ\text{C}$  for 30 mins, following which they are placed on ice and  $1/5$  volume of stop buffer/loading dye (see Section 2.1.5.6) is added. Activity was resolved in 1% agarose/TBE gels containing 0.05% ethidium bromide. TBE with 0.05% ethidium bromide was also used as the running buffer. Gels were run at 50-150 V until the dye front had moved approximately 5cm and then photographed using Type 55 film.

Inhibition of activity was performed using differing concentrations of VP16:  $5 \times 10^{-4}\text{M}$ ,  $5 \times 10^{-5}\text{M}$ ,  $5 \times 10^{-6}\text{M}$  and  $5 \times 10^{-7}\text{M}$ , incubated with samples. The drug was dissolved in DMSO with the final concentration of DMSO being 2%. This amount of DMSO was also added to no drug controls to ensure that it did not affect decatenation. Samples for inhibition assays were set up at room temperature and incubated with drug for 30 mins at  $37^\circ\text{C}$ .

## **2.2.12 Immunofluorescence** (as used in Coutts *et al.*, 1993)

*Details of solutions used in immunofluorescence are given in Section 2.1.5.7*

Cells were trypsinised from flasks and resuspended in fresh medium at a concentration of  $2 \times 10^5$  cells per ml. One ml of these diluted samples was then seeded per chamber of a Nunclon 4-well chamber slide. Slides were placed in a  $37^\circ\text{C}$ , 2%  $\text{CO}_2$  incubator overnight. Coverslips and chambers were removed prior to hybridisation with special care being taken to remove all silicon sealant from the slides (usually achieved with the aid of a scalpel). A number of slides were set up at once using L-DAN, CALU-3 and SK-MES-1, and those not used immediately in experiments were rinsed in PBS, air-dried, wrapped in Parafilm and frozen at  $-20^\circ\text{C}$ .

Remaining slides were also rinsed in PBS and then fixed for 1 minute in acetone/methanol (1:1). Blocking was performed in 3% BSA/PBST or 0.5% Boehringer Mannheim blocking reagent in PBST for 10 mins at room temperature, following which slides were washed briefly in PBST and incubated in primary antibody for 1-2 hours at 37°C in a humidified container.

Section 2.1.6 outlines all antibodies used in immunofluorescence and who they were supplied by. All primary antibodies were used at 1:50 dilution in block solution. The nucleolar control antibody obtained was part of a fluorescent ana test system kit from ImmunoConcepts, Sacramento and both primary, human anti-nucleoli and secondary anti-human-FITC antibodies came ready to use. Blocking peptides for topoisomerase II $\alpha$  and nm23H1/H2 antibodies were used to abolish antigen binding. For antibody blocking, 1 $\mu$ l of peptide was incubated with 1 $\mu$ l of primary antibody in a total volume of 10 $\mu$ l (8 $\mu$ l PBS) overnight at 4°C. The volume was made up to 50 $\mu$ l with blocking solution prior to use and used on one slide.

Following incubation with primary antibody, slides were washed in a large volume (approximately 400 mls) of PBST for 10 mins at room temperature. For detection of mouse monoclonal primary antibodies, anti-topoisomerase II $\beta$  and anti-ErbB2, a goat anti-mouse-FITC conjugated second antibody was used (Jackson Immunoresearch). For detection of rabbit polyclonal primary antibodies, anti-topoisomerase II $\alpha$  and anti-nm23H1/H2, a donkey anti-rabbit-FITC conjugated second antibody was used (Jackson Immunoresearch). For co-localisation studies using topoisomerase II $\beta$  and nucleolar control antibodies, the topoisomerase II $\beta$  antibody was detected with an anti-mouse-Cy5 conjugated second antibody. Slides were incubated with secondary antibodies at 1:100 dilution in blocking solution for 30 mins to 1 hour at room temperature. A final wash of 30 mins was performed in PBST as before and slides were then dehydrated and mounted as for FISH studies (Section 2.2.8.7), except slides were mounted under 22 x 32 cm coverslips. Slides were analysed as for FISH studies. In order to gain quantitative, comparative data, important when using blocked primary antibodies and normal antibodies in the same experiment, parameters used during image acquisition were set and remained unaltered during image collection by the scanning confocal microscope.

### **2.2.13 Flow Cytometry**

(adapted from Kaufmann *et al.*, 1991 and Prosperi *et al.*, 1992)

*Details of solutions used in FACS analysis are given in Section 2.1.5.8*

#### **2.2.13.1 Cell Cycle Analysis using Bromodeoxyuridine (BrdUrd) and Propidium Iodide (PI)**

Cells were seeded at around  $5 \times 10^5$  cells per flask, in duplicate for each cell line. Approximately 3 days after seeding, well before cells were confluent, the medium was removed from the flasks and replaced with fresh medium containing  $10\mu\text{M}$  freshly made BrdUrd. Cells were then incubated at  $37^\circ\text{C}$  for 4 hours to allow incorporation of the BrdUrd. Following this time the medium was removed and cells trypsinised as for normal tissue culture. The trypsin/cell solution was added to 5mls of medium and spun down at 1200rpm for 5 min. The cell pellet was fixed by the addition of 5ml ice-cold 70% ethanol while vortexing and kept at  $4^\circ\text{C}$  for at least 1 hour before continuing with the protocol to allow full penetration of the fixative. After this time, cells were washed twice in PBS, transferred to eppendorf tubes and each pellet resuspended in 1ml 2N HCl. Cells were left in acid for 30 mins at room temperature in order to partially denature the DNA. Centrifugation was then performed at 5000rpm for 5 min, the acid removed and each pellet resuspended in 1ml PBS. Cells were washed twice with this volume of PBS, once with PBT and then centrifuged as before. Each cell pellet was incubated with  $100\mu\text{l}$  of mouse anti-BrdUrd at 1:40 dilution in PBT for 1 hour at room temperature and then washed twice with PBT. Following these washes, cells were incubated with  $100\mu\text{l}$  of goat anti-mouse FITC at 1:40 dilution in PBT for 30 mins at room temperature. Samples were then washed once with PBT and once with PBS. It was at this point that a sample was dropped onto a clean glass slide, dried and mounted as for FISH analysis, to be examined under fluorescence microscopy. Remaining samples were stained with  $10\mu\text{g/ml}$  PI for 30 mins at room temperature or overnight at  $4^\circ\text{C}$ . Samples were centrifuged as described previously, resuspended in 0.5-1ml PBS depending on the cell number and analysed with a flow cytometer. Samples were stored in the dark at  $4^\circ\text{C}$ .

#### **2.2.13.2 FACS for Topoisomerase II $\alpha$**

Cells were trypsinised from  $75\text{ cm}^2$  flasks of subconfluent cells, fed the night prior to harvesting and pelleted at 2,500 rpm for 5 mins.

Cell pellets were then washed in PBS to remove any traces of medium and resuspended thoroughly in a small amount (100-200 $\mu$ l) of PBS. Five mls of 1:1 methanol/acetone was then added slowly to each sample and left at room temperature for 10-15 mins to ensure cells are infused with fixative. Cells were then spun as detailed above and the fixing and pelleting step repeated. All fix was removed from cell pellets using a P200 Gilson pipette and pellets resuspended in 1-2 mls of 0.5% Boehringer Mannheim blocking reagent in PBST. Cells were blocked at room temperature for 10 mins, spun down and resuspended in 50-100 $\mu$ l of primary antibody.

Three different topoisomerase II $\alpha$  antibodies were used, these being a rabbit polyclonal from Cambridge Research Biochemicals (CRB) and a rabbit polyclonal and a mouse monoclonal from TopoGEN. The CRB antibody was used at 1:100 dilution and the TopoGEN antibodies were used at 1:50 dilution. Cells were incubated with primary antibody for 1 hour at room temperature, following which they were spun down and washed twice with 3 mls of PBST. Secondary antibodies were used at 1:100 dilution with an anti-mouse-FITC antibody used for detection of the monoclonal topoisomerase II $\alpha$  antibody and anti-rabbit-FITC antibody used for detection of the polyclonal primary antibodies. One hundred microlitres of secondary antibody dilution was used per sample of cells and left for 1 hour at room temperature. Samples were again spun down and washed twice with PBST as before.

At this point, a drop of each sample was put on a clean glass slide, dried and mounted with anti-fade mountant, as for FISH samples. This enabled samples to be examined under the fluorescence microscope as well as by FACS. Following the final wash, cells were resuspended in 1 ml of PBS to which 10  $\mu$ l of a 10mg/ml propidium iodide was added. Cells were left to stain overnight at 4 $^{\circ}$ C and were then spun down and resuspended in approximately 500 $\mu$ l of PBS, depending on the number of cells per sample. FACS analysis was performed using a Coulter flow cytometer.

### **2.2.13.3 FACS for P-Glycoprotein and MRP**

CALU-3, CALU-3/10 $^{-5}$ M VP16, A2780, A2780/Adr, GLC $_4$  and GLC $_4$ /Adr were analysed by flow cytometry for P-glycoprotein and MRP status. Two different antibodies for P-glycoprotein were used, JSB-1 and MRK-16, as shown in Section 2.1.6 (kindly provided by Dr. Fiona Scott, MRC, Edinburgh). All antibodies were diluted to required strength in PBS with 3% BSA and 0.05% sodium azide. JSB-1 was used at 1 $\mu$ g/ml and MRK-16 was used at 0.2 $\mu$ g/ml. Three different dilutions of polyclonal anti-MRP

serum (kindly provided by Professor Melvin Center) were used, 1:5, 1:25 and 1:50. Cells were used in  $1 \times 10^7$  aliquots, obtained from trypsinised flasks. Samples of cells used for MRK-16 incubation were not fixed since this antibody recognises an external epitope of P-glycoprotein.

Cells were pelleted at 1500 rpm for 5 min at 4°C and then fixed in 70% ethanol in PBS at 4°C, if required. Samples were then washed twice in PBS at 4°C and incubated with 20µl of rabbit or goat serum for monoclonal or polyclonal primary antibodies respectively. Serum was incubated with cells for 10 mins at 4°C, following which samples were spun at 1500 rpm for 5 mins and serum removed. Cell pellets were then resuspended in 25µl of primary antibody and left on ice for 30 mins. Samples were then spun as before and washed three times in PBS/BSA/sodium azide. Following the final wash, the cell pellet was resuspended in 50µl of the appropriate secondary antibody and again incubated for 30 mins on ice. Cells were then washed for a further three times in PBS/BSA/sodium azide and finally resuspended in 500µl of PBS/BSA/sodium azide solution with 1mg/ml propidium iodide.

Samples were analysed on a Becton-Dickinson FACScan machine using Hewlett Packard software. Data was acquired using Consort 30 and analysed using LYSYS.

## CHAPTER 3

# CHARACTERISATION OF A 17q AMPLICON IN THE NON-SMALL CELL LUNG ADENOCARCINOMA CELL LINE, CALU-3

### 3.1 Introduction

From previous work on the non-small cell lung adenocarcinoma cell line, CALU-3 it is known that this cell line has amplification of ERBB2 and TOPO II $\alpha$  genes (Keith *et al.*, 1992). The ERBB2 gene has been found to be amplified in a variety of human adenocarcinomas including breast (Slamon *et al.*, 1987; van de Vijver *et al.*, 1987; Varley *et al.*, 1987), ovarian (Berchuck *et al.*, 1990; Slamon *et al.*, 1989; Zheng *et al.*, 1991) stomach (Park *et al.*, 1989) and lung (Kern *et al.*, 1990; Schneider *et al.*, 1989; Shi *et al.*, 1992). ERBB2 amplification and overexpression has also been associated with tumour development and poor prognosis in breast cancer (Gullick *et al.*, 1991; Lovekin *et al.*, 1991; Muss *et al.*, 1994; Slamon *et al.*, 1989; Winstanley *et al.*, 1991; Wright *et al.*, 1992). Cases of ERBB2 and TOPO II $\alpha$  co-amplification have previously been described in breast tumours (Keith *et al.*, 1993; Murphy *et al.*, in press; Smith *et al.*, 1993). This co-amplification is thought to arise because the two genes are situated in close proximity on chromosome 17q, both having been mapped previously to 17q21-22 (Fukushige *et al.*, 1986; Tan *et al.*, 1992; Tsai-Plugfelder *et al.*, 1988). Therefore, the situation of TOPO II $\alpha$  and ERBB2 co-amplification observed in CALU-3 appears to mimic that seen in a certain subset of breast tumours.

The co-amplification of ERBB2 and TOPO II $\alpha$  genes is also of interest from a clinical point of view since cell lines found to have this co-amplification appear to be more sensitive to topoisomerase II inhibitors than those lacking TOPO II $\alpha$  amplification (Keith *et al.*, 1993; Smith *et al.*, 1993). This could lead one to postulate that those tumours which have ERBB2 and TOPO II $\alpha$  co-amplification may be more sensitive to treatment with topoisomerase II inhibiting agents. The CALU-3 cell line has also been found to be very sensitive to the topoisomerase II targeting agents VP16 and doxorubicin (Merry *et al.*, 1987) and so may be a viable model for the study of changes around chromosome 17q which occur in breast cancer. There are a number of interesting genes on 17q including NF1, G-CSF, NM23H1, RAR $\alpha$

and PKC $\alpha$  as well as the BRCA1, familial breast cancer gene region. Thus, the aim of the work presented in this chapter was to further characterise the 17q amplicon in CALU-3 by investigating whether any of the above genes were also co-amplified.

Initial studies were performed using cDNA probes for the various genes in Southern blotting of CALU-3, L-DAN and SK-MES-1 DNA. Using this technique, the intensity of bands detected on an autoradiograph is indicative of the gene copy number of the probe used. However, Southern blotting does not provide any information on the chromosomal localisation of gene copies. In order to find out more structural information on the 17q amplicon in CALU-3, fluorescence *in situ* hybridisation (FISH) was performed. Using this technique, whole chromosomes, chromosome-specific centromeres and single-copy genes can be detected, as depicted in Figure 3A. Chromosome painting (Carter, 1994; Lichter *et al.*, 1988) was used with a flow-sorted chromosome 17 paint to specifically detect chromosome 17 sequences in metaphase spreads from L-DAN, CALU-3 and SK-MES-1. This particular kind of probe is extremely useful for detecting gross abnormalities of chromosomes, such as translocations. As shown in Figure 3A, chromosome-specific centromere probes are also available, or can readily be synthesised using PCR from alpha satellite arrays present at chromosome centromeres (Willard, 1990; Haaf & Willard, 1992). Such centromere probes are useful in checking that single-gene probes are hybridising to the correct chromosomes. Multiple single gene probes can also be used in the same hybridisation (Heppell-Parton *et al.*, 1994; Inazawa *et al.*, 1994). This is particularly useful for investigating possible co-localisation of genes on a chromosome and also for ordering of gene probes.

All FISH experiments performed in this chapter utilised chromosomes isolated from either normal lymphocytes or the three non-small cell lung cancer cell lines, L-DAN, CALU-3 or SK-MES-1, but FISH can also be performed on frozen or paraffin sections of tissue (Murphy *et al.*, in press) and in isolated interphase nuclei (Arnoldus *et al.*, 1991; Bar-Am *et al.*, 1992; Devilee *et al.*, 1988; Kallioniemi *et al.*, 1992b). Whatever the target material is, the basic methodology for FISH is the same. This is outlined in Figure 3B, using chromosomes as the target material. In this technique, chromosomes are isolated from cells by treatment of the cells with colcemid. This drug blocks cells at the metaphase stage of the cell cycle by interfering with spindle formation. Cells are then swollen with a hypotonic solution and fixed. Drops of the fixed cell suspension are dropped from a height onto clean glass slides.

## **Figure 3A**

### **General uses of fluorescence *in situ* hybridisation (FISH)**

This figure depicts the different chromosomal regions which can be detected using FISH and the uses of the different probes.

Black areas indicate normal, unhybridised chromosome sequence. Red or blue areas indicate hybridisation of probe.

Whole chromosome paints will hybridise to sequences along the entire length of a particular chromosome. These probes are extremely useful for analysis of chromosomal translocations.

Centromere probes that are specific for individual chromosomes are also available and can be used to ensure that a single-copy gene probe is hybridising to the correct chromosome.

Cosmids carrying sequences from single copy genes can be used to check actual gene copy number. Multiple single-copy gene cosmids can be used in hybridisations, provided different fluorochromes are used for their detection. This technique is useful when studying the co-localisation and order of genes.



Whole Chromosome  
Paint



Centromere  
Specific Probe



Chromosome  
Translocations



Single  
Gene  
Probe



Check Location of  
Gene Probe



Multiple Gene  
Probes



## **Figure 3B**

### **Basic methodology for FISH**

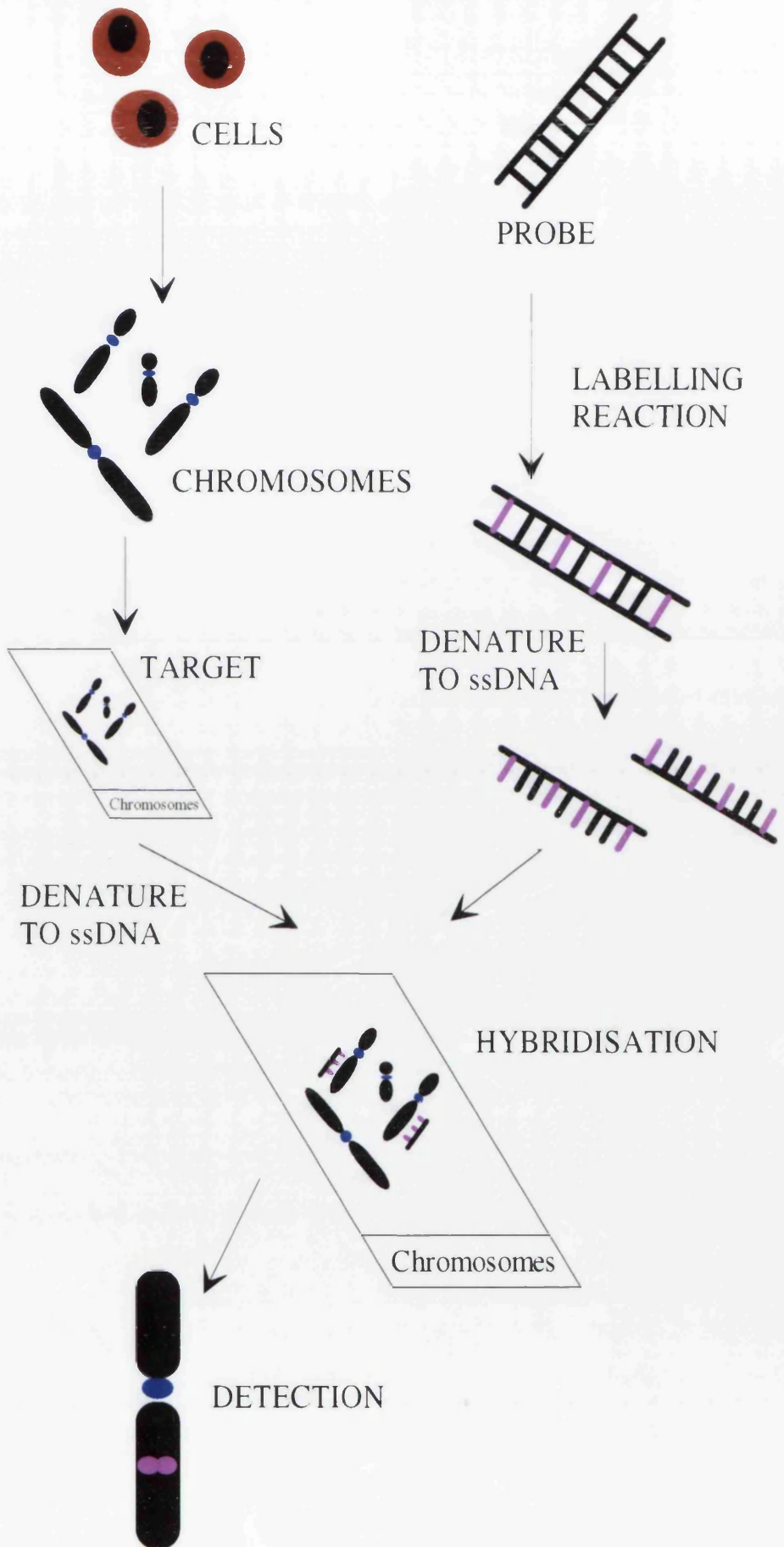
This figure depicts the basic protocol for FISH experiments using chromosomes as the target material.

Cells are treated in culture with colcemid which interferes with the spindle production during mitosis and thus traps cells at metaphase. Hypotonic treatment of these cells causes them to swell at which point cells are fixed in a mixture of methanol and acetic acid. When cells are then dropped onto clean glass slides, they burst and release the chromosomes to which probes can then be hybridised. Slides are then subjected to a further fixation step, RNase treatment (to digest any RNA present) and mild protease treatment, which aids probe penetration of the DNA. A short post-fixation step is then performed following which slides are treated with hot 70% formamide which denatures the dsDNA to ssDNA.

The required gene probe is labelled with either biotin or digoxigenin (DIG), achieved through a nick translation reaction using biotin or digoxigenin-conjugated nucleotide <sup>triphosphates</sup>. The probe is also denatured by heat treatment prior to hybridisation.

The denatured probe is then applied to the denatured chromosomes and incubated overnight at 37°C in a humidified chamber. Following this, numerous washes are performed to remove unhybridised probe and the probe can then either be detected using antibodies (in the case of DIG probes or biotin probes) or cycles of avidin-FITC/anti-biotin detection (only for biotin probes). Various different fluorochromes can be conjugated to the second antibody such as FITC, Texas Red or Cy<sup>5</sup>.

Samples are then analysed by confocal laser scanning microscopy.



The force of the cells hitting the slide causes them to burst thus the chromosomes are released from the nucleus. Once slides have been prepared they are fixed again, treated with RNase to digest any RNA which may cause background in the hybridisation and given a mild protease treatment. Following another fixation step the samples are denatured in hot 70% formamide solution. This treatment causes the dissociation of dsDNA to form ssDNA. The probe which is to be used in the hybridisation is labelled with a hapten, usually either biotin or digoxigenin. This is achieved by nick translation of the probe with biotin- or digoxigenin-conjugated nucleotides. Human CotI DNA is usually added to single-copy gene probes in order to compete out any repetitive DNA sequences which may be present (Lichter *et al.*, 1988). Labelled probe is resuspended in a formamide-based hybridisation solution. This solution can be made more or less stringent for probe binding depending on the concentration of formamide used (usually 50% for single-copy gene probes and 70% for repetitive sequence probes). Denaturation of the probe is then carried out, followed by a period of incubation at 37°C to allow reannealing of the repetitive sequences. Hybridisation of probe and sample is performed overnight at 37°C in a humidified chamber.

Probe detection can be achieved using antibodies, or biotin/avidin reactions with secondary antibody or avidin being conjugated to a fluorochrome. Multiple fluorochromes are required if more than one probe is used. Commonly used fluorochromes are fluorescein isothiocyanate (FITC), which produces green fluorescence, and Texas Red and Cy<sup>5</sup> which both produce red fluorescence. Once detected, samples can be analysed using conventional fluorescence microscopy or a laser scanning confocal microscope. Analysis by confocal microscopy enables use of fluorochromes which are not excited by ultra-violet light, such as Cy<sup>5</sup>.

As well as characterisation of genes involved in the 17q amplicon in CALU-3, the process of amplification is also of interest in this study. As mentioned in Chapter 1, amplification of genes is one mechanism whereby cells can override the growth restraints which are normally imposed on them. Thus the mechanism by which this amplification occurs is also extremely important. FISH analysis can be extremely informative in this respect since the location of genes are visualised on the chromosomes, and this technique has been used to previously to investigate mechanisms of amplification (Smith *et al.*, 1990; Trask & Hamlin, 1989; Windle *et al.*, 1991). Amplified DNA can be visualised either as extended chromosomal regions (ECRs), also referred to as homogeneously staining regions (HSRs), or as extrachromosomal elements, such as episomes or double minutes (DMs).

Double minutes are small, paired circular DNA molecules which lack centromeres. Replication of double minutes, initiated from replication origins (Carroll *et al.*, 1993), has been found to occur at approximately the same time as that of the corresponding sequences in the genome (Carroll *et al.*, 1991).

Double minutes carrying the c-MYC oncogene have been found in cases of acute myeloid leukaemia (Slovak *et al.*, 1994) and the P-glycoprotein encoding gene, MDR1, has also been localised to DMs in colchicine-selected cells (Schoenlein *et al.*, 1992). It is thought that double minutes are formed via deletion of gene sequences from chromosomes (Hahn, 1993; Wintersberger, 1994). Although DMs appear to be stable once formed, integration of DMs into chromosomes (to form HSRs) has been observed (Carroll *et al.*, 1988) and it has been proposed that double minutes are the precursors to HSRs in cells (Wahl, 1989). More details concerning characterisation and importance of DMs in gene amplification can be found in the recent review by (Hahn, 1993).

Homogeneously staining regions are a common source of amplified genes in mammalian cells. Analyses of such HSRs has been performed on drug-resistant rodent, and particularly hamster, cell lines since it has been discovered that certain genes become amplified on exposure to particular drugs (Flintoff *et al.*, 1984; Hyrien *et al.*, 1988; Kaufman & Schimke, 1981; Smith *et al.*, 1990; Trask & Hamlin, 1989). Chinese hamster ovary (CHO) cell lines appear to be particularly amenable to such gene amplification. When CHO cells are exposed to increasing concentrations of methotrexate (MTX), they become resistant to this drug via over-production of the enzyme dihydrofolate reductase (DHFR), which is the target of MTX. Therefore, the excess enzyme in the cell neutralises the MTX whilst enough DHFR is present to continue its normal role in the cell. Chinese hamster cells over-producing adenylate deaminase (AMPD) have also been isolated following exposure of the cells to cofomycin, an inhibitor of AMPD (Debatisse *et al.*, 1986; Hyrien *et al.*, 1988). These cells were found to possess 150 copies of an amplicon containing the gene for AMPD. Another model system utilised is that of amplification of the carbamoyl-P synthetase, aspartate transcarbamylase, dihydro-orotase (CAD) gene in Syrian hamster cells (Smith *et al.*, 1990; Smith *et al.*, 1992) which can be induced by exposure to the inhibitor N-phosphonoacetyl-L-aspartate (PALA). The CAD gene encodes a tri-functional protein involved in UMP biosynthesis. In the Syrian hamster cells, the amplified CAD genes are found in multiple copies of large regions of DNA, with each of these regions being tens of megabases in length.

The fact that the systems outlined above can be manipulated *in vitro* to produce these extended chromosomal regions means that they are also extremely useful for investigating mechanisms of DNA amplification. Many different models for mechanisms of gene amplification have been proposed recently reviewed in (Stark, 1993; Wintersberger, 1994). These proposed mechanisms can be divided into two groups based on the initial cause of the amplification, these being either over-replication from a replication origin or recombination between sister chromatids or chromosome homologues.

The earliest model proposed for gene amplification was the "onion-skin" model, depicted in Figure 3C. This mechanism was initially proposed to account for SV40 virus excision in transformed cells (Botchan *et al.*, 1979) but had also been extended to account for amplification in mammalian cells (Roberts *et al.*, 1983; Varshavsky, 1981; Schimke *et al.*, 1986). The mechanism proposes that a replication origin is initiated more than once per cell cycle. This causes "runaway" replication of the replicon resulting in the layered effect of replication bubbles, similar to the layers of an onion skin, hence the name. This final structure is thought to be very unstable and can break down to produce numerous structures including episomes and DNA duplexes containing amplified DNA sequences (Stark *et al.*, 1989). However, later experiments on gene amplification in mammalian cells attempting to repeat data already published implied that this mechanism may not be the basis for the genetic changes seen with gene amplification (Hahn *et al.*, 1986). It is now thought that this mechanism does not play a major role in the amplification of mammalian genes. This onion-skin model is used to explain amplification of developmentally regulated genes in *Drosophila* and *Sciara* (Delidakis & Kafatos, 1989; Kafatos *et al.*, 1985; Liang *et al.*, 1993).

Mechanisms of gene amplification in mammalian cells have been analysed mainly using the numerous hamster cell line models outlined previously. The mechanism of formation of an amplicon can only really be deduced, however, from the early stages of amplification (Ma *et al.*, 1993; Smith *et al.*, 1990; Trask & Hamlin, 1989; Windle *et al.*, 1991) since further amplification may be caused by additional mechanisms only permitted because of the resulting DNA structure after the initial genetic change. The four papers referred to above all conclude that the genetic changes observed in early gene amplification are most likely due to unequal sister chromatid exchange and subsequent bridge/breakage/fusion cycles. This mechanism for gene amplification is shown in Figure 3D (adapted from Wintersberger, 1994). This figure shows the possible pathways leading to gene amplification starting with a normal chromosome. The normal chromosome is shown with

### **Figure 3C**

#### **"Onion-skin" model for gene amplification by over-replication**

(adapted from Stark *et al.*, 1989)

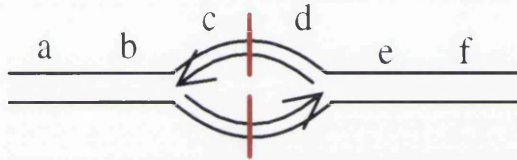
This figure shows one of the first models proposed for gene amplification.

The red lines show origins of replication and the arrowed lines represent replication forks moving in the direction of the arrowhead.

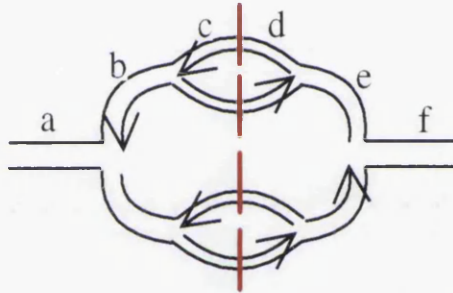
The model begins with normal replication proceeding from a replication origin. This produces a bubble of DNA consisting of the two parental strands and two newly replicated, daughter strands. Some obstruction in replication then occurs which prevents this structure from being resolved and causes the replication origin to fire again, resulting in the replication of the daughter strands. This cycle could be repeated many times, thus forming layers of partially replicated DNA duplexes. This structure is extremely unstable and could resolve by intra- or inter-duplex DNA recombination to produce episomes or large arrays of amplified genes, respectively.



REPLICATION



UNSCHEDULED REPLICATION



UNSCHEDULED REPLICATION

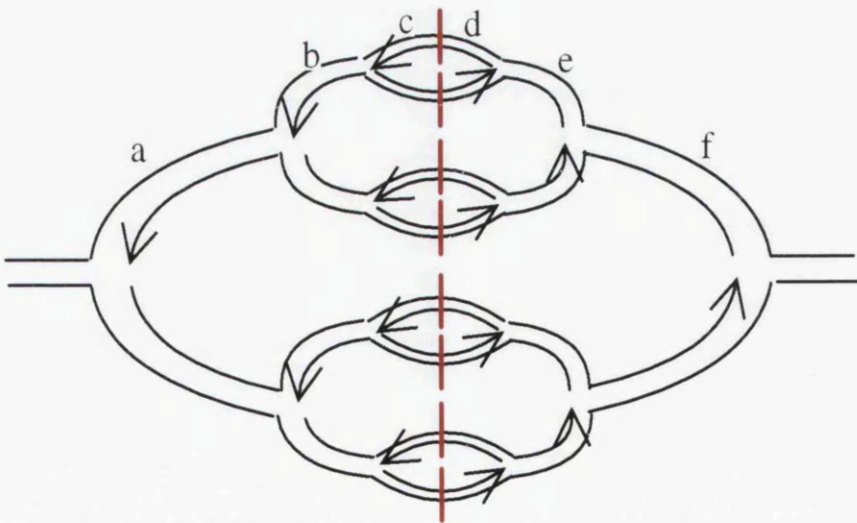


## **Figure 3D**

### **Sister chromatid exchange and bridge/breakage/fusion model of gene amplification**

(adapted from Wintersberger, 1994)

This figure shows the most popular proposed model for mammalian gene amplification.

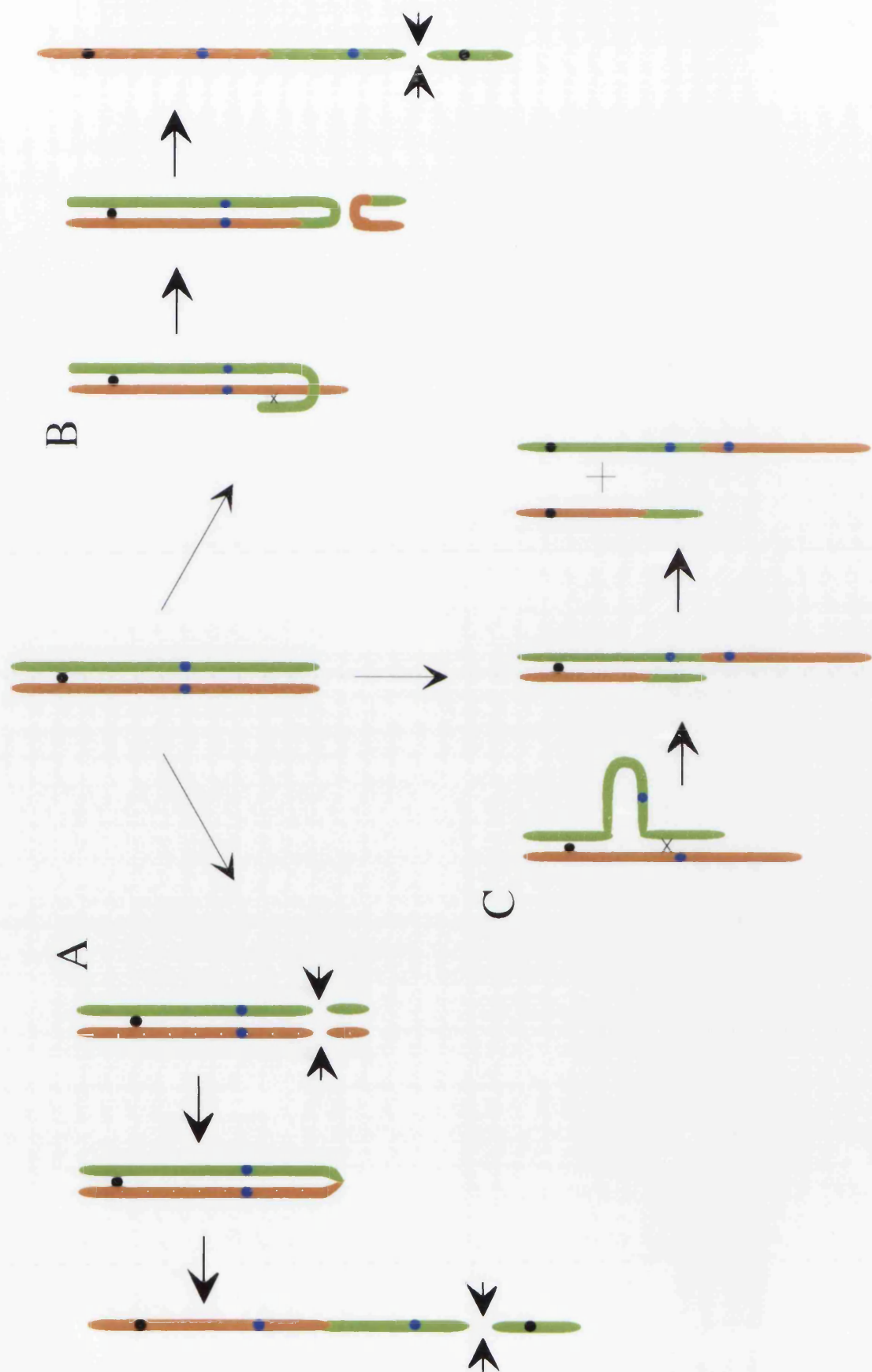
The model begins with a normal chromosome depicted as having orange and green sister chromatids, for ease of distinction of chromatids. The black circle represents a centromere and the blue circle represents the gene to be amplified.

There are three possible pathways which this chromosome can follow in order to produce gene amplification:

Pathway A is a simple telomere breakage-fusion model where a break occurs by the telomere region of each sister chromatid. This creates frayed chromosome ends which are healed by sister chromatid fusion. A dicentric chromosome is thus produced which breaks during the next round of DNA replication to produce one chromosome with two copies of the gene and one lacking any copies.

Pathway B also results in the formation of a dicentric chromosome, but in this pathway it is formed by unequal sister chromatid exchange occurring between the gene and the telomere followed by DNA breakage. An acentric chromosomal fragment is also formed which will probably be lost during the following round of DNA replication.

Pathway C results in the formation of two monocentric chromosomes via unequal sister chromatid exchange occurring above the gene in one chromatid and below the gene in the other. Therefore, one chromosome carries both copies of the gene and the other lacks any copies.



orange and green sister chromatids (for ease of distinction of chromatids), the blue circle is the gene to be amplified and the black circle is the centromere. In pathway A, frayed telomeres are created, presumably by incorrect DNA replication or repair causing DNA breakage, and the sister chromatids then fuse at the free ends. This process creates a dicentric chromosome which will break at the next round of replication to produce one chromosome with two copies of the gene and a chromosome fragment, which retains a centromere. Both of these molecules will only have one intact telomere, thus the cycle of bridge/fusion and breakage could continue into the next round of replication. Pathway B results in the same dicentric chromosome as pathway A, but this arises through unequal sister chromatid exchange rather than telomere loss. Pathway C again shows a method involving non-homologous recombination, but the end results of this exchange are two monocentric chromosomes, one of which lacks the gene in question and one of which has both copies.

Abnormalities of telomeres have been observed in a variety of different tumour types, such as renal (Holzmann *et al.*, 1993; Mehle *et al.*, 1994), brain (Sawyer *et al.*, 1993), melanoma (Melzter *et al.*, 1993) and colorectal (Hastie *et al.*, 1990). The most common abnormality appears to involve shortening of the telomere which makes the telomere unstable and creates a "sticky" end to which other chromosomes may associate. It has also been shown using Chinese hamster ovary cells that telomeric DNA sequences are more likely to break following exposure to ionising radiation than any other part of the total genome (Alvarez *et al.*, 1993). This evidence lends more weight to the suggested telomere-breakage model of gene amplification previously proposed. Indeed, when the early steps of gene amplification are studied, chromosomal changes which could be explained by the unequal sister chromatid exchange and bridge/breakage/fusion model are found (Ma *et al.*, 1993; Smith *et al.*, 1990; Smith *et al.*, 1992; Toledo *et al.*, 1992; Trask & Hamlin, 1989; Windle *et al.*, 1991). The general chromosomal changes observed in all the above studies include the formation of dicentric chromosomes and the discovery that the original copy of the gene appears to remain associated with the amplified region. Also, inverted duplication of sequences is commonly observed which would be indicative of telomeric fusion of sister chromatids.

The work presented in this chapter uses various methods of genetic analysis to further characterise the chromosome 17q amplicon found in the NSCLC cell line CALU-3. Initial detection of amplified genes from chromosome 17 was achieved using Southern analysis. More detailed genetic

analysis has been performed using the technique of fluorescence *in situ* hybridisation.

## **3.2 Results**

In this chapter, genetic changes to chromosome 17 have been analysed by Southern blot hybridisation and fluorescence *in situ* hybridisation (FISH) in the three non-small cell lung cancer cell lines L-DAN, CALU-3 and SK-MES-1. Previous work by Keith *et al.* has shown CALU-3 to have amplified TOPO II $\alpha$  and ERBB2 genes (Keith *et al.*, 1992). The results shown here demonstrate the use of other gene probes from the 17q region, as well as those for ERBB2 and TOPO II $\alpha$  genes, in a more detailed study of the chromosome 17 amplicon in CALU-3. L-DAN and SK-MES-1 were included as examples of NSCLC cell lines which show no evidence of amplification of chromosome 17q.

### **Characterisation of the 17q Amplicon by Southern Analysis**

Southern blot hybridisation was performed using DNA isolated from CALU-3, L-DAN and SK-MES-1 in order to detect amplified gene sequences from the long arm of chromosome 17. Figures 3.1 and 3.2 show the results of Southern analysis of L-DAN, CALU-3 and SK-MES-1 with a number of different probes from genes on 17q. Figure 3.1 shows the same Southern filter re-probed with 4 different 17q gene probes (TOPO II $\alpha$ , ERBB2, RAR $\alpha$  and NM23H1). An immunoglobulin probe from chromosome 14, pHJi, was also used to assess samples. From the results of the pHJi probing, all the lanes appear to be relatively equal in signal and are therefore equally loaded. Thus the amplified signal seen in the CALU-3 lanes (1, 4, 7 and 10) in those panels showing results of TOPO II $\alpha$ , ERBB2 and RAR $\alpha$  gene probings is not due to overloading of CALU-3 DNA. The amplification of TOPO II $\alpha$  and ERBB2 seen in CALU-3 in Figure 3.1 also agrees with the results previously obtained by Keith *et al.*, as mentioned above. From the NM23H1 probed filter it can be seen that there does not appear to be amplification of this gene in any of the three cell lines. Figure 3.2, panel (a) demonstrates that there is also low level amplification of the G-CSF gene in CALU-3 (lanes 1, 4, 7, 10, 13 and 16). Panel (b) shows pHJi probing of the same filter from panel (a). It can therefore be seen that the CALU-3 lanes are not overloaded, thus the amplification seen in panel (a) is genuine. Panels (c) and (d) in Figure 3.2 show the results of PKC $\alpha$  and pHJi probing of a filter with CALU-3 DNA present in lanes 3, 6, 9 and 12. Panel (d) shows that there is equal DNA loading of the samples. Therefore, as seen in the NM23H1

### **Figure 3.1**

#### **Southern blot analysis of L-DAN, CALU-3 and SK-MES-1.**

The same blot was probed with SP1 (TOPO II $\alpha$ ), pCer204 (ERBB2), p63 (RAR $\alpha$ ), nm23H1 (NM23H1)

The pHJi probe was used as a loading control

Marker sizes in kilobases are shown on the right of each panel

**Lanes 1, 4, 7 & 10: CALU-3 , Lanes 2, 5, 8 & 11: L-DAN,  
Lanes 3, 6, 9 & 12: SK-MES-1**

DNA loaded in lanes 1-3 was digested with *TaqI*

DNA loaded in lanes 4-6 was digested with *EcoRI*

DNA loaded in lanes 7-9 was digested with *PstI*

DNA loaded in lanes 10-12 was digested with *BamHI*

In the panels which show the results of TOPO II $\alpha$ , ERBB2 and RAR $\alpha$  probings, a more intense signal can be seen in the CALU-3 lanes (1,4,7 and 10) than in the L-DAN or SK-MES-1 lanes.

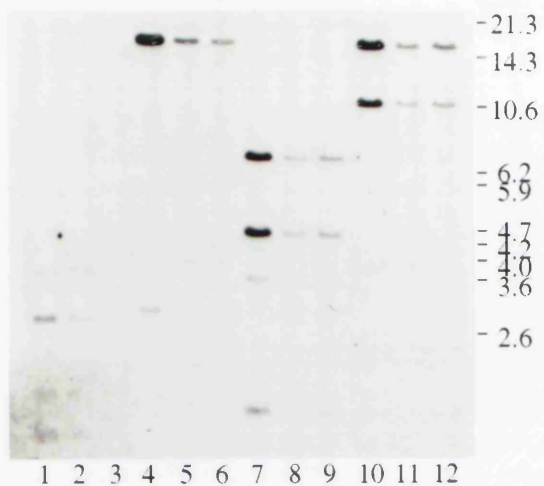
The signal observed in the NM23H1-probed blot is very similar between all the samples.

DNA loading is almost equal between the samples, as can be seen from the pHJi-probed blot.

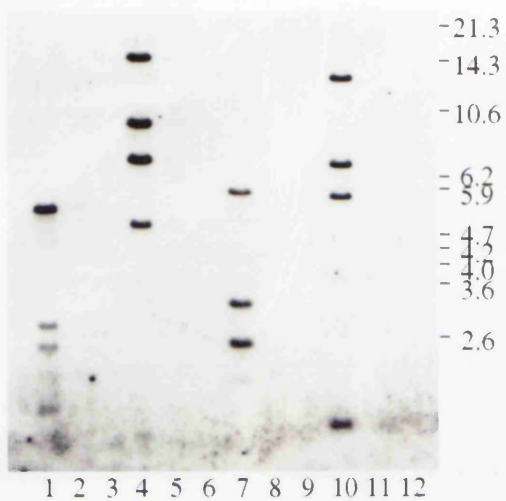
Therefore, by Southern blotting the CALU-3 cell line appears to have amplification of TOPO II $\alpha$ , ERBB2 and RAR $\alpha$  genes. The NM23H1 gene is not amplified in CALU-3.

No differences are observed in digest patterns between L-DAN, CALU-3 and SK-MES-1, thus there do not appear to be any rearrangements within those genes amplified in CALU-3.

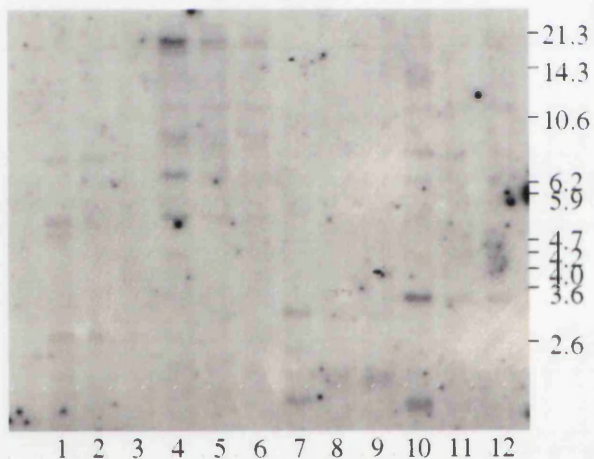
### TOPO II $\alpha$



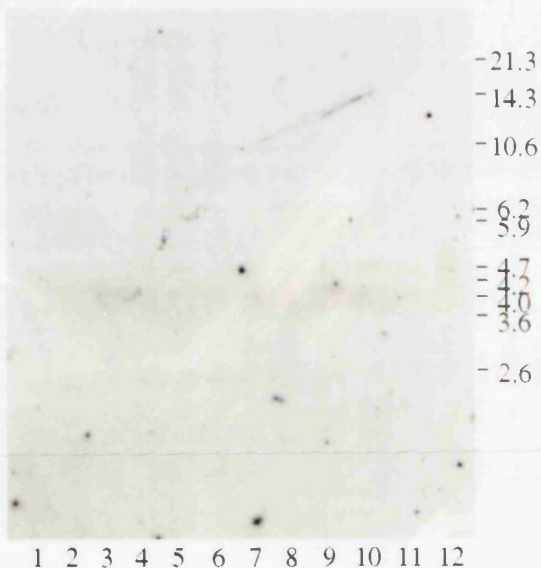
### ERBB2



### RAR $\alpha$



### NM23H1



### pHJi

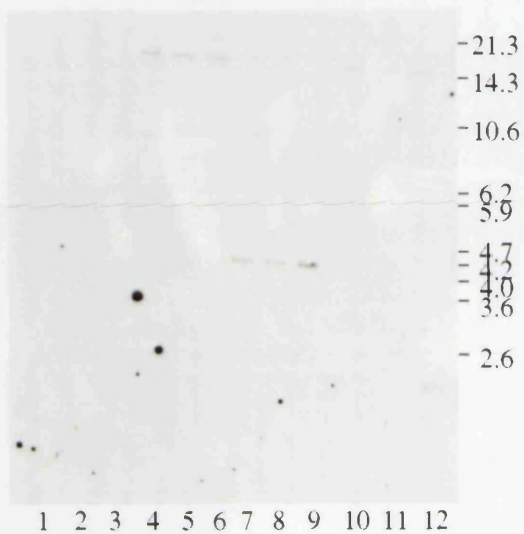


## **Figure 3.2**

### **Further Southern blot analysis of L-DAN, CALU-3 and SK-MES-1.**

Panels (a) & (b) show the same blot probed with G-CSF and pHJi probes,  
respectively

**Lanes 1, 4, 7, 10, 13 & 16: CALU-3, Lanes 2, 5, 8, 11, 14 & 17: L-DAN**

**Lanes 3, 6, 9, 12, 15 & 18: SK-MES-1**

DNA loaded in lanes 1-3 was digested with *XmnI*

DNA loaded in lanes 4-6 was digested with *PstI*

DNA loaded in lanes 7-9 was digested with *TaqI*

DNA loaded in lanes 10-12 was digested with *BglII*

DNA loaded in lanes 13-15 was digested with *BamHI*

DNA loaded in lanes 16-18 was digested with *EcoRI*

Panels (c) & (d) show the same blot probed with PKC $\alpha$  and pHJi probes,  
respectively

**Lanes 1, 4, 7, & 10: SK-MES-1, Lanes 2, 5, 8, & 11: L-DAN**

**Lanes 3, 6, 9 & 12: CALU-3**

DNA loaded in lanes 1-3 was digested with *TaqI*

DNA loaded in lanes 4-6 was digested with *EcoRI*

DNA loaded in lanes 7-9 was digested with *PstI*

DNA loaded in lanes 10-12 was digested with *BamHI*

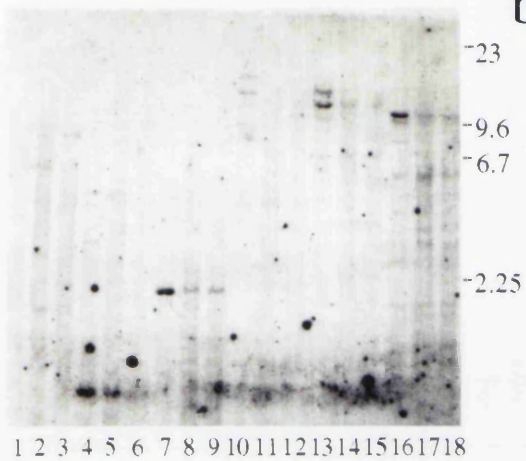
pHJi was used as a loading control

Marker sizes are shown in kilobases on the right of each panel

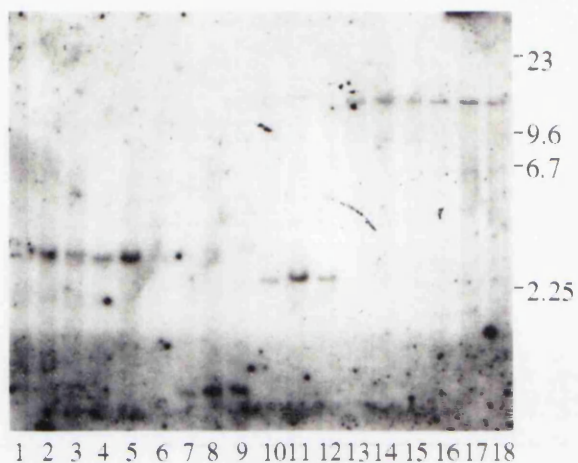
In panel (a), which shows the result of G-CSF gene probing, the strongest signal is observed in lanes containing CALU-3 DNA. DNA loading is fairly consistent between L-DAN, CALU-3 and SK-MES-1, as can be seen from panel (b). Therefore, CALU-3 also appears to have amplification of the G-CSF gene.

Panel (c) shows the result of PKC $\alpha$  gene probing. The strongest signals on this filter appears to be in the lanes containing SK-MES-1 DNA. From panel (d) these lanes are also found to have the highest DNA loading. Therefore, the PKC $\alpha$  gene is not amplified in CALU-3.

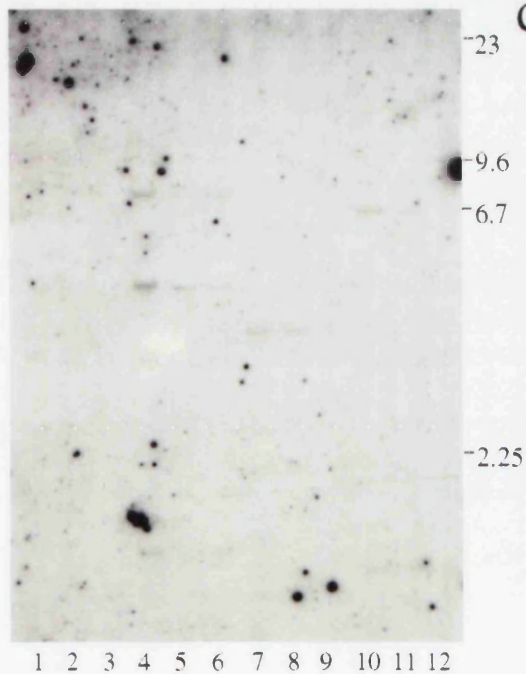
a



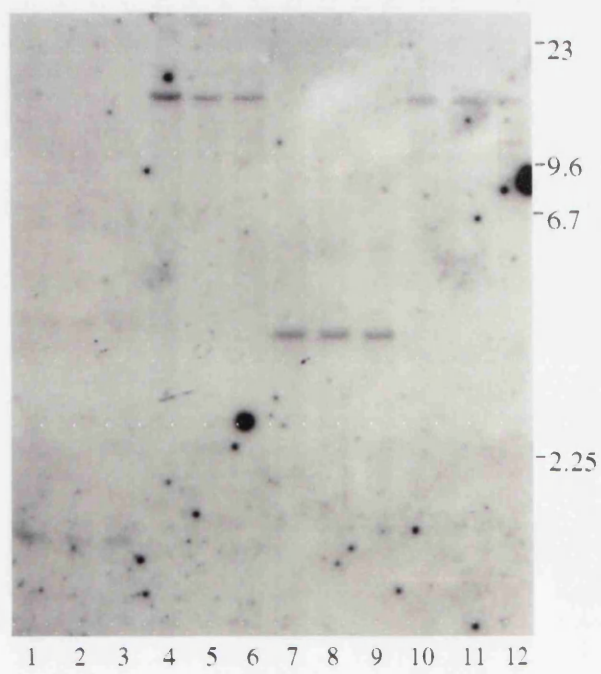
b



c



d



probed blot in Figure 3.1 there does not appear to be any amplification of this gene in CALU-3, L-DAN or SK-MES-1. Various enzyme digests were performed on the samples in order to detect any possible rearrangement of the genes to be analysed. However, no differences in banding patterns were observed between CALU-3, L-DAN and SK-MES-1, thus none of the genes analysed appear to be rearranged in CALU-3.

Thus, in CALU-3 an amplicon exists which contains the TOPO II $\alpha$ , ERBB2, RAR $\alpha$  and G-CSF genes, as detected by Southern analysis. The NM23H1 and PKC $\alpha$  genes are outside this region of amplification in CALU-3. None of the genes analysed in this section by Southern blot analysis are amplified in L-DAN or SK-MES-1.

### **Isolation of Cosmid Probes for NM23H1, RAR $\alpha$ , TOPO II $\alpha$ and NF1**

Cosmid probes for genes on 17q were required for fluorescence *in situ* hybridisation (FISH) studies. Cosmid probes for NM23H1, RAR $\alpha$ , TOPO II $\alpha$  and NF1 were all obtained from the Imperial Cancer Research Fund Reference Library-DataBase (ICRF RLDB) (Lehrach, 1990). The retinoic acid receptor alpha cosmids (digests of which are shown in Figure 3.3) were obtained through screening of chromosome 17 library filters with both  $\alpha$ -32P-dCTP-labelled oligos from the RAR $\alpha$  gene and the p63 RAR $\alpha$  plasmid probe used in Southern analysis. Positive clones were identified, co-ordinates calculated and these co-ordinates sent back to the ICRF RLDB. Agar stabs of positive clones were then received and the cosmids isolated as outlined in Section 2.2.8.4. Cosmids for NM23H1, TOPO II $\alpha$  and NF1 genes were also requested from the ICRF RLDB.

Panel (a) in Figure 3.3 shows an ethidium bromide stained Southern gel on which digested DNA of TOPO II $\alpha$ , RAR $\alpha$  and NM23H1 cosmids has been run. Panel (b) shows the autoradiograph which resulted from probing of the filter from this gel with the NM23H1 gene probe, previously used in Southern analysis. Thus it can be seen that only lanes (a) and (b), which contain undigested and digested DNA from the NM23H1 gene cosmid, respectively, show positivity following this probing. The smear seen in one of the lanes containing TOPO II $\alpha$  cosmid DNA was caused by detection of repetitive DNA sequences and is not specific. Therefore, the ICRFc105H12160 cosmid is specific for the NM23H1 gene.

Panel (c) shows an ethidium stained Southern gel of undigested and digested TOPO II $\alpha$  cosmids received from the ICRF RLDB. The filter produced from this gel was hybridised with the SP1, TOPO II $\alpha$  gene probe,

### **Figure 3.3**

#### **Confirmation of identity of ICRF NM23H1 and TOPO II $\alpha$ cosmids by Southern analysis.**

**Panel (a):** Ethidium bromide stained Southern gel showing undigested and digested TOPO II $\alpha$  (as marked), RAR $\alpha$  (as marked) and NM23H1 cosmid (lanes a and b).

**Panel (b):** Autoradiograph resulting from incubation of filter from gel in panel (a) with NM23H1 Southern probe.

Lane a: ICRFc105H12160, undigested

Lane b: ICRFc105H12160, *EcoRI* digested

**Panel (c):** Ethidium bromide stained Southern gel showing undigested and digested ICRF TOPO II $\alpha$  cosmids.

**Panel (d):** Autoradiograph resulting from incubation of filter from gel in panel c with TOPO II $\alpha$  (SP1) Southern probe.

Lanes 1 & 2: ICRFc105G0847, Lanes 3 & 4: ICRFc105G01101,  
Lanes 5 & 6: ICRFc105C0867, Lanes 7 & 8: ICRFc105C0913,  
Lanes 9 & 10: ICRFc105H01119, Lanes 11 & 12: ICRFc105C1056,  
Lanes 13 & 14: ICRFc105B04155, Lanes 15 & 16: ICRFc105A09111,  
Lanes 17 & 18: ICRFc105A07140  
Lanes 19 & 20: ICRFc105C0967,  
Lanes 21 & 22: ICRFc105E1029,  
Lanes 23 & 24: ICRFc105G1239.  
M: Lambda x *HindIII* Marker

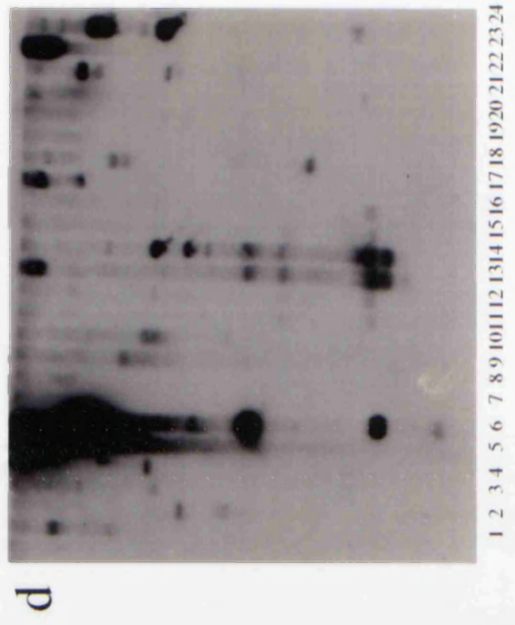
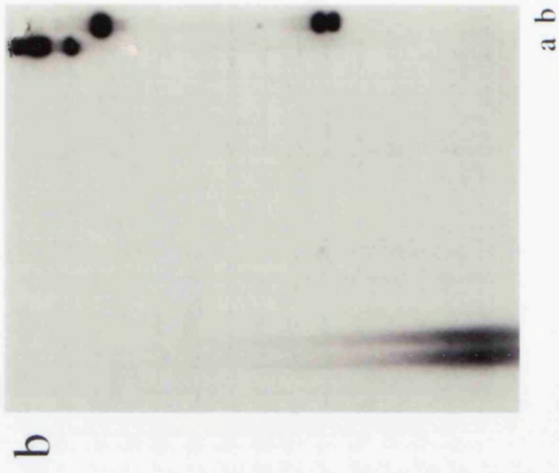
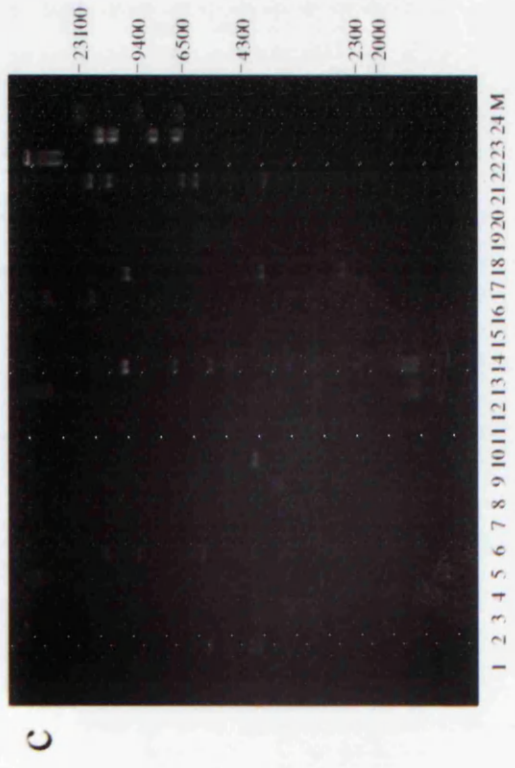
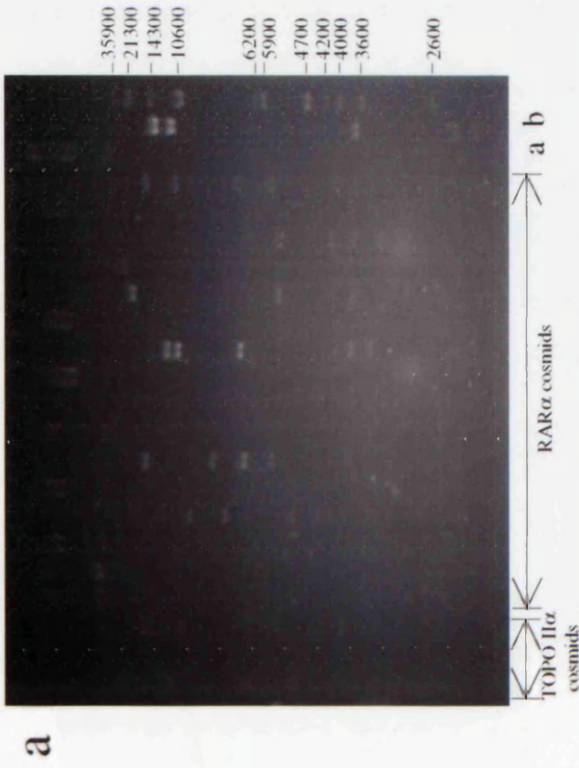
Odd numbers: Undigested cosmid DNA

Even numbers: *EcoRI* digested cosmid DNA

Marker sizes in base pairs are shown on the right of panels (a) and (c)

Panel (b) shows that only the NM23H1 cosmid, ICRFc105H12160, hybridises with the NM23H1 gene probe.

Panel (d) shows that all the TOPO II $\alpha$  cosmids hybridise with the SP1 probe.



1 2 3 4 5 6 7 8 9 10 11 12 13 14 15 16 17 18 19 20 21 22 23 24 M

1 2 3 4 5 6 7 8 9 10 11 12 13 14 15 16 17 18 19 20 21 22 23 24

and the resulting autoradiograph is shown in panel (d). Therefore, all TOPO II $\alpha$  cosmids received from the ICRF hybridise to this probe. From panels (c) and (d), the largest clones were chosen for use in FISH analysis, these being ICRFc105B04155 and ICRFc105H01119. All eight RAR $\alpha$  cosmids received from the ICRF were used in FISH analysis and ICRFc105F1255 was chosen for use in further experiments due to its' hybridisation efficiency.

### **Investigation of Gross Genetic Changes to Chromosome 17 in L-DAN, CALU-3 and SK-MES-1 by FISH**

Initial FISH experiments with L-DAN, CALU-3 and SK-MES-1 were performed using whole chromosome 17 paints and chromosome 17-specific centromere probe. These probes enable any gross changes to chromosome 17 to be investigated since the paint probe will identify sequences from anywhere along the length of chromosome 17, thus making it possible to detect translocations involving this chromosome.

Figure 3.4 shows the results of using both the whole chromosome 17 paint and chromosome 17-specific centromere probe on normal lymphocyte (panels a & e), CALU-3 (panels b & f), L-DAN (panels c & g) and SK-MES-1 (panels d & h) metaphase chromosome spreads. In lymphocytes, two copies of chromosome 17 are observed (panel a), as shown by the two chromosomes which are visualised in green. Two copies of chromosome 17 centromere are also observed in normal lymphocytes (panel e), as shown by the two green spots on two of the chromosomes in the spread. When these probes are used on CALU-3 chromosomes, the results appear to be very different from those seen in lymphocytes. No single chromosome within the CALU-3 metaphase spread hybridises in its entirety to chromosome 17 paint (panel b). Instead, there appear to be seven different chromosomal regions to which the paint hybridises. When chromosome 17-specific centromere probe was used (panel f), five chromosomes were seen to react with this probe. This indicates that not all of the chromosome 17 regions detected by chromosome 17 paint are associated with a chromosome 17 centromere sequence.

When L-DAN chromosomes were hybridised with chromosome 17 paint and centromere probes (panels c and g respectively) it was discovered that this cell line appears to have three copies of chromosome 17, and three chromosome 17 centromeres. Therefore, it appears that these three chromosomes still possess chromosome 17 centromeres. However, it cannot be said that these chromosomes are normal copies of chromosome 17,

### **Figure 3.4**

#### **Detection of chromosome 17 and chromosome 17 centromere in lymphocytes and lung tumour cell lines by FISH.**

**Panels (a) & (e): Normal lymphocytes**

**Panels (b) & (f): CALU-3**

**Panels (c) & (g): L-DAN**

**Panels (d) & (h): SK-MES-1**

Chromosomes were visualised with PI (pseudocoloured red). Chromosome 17 and chromosome 17-specific centromere signals were visualised with FITC (pseudocoloured green).

Chromosome 17 paint from Cambio was used to detect chromosome 17 sequences. Our own PCR-produced centromere 17-specific alpha satellite probe was used to detect chromosome 17 centromere sequences.

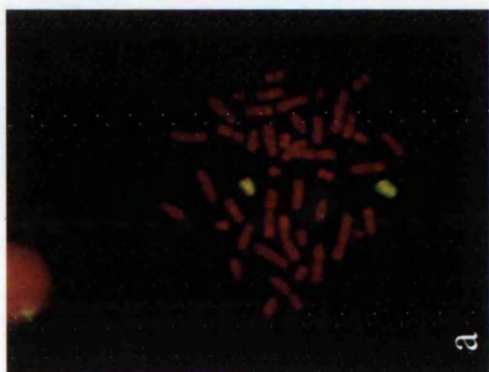
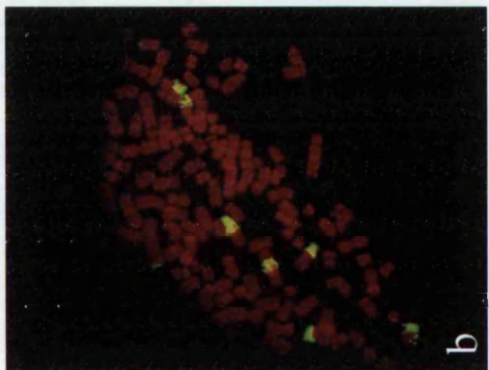
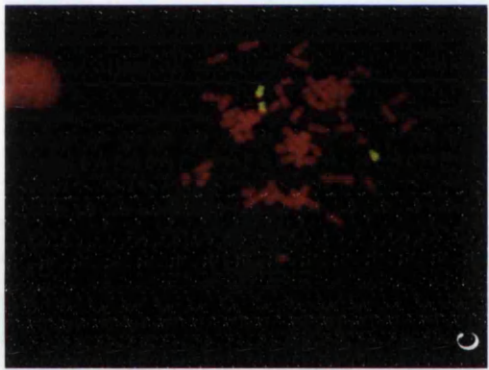
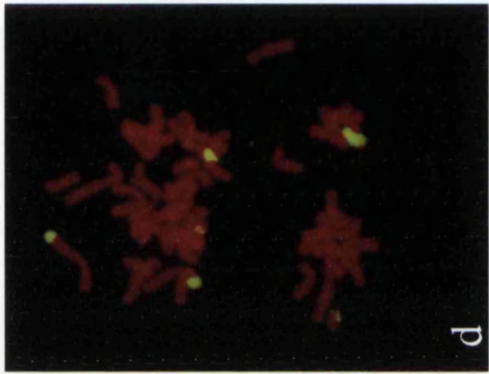
In lymphocytes, two copies of chromosome 17 (panel a) and chromosome 17 centromere (panel e) are observed, as would be expected in a normal cell.

CALU-3 appears not to have any intact chromosome 17s', but has 7 major regions of hybridisation to the chromosome 17 paint (panel b). Panel f shows CALU-3 to have 5 chromosome 17 centromere sequences.

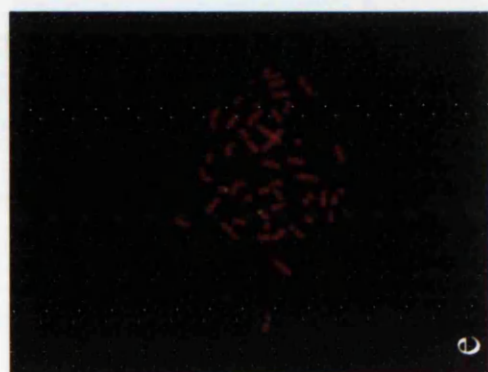
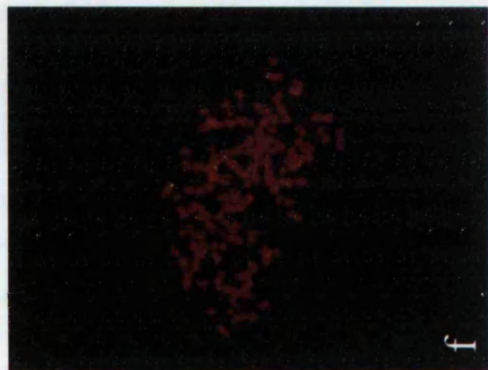
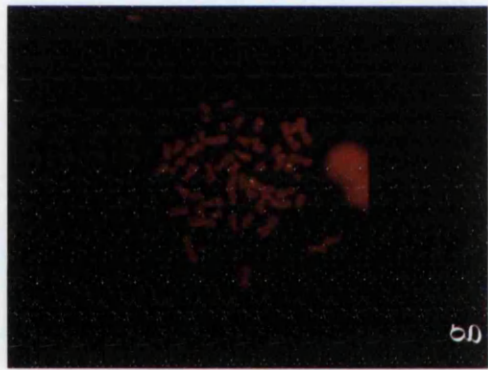
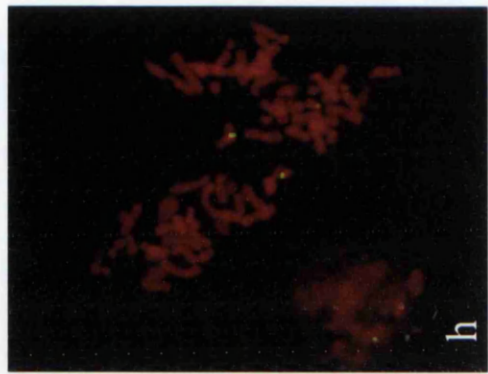
L-DAN appears to have three copies of chromosome 17 and chromosome 17 centromere (panels c and g, respectively).

SK-MES-1 appears to have six regions of hybridisation to the chromosome 17 paint (panel d) and three chromosome 17 centromere sequences (panel h).

chromosome  
17 paint



chromosome  
17 centromere



since this analysis can only detect gross changes to chromosomes. Panels (d) and (h) show the results of whole chromosome 17 painting and chromosome 17 centromere detection in SK-MES-1. This cell line appears to have six regions of chromosome 17 paint hybridisation (panel d) and three chromosome 17 centromere sequences (panel h). Therefore, as in CALU-3, some of the chromosome 17 detected regions are not associated with chromosome 17 centromeres.

### **Co-hybridisation of Single-Copy Gene Cosmids with Chromosome 17-Specific Centromere Probe in Lymphocytes**

To confirm the co-localisation of gene cosmids to particular chromosomes, single-copy gene cosmids can be co-hybridised with chromosome-specific centromere probes. Figure 3.5 shows double hybridisation of all single-copy gene cosmids used in FISH analysis with the chromosome 17-specific centromere probe in lymphocytes. Green signal indicates hybridisation of single-copy probe and red signal indicates hybridisation of chromosome 17 centromere probe. In all panels, four single-copy gene signals can be seen on each metaphase spread. This is a result of the gene being detected on both chromatids of each chromosome 17. Thus it can be seen that all the cosmids used do hybridise to chromosome 17 in lymphocytes.

Three different TOPO II $\alpha$  gene cosmids were available for use in FISH, pC5, ICRFc105H01119 and ICRFc105B041155. To discover if there was any difference in results obtained from using the different probes in FISH, counts were made of hybridisation signals from 20 lymphocyte metaphase spreads. These counts are shown in Table 3.1. In each case 20 metaphase spreads were counted and it was assumed that the maximum total number of hybridisation counts possible was 80 (four per metaphase spread). Therefore, the final percentage hybridisation frequency was calculated as total counts from that experiment divided by 80 and multiplied by 100. Hybridisation frequencies in Table 3.1 show that the ICRFc105B041155 cosmid has the highest frequency and thus is the most efficient at detecting the TOPO II $\alpha$  gene. Hybridisation frequencies were also calculated for NF1, NM23H1, RAR $\alpha$  and C05123 cosmids on lymphocyte metaphase spreads. These frequencies are shown in Table 3.2.

Since all the gene probes used were all situated around the same region of chromosome 17, it was very difficult to deduce an order for the probes by eye. Therefore, photographs of hybridisations in lymphocytes were

### **Figure 3.5**

#### **Double hybridisation of single-copy gene cosmids and chromosome 17 centromere probe in lymphocytes.**

Each panel shows a different single copy gene cosmid (from the 17q region) hybridised in conjunction with the PCR-produced chromosome 17-specific centromere probe to metaphase spreads prepared from normal lymphocytes.

Single gene cosmids used: ICRFc105B041155 (TOPO II $\alpha$ )  
C05123 (BRCA1 region)  
ICRFc105C0861 (NF1)  
Neu1 and Neu4 (ERBB2)  
ICRFc105F1255 (RAR $\alpha$ )  
ICRFc105H12160 (NM23H1)

Chromosomes were visualised with PI (pseudocoloured blue), single gene cosmids were visualised with FITC (pseudocoloured green) and chromosome 17 centromere sequence was visualised with Cy<sup>5</sup> (pseudocoloured red).

In each panel two chromosome 17s are observed, both with single gene cosmid signal (green) and centromere signal (red). Two cosmid signals are seen on each chromosome (four per metaphase spread) due to detection of the single-copy gene on each of the chromosome arms.

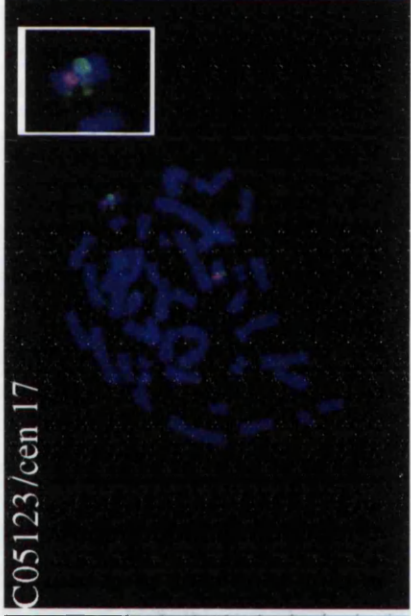
Small panel within each picture shows close-up of a chromosome 17 from that spread.

Therefore, this confirms that all of the single gene cosmids used do hybridise to chromosome 17 in normal lymphocytes.

TOPO II $\alpha$ /cen 17



C05123/cen 17



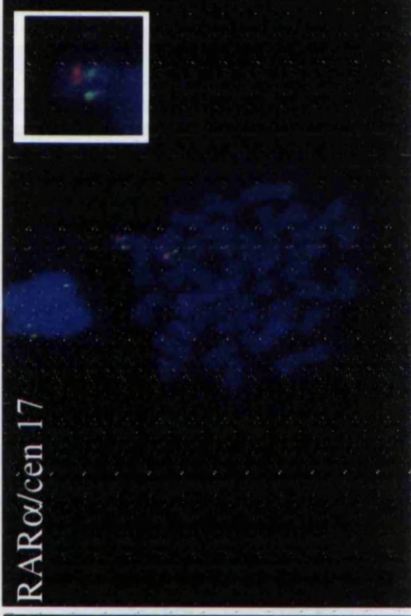
NF1/cen 17



ERBB2/cen 17



RAR $\alpha$ /cen 17



NM23H1/cen 17



**Table 3.1**

**Relative hybridisation frequencies of the three TOPO II $\alpha$  cosmids, pC5, ICRFc105H01119 and ICRFc105B041155 on lymphocyte metaphase spreads.**

<b>Cosmid Used</b>	<b>No. of chr. spreads counted</b>	<b>Total no. of chr. with signal</b>	<b>Total no. of signals</b>	<b>%age hybridisation frequency</b>
pC5	20	34	63	<b>78%</b>
H01119	20	38	72	<b>90%</b>
B041155	20	39	73	<b>91%</b>

**Table 3.2**

**Hybridisation frequencies of NF1, NM23H1, RAR $\alpha$  and C05123 cosmids on lymphocyte metaphase spreads.**

<b>Gene Locus</b>	<b>Cosmid Used</b>	<b>No. of chr. spreads counted</b>	<b>Total no. of chr. with signal</b>	<b>Total no. of signals</b>	<b>%age hybrid<sup>n</sup> frequency</b>
NF1	C0861	20	40	63	<b>78%</b>
NM23H1	H12160	20	39	67	<b>83%</b>
RAR $\alpha$	F1255	20	40	77	<b>96%</b>
Unknown	C05123	20	39	67	<b>83%</b>

Percentage hybridisation efficiency was calculated on the basis of 4 signals (doublets) being detected per metaphase spread.

used to obtain fractional length measurements for each of the single-copy gene cosmids (Tanner *et al.*, 1994). The SigmaScan programme on PC was used to take these measurements. Measurements were taken from the tip of the p arm of chromosome 17 down to the single-copy cosmid signal (FL1), and then from the single gene signal down to the tip of the q arm (FL2). Fractional length measurement 1 (FL1) was then expressed as a fraction of the sum of FL1 and FL2.

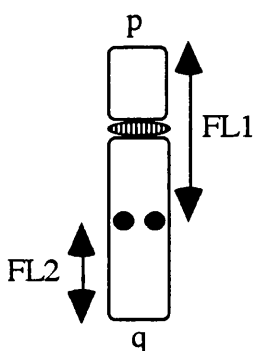


Table 3.3 shows the mean, median and standard deviation of fractional length measurements taken for all the gene cosmids used in FISH. Figure 3.6 shows the distances of the genes from the p arm of chromosome 17 according to the mean fractional length measurement. Mann-Whitney analysis of all possible gene combinations was also performed using the median FL. Results of this analysis are shown in Table 3.4. These results show that the distances between almost all the gene pairs are significant if level of significance is set at 10% ( $p=0.1$ ). Gene pairs analysed which give a p-value greater than or close to 0.1 are assumed to be located very close together on chromosome 17q. Therefore, fractional length measurements enabled ordering of the gene cosmids used in FISH analysis.

### **Analysis of TOPO II $\alpha$ and ERBB2 gene copy number in L-DAN and SK-MES-1**

Since Southern data has been accumulated on L-DAN and SK-MES-1, it was also of interest to perform FISH on these cell lines with TOPO II $\alpha$  and ERBB2 gene cosmids. This work was carried out prior to receipt of the ICRF cosmids, thus the pC5 cosmid was used to detect TOPO II $\alpha$  in these experiments. Figure 3.7 shows the results of detection of TOPO II $\alpha$  and ERBB2 in L-DAN and SK-MES-1. Panels (a) and (c) show hybridisation of TOPO II $\alpha$  and ERBB2 cosmids, respectively in L-DAN. In panel (b) three copies of ERBB2 can also be seen in the interphase nuclei. Six signals are detected due to there being one gene copy per chromatid arm.

**Table 3.3**

**Table showing mean, median and standard deviation of fractional length measurements for all genes studied by FISH.**

<b>Gene</b>	<b>No. of chromatids counted</b>	<b>Mean Fractional Length</b>	<b>Median Fractional Length</b>	<b>Standard Deviation</b>
<b>NF1</b>	22	0.40	0.41	0.042
<b>ERBB2</b>	25	0.47	0.47	0.043
<b>TOPO II<math>\alpha</math></b>	22	0.49	0.50	0.034
<b>RAR<math>\alpha</math></b>	16	0.52	0.52	0.060
<b>CO5123</b>	21	0.55	0.55	0.047
<b>NM23H1</b>	17	0.59	0.60	0.055

**Table 3.4**

**Table showing p-values from Mann-Whitney analysis for all gene pair combinations.**

<b>Gene Pair Tested</b>	<b>p-value</b>
NF1-NM23H1	0.00
NF1-CO5123	0.00
NF1-RAR $\alpha$	0.00
NF1-TOPO II $\alpha$	0.00
NF1-ERBB2	0.00
ERBB2-NM23H1	0.00
ERBB2-CO5123	0.00
ERBB2-RAR $\alpha$	0.00
ERBB2-TOPO II $\alpha$	0.14
TOPO II $\alpha$ -NM23H1	0.00
TOPO II $\alpha$ -CO5123	0.00
TOPO II $\alpha$ -RAR $\alpha$	0.09
RAR $\alpha$ -NM23H1	0.00
RAR $\alpha$ -CO5123	0.12
CO5123-NM23H1	0.02

### **Figure 3.6**

#### **Diagram showing positions of genes on 17q according to mean fractional length measurement (FLM)**

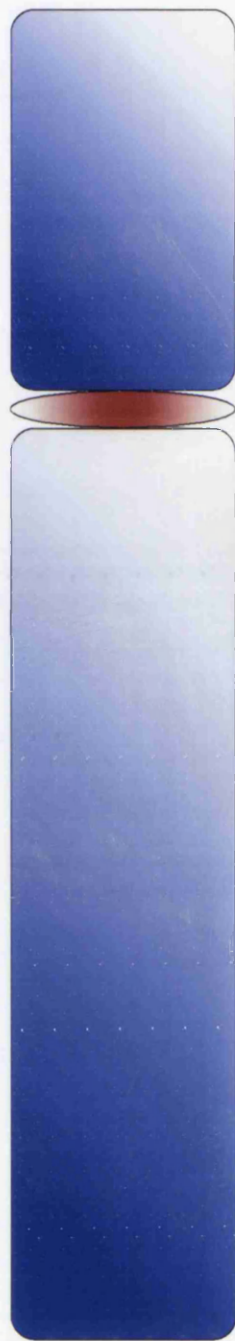
Fractional length measurements were calculated from single gene cosmid hybridisations on lymphocytes (using SigmaScan) in order to obtain mapping data. Measurements were taken from the tip of the p arm to the gene signal and then from the gene signal to the tip of the q arm. The fractional length of the gene signal from 17p was then calculated from these measurements.

The cosmids used were:

ICRFc105B041155	(TOPO II $\alpha$ )
C05123	(BRCA1 region)
ICRFc105C0861	(NF1)
Neu1 and Neu4	(ERBB2)
ICRFc105F1255	(RAR $\alpha$ )
ICRFc105H12160	(NM23H1)

This diagram shows the order of the above genes on chromosome 17 according to the calculated mean fractional length of each cosmid hybridisation. Further statistical details of samples, such as number of chromatids counted and the standard deviation, are shown in Table 3.1.

Diagram showing positions of genes on 17q according to mean fractional length measurement (FLM)



GENE	MEAN FLM
NF1	0.40
ERBB2	0.47
TOPO II $\alpha$	0.49
RAR $\alpha$	0.52
C05123	0.55
NM23H1	0.59

**Chromosome 17**

### **Figure 3.7**

#### **Analysis of TOPO II $\alpha$ and ERBB2 copy number in L-DAN and SK-MES-1 using FISH.**

**Panel (a):** L-DAN chromosomes hybridised with TOPO II $\alpha$  gene cosmid (pC5)

**Panel (b):** L-DAN chromosomes hybridised with ERBB2 gene cosmids (Neu1 and Neu4)

**Panel (c):** SK-MES-1 chromosomes hybridised with TOPO II $\alpha$  gene cosmid (pC5)

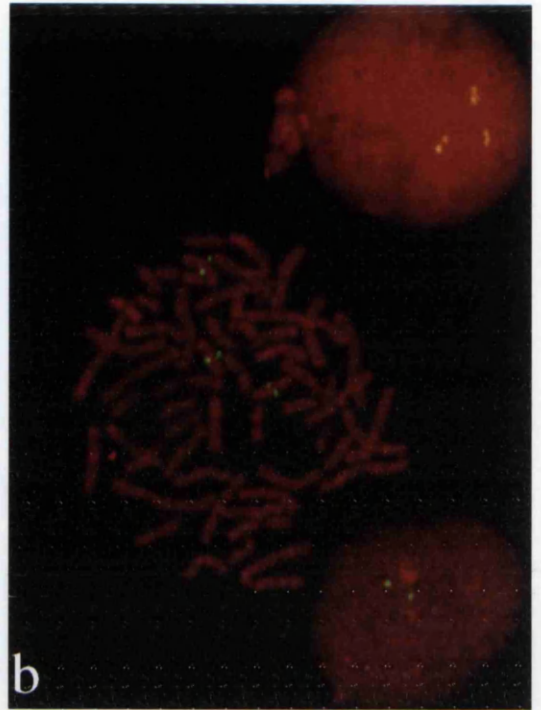
**Panel (d):** SK-MES-1 chromosomes hybridised with ERBB2 gene cosmids (Neu1 and Neu4)

Chromosomes were visualised with PI (pseudocoloured red), single copy gene cosmids were visualised with FITC (pseudocoloured green).

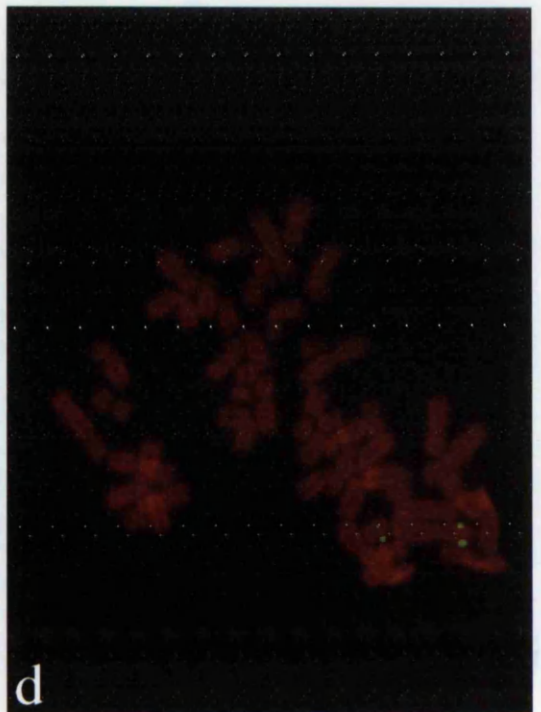
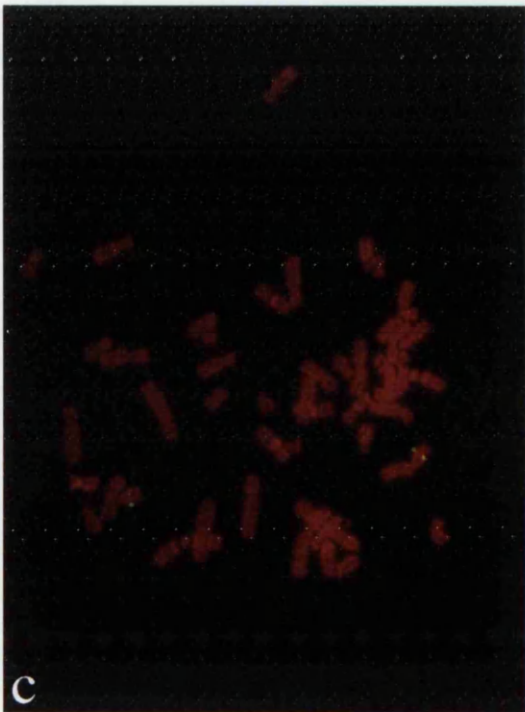
Panels (a) and (b) show L-DAN to have three copies of the TOPO II $\alpha$  and ERBB2 genes. Six signals are visualised since there is one copy of the gene on each chromatid. The finding of three copies of these genes correlates with the detection of the three seemingly intact chromosome 17s' by chromosome 17 painting (Figure 3.4).

Panels (c) and (d) show SK-MES-1 to have two copies of both TOPO II $\alpha$  and ERBB2. Therefore, there does not appear to be any changes in the copy number of these genes in SK-MES-1. However, it appears that one of the chromosomes on which signal is being detected is much larger than a normal chromosome 17. Thus it appears that a translocation may have occurred between a chromosome 17 and another chromosome in SK-MES-1.

L-DAN



SK-MES



Therefore, it appears that L-DAN has three copies of TOPO II $\alpha$  and ERBB2 genes. This data agrees with previous data showing that L-DAN has three copies of chromosome 17 and three chromosome 17 centromeres (Figure 3.4, panels c and g). Figure 3.7, panels (c) and (d) show the results of TOPO II $\alpha$  and ERBB2 cosmid hybridisation in SK-MES-1. Therefore, there does not appear to be any changes in the copy number of these genes in this cell line. However, although one pair of signals appears to be on a 'normal' chromosome 17, the other chromosome on which cosmid signals are detected is much larger. Thus it is proposed that a translocation has occurred in SK-MES-1 between one chromosome 17 and another chromosome.

### **Further Characterisation of the Chromosome 17 Amplicon in CALU-3 using FISH**

From previous work by Keith *et al.*, (1992) it is known that the TOPO II $\alpha$  and ERBB2 genes are co-amplified in CALU-3. One of the main aims of this project was to discover if there was amplification of any other genes from this region of chromosome 17. Figures 3.1 and 3.2 have demonstrated that the RAR $\alpha$  and G-CSF genes are also contained within the chromosome 17 amplicon, whereas NM23H1 and PKC $\alpha$  genes are outside the region of amplification. However, the structure of the amplicon is still unknown. By FISH analysis, the precise location of these amplified genes can be observed on the chromosomes. Figure 3.4, panels (b) and (f) showed that CALU-3 has seven regions of chromosome 17 sequence and five chromosome 17 centromeres. Figure 3.8 shows double hybridisation of the chromosome 17-specific centromere probe and six single-copy gene probes (for TOPO II $\alpha$ , ERBB2, RAR $\alpha$ , NM23H1, NF1 genes and C05123 for the BRCA1 region) on CALU-3 metaphases. All these panels show that regions of hybridisation to the single gene probes (green signal) are associated with chromosome 17 centromere sequences (red signal).

With the ERBB2 cosmids, three regions of amplification are observed. Three regions of TOPO II $\alpha$  amplification are also observed, along with 2 single copies of the gene on the remaining two chromosomes which have chromosome 17 centromeres. The same finding of three amplified regions and 2 single gene copies was also seen when C05123 and RAR $\alpha$  cosmids were hybridised to CALU-3 metaphases. NM23H1 and NF1 cosmid hybridisations resulted in the detection of 5 copies of each of these genes, one associated with each chromosome 17 centromere. Interestingly, it appears that there may have been an inversion of this region of chromosome 17 as well as

### **Figure 3.8**

#### **Double hybridisation of single-copy gene cosmids and chromosome 17 centromere probe in CALU-3.**

Each panel shows a different single copy gene cosmid (from the 17q region) hybridised in conjunction with the PCR-produced chromosome 17-specific centromere probe to metaphase spreads prepared from CALU-3.

Single gene cosmids used: ICRFc105B041155 (TOPO II $\alpha$ )  
C05123 (BRCA1 region)  
ICRFc105C0861 (NF1)  
Neu1 and Neu4 (ERBB2)  
ICRFc105F1255 (RAR $\alpha$ )  
ICRFc105H12160 (NM23H1)

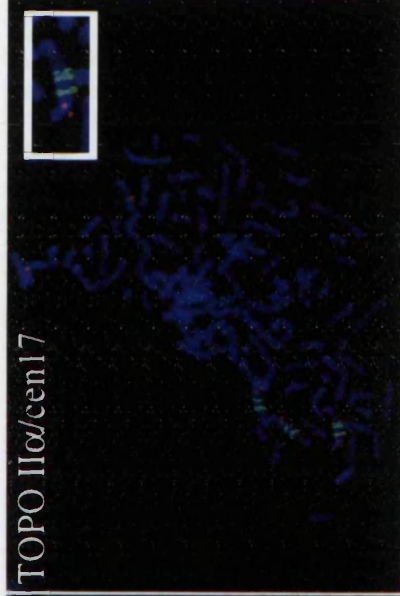
Chromosomes were visualised with PI (pseudocoloured blue), single gene cosmids were visualised with FITC (pseudocoloured green) and chromosome 17 centromere sequence was visualised with Cy<sup>5</sup> (pseudocoloured red).

CALU-3 has 3 regions of amplification of ERBB2, all of which are associated with chromosome 17 centromere sequence. The TOPO II $\alpha$  gene amplification is also found on three chromosomes, with two single copies of the gene present on the other chromosomes with 17 centromere signal. Both C05123 and RAR $\alpha$  genes show amplification on three chromosomes, although not to the same extent as ERBB2 or TOPO II $\alpha$  genes. Single copies of these genes are also seen associated with the other two chromosome 17 signals. CALU-3 appears to have 5 copies of both the NM23H1 and NF1 genes, all linked to chromosome 17 centromere signals.

ERBB2/cen17



TOPO II $\alpha$ /cen17



CO5123/cen17



RAR $\alpha$ /cen17



NM23H1/cen17



NF1/cen17



the amplification since the NM23H1 gene appears to be very close to the centromere. From fractional length measurements shown in Figure 3.6, NM23H1 should be located towards the |q ter of chromosome 17 below all the other genes. The close-up pictures of chromosomes with ERBB2 and TOPO II $\alpha$  hybridisation also show the laddering pattern of signal.

Figure 3.9 shows close up images of the three chromosomes on which the 17q amplicon is present following hybridisation of the six single gene cosmids. The ladderised banding pattern of signal hybridisation is shown very clearly in the panels from ERBB2, TOPO II $\alpha$ , RAR $\alpha$  and C05123 experiments. It can also be seen that RAR $\alpha$  and C05123 genes are not amplified to the same extent as TOPO II $\alpha$  and ERBB2 genes. Hybridisation frequencies were calculated from these experiments and are shown in Table 3.5. Total number of hybridisation signals was not determined for TOPO II $\alpha$ , ERBB2, RAR $\alpha$  or C05123 cosmids since resolution of hybridisation was not good enough to enable counting of individual signals.

Figure 3.10 shows co-hybridisation of the TOPO II $\alpha$  cosmid with ERBB2 and RAR $\alpha$  cosmids (upper and lower panels, respectively) in CALU-3. In the upper panel (ERBB2/TOPO II $\alpha$  hybridisation), TOPO II $\alpha$  cosmid hybridisation is visualised in green and ERBB2 cosmid hybridisation is visualised in red. Where there is overlap of these colours, yellow signal is seen. In the lower panel (TOPO II $\alpha$ /RAR $\alpha$  hybridisation) RAR $\alpha$  cosmid hybridisation is visualised in green and TOPO II $\alpha$  cosmid hybridisation is visualised in red. Again, overlap of red and green signal results in yellow. Both these images show that signals from the gene cosmids used are detected on the same distinct chromosomal regions in CALU-3. Clear laddering of cosmid signal can be seen in the TOPO II $\alpha$ /ERBB2 panel. Figure 3.11 shows co-hybridisation of the TOPO II $\alpha$  cosmid with NF1 and NM23H1 cosmids (upper and lower panels, respectively). In both these panels TOPO II $\alpha$  cosmid hybridisation is shown in red and NF1 and NM23H1 hybridisation is shown in green. Five copies of the NF1 and NM23H1 cosmids are detected in CALU-3, with TOPO II $\alpha$  amplification associated with three of these gene copies.

## **Figure 3.9**

### **Hybridisation of single-copy gene cosmids in CALU-3.**

Each panel shows a different single-copy gene cosmid (from the 17q region) hybridised to CALU-3 chromosomes. Only the three chromosomes which carry the amplicon are shown in each panel, at a slightly higher magnification in order to show the structure of amplified genes in the 17q region.

Single gene cosmids used: ICRFc105B041155 (TOPO II $\alpha$ )  
C05123 (BRCA1 region)  
ICRFc105C0861 (NF1)  
Neu1 and Neu4 (ERBB2)  
ICRFc105F1255 (RAR $\alpha$ )  
ICRFc105H12160 (NM23H1)

Chromosomes were visualised with PI (pseudocoloured red) and gene cosmids were visualised with FITC (pseudocoloured green).

These figures show a more detailed view of the gene amplification in CALU-3. Two stripes of green signal (indicating cosmid hybridisation) can clearly be seen in the panels showing ERBB2, TOPO II $\alpha$ , RAR $\alpha$  and C05123 hybridisations.

Only single copies of NF1 and NM23H1 appear to be present on these chromosomes.

ERBB2



TOPO II $\alpha$



RAR $\alpha$



NM23H1



NF1



C05123



**Table 3.5**

**Hybridisation frequencies of TOPO II $\alpha$ , ERBB2, NF1, NM23H1, RAR $\alpha$  and C05123 cosmids on CALU-3 metaphase spreads.**

<b>Gene Locus</b>	<b>Cosmid Used</b>	<b>No. of chr. spreads counted</b>	<b>Total no. of chr. with signal</b>	<b>Total no. of signals</b>	<b>%age hybrid<sup>n</sup> frequency</b>
Topo II $\alpha$	B041155	20	85	ND	<b>ND*</b>
ERBB2	Neu1/Neu4	20	60	ND	<b>ND</b>
NF1	C0861	20	99	145	<b>72%</b>
NM23H1	H12160	20	100	175	<b>87%</b>
RAR $\alpha$	F1255	20	100	ND	<b>ND</b>
Unknown	C05123	20	100	ND	<b>ND</b>

ND: Not Determined

\*: Each spread was seen to have 1 or 2 single copies of the TOPO II $\alpha$  gene on separate chromosomes from those carrying the amplification.

Percentage hybridisation efficiency was calculated on the basis of 4 signals (doublets) being detected per metaphase spread.

### **Figure 3.10**

#### **Double hybridisation of single-copy gene cosmids in CALU-3.**

Upper panel shows double hybridisation of TOPO II $\alpha$  and ERBB2 gene cosmids to a metaphase spread from CALU-3

Chromosomes were visualised with PI (pseudocoloured blue), TOPO II $\alpha$  was visualised with FITC (pseudocoloured green) and ERBB2 was visualised with Cy<sup>5</sup> (pseudocoloured red).

Lower panel shows double hybridisation of TOPO II $\alpha$  and RAR $\alpha$  cosmids to a metaphase spread from CALU-3

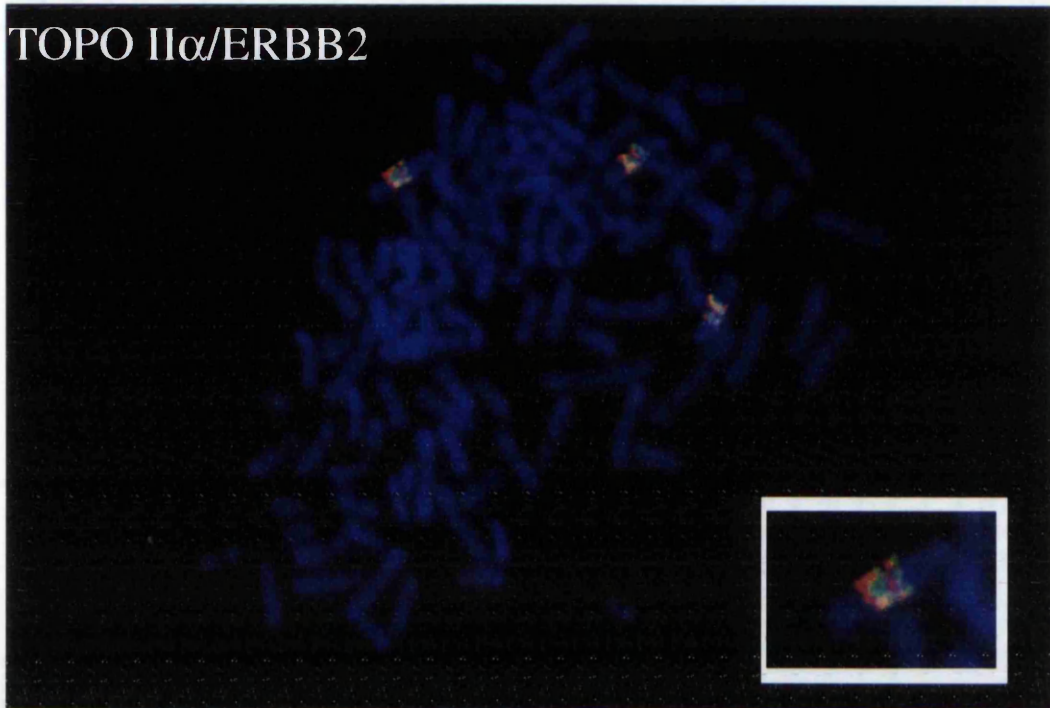
Chromosomes were visualised with PI (pseudocoloured blue), RAR $\alpha$  was visualised with FITC (pseudocoloured green) and TOPO II $\alpha$  was visualised with Cy<sup>5</sup> (pseudocoloured red).

Inset boxes show close-up of chromosome with double hybridisation. Yellow signal denotes overlap of green and red colours.

Single gene cosmids used: ICRFc105B041155 (TOPO II $\alpha$ )  
Neu1 and Neu4 (ERBB2)  
ICRFc105F1255 (RAR $\alpha$ )

These figures show the co-hybridisation of signals for ERBB2 and RAR $\alpha$  with TOPO II $\alpha$  on three distinct chromosomal regions in CALU-3.

TOPO II $\alpha$ /ERBB2



TOPO II $\alpha$ /RAR $\alpha$

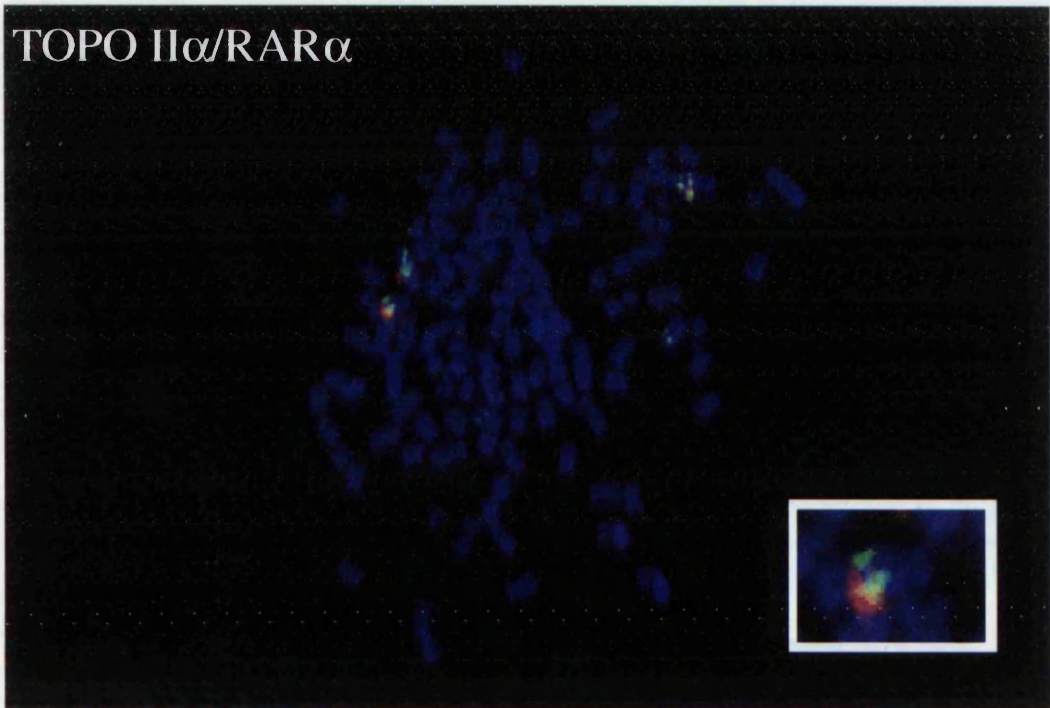


### **Figure 3.11**

#### **Double hybridisation of single-copy gene cosmids in CALU-3.**

Upper panel shows double hybridisation of TOPO II $\alpha$  and NF1 gene cosmids to a metaphase spread from CALU-3. Chromosomes were visualised with PI (pseudocoloured blue), NF1 was visualised with FITC (pseudocoloured green) and TOPO II $\alpha$  was visualised with Cy<sup>5</sup> (pseudocoloured red).

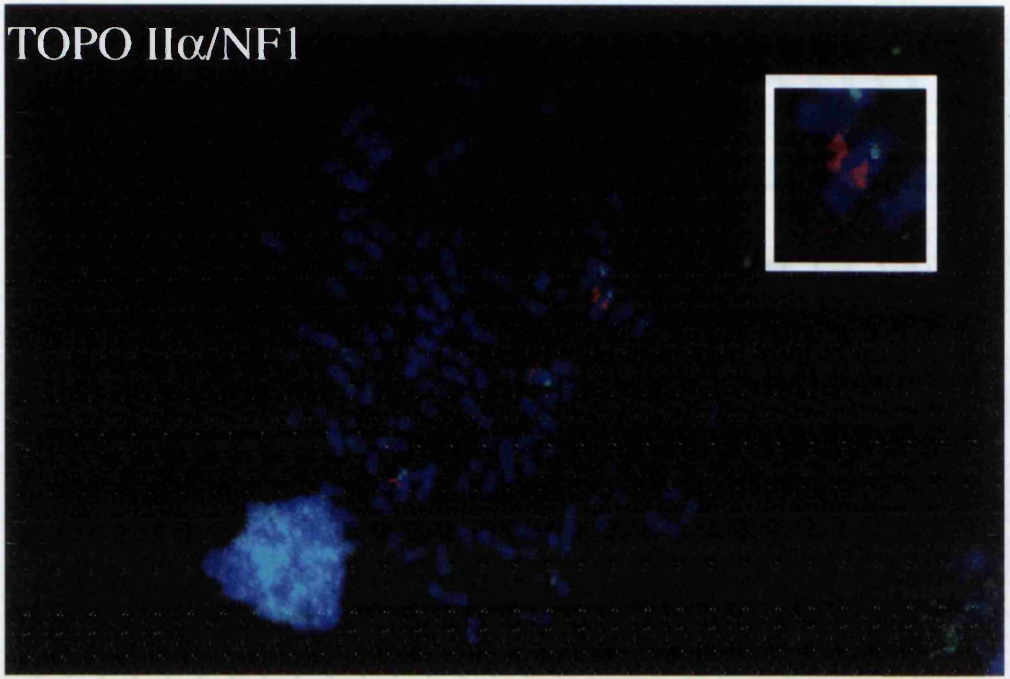
Lower panel shows double hybridisation of TOPO II $\alpha$  and NM23H1 cosmids to a metaphase spread from CALU-3. Chromosomes were visualised with PI (pseudocoloured blue), NM23H1 was visualised with FITC (pseudocoloured green) and TOPO II $\alpha$  was visualised with Cy<sup>5</sup> (pseudocoloured red).

Inset boxes show close-up of chromosome with double hybridisation. Yellow signal denotes overlap of green and red colours.

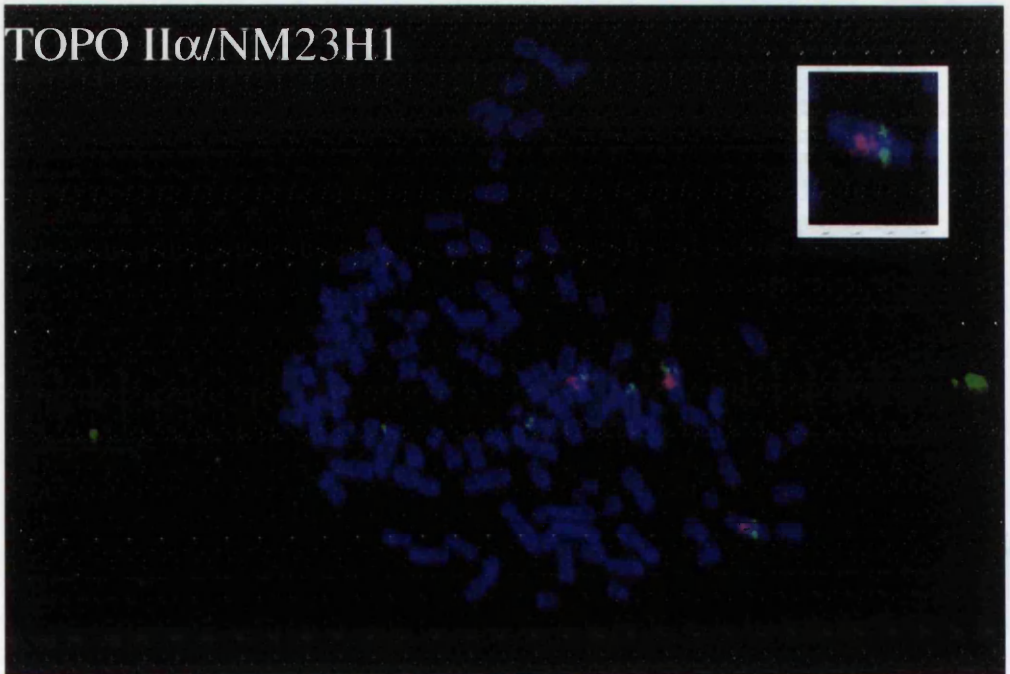
Single gene cosmids used: ICRFc105B041155 (TOPO II $\alpha$ )  
ICRFc105C0861 (NF1)  
ICRFc105H12160 (NM23H1)

These figures show the co-hybridisation of signals for NF1 and NM23H1 with TOPO II $\alpha$  on three distinct chromosomal regions in CALU-3.

TOPO II $\alpha$ /NF1



TOPO II $\alpha$ /NM23H1



### **3.3 Discussion**

The work presented in this chapter deals with further characterisation of the amplicon on chromosome 17 in the NSCLC cell line, CALU-3. As mentioned in the introduction to this chapter, co-amplification of TOPO II $\alpha$  and ERBB2 genes has been observed in certain cases of breast cancer (Keith *et al.*, 1993; Murphy *et al.*, in press; Smith *et al.*, 1993). Amplification of the ERBB2 gene, however, has also been shown without involvement of the TOPO II $\alpha$  gene (Keith *et al.*, 1993; Smith *et al.*, 1993). Thus one could propose that ERBB2 is the driving force for the amplification of this region of chromosome 17. This would seem to make sense since it is known that the product of the ERBB2 gene is a growth factor receptor and overexpression of such a receptor would be an obvious advantage to cellular growth, although amplification of a gene does not necessarily mean that the gene is being overexpressed (Lafage *et al.*, 1990; Tsuda *et al.*, 1989; van de Vijver *et al.*, 1987). The study of expression of the ERBB2 gene in CALU-3 is dealt with in Chapter 4.

Analysis of co-amplification of genes on 17q in breast cancer (Keith *et al.*, 1993) indicates, however, that ERBB2 may not necessarily be the driver for amplification of genes in this region. In 3 tumours which demonstrated co-amplification of TOPO II $\alpha$ , RAR $\alpha$  and ERBB2 genes by Southern blot analysis, the RAR $\alpha$  locus was seen to be amplified to a greater degree than ERBB2 in all 3 cases. Two of these tumours also showed higher amplification of TOPO II $\alpha$  than ERBB2. Therefore, it may be that higher levels of RAR $\alpha$  and TOPO II $\alpha$  have been selected for during the process of carcinogenesis, since it is not clear what affect overexpression of these genes would have on a cell. It could also be that these differences in gene amplification levels are a result of the mechanism of amplification. As mentioned above, this investigation was performed using Southern blot hybridisation. Such analysis, however, does not give any information on the precise copy number of the genes studied, nor does it provide information on location of the genes. Also, perhaps more importantly, Southern analysis does not show possible relationships between genes. For example, in the above study there may be specific areas of the breast tumours where only TOPO II $\alpha$  and ERBB2 gene amplification are seen, with only certain cells having co-amplification of all three genes. This kind of information can be obtained, however, by performing FISH analysis on tumour sections, and such work has been carried out using repetitive and single-copy gene probes on both paraffin

sections and touch preparations of tumours (Kallioniemi *et al.*, 1992b; Kim *et al.*, 1993; Murphy *et al.*, in press; Persons *et al.*, 1993; Stock *et al.*, 1993).

Following the detection of amplified genes in CALU-3 by Southern analysis, a more detailed approach was taken using fluorescence in situ hybridisation. Since cosmid probes for some of the genes of interest on chromosome 17q were not commercially available, it was necessary to develop and map new cosmids. This was achieved for RAR $\alpha$ , NM23H1 and NF1 genes. All cosmids used were shown to co-localise with chromosome 17-specific centromere sequences (Figure 3.5) and mapping data was derived by taking fractional length measurements from cosmid hybridisations with lymphocyte chromosomes (Figure 3.6). There has been a lot of interest generated in chromosome 17q because of the linkage of the early onset breast cancer gene to this region. Previous mapping data obtained for 17q (Abel *et al.*, 1993; Anderson *et al.*, 1993; Flejter *et al.*, 1993) shows a very similar ordering of the ERBB2, TOPO II $\alpha$  and NM23H1 (or NME1) genes, although mapping data for the RAR $\alpha$  gene places it between the ERBB2 and TOPO II $\alpha$  genes (Abel *et al.*, 1993). In order to resolve these cosmids more accurately, FISH could be performed either on interphase cells or on stretched DNA (DIRVISH) using three colour mapping (Flejter *et al.*, 1993; Parra & Windle, 1993).

Differences in resolution between Southern and FISH analyses were also observed in this chapter. By Southern analysis, there did not appear to be any difference in TOPO II $\alpha$  or ERBB2 gene copy number between L-DAN and SK-MES-1 (Figure 3.1). By FISH analysis, however, 3 copies of both TOPO II $\alpha$  and ERBB2 were detected in L-DAN and 2 copies of each of these genes were detected in SK-MES-1 (Figure 3.7). This example highlights the usefulness of FISH in being able to visualise the exact copy number of a gene. The apparent translocation of chromosome 17 detected in SK-MES-1 would also have remained undetected by Southern analysis.

FISH analysis of CALU-3 (Figures 3.8, 3.9, 3.10 and 3.11) has shown that there is amplification of TOPO II $\alpha$ , ERBB2 and RAR $\alpha$  genes. The region of the C05123 cosmid was also found to be amplified. Therefore, the amplicon in CALU-3 encompasses five loci, ERBB2, TOPO II $\alpha$ , RAR $\alpha$ , G-CSF and C05123. It is interesting that the TOPO II $\alpha$  and ERBB2 genes appear to be more highly amplified than RAR $\alpha$ , G-CSF and C05123 sequences. With RAR $\alpha$ , the FISH data therefore agrees with Southern data which also showed lower levels of amplification of this gene (Figure 3.1). Therefore, there are three chromosomes carrying the amplified sequences in CALU-3, with two other chromosomes carrying single copy loci. Both the

single copy regions and the regions of amplification in CALU-3 are still associated with chromosome 17 sequences, as is shown by the co-hybridisation of chromosome 17-specific centromere sequence (Figure 3.8). Co-hybridisation of cosmids detecting the TOPO II $\alpha$ , ERBB2 and RAR $\alpha$  genes in CALU-3 indicates that these genes are truly co-amplified on the same region of the chromosome arm (Figure 3.10). There also appears to be an inversion of the region of amplification in CALU-3 since the NM23H1 gene is detected in close association with the centromere region (Figure 3.8). The exact copy number of TOPO II $\alpha$  and ERBB2 genes in CALU-3 could not be calculated due to the proximity of hybridisation signals within the amplicon. It would be of interest to obtain quantitative fluorescence measurements on these hybridisations, which compares to performing densitometry on autoradiographs. The advantage of measuring quantitative fluorescence is that measurement of a true single-copy signal can be taken and compared to the fluorescence of an amplified region.

It was previously published that CALU-3 was observed to have five copies of TOPO II $\alpha$ , three of which were clustered on one chromosome (Coutts *et al.*, 1993). The data presented in this chapter has shown much higher levels of TOPO II $\alpha$  amplification in CALU-3. The most likely explanation for this is that there has been selection and outgrowth of a clone with higher levels of gene amplification. The amplicon described above, in CALU-3, appears to represent a stable genotype since a number of independent chromosome preparations have been used in this analysis and have produced the same results.

It is of interest to note the pattern of amplified genes in CALU-3 since there appear to be two distinct stripes of ERBB2, TOPO II $\alpha$ , RAR $\alpha$  and C05123 hybridisation. Such stripe patterns were also reported in the papers concerning mechanisms of amplification, and the unequal sister chromatid exchange model, in particular, as outlined in Figure 3D (Smith *et al.*, 1990; Trask & Hamlin, 1989). Also noted in the paper by Trask and Hamlin are that single copies of the gene remain associated with the original locus. A similar phenomenon is noted in CALU-3 with single copies of the TOPO II $\alpha$ , RAR $\alpha$  and C05123 loci detected independently of the chromosomes carrying the amplicon. Since CALU-3 has now been passaged for many years in culture, it would be extremely difficult to deduce the initial mechanism of amplification. It would also be impossible to tell whether the inversion of this region occurred before or after the amplification. However, the genetic changes observed in CALU-3 could probably be accounted for by the unequal sister chromatid exchange and bridge/breakage/fusion model

(Smith *et al.*, 1990; Trask & Hamlin, 1989, Figure 3D). Figure 3E shows an extended version of this model, with a further cycle of bridge and breakage shown. The red and blue triangles in this diagram indicate two hypothetical genes and their orientation. Therefore, as the cycles of breakage and fusion occur, the changes to gene copy number and direction can be followed. This figure depicts formation of a bridge structure at D, thus at E head-to-tail arrays of the genes are observed. Alternatively, non-homologous exchange could occur between sister chromatids at D, as could breakage at a different telomere site which would possibly create a different outcome at E.

This theory of gene amplification could be tested in CALU-3 by analysing the amplicon in more detail. In order to do this, the region of amplification would need to be microdissected and then PCR-amplified. A microclone library could then be generated from the PCR products. Clones could then be analysed by Southern blotting to check which gene or genes they contained. Clones positive for two genes would be very interesting to study since they would contain the joining regions, thus by sequencing the DNA it would be possible to deduce the orientation of the genes. This technique of microdissection and microcloning has been used to study amplicons found in melanoma cell lines (Zhang *et al.*, 1993), neuroblastoma cell lines (Schneider *et al.*, 1992) and drug-resistant lung cancer cell lines (Ray *et al.*, 1994).

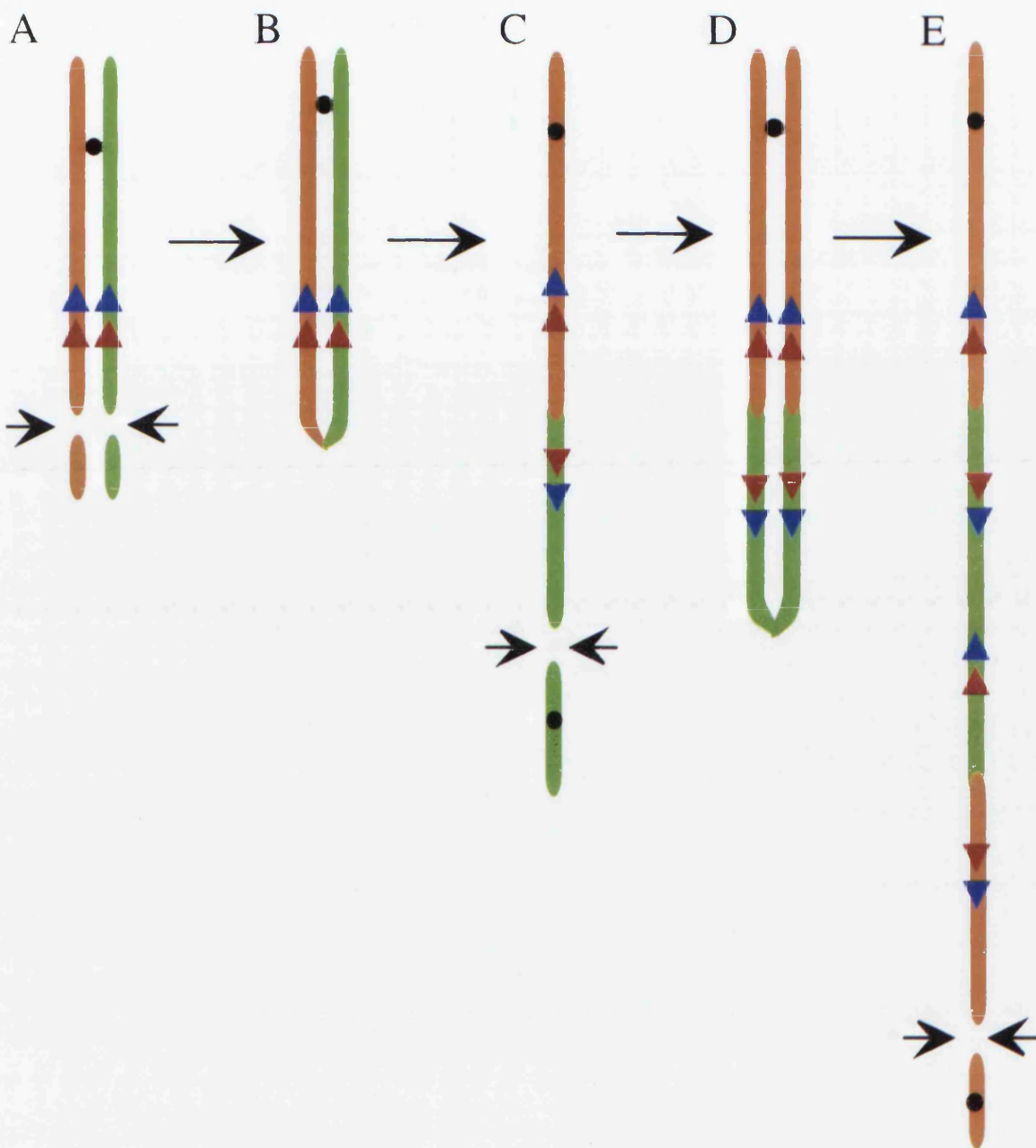
## **Figure 3E**

### **Extended model of gene amplification for CALU-3**

This figure shows an extended version of Figure 3D, with the red and blue triangles representing two hypothetical genes and their orientation. The sister chromatids are depicted in orange and green and the centromere is shown as a black circle.

This pathway begins at A with a normal chromosome which undergoes chromosomal breakage near the telomeres. This creates frayed ends which are then healed by fusion of the two sister chromatids (B). Following replication, the chromosome shown in C is produced. At this stage it can be seen that the gene copies from the green sister chromatid have become reversed in orientation. Another breakage then occurs at the telomere of this chromosome which again is healed by telomere fusion (D). A further round of DNA replication results in the chromosome shown in E. Therefore, as the copy number of the two genes increases, it can be seen that their orientation is also being changed.

There does not necessarily have to be telomere breakage at C, however. The model could also be continued by non-homologous exchange between the sister chromatids which may result in different copy numbers or orientations of the genes from that depicted in E.



## CHAPTER 4

# CHROMOSOME 17q AMPLICON: ANALYSIS OF GENE EXPRESSION

### 4.1 Introduction

This chapter will deal with expression of genes on chromosome 17q in CALU-3, as analysed using a variety of techniques. As mentioned in Chapter 1, topoisomerase II is the target for a number of commonly used chemotherapeutic agents. Where treatment with such topoisomerase II inhibitors is used, the level of expression of topoisomerase II within the tumour may be an important factor in the success of that treatment. Resistance to topoisomerase II inhibitors is now a major problem in the clinic and numerous studies have attempted to investigate the relationship between topoisomerase II expression levels in cells and sensitivity to drugs such as amsacrine (mAMSA) and etoposide (VP16) (Davies *et al.*, 1988; Fry *et al.*, 1991). Both of these studies report a correlation between topoisomerase II levels in cells and their chemosensitivity, with a higher level of topoisomerase II resulting in greater sensitivity of the cells to topoisomerase II inhibitors. It has also been shown in yeast cells that constitutive overexpression of a plasmid-borne TOP2 gene (encoding yeast topoisomerase II) leads to hypersensitivity of these cells to mAMSA and etoposide (Nitiss *et al.*, 1992).

Conversely, low levels of topoisomerase II alone have been associated with drug resistance in both cell lines derived from tumours and those having undergone *in vitro* drug selection (Giaccone *et al.*, 1992; Potmesil *et al.*, 1988; Ritke *et al.*, 1994; Webb *et al.*, 1991). This mechanism of drug resistance may be extremely important in certain tumour types where traditional drug resistance mechanisms, such as P-glycoprotein are rarely observed. However, it is not only low levels of topoisomerase II expression which can lead to drug resistance. Alterations to the topoisomerase II protein have also been found in cells selected for drug resistance *in vitro*. Such alterations may be in the form of point mutations, which result in a single amino acid changes in the protein (Bugg *et al.*, 1991; Danks *et al.*, 1993; Hinds *et al.*, 1991; Lee *et al.*, 1992) These changes are most commonly found to occur between residues 1346 and 1555, the site of consensus sequences which are known to bind ATP in other proteins, although alterations have also been found around the active site tyrosine at amino acid position 804 (Danks

*et al.*, 1993; Patel & Fisher, 1993). This is an important region of the topoisomerase II molecule because it is known that this tyrosine residue binds covalently to DNA during the catalytic cycle. Gross alterations to topoisomerase II have also been reported in connection with drug resistance (Mirski *et al.*, 1993). In this case a topoisomerase II $\alpha$ -related protein was observed in the derived resistant cell line, with an apparent molecular weight of 160kD as opposed to the normal 170kD mass of topoisomerase II $\alpha$ . A smaller mRNA molecule was also observed. Cell lines selected *in vitro* for resistance in VP16, VM26, adriamycin, mAMSA or mitoxantrone have sometimes been found to overexpress either P-glycoprotein or the multidrug resistance-associated protein MRP as well as having decreased levels of topoisomerase II (Cole *et al.*, 1991; de Jong *et al.*, 1993; Kamath *et al.*, 1992; Schneider *et al.*, 1994).

Thus, it can be seen that topoisomerase II plays an important role in both drug sensitivity and resistance in a variety of cell lines and tumours. Work outlined above demonstrates that alteration of topoisomerase II expression by amplification, mutation or deletion during tumour development could determine the response of those cells to topoisomerase inhibitors. A paper by Keith *et al.* in 1992 demonstrated the co-amplification of TOPO II $\alpha$  with the ERBB2 gene in a non-small cell lung adenocarcinoma cell line, CALU-3 (Keith *et al.*, 1992). It is presumed that this situation has arisen because of the proximity of TOPO II $\alpha$  to ERBB2 on 17q. Results shown in Chapter 3 confirm this co-amplification and also demonstrate the amplification of RAR $\alpha$  and G-CSF genes in CALU-3. It is therefore of interest to study the expression of the topoisomerase II $\alpha$  gene in CALU-3, to determine if amplification of this gene has led to increased levels of expression.

Some of the genes around this region of chromosome 17q have been implicated in the process of carcinogenesis, including ERBB2, RAR $\alpha$  and NM23H1. The ERBB2 gene (mapped to chromosome 17q21 by Fukushige *et al.* in 1986) was originally discovered, in two independent studies, by its homology with the v-ERBB gene and its amplification in the tumours analysed (King *et al.*, 1985; Semba *et al.*, 1985). The same gene had previously been identified as the transforming oncogene, NEU, in a series of rat neuroblastoma cells (Schechter *et al.*, 1984). The protein which ERBB2 encodes (a tyrosine-specific kinase receptor, p185<sup>neu</sup>) was found to display a strong homology to the epidermal growth factor (EGF) receptor (Coussens *et al.*, 1985; Yamamoto *et al.*, 1986) and its amplification and overexpression has been associated with tumour development and poor prognosis in breast

cancer (Gullick *et al.*, 1991; Lovekin *et al.*, 1991; Muss *et al.*, 1994; Slamon *et al.*, 1989; Winstanley *et al.*, 1991; Wright *et al.*, 1992).

Retinoids (derivatives of vitamin A) are important molecules in terms of cellular development and differentiation see Holdener & Bollag, 1993 and Leid *et al.*, 1992 for reviews. Three members of the retinoic acid receptor family have so far been isolated,  $\alpha$ ,  $\beta$  and  $\gamma$  (Elder *et al.*, 1991; Zelent *et al.*, 1989), with multiple isoforms found of RAR $\alpha$  and  $\gamma$  (Gaub *et al.*, 1992; Lazega *et al.*, 1993). The RAR $\alpha$  gene (mapped to chromosome 17q21 by Mattei *et al.* in 1988) is commonly found to be rearranged and fused to a novel gene, PML, in acute promyelocytic leukaemia (APL) (Chang *et al.*, 1991; de The *et al.*, 1990). It is thought that the PML gene product may be involved in RNA processing because of its speckled nuclear localisation and also some of the domains within the protein are found in components of ribonucleoprotein complexes (Kastner *et al.*, 1992).<sup>\*</sup> The RAR $\alpha$ -PML gene translocation results in the production of two reciprocal fusion proteins, PML/RAR $\alpha$  and RAR $\alpha$ /PML (Kastner *et al.*, 1992; Pandolfi *et al.*, 1991), with PML/RAR $\alpha$  thought to play the primary role in leukaemogenesis, since this isoform contains the functional domains of both proteins and is found in all patients with t(15;17) translocation. The finding of this translocation was of great interest since APL patients were known to undergo complete remission after a few weeks of treatment with retinoic acid (Castaigne *et al.*, 1990; Meng-Er *et al.*, 1988; Warrell *et al.*, 1991; Gillard & Solomon, 1993). Retinoids are also used as adjuvant therapy in cancer chemotherapy due to their ability to cause cellular differentiation (Bollag & Holdener, 1992; Costa, 1993; Holdener & Bollag, 1993).

The NM23H1 gene was initially discovered by Steeg *et al.* by differential colony hybridisation of a panel of related murine melanoma cell lines with varying metastatic potential (Steeg *et al.*, 1988a). A second NM23 gene was subsequently identified, having significant homology to NM23H1 (Stahl *et al.*, 1991). It is thought that the two genes are differentially regulated since RNA levels are seen to differ for each gene in the same tumour. Expression of the NM23H1 gene (mapped by Varesco *et al.*, (1992) to 17q22) has been investigated in CALU-3 as the protein product is proposed to have an effect on the metastatic potential of certain tumour cells (Leone *et al.*, 1993a; Leone *et al.*, 1993b; Steeg *et al.*, 1988b; Wang *et al.*, 1993). Expression of the NM23H1 gene has been correlated with the proliferative stages of the cell cycle (Igawa *et al.*, 1994). The nm23H1 and H2 proteins were recently identified as being nucleoside diphosphate (NDP) kinase A and NDP kinase B, respectively (Gilles *et al.*, 1991; Wallet *et al.*, 1990). Cellular NDP kinase

is an oligomer of these individual NDP subunits. NDP kinases play major roles in the synthesis of nucleoside triphosphates (other than ATP), regulation of microtubule assembly and disassembly and are also found associated with GTP-binding proteins, so may be involved in regulation of some signal transduction pathways (Liotta & Steeg, 1990). Thus it can be seen how alterations in expression of these proteins could affect both cellular motility and proliferation.

Analysis of gene expression in CALU-3 has been performed using a variety of techniques on both amplified and non-amplified genes. Northern analysis was initially carried out to investigate any alterations in expression of the three topoisomerase genes, I, II $\alpha$  and II $\beta$  at the RNA level. A number of small cell lung cancer (SCLC) cell lines were screened on this Northern at the same time as the non-small cell lung cancer (NSCLC) cell lines. Western and immunofluorescence analysis has also been performed on CALU-3, L-DAN and SK-MES-1 using antibodies against the TOPO II $\alpha$ , ERBB2, RAR $\alpha$  and NM23H1/2 gene products. Western analysis enables quantitative measurement of topoisomerase II $\alpha$  protein levels, whereas immunofluorescence shows cellular localisation of the enzyme, and any differences in expression amongst cells of the same population. Any qualitative differences in topoisomerase II between the three cell lines were detected using biochemical and band depletion assays. Flow cytometry was used to investigate cellular proliferation in L-DAN, CALU-3 and SK-MES-1, and the cell cycle regulation of topoisomerase II $\alpha$ , nm23H1/H2 and erbB2 expression in these cell lines. The possibility of alterations in the chromatin structure around the TOPO II $\alpha$  and TOPO II $\beta$  genes was also investigated by analysis of methylation status of these genes.

The expression analyses undertaken in this chapter utilised the non-small cell lung cancer cell lines L-DAN and SK-MES-1 as examples of cell lines with no evidence of TOPO II $\alpha$  gene amplification.

## **4.2 Results**

In this part of the study, expression analysis of a number of genes in the 17q12-telomere region has been undertaken. From Chapter 3 it is known that the loci for ERBB2, RAR $\alpha$ , G-CSF and TOPO II $\alpha$  genes, are amplified in CALU-3. Southern data shows the NM23H1 and protein kinase C alpha (PKC $\alpha$ ) genes are outside the amplicon in CALU-3. To investigate whether amplified genes are overexpressed in CALU-3, and to determine if an elevated level of the topoisomerase II $\alpha$  enzyme is the cause of the sensitivity of CALU-3 to topoisomerase II inhibitors, a number of different techniques have been utilised.

### **Northern Blot Analysis of TOPO II $\alpha$ Expression**

Northern blotting was initially used to investigate TOPO II $\alpha$  expression in L-DAN, CALU-3 and SK-MES-1. Figure 4.1 shows an example of a Northern with these three non-small cell lung tumour cell lines plus a number of other cell lines derived from small cell lung tumours. The same blot was reprobbed 4 times with cDNA probes for TOPO II $\alpha$  (panel a), TOPO II $\beta$  (panel b), TOPO I (panel c) and 7S (panel d) genes. From Figure 4.1 (lane 1) CALU-3 was seen to express high levels of TOPO II $\alpha$  mRNA. No overexpression of TOPO II $\beta$  or TOPO I was observed relative to L-DAN or SK-MES-1. SK-MES-1 (lane 3) was seen to express all three topoisomerases. L-DAN (lane 2) was underloaded so expression of TOPO II $\beta$  and TOPO I genes was difficult to detect (panels b and c respectively). Thus, of these three non-small cell lung tumour cell lines, CALU-3 has the highest expression of topoisomerase II $\alpha$  mRNA, which may be presumed to be a result of the amplification of the TOPO II $\alpha$  gene.

A number of small cell lung tumour cell lines were screened at the same time, although no further analysis was performed. Lanes 4-9 contain samples of RNA from these cell lines. LS263 (Lane 4) was developed from a post-therapy biopsy of a neck node metastasis which appeared to be intrinsically resistant to treatment in the clinic (3 cycles of cyclophosphamide, doxorubicin, vincristine, etoposide and verapamil). From blots a, b and c it can be seen that this tumour expresses very low levels of all three topoisomerases. LS277 (Lane 5) was derived from a pre-treatment biopsy of a chemosensitive small cell lung tumour. Blot a shows that this cell line has a relatively high level of TOPO II $\alpha$  RNA expression. The samples in lanes 6

## **Figure 4.1**

### **Detection of topoisomerase RNA expression levels by Northern blot analysis.**

**(a): TOPO II $\alpha$  (SP1), (b): TOPO II $\beta$  (SP12),  
(c): TOPO I (ScI70), (d): 7S**

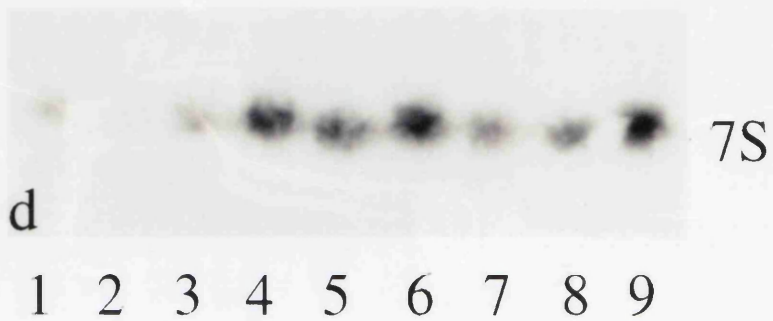
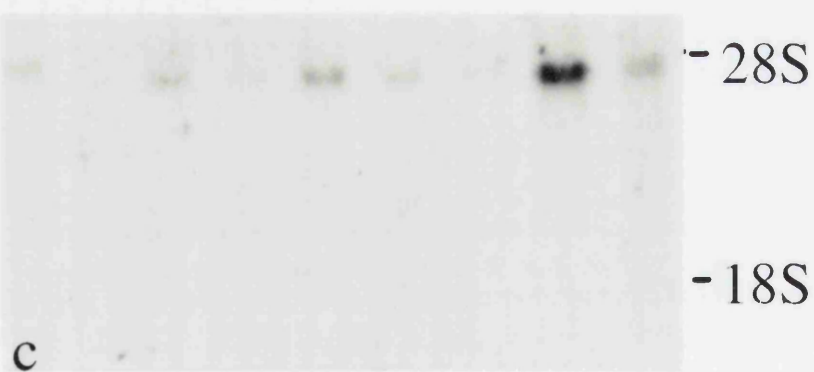
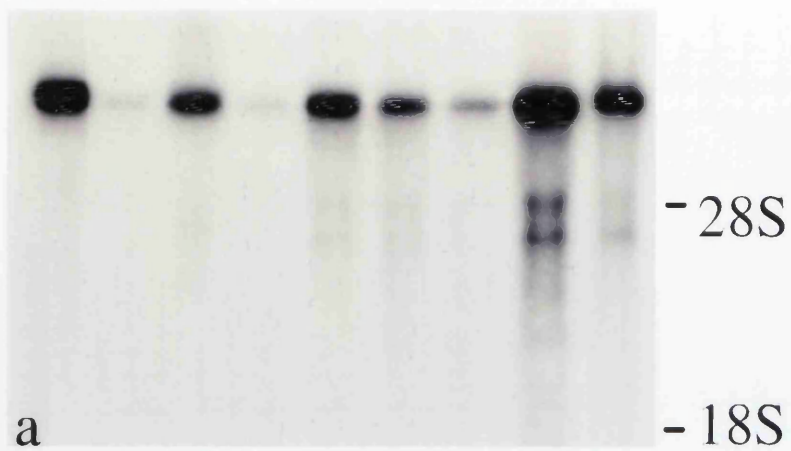
**Lane 1: CALU-3, Lane 2: L-DAN, Lane 3: SK-MES-1,  
Lane 4: LS263, Lane 5: LS277, Lane 6: LS274,  
Lane 7: LS310, Lane 8: LS112, Lane 9: LS112ST**

Sizes of mRNA detected:

28S= ~5kb, 18S= ~2kb, TOPO II $\alpha$ = 6.5kb, TOPO II $\beta$ = 6.5kb,  
TOPO I= 4.1kb

CALU-3, L-DAN and SK-MES-1 are all non-small cell lung carcinoma cell lines. All other cell lines mentioned were derived within the Department of Medical Oncology from biopsies of small cell lung tumours (or their metastases). The 7S RNA probe was used as a loading control.

From blot (a) it is clear that CALU-3 (Lane 1) overexpresses mRNA from the TOPO II $\alpha$  gene when compared to the other cell lines. It does not overexpress RNA from either the TOPO II $\beta$  or TOPO I genes.



1 2 3 4 5 6 7 8 9

and 7 (LS274 and LS310) were derived from pre- and post-treatment (4 cycles of therapy as for LS263 but without verapamil) biopsies respectively. Although there appears to be some drop in TOPO II $\alpha$  expression in LS310, there is a slight imbalance in loading between the two samples which may account for this result. LS112 (Lane 8) was developed from a very advanced tumour and is seen to express high levels of all three topoisomerases. LS112ST is a more adherent derivative of LS112 and appears to show lower levels of topoisomerase expression.

### **Western Blot and Immunofluorescence Analysis of TOPO II $\alpha$ Expression**

Having found increased expression of TOPO II $\alpha$  mRNA, Western blotting was used to detect topoisomerase II $\alpha$  protein expression in CALU-3. Figure 4.2 shows the high levels of topoisomerase II $\alpha$  protein seen in CALU-3 (lane 2). Densitometric analysis of this autoradiograph showed CALU-3 to express 10-15 times more protein than either L-DAN or SK-MES-1. Therefore, overexpression of TOPO II $\alpha$  mRNA appears to lead to enhanced production of the enzyme in CALU-3. Immunofluorescence was also used to examine topoisomerase II $\alpha$  enzyme levels in the three cell lines. This technique detects subcellular localisation of the topoisomerase II $\alpha$  protein and its cell to cell distribution in a cell population. As can be seen in Figure 4.3, topoisomerase II $\alpha$  is detected in CALU-3 cells only (panel b). Figure 4.3 also shows the nucleoplasmic localisation of topoisomerase II $\alpha$  and the heterogeneous nature of expression amongst this population of cells. Very high expression of the protein is seen in the mitotic cell in panel (b), which correlates with the upregulation of topoisomerase II $\alpha$  protein known to occur at the G2/M phase of the cell cycle (Kaufmann *et al.*, 1991; Prosperi *et al.*, 1994; Prosperi *et al.*, 1992).

### **Biochemical Assays for Topoisomerase II**

In order to prove that the topoisomerase II enzyme produced in CALU-3 had catalytic activity, decatenation assays were performed using a kit supplied by TopoGEN (see section 2.2.11 for details). This assay uses the ability of topoisomerase II to decatenate kinetoplast DNA to minicircles (via DNA breakage and strand passage) as a measurement of the enzymes' activity in that sample. It does not, however, distinguish between the alpha and beta forms of topoisomerase II. The same extracts were used in these assays and the Western analysis (Figure 4.2). Figure 4.4 shows the results of one such

## **Figure 4.2**

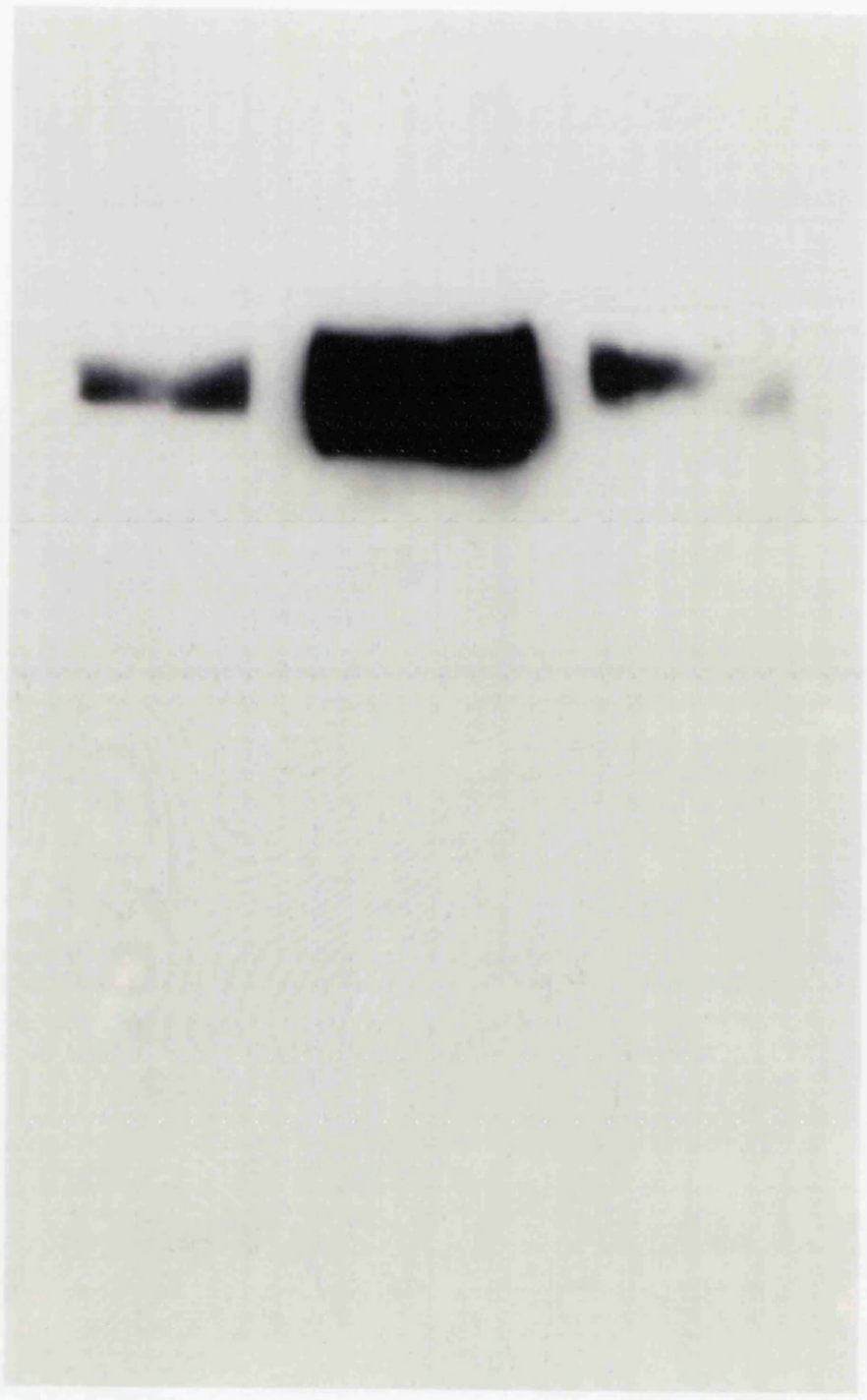
### **Detection of topoisomerase II $\alpha$ expression by Western blot analysis.**

**Lane 1: L-DAN, Lane 2: CALU-3, Lane 3: SK-MES-1**

Molecular mass of topoisomerase II $\alpha$ = 170kD

Fifty microgrammes of nuclear extract were run per lane. Molecular mass standards in kiloDaltons are shown to the right of the autoradiograph. A polyclonal antibody from Cambridge Research Biochemicals was used to detect topoisomerase II $\alpha$  expression.

The CALU-3 extract (Lane 2) is seen to contain higher levels of topoisomerase II $\alpha$  than either of the other two cell extracts. Thus amplification of the TOPO II $\alpha$  gene, and enhanced mRNA level in CALU-3 appear to lead to a greater production of the enzyme.



-206

-110

1

2

3

### **Figure 4.3**

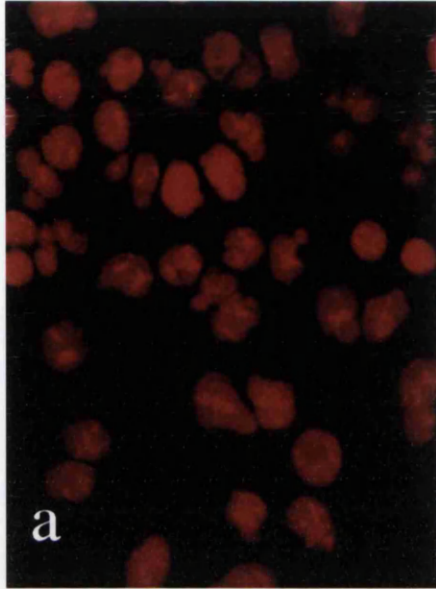
#### **Detection of TOPO II $\alpha$ gene expression by immunofluorescence.**

**(a):** L-DAN, **(b):** CALU-3, **(c):** SK-MES-1

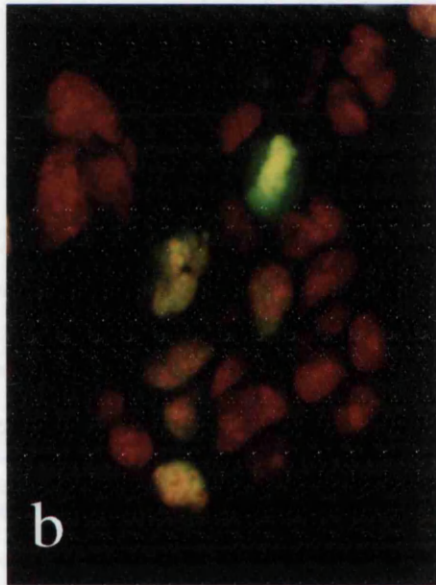
Nuclei are counterstained with propidium iodide (pseudocoloured red), topoisomerase II $\alpha$  detected with FITC (pseudocoloured green). A polyclonal antibody from TopoGEN was used to detect topoisomerase II $\alpha$ .

As can be seen from panel (b), topoisomerase II $\alpha$  expression (green signal) is only detectable in CALU-3, where there is known amplification of this gene. Expression of topoisomerase II $\alpha$  is found within the entire nucleoplasm of the cell and is also heterogeneous within a cell population.

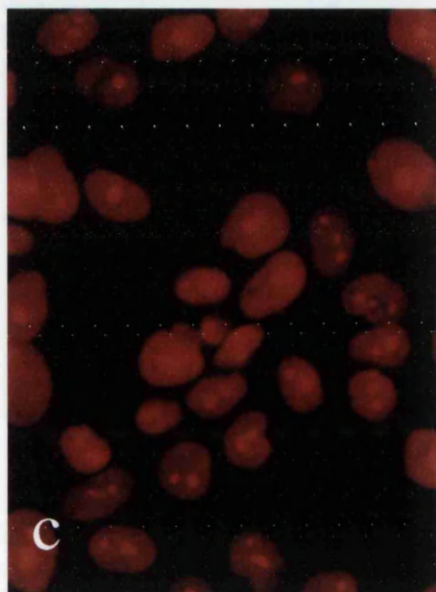
The cell with the strongest green signal in panel (b) is undergoing mitosis, as indicated by the condensed nature of the DNA. This correlates with the fact that topoisomerase II $\alpha$  expression is upregulated at the G2/M phase of the cell cycle.



L-DAN



CALU-3



SK-MES-1

## **Figure 4.4**

### **Decatenation of kinetoplast DNA by cellular extracts from (a): L-DAN, (b): CALU-3 and (c): SK-MES-1.**

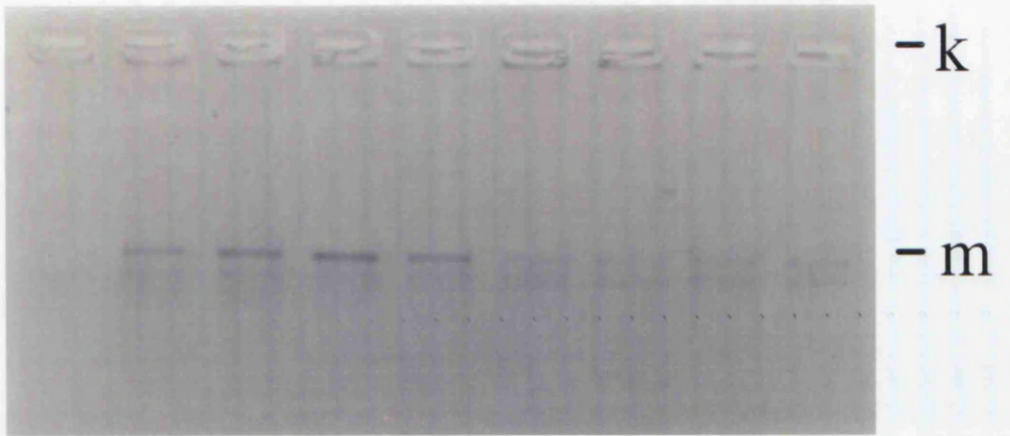
Serial dilutions of crude nuclear extracts were assayed for topoisomerase II activity:

**Lane 1: 0 $\mu$ g, Lane 2: 5 $\mu$ g, Lane 3: 2.5 $\mu$ g, Lane 4: 1.25 $\mu$ g,  
Lane 5: 0.625 $\mu$ g, Lane 6: 0.312 $\mu$ g, Lane 7: 0.156 $\mu$ g,  
Lane 8: 0.078 $\mu$ g, Lane 9: 0.039 $\mu$ g**

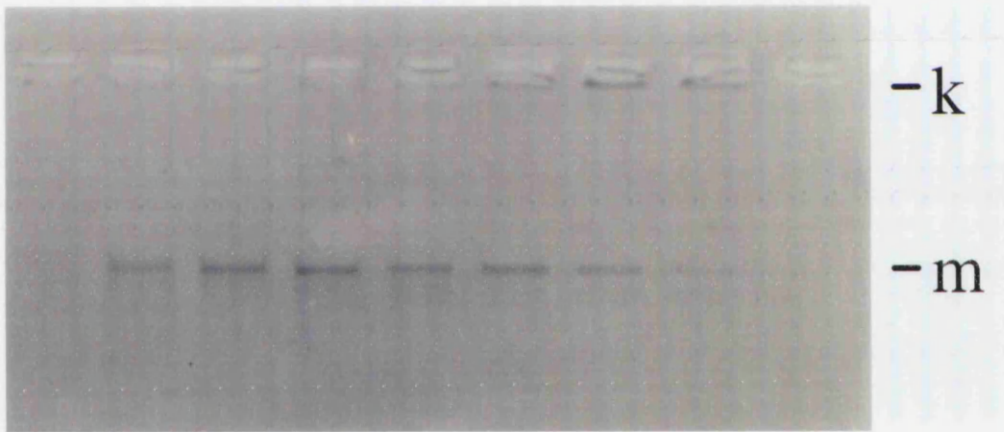
Topoisomerase II activity decatenates kinetoplast DNA to monomer minicircles (m). In the absence of cellular extract, kinetoplast DNA (k) remains in the well of the gel (Lane 1).

By comparing the three gels it can be seen that CALU-3 displays at least a four-fold increase in topoisomerase II activity since monomeric kDNA can be seen down to a protein concentration of 0.156 $\mu$ g. L-DAN and SK-MES-1 show minicircle formation down to a protein concentration of 0.625 $\mu$ g.

a



b



c



1 2 3 4 5 6 7 8 9

assay, with CALU-3 extract shown in panel (b). From this figure it is clear that decatenation activity (production of minicircles) occurs with lower concentrations of cell extract in CALU-3 (0.078 $\mu$ g) when compared with L-DAN or SK-MES-1 (0.625 $\mu$ g). Therefore, CALU-3 has at least eight-fold more topoisomerase II activity than either L-DAN or SK-MES-1. These other two cell lines have almost equivalent topoisomerase II activity.

Since the TOPO II $\alpha$  gene is amplified in CALU-3, it is possible that the gene may contain alterations rendering the protein insensitive to topoisomerase II inhibiting drugs (Takano *et al.*, 1992). To investigate this, decatenation assays were performed in the presence of the topoisomerase II interactive drug VP16. This drug stabilises the cleavable complex formed by topoisomerase II during its catalytic cycle thus inhibiting dissociation of the enzyme from the DNA. Therefore, when VP16 is added to a decatenation reaction, decatenation of kinetoplast DNA will be inhibited. If the topoisomerase II enzyme produced by CALU-3 is altered in a way which disturbs the binding of drug to enzyme then decatenation would not be affected. Figure 4.5 shows the affect of varying concentrations of VP16 on decatenation reactions containing L-DAN (panel a), CALU-3 (panel b) and SK-MES-1 (panel c) crude nuclear extract. A lower protein concentration was used per reaction for CALU-3 as for the other two cell lines because of the enhanced topoisomerase II activity seen in CALU-3. From lane 3 onwards the amount of minicircle DNA produced from the kinetoplast DNA is seen to be reduced in all three cell lines. In lane 5 of panels (a), (b) and (c) the reaction appears to have been almost completely inhibited. Therefore, VP16 is still capable of inhibiting topoisomerase II activity in all three cell lines, including CALU-3.

### **Band Depletion Assay**

As well as using extracts from the cell lines to study topoisomerase II activity, a whole cell approach, the band depletion assay, was also used to study interaction of topoisomerase II with VP16. By using antibodies against topoisomerase II $\alpha$  at the Western blotting step, interactions between this isozyme only and VP16 can be studied. The band depletion assay involves treating living cells in culture with varying concentrations of VP16 (described in section 2.2.10.3), making extracts from these cells and analysing the extracts using Western blotting. When cells are treated with drugs such as VP16, the catalytic cycle of topoisomerase II $\alpha$  is disturbed. Normally during the strand passage/religation reaction, where VP16 acts, the topoisomerase II $\alpha$

## **Figure 4.5**

### **Inhibition of topoisomerase II activity by VP16.**

**(a): L-DAN, (b): CALU-3, (c): SK-MES**

Crude nuclear extracts from the above three cell lines were assayed for decatenation activity in the presence of increasing concentrations of VP16.

**Lane 1:** no drug, no nuclear extract,

**Lane 2:** no drug, DMSO diluant control, **Lane 3:** 10 $\mu$ M VP16,

**Lane 4:** 100 $\mu$ M VP16, **Lane 5:** 200 $\mu$ M VP16

k= kinetoplast DNA, m=monomer minicircles

2.5 $\mu$ g of protein was used in assays (a) and (c). 1.25 $\mu$ g protein was used in assay (b) due to the increased topoisomerase II activity seen in CALU-3.

From this figure it can be seen that VP16 is capable of inhibiting topoisomerase II activity in L-DNA, CALU-3 and SK-MES-1.

a



- k

- m

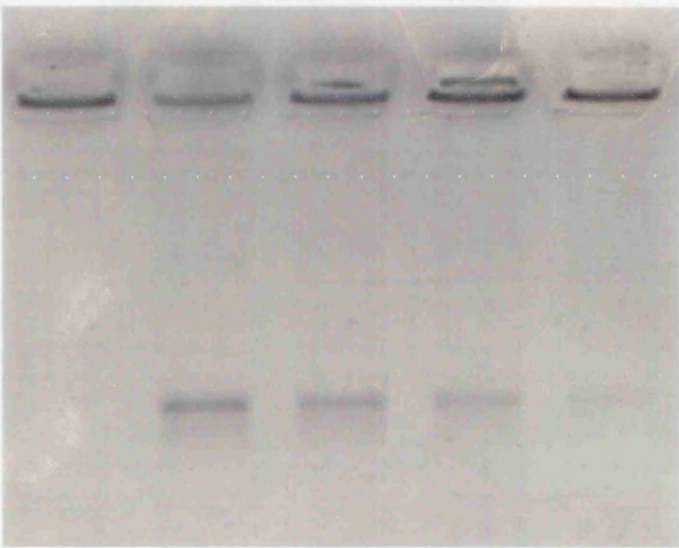
b



- k

- m

c



- k

- m

1 2 3 4 5

molecule is free to dissociate from the DNA. Once cells are treated, however, the drug stabilises these protein/DNA interactions and large complexes of drug, protein and DNA are formed (as in the decatenation inhibition reactions above). If a protein extract is then made from these cells, detection of the topoisomerase II $\alpha$  is prevented since the complex cannot be resolved on a polyacrylamide gel. Figure 4.6 depicts this technique diagrammatically, with concentration of VP16 increasing from left to right. Theoretically, therefore, little topoisomerase II $\alpha$  should be detected at high drug concentrations. Figure 4.7 shows an autoradiograph developed from a band depletion assay. The highest concentration of drug was used in samples run in lanes 2, 6 and 10, where a visible depletion in the amount of topoisomerase II $\alpha$  can be seen compared to no drug controls (lanes 1, 5 and 9) in L-DAN, CALU-3 and SK-MES-1. Thus the topoisomerase II $\alpha$  enzyme from each cell line is still able to be trapped by VP16 on genomic DNA.

### **Flow Cytometry**

Flow cytometry was used as a method to investigate both normal cellular proliferation of L-DAN, CALU-3 and SK-MES-1 and the cell cycle regulation of topoisomerase II $\alpha$ , nm23H1/H2 and erbB2 expression in these cell lines. The cell cycle analysis was performed using bromodeoxyuridine (BrdUrd), which incorporates into DNA during replication. Therefore, this technique detects those cells which have been through S phase. Figure 4.8 shows the results from a FACS experiment after cells have been incubated with BrdUrd for 4 hours. The left-hand panels, (a) L-DAN, (c) CALU-3 and (e) SK-MES-1, show FACS printouts in which cells in G0/G1, G1-S and G2/M phases can be distinguished by the amount of BrdUrd incorporation (FITC fluorescence), together with intensity of PI staining. FITC fluorescence is measured along the LFL1 axis and FL3 measures PI fluorescence. Thus cells in box 1 can be said to be in G0 or G1 with a 2n DNA content and cells in box 4 are in G2 or M phase with a 4n DNA content, since these cells have been through S phase. Cells in box 2 are progressing into S phase from G1 and cells in box 3 are progressing through S phase. Table 4.1 shows the percentages of cells in the different stages of the cell cycle for L-DAN, CALU-3 and SK-MES-1 calculated from this experiment. From this data there appears to be strong agreement between duplicate samples and little difference in the distribution between the cell cycle phases in the three cell lines.

## **Figure 4.6**

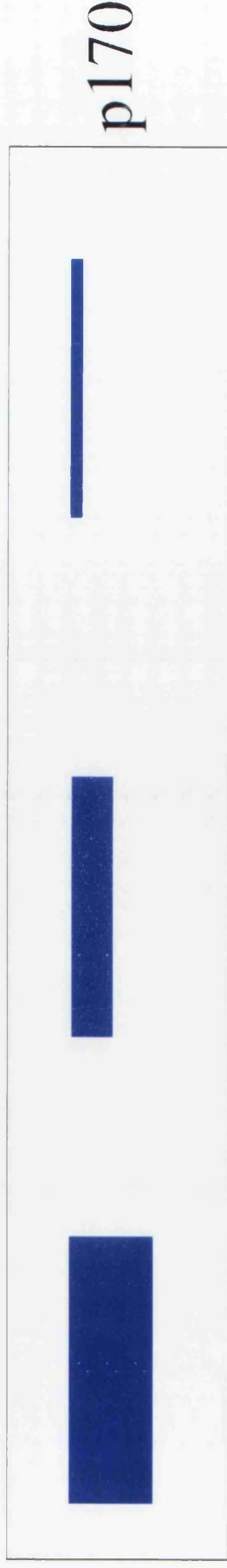
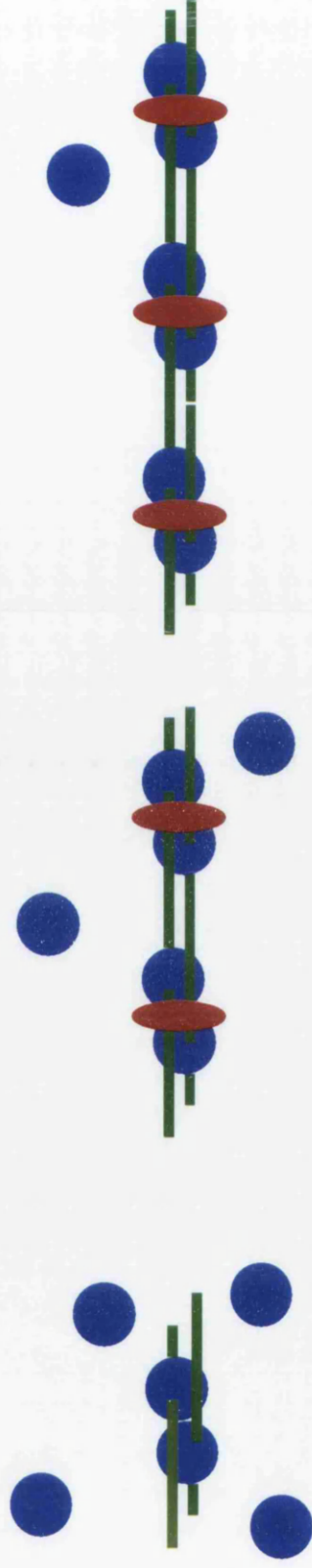
### **Diagrammatic explanation of the band depletion assay**

Three situations are outlined in this diagram. On the far left is an untreated cell, where the topoisomerase II enzyme is free to bind to and dissociate from the DNA. When Western analysis for topoisomerase II $\alpha$  is performed using protein extract from this cell, a large amount of topoisomerase II $\alpha$  is detected.

The middle panel depicts the situation where cells have been incubated with fairly low concentrations of drug. The drug has bound to the topoisomerase II $\alpha$ /DNA complexes, but there is still some topoisomerase II $\alpha$  free in the nucleus. It is this free topoisomerase II which is detected following Western analysis.

The final diagram depicts the results when using high concentrations of drug. Most of the topoisomerase II $\alpha$  is bound in stable drug/DNA complexes and unable to be resolved upon Western analysis. Thus very little topoisomerase II $\alpha$  is detectable on the Western blot.

## Band Depletion Assay



## Western Analysis

● = topo IIα    ● = VP16    — = dsDNA

## **Figure 4.7**

### **Band depletion assay of topoisomerase II $\alpha$ using whole cell lysates, analysed by Western blot.**

Cells were incubated with decreasing amounts of VP16 for 2 hours at 37°C and then lysed in protein lysis buffer. Samples were resolved on a 6% polyacrylamide gel (see Section 2.2.10.3).

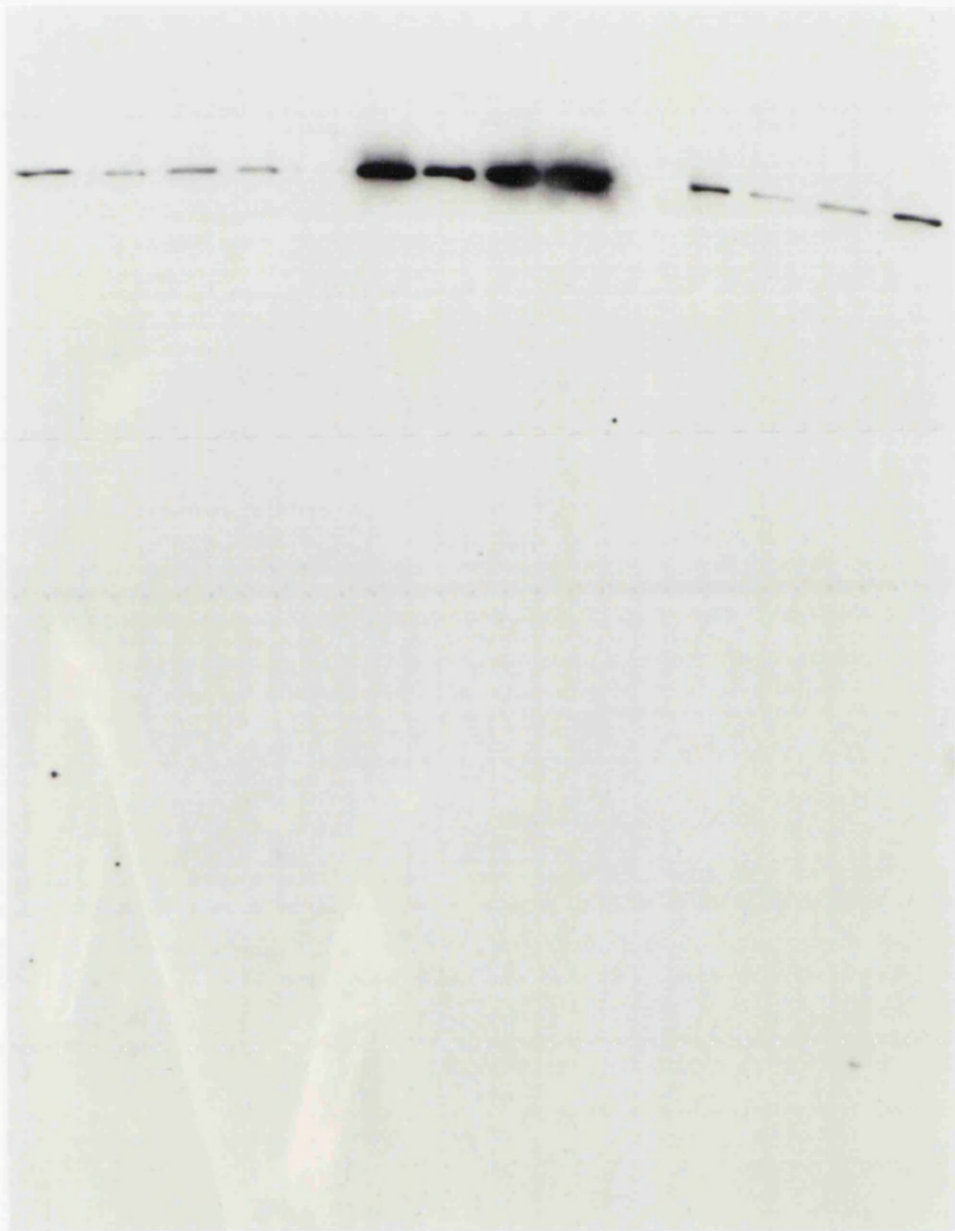
**Lanes 1-4: L-DAN, Lanes 5-8: CALU-3,  
Lanes 9-12: SK-MES-1**

Cells in lanes 1,5 and 9 were not treated with drug, those in lanes 2,6 and 10 were treated with  $5 \times 10^{-4}$ M VP16, those in lanes 3,7 and 11 were treated with  $5 \times 10^{-5}$ M VP16 and those in lanes 4, 8 and 12 were treated with  $5 \times 10^{-6}$ M VP16.

Molecular mass standards in kiloDaltons are shown to the right of the autoradiograph. A polyclonal antibody from Cambridge Research Biochemicals was used to detect topoisomerase II $\alpha$ .

From the autoradiograph it can be seen that cells treated with higher concentrations of VP16 show a decrease in the amount of topoisomerase II $\alpha$  detected on the Western. This depletion of band intensity is caused by the topoisomerase enzyme becoming trapped in a DNA/drug/enzyme complex which is unable to migrate in a polyacrylamide gel due to its large molecular size.

L-DAN, CALU-3 and SK-MES-1 all show a depletion in the amount of topoisomerase II $\alpha$  detected when cells are challenged with VP16. Therefore the enzyme from each cell line is still able to be trapped by VP16 on genomic DNA.



- 206

- 110

- 70

- 43

- 28

1 2 3 4 5 6 7 8 9 10 11 12

## **Figure 4.8**

### **Cell cycle analysis using bromodeoxyuridine incorporation.**

**(a) & (b): L-DAN, (c) & (d): CALU-3, (d) & (e): SK-MES-1**

Nuclei were stained with PI (visualised in red in panels b, d and f).

BrdUrd was detected with a mouse anti-BrdUrd antibody. The secondary anti-mouse antibody was conjugated to FITC (visualised in green in panels b, d and f).

LFL1: Log FITC value

FL3: PI value

Box 1: G0/G1 phase

Box 2: G1-S phase

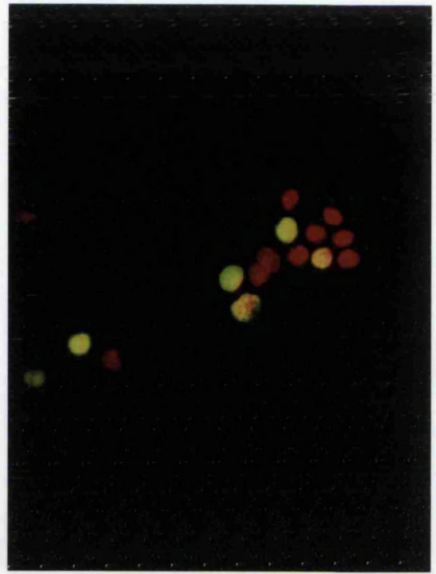
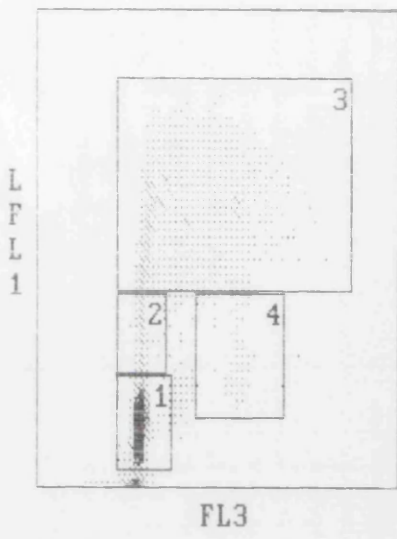
Box 3: S phase

Box 4: G2/M phase

Panels (a), (c) and (e) show FACS results for cell cycle analysis after a four hour BrdUrd incubation period.

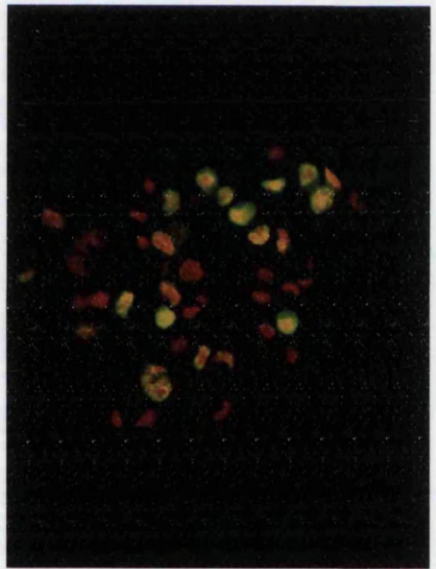
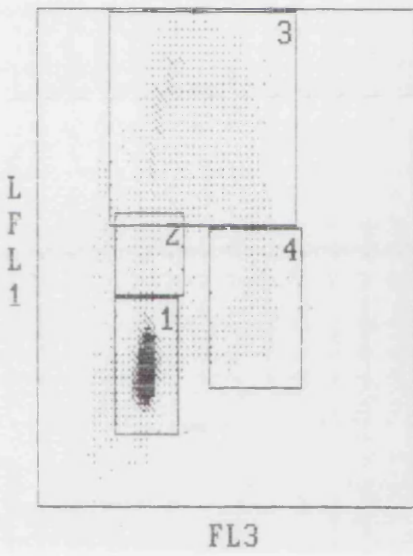
Panels (b), (d) and (f) show the same FACS samples as in (a), (c) and (e) analysed by fluorescence microscopy.

From panels (a), (c) and (e) it can be seen that all three cell lines undergo a routine cell cycle, with cells observed at all different phases. Panels (b), (d) and (f) show that green fluorescence is observed in a proportion of the cells from L-DAN, CALU-3 and SK-MES-1 when analysed by fluorescence microscopy, indicating BrdUrd incorporation and therefore cells in S phase.



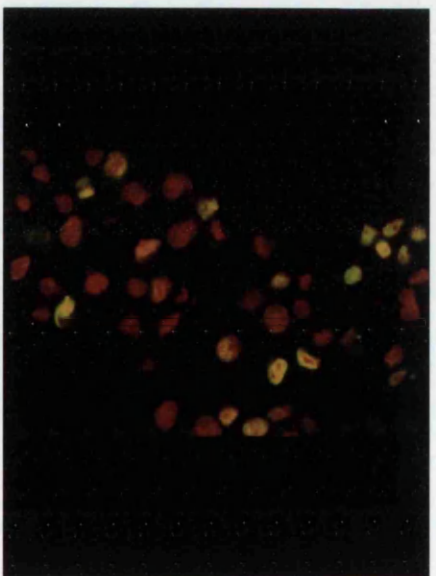
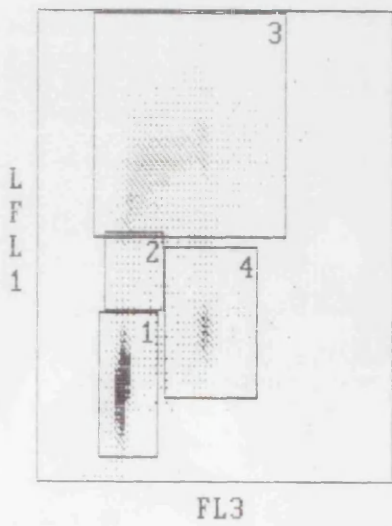
a

b



c

d



e

f

**Table 4.1****Percentage of cells in the different stages of the cell cycle**

	<b>% G0/G1</b>	<b>% G1/S</b>	<b>% S</b>	<b>% G2/M</b>
<b>L-DAN (1)</b>	47.3%	4.3%	40.9%	2.3%
<b>L-DAN (2)</b>	43.5%	3.8%	45.8%	3.0%
<b>CALU-3 (1)</b>	57.2%	4.2%	29.0%	5.5%
<b>CALU-3 (2)</b>	47.8%	6.4%	37.7%	9.2%
<b>SK-MES-1 (1)</b>	39.9%	4.3%	41.2%	8.9%
<b>SK-MES-1 (2)</b>	43.5%	4.0%	41.2%	10.1%

In Figure 4.8, the right-hand panels, (b) L-DAN, (d) CALU-3 and (f) SK-MES-1 show the same BrdUrd FACS samples from (a), (c) and (e) analysed by fluorescence microscopy. By using this type of analysis, FITC and PI fluorescence can be visualised (green signal and red signal respectively). Therefore, this can be used as a control for the FACS printouts since the fluorescence can actually be seen down the microscope. Panels (b), (d) and (f) clearly show the different intensities of FITC fluorescence in L-DAN, CALU-3 and SK-MES-1 indicating differential incorporation of BrdUrd. Differences in PI fluorescence are more difficult to see since these images merge both PI and FITC signals. Thus, from Figure 4.8 it appears that L-DAN, CALU-3 and SK-MES-1 undergo a routine cell cycle with cells observed in all stages of the cycle.

Figure 4.9 shows the results of FACS analysis of topoisomerase II $\alpha$  expression in L-DAN (a and b), CALU-3 (c and d) and SK-MES-1 (e and f). From panels (a) and (e), it can be seen that there are low levels of topoisomerase II $\alpha$  expression in L-DAN and SK-MES-1, with the highest peak of expression (high level of FITC fluorescence) seen in box 4. This equates with the G2/M phase of the cell cycle which is where highest expression of topoisomerase II $\alpha$  has been observed previously (Kaufmann *et al.*, 1991; Prosperi *et al.*, 1994; Prosperi *et al.*, 1992). Panel (c) shows the very high level of topoisomerase II $\alpha$  observed in CALU-3, in which the highest peak of topoisomerase II $\alpha$  expression still appears to be in G2/M. Panels (b), (d) and (f) also show the levels of topoisomerase II $\alpha$  expression in L-DAN, CALU-3 and SK-MES-1, shown by green signal. Again, low numbers of topoisomerase II $\alpha$  expressing cells are visible in L-DAN and SK-MES-1 with a higher number of expressing cells visible in CALU-3. Table 4.2 shows the number of cells in different stages of the cell cycle, calculated from the experiment shown in panels (a), (c) and (e) in Figure 4.9. All the figures shown in this table have been adjusted against a no primary antibody control experiment which was performed in parallel. Table 4.3 shows percentages for each cell cycle stage calculated from the data presented in Table 4.2. From Table 4.3 it can be seen that although the percentages are markedly higher for CALU-3, there is still a rise in the percentage of cells expressing topoisomerase II $\alpha$  from G1 to G2/M. Therefore, it appears that CALU-3 still has cell cycle regulation of topoisomerase II $\alpha$  expression.

FACS analysis was also performed using the antibody against nm23H1/H2 proteins. The results from this experiment are shown in Figure 4.10. Panels (a), (c) and (e) show FACS printouts of nm23H1/H2 expression for L-DAN, CALU-3 and SK-MES-1 respectively. Panels (b), (d) and (f)

## **Figure 4.9**

### **Cell cycle regulation of topoisomerase II $\alpha$ expression by FACS.**

**(a) & (b): L-DAN, (c) & (d): CALU-3, (e) & (f): SK-MES-1**

Nuclei were stained with PI (visualised in red in panels b, d and f).

Topoisomerase II $\alpha$  protein was detected with a polyclonal antibody from CRB and the secondary antibody was conjugated to FITC (visualised in green in panels b, d and f).

FL1: FITC value

FL3: PI value

Panel (a):           Box 1: G1, topoisomerase II $\alpha$  negative  
                          Box 3: G1, topoisomerase II $\alpha$  positive  
                          Box 2: G2, topoisomerase II $\alpha$  negative  
                          Box 4: G2, topoisomerase II $\alpha$  positive

Panels (c) & (e):   Box 1: G1, topoisomerase II $\alpha$  negative  
                          Box 2: G1, topoisomerase II $\alpha$  positive  
                          Box 3: G2, topoisomerase II $\alpha$  negative  
                          Box 4: G2, topoisomerase II $\alpha$  positive

Panels (a), (c) and (e) show FACS results of topoisomerase II $\alpha$  expression in L-DAN, CALU-3 and SK-MES-1 respectively.

Panels (b), (d) and (f) show the same FACS samples as in (a), (c) and (e) analysed by fluorescence microscopy.

From panels (a), (c) and (e) it can be seen that all three cell lines express topoisomerase II $\alpha$  in the G1 and G2/M stages of the cell cycle (boxes 3 and 4 in a, boxes 2 and 4 in c and e). Panels (c) and (d) show high expression of topoisomerase II $\alpha$  in CALU-3.

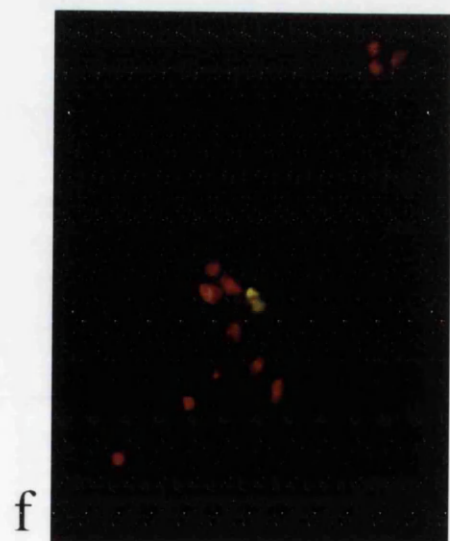
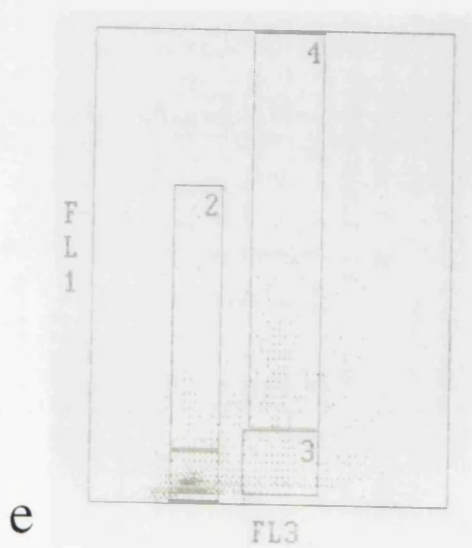
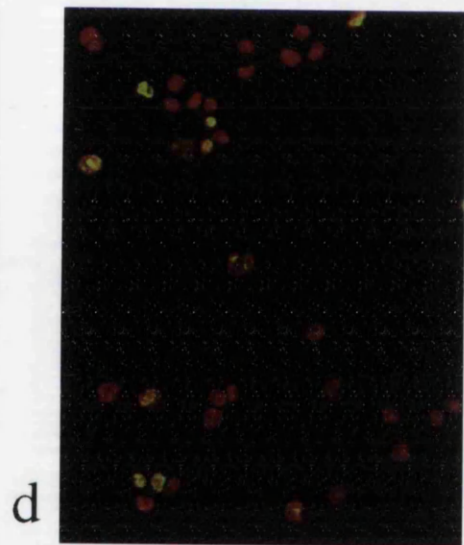
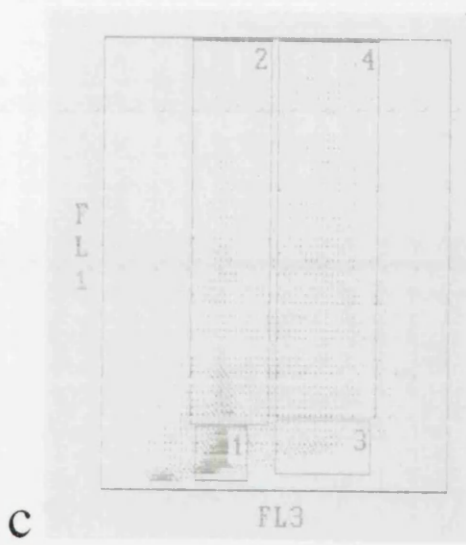
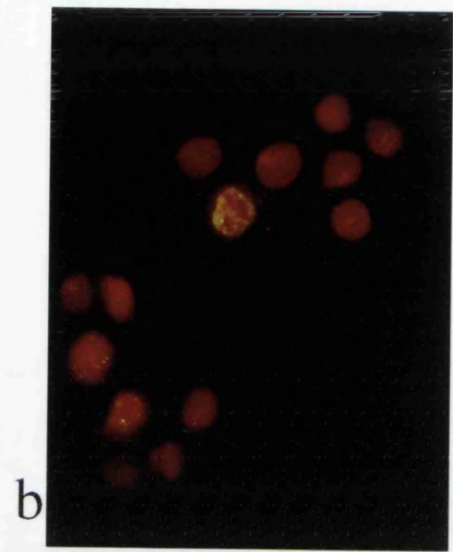
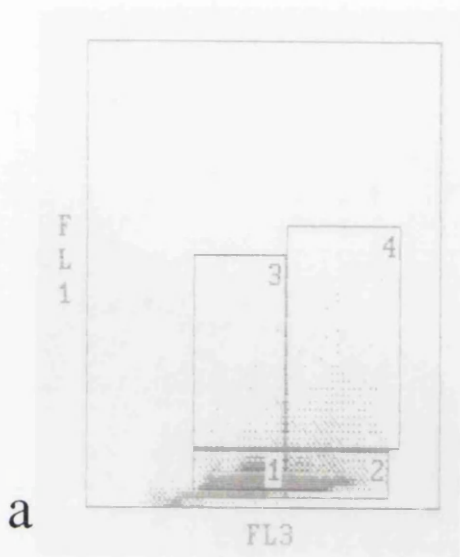


**Table 4.2**

**Number of cells in different stages of the cell cycle in a topoisomerase II $\alpha$  FACS experiment (polyclonal antibody)**

	<b>G1 total cell no.</b>	<b>G1 Topo II<math>\alpha</math> +ve cells</b>	<b>G2/M total cell no.</b>	<b>G2/M Topo II<math>\alpha</math> +ve cells</b>
<b>L-DAN (a)</b>	36270	1057	3151	494
<b>L-DAN (b)</b>	26634	122	3060	488
<b>CALU-3 (a)</b>	10597	4362	4268	3191
<b>CALU-3 (b)</b>	8957	5242	3956	3248
<b>SK-MES-1 (a)</b>	2903	155	420	136
<b>SK-MES-1 (b)</b>	1634	55	372	95

All numbers listed have been corrected against a no primary antibody control experiment

**Table 4.3**

**Percentage of cells positive for topoisomerase II $\alpha$  expression in G1 and G2/M (polyclonal antibody)**

	<b>% G1 positive cells</b>	<b>% G2 positive cells</b>
<b>L-DAN (a)</b>	3%	15%
<b>L-DAN (b)</b>	0.5%	15%
<b>CALU-3 (a)</b>	41%	74%
<b>CALU-3 (b)</b>	58%	82%
<b>SK-MES-1 (a)</b>	5%	32%
<b>SK-MES-1 (b)</b>	3%	25%

## **Figure 4.10**

### **FACS analysis of nm23H1/H2 expression.**

**(a) & (b): L-DAN, (c) & (d): CALU-3, (d) & (e): SK-MES-1**

Nuclei were stained with PI (visualised in red in panels b, d and f).

Nm23H1 and H2 proteins were detected with a polyclonal antibody from CRB and the secondary antibody was conjugated to FITC (visualised in green in panels b, d and f).

FL1: FITC value

FL3: PI value

Box 1: G1, nm23H1/H2 negative

Box 2: G1, nm23H1/H2 positive

Box 3: G2, nm23H1/H2 negative

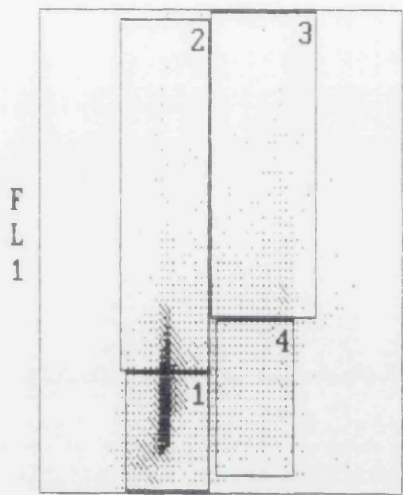
Box 4: G2, nm23H1/H2 positive

Panels (a), (c) and (e) show FACS results of nm23H1/H2 expression in L-DAN, CALU-3 and SK-MES-1 respectively.

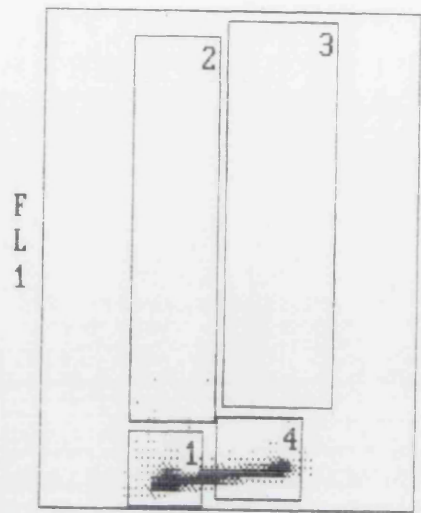
Panels (b), (d) and (f) show results of a FACS experiment using peptide-blocked anti-nm23H1/H2 antibody.

From panels (a), (c) and (e) it can be seen that all three cell lines express nm23H1 and H2. There does not appear to be any cell cycle regulation of these proteins in L-DAN, CALU-3 or SK-MES-1.

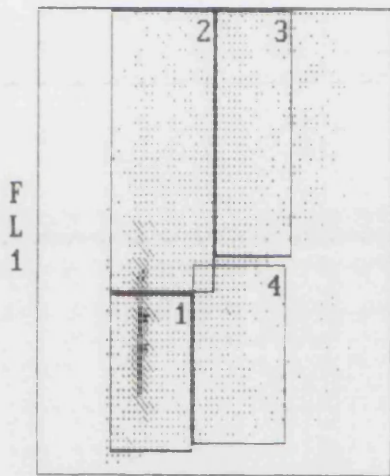
Panels (b), (d) and (f) show that when blocked primary antibody is used, very little expression of the nm23 proteins is observed.



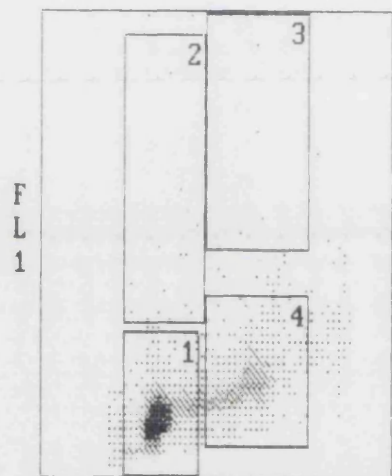
a



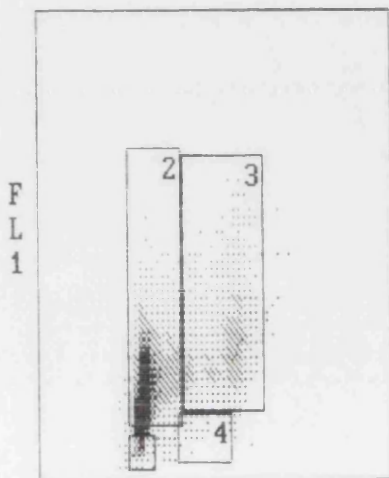
b



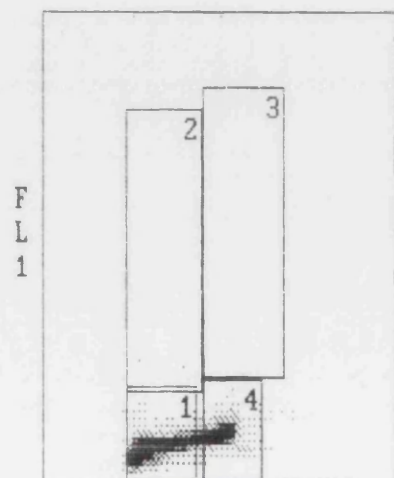
c



d



e



f

show a parallel experiment in which peptide-blocked primary antibody was used, and shows that there was very little nm23H1/H2 expression detectable. From the results shown in (a), (c) and (e) it can be seen that all three cell lines express the nm23 proteins, and that there does not appear to be any cell cycle regulation of nm23. When the anti-erbB2 antibody was used in FACS analysis, expression was observed only in CALU-3 and also did not appear to be cell cycle regulated (data not shown).

### **Investigation into the methylation status of the TOPO II $\alpha$ and TOPO II $\beta$ genes**

Changes in the methylation status of genes are known to have an effect on gene expression reviewed in Baylin *et al.*, 1991. Alterations in methylation state are also thought to play a role in the organisation of DNA structure, with heavily methylated regions being apparently inaccessible to the transcription machinery and thus not being expressed, and under methylated regions of DNA being much more loosely organised and thus more open to transcription (Antequera *et al.*, 1990; Tazi & Bird, 1990). Hypermethylation of DNA has been found in lung and colon carcinomas, particularly in regions of chromosomes where loss of heterozygosity occurs (Makos *et al.*, 1992). It is thought that DNA methylation inhibits the expression of genes (Cedar, 1988), and thus hypomethylation of genes could result in overexpression. Hypomethylation of genes has been observed in colon carcinomas, with increased hypomethylation in metastatic tumours (Feinberg & Vogelstein, 1983; Goelz & Vogelstein, 1985). Therefore, the methylation state of DNA may play a role in the tumorigenic process. Figure 4.11 shows the autoradiographs resulting from an investigation of hypomethylation of the TOPO II genes. A number of different tumour types were analysed, including the NSCLC cell lines L-DAN (lanes 15 & 16) and CALU-3 (lanes 17 & 18). In this study, the restriction enzymes *MspI* and *HpaII* were utilised. *MspI* will cleave DNA irrespective of its' methylation status. *HpaII*, on the other hand, will only cleave its' restriction site if it is not methylated. Since *MspI* and *HpaII* enzymes have the same restriction site, hypomethylated DNA would produce identical restriction fragments with both enzymes. From the data shown in Figure 4.11, however, there does not appear to be any evidence for hypomethylation of either the TOPO II $\alpha$  or TOPO II $\beta$  genes in any of the samples analysed.

## **Figure 4.11**

### **Investigation into the methylation status of TOPO II $\alpha$ and II $\beta$ genes, using Southern analysis.**

The same blot was probed with SP1 (TOPO II $\alpha$ ) and SP12 (TOPO II $\beta$ ) probes

**Lanes 1 & 2: R3E2, Lanes 3 & 4: Sample of lung tumour DNA,  
Lanes 5 & 6: LS274, Lanes 7 & 8: LS310,  
Lanes 9 & 10: LS112, Lanes 11 & 12: LS112ST,  
Lanes 13 & 14: LS112Adr, Lanes 15 & 16: CALU-3,  
Lanes 17 & 18: L-DAN**

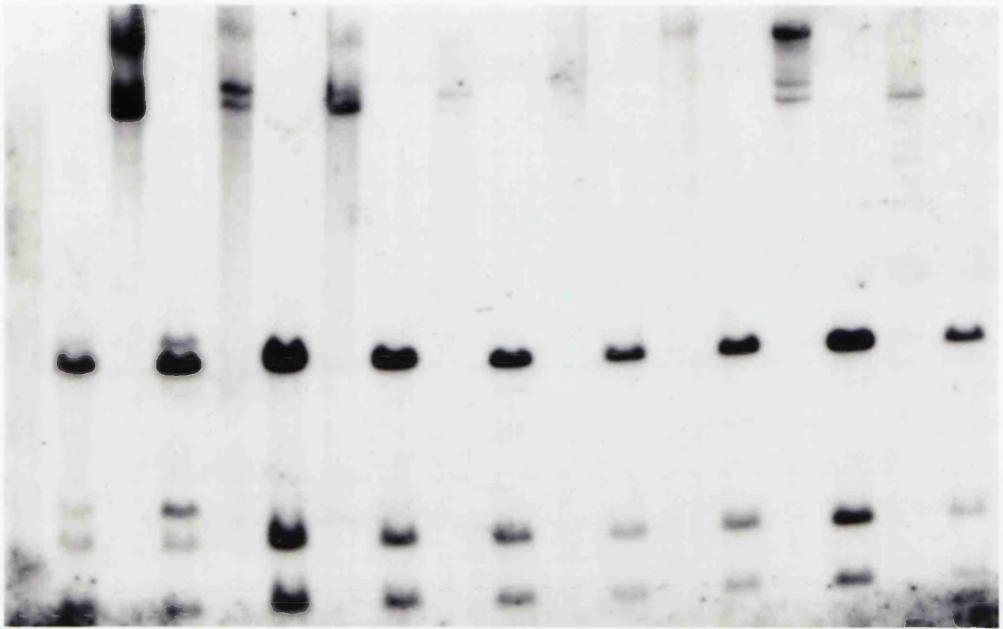
DNA loaded in odd-numbered lanes was digested with *HpaII*  
DNA loaded in even-numbered lanes was digested with *MspI*

R3E2 is a cell line derived from normal bowel. LS274, LS310, LS112, LS112ST and LS112Adr are all small cell lung tumour cell lines. CALU-3 and L-DAN are both non-small cell lung tumour cell lines.

The restriction enzyme *HpaII* will not cleave DNA if its' cleavage site is methylated. The *MspI* restriction enzyme will cleave DNA irrespective of its methylation status. Therefore, hypomethylation of the TOPO II $\alpha$  or II $\beta$  genes, which could result in enhanced transcription levels, would be evident by production of identically sized restriction fragments as in *MspI* digests in the *HpaII* digests.

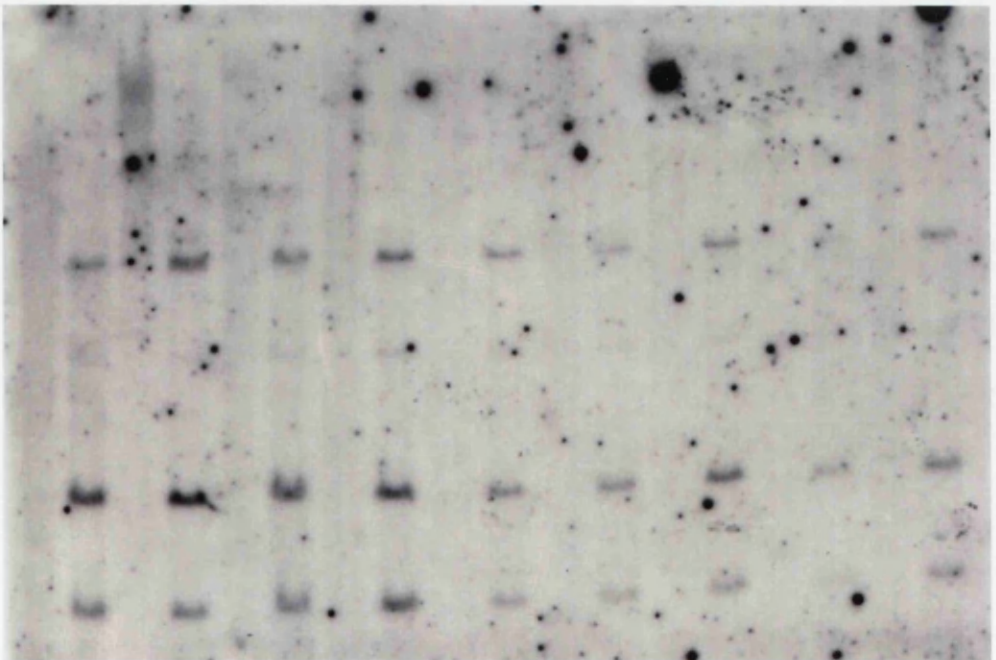
There does not appear to be any evidence for hypomethylation in any of the samples analysed.

TOPO II $\alpha$



1 2 3 4 5 6 7 8 9 10 11 12 13 14 15 16 17 18

TOPO II $\beta$



1 2 3 4 5 6 7 8 9 10 11 12 13 14 15 16 17 18

## **Expression of Other Loci on 17q**

As mentioned previously, CALU-3 has a number of genes co-amplified on chromosome 17 including ERBB2, TOPO II $\alpha$  and RAR $\alpha$ . All of these genes have been implicated in the process of carcinogenesis. ERBB2 amplification has been linked with poor prognosis in a variety of tumour types, including breast and ovarian (Hynes, 1993; Perren, 1991; Slamon *et al.*, 1989), TOPO II $\alpha$  expression levels are thought to play a role in sensitivity of cells to topoisomerase II inhibitors (Davies *et al.*, 1988; Fry *et al.*, 1991; Nitiss *et al.*, 1992) and translocation of the RAR $\alpha$  gene is commonly found in acute promyelocytic leukaemia (Chang *et al.*, 1991; Dong *et al.*, 1993; Kastner *et al.*, 1992). The expression of NM23H1 was also investigated since there is evidence that this protein may influence the metastatic potential of tumour cells (Hennessy *et al.*, 1991; Leone *et al.*, 1993a; Leone *et al.*, 1993b; Wang *et al.*, 1993).

In order to investigate ERBB2 expression in CALU-3, immunofluorescence analysis was performed using a monoclonal antibody against the erbB2 protein. Results from this experiment are shown in Figure 4.12. No expression of erbB2 was detected in either L-DAN or SK-MES-1. CALU-3, however, was found to express erbB2 in the cell membrane of every cell in the population. This high expression therefore correlates with the gene amplification seen in this cell line. Expression analysis of the RAR $\alpha$  gene was carried out using Western analysis. Figure 4.13 shows the results of a Western detected with a polyclonal antibody against the retinoic acid receptor alpha protein. No overexpression of this protein was detected in CALU-3, shown in lane 2, when compared to expression levels in L-DAN (lane 1) and SK-MES-1 (lane 3).

Although NM23H1 is known to be outside the region of amplification in CALU-3, expression of this gene is of interest because of its proposed role in anti-metastasis. Both nm23H1 and H2 proteins were detected by the antibody used in this analysis. Figure 4.14 shows the results of a Western blot where one half was probed with anti-nm23 antibody (a) and the other half with peptide-blocked anti-nm23 antibody (b). The blot in panel (a) shows the two bands expected for nm23H1 and H2 at 17 and 18.5 kD respectively. When detected with peptide-blocked primary antibody these bands are abolished (panel b). Figure 4.15 shows immunofluorescence detection of nm23H1 and H2 using the same antibody as in Western analysis. Panels (a), (c) and (e) show nm23 expression to be cytoplasmic and in every

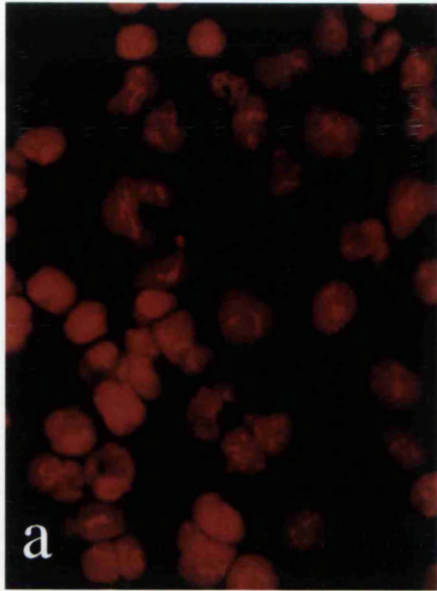
## **Figure 4.12**

**Detection of ERBB2 gene expression by immunofluorescence.**

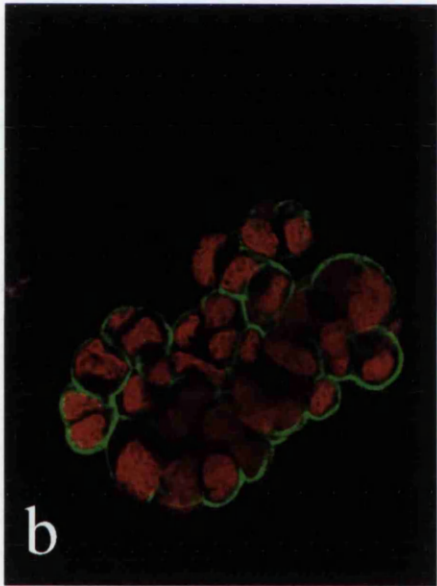
**(a): L-DAN, (b): CALU-3, (c): SK-MES-1**

Nuclei are counterstained with propidium iodide (pseudocoloured red), erbB2 protein detected with FITC (pseudocoloured green). ERBB2 expression was detected using the monoclonal antibody NCL-CB11 from Novocastra.

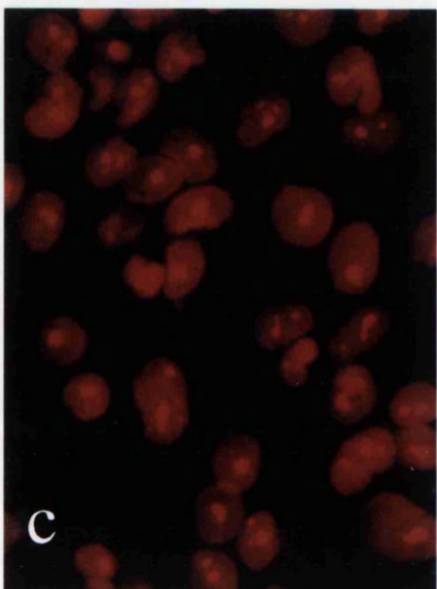
As can be seen from panel (b), ERBB2 expression (green signal) was only detectable in CALU-3, where this gene is amplified. Expression of ERBB2 was detected only in the cell membrane and in every cell of the population.



L-DAN



CALU-3



SK-MES-1

**Figure 4.13**

**Detection of retinoic acid receptor alpha (RAR $\alpha$ ) expression by Western blot analysis.**

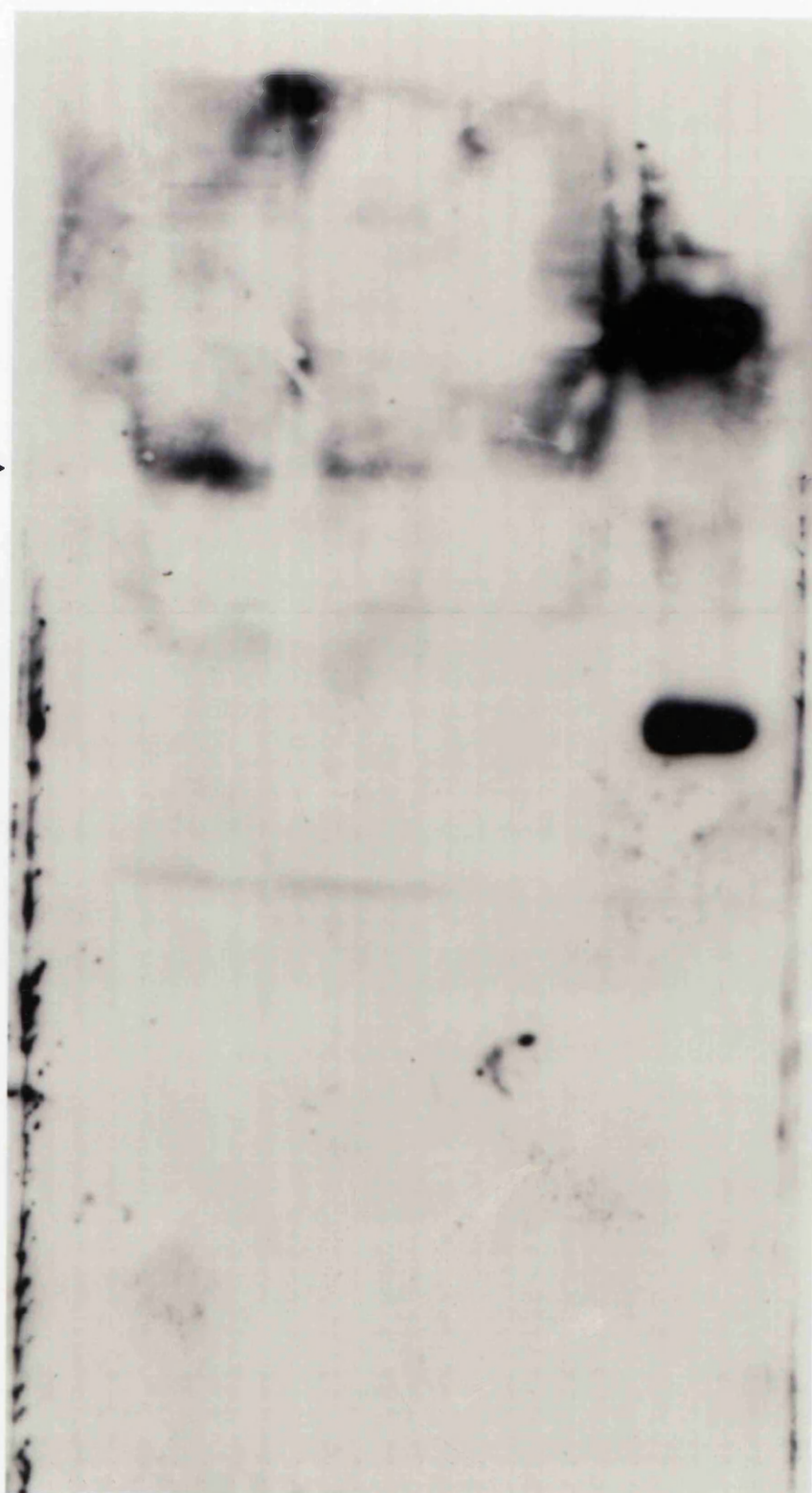
**Lane 1: L-DAN, Lane 2: CALU-3, Lane 3: SK-MES-1.  
M=Markers**

Molecular mass of RAR $\alpha$ = 45kD

Whole cell lysates from  $1 \times 10^5$  cells were loaded per lane. Molecular mass standards in kiloDaltons are shown to the right of the autoradiograph. RAR $\alpha$  was detected using a polyclonal antibody from Affinity BioReagents.

Despite the fact that CALU-3 has an amplified RAR $\alpha$  gene, there is no evidence of overexpression of that gene when compared to expression levels in L-DAN and SK-MES-1.

RAR $\alpha$  →



1

2

3

M

## **Figure 4.14**

### **Detection of nm23H1/H2 expression by Western blot analysis.**

- (a): blot incubated with anti-nm23H1/H2 antibody.  
(b): blot incubated with peptide blocked anti-nm23H1/H2 antibody

**Lane 1: L-DAN, Lane 2: CALU-3, Lane 3: SK-MES-1.**

Molecular mass of nm23H1= 17kD

Molecular mass of nm23H2=18.5kD

Whole cell lysates from  $1 \times 10^5$  cells were loaded per lane. Molecular mass standards in kiloDaltons are shown to the right of the autoradiograph. A polyclonal antibody against both nm23H1 and nm23H2 was used from Cambridge Research Biochemicals.

Both nm23H1 and nm23H2 are detected by the primary antibody, as observed in image (a). When a complementary peptide is used to block primary antibody binding these bands are abolished, as observed in image (b).

As shown by Southern analysis, the NM23H1 gene is not amplified in CALU-3, thus expression of this protein is similar among the three cell lines.

a



1 2 3

b



1 2 3

-43

-28

-17

-15

## **Figure 4.15**

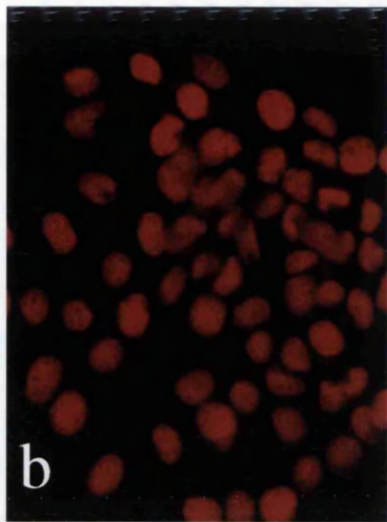
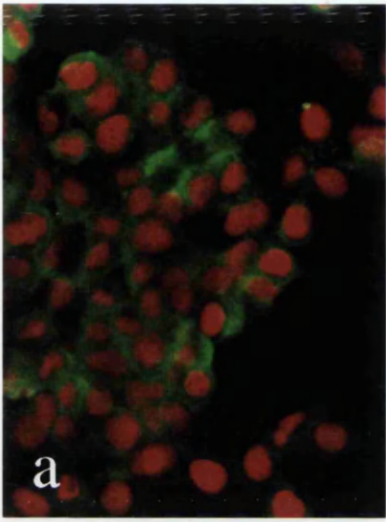
### **Detection of NM23H1/H2 gene expression by immunofluorescence.**

**(a), (c) and (e):** L-DAN, CALU-3 and SK-MES-1 reacted with anti-nm23H1/H2 antibody

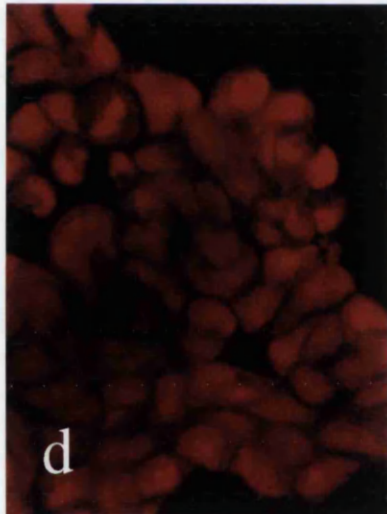
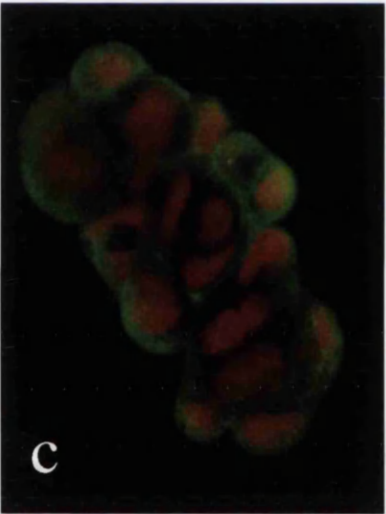
**(b), (d) and (f):** L-DAN, CALU-3 and SK-MES-1 reacted with peptide-blocked anti-nm23H1/H2 antibody

Nuclei are counterstained with propidium iodide (pseudocoloured red), nm23H1/H2 proteins detected with FITC (pseudocoloured green). Nm23H1/H2 was detected using a polyclonal antibody from Cambridge Research Biochemicals.

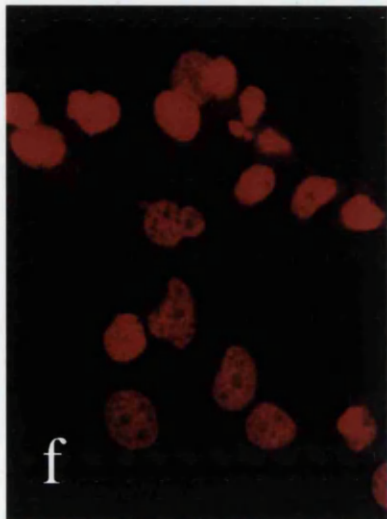
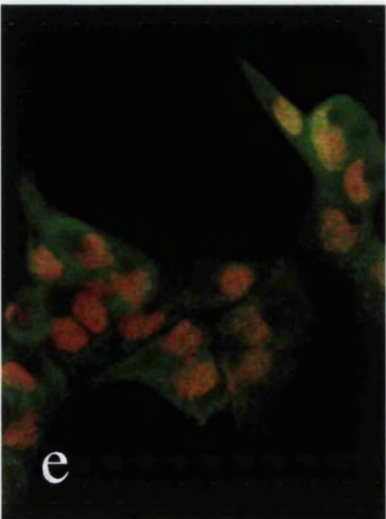
NM23H1/H2 expression (green) was detectable in the cytoplasm of all cells in L-DAN, CALU-3 and SK-MES-1 (panels a,c and e). No expression was detected when peptide-blocked primary antibody was used (panels b,d and f).



L-DAN



CALU-3



SK-MES-1

cell in L-DAN, CALU-3 and SK-MES-1. Again, with peptide-blocked primary antibody all signal was abolished.

### **4.3 Discussion**

The expression data shown here for CALU-3 demonstrate that this cell line has high expression of topoisomerase II $\alpha$  both at the mRNA and protein level (Figures 4.1, 4.2 and 4.3). Although the Northern gel was underloaded for L-DAN, CALU-3 and SK-MES-1, it is still clear that CALU-3 expresses the TOPO II $\alpha$  gene very highly when loading and expression levels of all the other cell lines are compared. It is difficult to comment on the expression of the topoisomerase genes in L-DAN due to the concentration of RNA loaded for this sample, although a faint band of TOPO II $\alpha$  expression can be seen in panel (a). The TOPO II $\alpha$  and II $\beta$  genes have an approximate 75% overall homology at the nucleotide level (Jenkins *et al.*, 1992; Austin *et al.*, 1993) thus there is a possibility that probes may cross-hybridise on Southern and Northern blots. This is an important issue at the RNA level since, as shown in Figure 4.1, the messages for TOPO II $\alpha$  and II $\beta$  genes are the same size (6.5kb). The same cDNA clones (SP1 and SP12) were initially used by Chung *et al.* in 1989. This group used oligos from the most distinct part of HeLa topoisomerase II $\alpha$  and the putative topoisomerase II $\beta$  sequence in competition hybridisation experiments. They found that the signal from each oligo was only competed out by unlabelled identical oligo, thus implying that the oligos derived from the cDNA clones were specific for the TOPO II $\alpha$  and II $\beta$  genes (Chung *et al.*, 1989). Also, if the signals from panels (a) and (b) are compared, it can be seen that CALU-3 has a much lower mRNA signal for TOPO II $\beta$  than for II $\alpha$ . If this were cross-hybridisation of signal, one would perhaps expect a similar intensity between the two probes. The difference in expression of the two genes is also shown in lanes 6 and 7 (LS274 and LS310, respectively), where with the TOPO II $\alpha$  probe LS274 has greater expression than LS310 but with the TOPO II $\beta$  probe, the two cell lines appear to show a very similar level of expression. To avoid the problem of cross-hybridisation, but still study mRNA levels in these cell lines, RNase protection assays could be performed. Such assays for TOPO II $\alpha$  and TOPO II $\beta$  have recently been described (Jenkins *et al.*, 1992), with distinct sizes of protected fragments isolated for topoisomerase II $\alpha$ - and topoisomerase II $\beta$ -specific probes. None of the NSCLC cell lines showed high expression of TOPO I. Previous work on the SCLC cell lines was performed in the Department of Medical Oncology by Dr. N. Keith and Dr. J. Plumb (unpublished). The data obtained here was found to agree with this previous work.

From densitometric analysis of the Western blot shown in Figure 4.2, CALU-3 was found to express approximately 10-15 fold more topoisomerase II $\alpha$  than either L-DAN or SK-MES-1. Thus the high TOPO II $\alpha$  mRNA level in CALU-3 appears to correlate with a greater production of enzyme. Immunofluorescence analysis shows that the topoisomerase II $\alpha$  enzyme level is not high in all CALU-3 cells, but that more positive cells are present in CALU-3 than either L-DAN or SK-MES-1. A very high level of the enzyme was detected in a mitotic cell, which agrees with many previous studies on the regulation of topoisomerase II during the cell cycle (Heck *et al.*, 1988; Kaufmann *et al.*, 1991; Prosperi *et al.*, 1994; Prosperi *et al.*, 1992; Woessner *et al.*, 1991). The intense topoisomerase II $\alpha$  signal in this cell looks to be associated with the metaphase chromosomes, unlike the other interphase cells where topoisomerase II $\alpha$  expression appears to be speckled throughout the nucleoplasm. Localisation of topoisomerase II $\alpha$  to metaphase chromosomes has been observed previously (Boy de la Tour & Laemmli, 1988; Earnshaw & Heck, 1985; Gasser *et al.*, 1986; Saitoh *et al.*, 1994) with immunopositivity observed along the entire length of the chromatid in expanded chromosomes (Earnshaw & Heck, 1985; Gasser *et al.*, 1986). In fact, topoisomerase II $\alpha$  has been proposed to be the most abundant non-histone protein in the metaphase scaffold representing 1-2% of the total protein mass in metaphase chromosomes. The lower levels of topoisomerase II $\alpha$  expression detected in L-DAN and SK-MES-1 by Western blot analysis were confirmed by immunofluorescence. However, due to the settings for digital image analysis required to maintain optimal visualisation conditions of topoisomerase II $\alpha$  in CALU-3, topoisomerase II $\alpha$  expression in these other two cell lines was almost undetectable.

Biochemical assays have shown CALU-3 to possess an approximate eight-fold increase in topoisomerase II activity when compared to the two cell lines without amplification of TOPO II $\alpha$  (Figure 4.4). This figure was deduced through independent analysis of the original negatives by at least two individuals and was taken as the protein concentration required to initiate decatenation. It cannot definitely be said that the increased activity observed in these assays is due to an increase in TOPO II $\alpha$  gene copy number since the biochemical assays do not distinguish between the topoisomerase II $\alpha$  and II $\beta$  isozymes. More detail is given on the topoisomerase II $\beta$  isozyme in Chapter 5, which concentrates on TOPO II $\beta$  expression and attempted detection of the 180kD protein.

Both the VP16 inhibition of catalytic assays and use of the band depletion assay show that the topoisomerase II enzyme produced by

CALU-3 and the other two cell lines is still sensitive to drug interaction. The catalytic assays show an *in vitro* approach to investigation of topoisomerase II activity, using a crude nuclear extract. However, as mentioned previously, it is not known whether the topoisomerase II $\beta$  isozyme is also a target for VP16 in these assays. The band depletion assay enables an *in vivo* study of topoisomerase II/drug interactions since it is performed in whole cells. Also, this assay allows one to distinguish between the alpha and beta isoforms by using Western analysis to investigate the treated cell extracts. Thus, from the band depletion assay and resultant Western, it can be said that topoisomerase II $\alpha$  from all three cell lines is capable of forming stabilised cleavable complexes in the presence of VP16.

Cell cycle analysis of L-DAN, CALU-3 and SK-MES-1 was performed by flow cytometry following bromodeoxyuridine (BrdUrd) incorporation. From the results shown in Table 4.1 there do not appear to be any major differences between the percentages of cells at any particular stage of the cell cycle in the three cell lines. These results will, of course, depend on how confluent the cells were when the experiment was carried out. However, it is clear from Figure 4.8 that cells from L-DAN, CALU-3 and SK-MES-1 all undergo a normal cell cycle in as much as cells are seen progressing from G0/G1 (boxes 1 and 2), through S phase (box 3) and into G2 (box 4). It appears from the topoisomerase II $\alpha$  FACS experiment that CALU-3 still retains some cell cycle regulation of topoisomerase II $\alpha$  expression, since the percentage of topoisomerase II $\alpha$  positive cells increases by 30-40% between G1 and G2/M (Table 4.3). Much lower levels of expression were detected in L-DAN and SK-MES-1. Experiments using a monoclonal antibody against topoisomerase II $\alpha$  were also performed (Tables 4.4 and 4.5). Using this antibody, topoisomerase II $\alpha$  expression was only detectable in CALU-3. This suggests that the monoclonal antibody was not sensitive enough to detect the topoisomerase II $\alpha$  expression in L-DAN and SK-MES-1. It is not known whether the topoisomerase II $\alpha$  positive cells detected in G0/G1 in CALU-3 (Figure 4.9, panel c) are expressing topoisomerase II $\alpha$  *de novo* at this stage of the cycle, or whether these are cells which are still expressing topoisomerase II $\alpha$  from G2/M. One way of finding the answer to this would be to carry out topoisomerase II $\alpha$  FACS analysis using cells treated with hydroxyurea. Hydroxyurea causes cells to block after the G1 phase of the cell cycle. Therefore, if this expression is caused by detection of topoisomerase II $\alpha$  still present in cells from G2/M, the hydroxyurea treated cells would probably be negative for topoisomerase II $\alpha$  expression, since most of the topoisomerase II $\alpha$  enzyme would degrade during

**Table 4.4**

**Number of cells in different stages of the cell cycle in a topoisomerase II $\alpha$  FACS experiment (monoclonal antibody)**

	<b>G1 total cell no.</b>	<b>G1 Topo II<math>\alpha</math> +ve cells</b>	<b>G2/M total cell no.</b>	<b>G2/M Topo II<math>\alpha</math> +ve cells</b>
<b>L-DAN</b>	-	ND	-	ND
<b>CALU-3 (a)</b>	11861	4284	3991	2804
<b>CALU-3 (b)</b>	13229	6154	3483	2567
<b>SK-MES-1</b>	-	ND	-	ND

All numbers listed have been corrected against a no primary antibody control experiment

**Table 4.5**

**Percentage of cells positive for topoisomerase II $\alpha$  expression in G1 and G2/M (monoclonal antibody)**

	<b>% G1 positive cells</b>	<b>% G2/M positive cells</b>
<b>L-DAN</b>	ND	ND
<b>CALU-3 (a)</b>	36%	70%
<b>CALU-3 (b)</b>	46%	73%
<b>SK-MES-1</b>	ND	ND

ND: Not Detected

the blocking procedure. If expression was *de novo* at G1, topoisomerase II $\alpha$  expression would still be detected. Ideally, further repetitions of the topoisomerase II $\alpha$  FACS experiments already performed, plus additional ones as outlined above, are required in order to have a full understanding of the cell cycle regulation of topoisomerase II $\alpha$  expression in CALU-3.

Using a basic method for detecting the methylation status of DNA, there was no evidence for hypomethylation of the TOPO II $\alpha$  or TOPO II $\beta$  genes in CALU-3, or any of the other samples analysed, as was shown in Figure 4.11. This would indicate that there are no gross changes to the chromatin structure around these genes in CALU-3, thus loosening of the chromatin scaffold, often associated with under methylated regions of DNA, (Tazi & Bird, 1990), does not appear to play a role in the overexpression of the TOPO II $\alpha$  gene in this cell line.

Using immunofluorescence, the erbB2 protein was detectable in CALU-3, where the gene is known to be amplified (Figure 4.12). Expression of this protein was visualised in the membrane of every cell. Expression of erbB2 has been observed in both the cytoplasm and membranes of cells (Gullick *et al.*, 1987; Ramachandra *et al.*, 1990; Winstanley *et al.*, 1991), although a recent report has suggested that membranous staining is the more prognostically relevant of the two when expression of erbB2 is studied in breast cancer (Tetu & Brisson, 1994). It has already been proposed that the ERBB2 gene is the driving force for the amplicon in CALU-3 since studies of gene amplification in breast cancer have shown that the ERBB2 gene is frequently found to be amplified alone, without involvement of the TOPO II $\alpha$  gene (Keith *et al.*, 1993; Smith *et al.*, 1993). The overexpression of erbB2 would give the tumour an obvious growth advantage since each cell would possess a higher number of growth factor receptors than a normal cell and thus, depending on growth conditions, could grow and divide at a greater rate. Overexpression of topoisomerase II $\alpha$  enzyme may also be important. Calf thymus DNA topoisomerase II has been found to mediate illegitimate recombination in an *in vitro* situation between two phage  $\lambda$  DNA molecules (Bae *et al.*, 1988) and putative topoisomerase II DNA-binding sites have been found at points of DNA insertion, deletion and translocation (Negrini *et al.*, 1993; Sperry *et al.*, 1989). Therefore, cells expressing large amounts of topoisomerase II $\alpha$  may display more of a tendency to undergo such cytogenetic changes due to an increase in the number of topoisomerase II molecules free to bind to these sites in the nucleus. There was no detectable expression of erbB2 in either L-DAN or SK-MES. This could be due to lack of expression of this protein by these cell lines, or low levels of expression

which are not detectable by this technique. To clarify this point, Western blot analysis could be performed using whole cell extracts from L-DAN and SK-MES-1.

As mentioned previously, the NM23H1 and RAR $\alpha$  genes are also situated around the region of the amplicon on chromosome 17 in CALU-3. From the results in Chapter 3 it was shown that the RAR $\alpha$  gene is amplified (CALU-3 having at least 8 copies), although apparently not as highly as TOPO II $\alpha$  or ERBB2 genes. The NM23H1 gene was found to be outside the region of amplification (5 copies found in CALU-3). Western analysis of the retinoic acid receptor alpha (Figure 4.13) has shown the protein not to be overexpressed in CALU-3 in comparison to L-DAN and SK-MES-1. This result was repeated in 3 other Western experiments. Although this may seem unusual, there are cases where genes are amplified and no expression is detected. For example, in the 11q amplicon, which has been reported in a variety of human tumours including breast and squamous cell carcinomas (see (Lammie & Peters, 1991) for review), the INT2 and HSTF1 genes are commonly within the amplicon but are not reported to be overexpressed (Fantl *et al.*, 1990; Lafage *et al.*, 1990; Tsuda *et al.*, 1989). Also the ERBA1 gene has been reported to be co-amplified with ERBB2 in breast tumours with there being no evidence for subsequent overexpression (van de Vijver *et al.*, 1987). Another suggestion to explain the apparent lack of overexpression in CALU-3 is that the expression seen may be very high for this cell line, since the RAR $\alpha$  expression level was not known previous to the occurrence of the gene amplification. The two fainter bands in Figure 4.13 are presumed to be degradation products from the main 45kD retinoic acid receptor alpha protein. Immunofluorescence was attempted using the same antibody as for Western analysis, but no specific signal could be obtained (data not shown).

The nm23H1/H2 proteins were detected in L-DAN, CALU-3 and SK-MES-1 by flow cytometry (Figure 4.10), Western analysis (Figure 4.14) and immunofluorescence (Figure 4.15). By immunofluorescence analysis, expression was observed to be cytoplasmic. This pattern of expression has been previously reported for nm23H1 and H2 (Igawa *et al.*, 1994; Lacombe *et al.*, 1991; Simpson *et al.*, 1994; Yamaguchi *et al.*, 1994). The minor bands detected in Figure 4.14 are assumed to be non-specific binding of the secondary antibody, since they are also present in the peptide-blocked primary antibody control (panel b). Specific detection of the nm23 proteins was confirmed using a blocking peptide, to which the antibody had initially been raised. This was successful in blocking primary antibody signal in both Western and immunofluorescence analysis. No investigation has been

performed into whether this expression correlates with the metastatic potential of these cell lines.

From Chapter 3 it is known that CALU-3 has amplification of TOPO II $\alpha$ , ERBB2, RAR $\alpha$  and G-CSF genes. It was also discovered that L-DAN has three copies of both TOPO II $\alpha$  and ERBB2 and SK-MES-1 has two copies of each of these genes. Expression analysis of TOPO II $\alpha$  and ERBB2 has shown these genes to be overexpressed in CALU-3 when compared to L-DAN and SK-MES-1. No alterations were found in the activity or drug binding capability of the topoisomerase II $\alpha$  enzymes in any of the cell lines. CALU-3 has previously been found to be 35-52-fold more sensitive to VP16 than either L-DAN or SK-MES-1, and 12-25-fold more sensitive to doxorubicin (Merry *et al.*, 1987). Therefore, it is proposed that expression of the amplified TOPO II $\alpha$  gene sequences in CALU-3 cause enhanced production of topoisomerase II alpha enzyme and this plays a major role in the sensitivity of CALU-3 to topoisomerase II inhibitors. This finding may be of importance in a clinical situation since tumours which are found to carry such a gene amplification may, therefore, respond preferentially to treatment with topoisomerase II inhibitory drugs (Keith *et al.*, 1993; Smith *et al.*, 1993).

# CHAPTER 5

## EXPRESSION ANALYSIS OF TOPOISOMERASE II $\beta$

### 5.1 Introduction

This chapter will deal with expression analysis of the topoisomerase II beta enzyme in L-DAN, CALU-3 and SK-MES-1. The beta isoform of topoisomerase II was initially described by Drake *et al.* in 1987 when they purified topoisomerase II from amsacrine-resistant P388 leukaemia cells (Drake *et al.*, 1987). After performing SDS-polyacrylamide gel electrophoresis with their purified topoisomerase II, two bands were noticed at 170 (p170) and 180kD (p180). When antibodies were raised to these specific proteins, each antibody was found only to react to the protein it was raised against. Other data was also obtained which led the authors to conclude that there were two forms of topoisomerase II, including the finding that each protein had catalytic activity, each produced distinct proteolytic fragments upon digestion with *Staphylococcus* V8 protease and the relative levels of the p170 and p180 forms between amsacrine-resistant P388 and amsacrine-sensitive P388 cells were found to be consistently different. In 1989 the same group isolated p170 and p180 proteins from U937 cells and proceeded to study the biochemical and pharmacological properties of each isozyme (Drake *et al.*, 1989). In this study it was discovered that the isozymes could be distinguished in a number of ways. The optimal salt concentration for catalytic activity was found to be higher for the p180 enzyme than for p170. Thermal stability of the two proteins was found to be very different with the half life of p180 shown to be half of that for p170 and the drug sensitivity of the two isozymes differed in that higher concentrations of both teniposide and merbarone were required for inhibition of catalytic activity in reactions with p180. Investigations into drug-induced cleavage sites found that p170 appeared to prefer A-T-rich binding sites, whereas p180 appeared to prefer G-C rich sites. Finally, when expression of the two isozymes during the cell cycle was investigated, it was discovered that p170 levels were highest during logarithmic growth and dropped as cells reached the plateau stage of growth (as described in Chapter 4). Expression of p180 appeared to be the opposite to this, with low expression during logarithmic growth and higher expression as the plateau phase was reached. Therefore, it appeared that the initial proposal

of the existence of two topoisomerase II proteins was correct, although there was still no genetic data showing the existence of two genes for topoisomerase II.

However, in 1989 the first publication appeared reporting the characterisation of two human TOPO II cDNA clones (Chung *et al.*, 1989). The cDNAs described in this paper are the same ones which were used for the Southern and Northern blotting previously described in Chapters 3 and 4. By screening a cDNA library made from a nitrogen mustard-resistant human Burkitt lymphoma cell line (Raji-HN<sub>2</sub>) previously used by Tan *et al.* in 1988, two classes of TOPO II clones were pulled out. One member of the first class was found to be identical to part of a HeLa cell TOPO II cDNA (SP1), whereas members of the second class (SP11 and SP12) displayed a 75% nucleotide and 92% predicted peptide similarity to the first two-thirds of this HeLa TOPO II clone, leading to the suspicion that they were cDNAs from different genes. When antibodies were raised against peptides specific to each cDNA, SP1-peptide antibodies were found only to recognise the p170 form of topoisomerase II and SP11-peptide antibodies to only recognise the p180 form. Hybridisation of oligos from the SP1 and SP11 cDNAs to Northern blots resulted in the detection of a 6.5 kb mRNA for each class, although when competition experiments were performed, hybridisation of oligo from one class was not competed out by oligo specific for the other, ruling out the possibility that the probes were detecting the same message. Therefore, this paper provided both genetic and immunological evidence for the existence of two TOPO II genes. It was also in this paper that the suggestion was made to adopt the terms II $\alpha$  (p170) and II $\beta$  (p180) for the two topoisomerase II isozymes. In 1990, another group reported the finding of a novel topoisomerase II homologue from HeLa cells (Austin & Fisher, 1990), again finding 60-70% nucleotide and peptide sequence homology with a region of HeLa cell TOPO II cDNA. It was later published that this clone encoded a C-terminal segment from the TOPO II $\beta$  gene (Austin *et al.*, 1993).

The TOPO II gene had already been localised to chromosome 17q21-22 (Tsai-Plugfelder *et al.*, 1988), although confirmation that this was the TOPO II $\alpha$  gene had to wait until the beginning of 1992 when Tan *et al.* reported the mapping of the TOPO II $\alpha$  and II $\beta$  genes using the SP1 and SP12 cDNA clones (Tan *et al.*, 1992). It was then confirmed that the human genome possessed two genes for topoisomerase II, one of which was located on 17q21-22 and the other on chromosome 3. Further mapping of the TOPO II $\beta$  gene localised it to chromosome 3p24 (Jenkins *et al.*, 1992). It has subsequently been reported that there are two differentially spliced forms of

topoisomerase II $\beta$  expressed in human cells, with the  $\beta$ -2 form containing a sequence which would encode an extra 5 amino acids in the topoisomerase II $\beta$  protein. However, in all cases it appeared that the  $\beta$ -1 form was the major form expressed, with consistently higher levels of  $\beta$ -1 RNA seen than  $\beta$ -2 (Davies *et al.*, 1993).

Analysis of topoisomerase II expression in normal human lymphocytes has shown that topoisomerase II $\beta$  expression is higher than topoisomerase II $\alpha$  expression in non-cycling cells, and that levels of both isoforms rose between G<sub>1</sub> and G<sub>2</sub>-M following phytohaemagglutinin stimulation of the lymphocytes (Prosperi *et al.*, 1994). Other studies commenting on differential expression of the topoisomerase II $\alpha$  and II $\beta$  enzymes in tumour cells during the cell cycle have also reported a higher level of topoisomerase II beta in resting cells when compared to topoisomerase II alpha expression (Kimura *et al.*, 1994; Negri *et al.*, 1992; Prosperi *et al.*, 1992; Woessner *et al.*, 1991). A study of the patterns of TOPO II $\alpha$  and TOPO II $\beta$  gene expression in various differentiated tissues in mice also found expression of the beta gene in tissues with no proliferating cells (Capranico *et al.*, 1992). However, topoisomerase II $\beta$  expression has been difficult to analyse because of the instability of the beta protein (Drake *et al.*, 1989; Negri *et al.*, 1993).

As well as cell cycle regulation, a number of groups have investigated the subcellular localisation of the two isoforms in cells. As presented in Chapter 4, topoisomerase II alpha is localised to the nucleoplasm of cells. Topoisomerase II $\beta$  expression was initially observed only in the nucleoli of cells (Negri *et al.*, 1992; Zini *et al.*, 1992), although a more recent study has suggested that the beta isozyme may be present in both the nucleoli and the nucleoplasm (Petrov *et al.*, 1993). Investigations of topoisomerase II expression in *Xenopus* oocytes also found topoisomerase II expression in both nucleoli and nucleoplasm, although this work was performed using a polyclonal antibody which recognised both 170 and 180kD proteins, which may explain this result (Fischer *et al.*, 1994). The discovery that the two isoforms appear to be expressed in different locations has led to the proposal that they may play different roles within the cell, with the beta isoform possibly involved in the regulation of transcription of the ribosomal genes.

The analysis of topoisomerase II $\beta$  expression detailed in this chapter has been undertaken using a variety of techniques in an attempt to overcome the major problem associated with the detection of this protein, that being degradation. The mouse monoclonal antibody used, 8F8 (kindly provided by Dr. Astaldi Ricotti), has been characterised previously in various analyses of topoisomerase II beta expression (Negri *et al.*, 1992; Negri *et al.*,

1993; Prosperi *et al.*, 1994; Prosperi *et al.*, 1992; Zini *et al.*, 1992). The NSCLC cell lines CALU-3, L-DAN and SK-MES-1 were also used in this analysis.

## **5.2 Results**

This chapter deals with expression of the beta isozyme of topoisomerase II. This protein has been notoriously difficult to isolate, as was hinted at in the previous chapter. The main factor for successful detection of the intact, 180kD topoisomerase II $\beta$  protein by Western blotting appears to be the time taken from preparation of the cell lysates to loading the Western. Therefore, in an attempt to detect the 180kD topoisomerase II $\beta$  protein a number of different protocols and antibodies have been tried. However, the only antibody which routinely detected a signal in the cell lines used was a mouse monoclonal against topoisomerase II $\beta$ , 8F8, (Negri *et al.*, 1992), kindly given to us by Dr. Giulia Astaldi Ricotti from Pavia, Italy.

### **Dot Blot Analysis for Topoisomerase II $\beta$**

Dot blotting was initially used to see if the antibody would detect any topoisomerase II $\beta$  signal from the three cell lines. Figure 5.1 shows the results of two identical dot blots, of which one was incubated in the anti-topoisomerase II $\beta$  primary antibody (panel a) and a control one in which the primary antibody was omitted (panel b). Doubling dilutions of nuclear extract were applied to the filter from 50 $\mu$ g (darkest signal) down to 0.39 $\mu$ g for each cell line. As can be seen from panel (a), topoisomerase II $\beta$  protein was detected in L-DAN (lane 1), CALU-3 (lane 2) and SK-MES-1 (lane 3) down to a protein concentration of 0.78 $\mu$ g. Very little background from the secondary antibody was observed (panel b). The lanes marked here are the same as in panel (a). From Figure 5.1, panel (a), it appears that L-DAN and SK-MES-1 express very similar amounts of topoisomerase II $\beta$  protein, with CALU-3 expressing slightly less. It is not clear from this data whether it is the intact or degraded form of topoisomerase II $\beta$  which is being detected.

### **Western Blot Analysis for Topoisomerase II $\beta$**

The same anti-topoisomerase II $\beta$  antibody was subsequently used in Western analysis in an attempt to detect the intact 180kD topoisomerase II $\beta$  protein. Figure 5.2 shows the results of Western blots for both topoisomerase II $\alpha$  and topoisomerase II $\beta$  enzymes. Following incubation of the filter with anti-topoisomerase II $\alpha$  antibodies, CALU-3 (lane 2) can be seen to overexpress the 170kD topoisomerase II $\alpha$  protein when

## **Figure 5.1**

### **Detection of topoisomerase II $\beta$ using dot blot analysis.**

- (a): Dot blot using a mouse monoclonal primary antibody 8F8 against the topoisomerase II $\beta$  enzyme
- (b): Control dot blot without using primary antibody

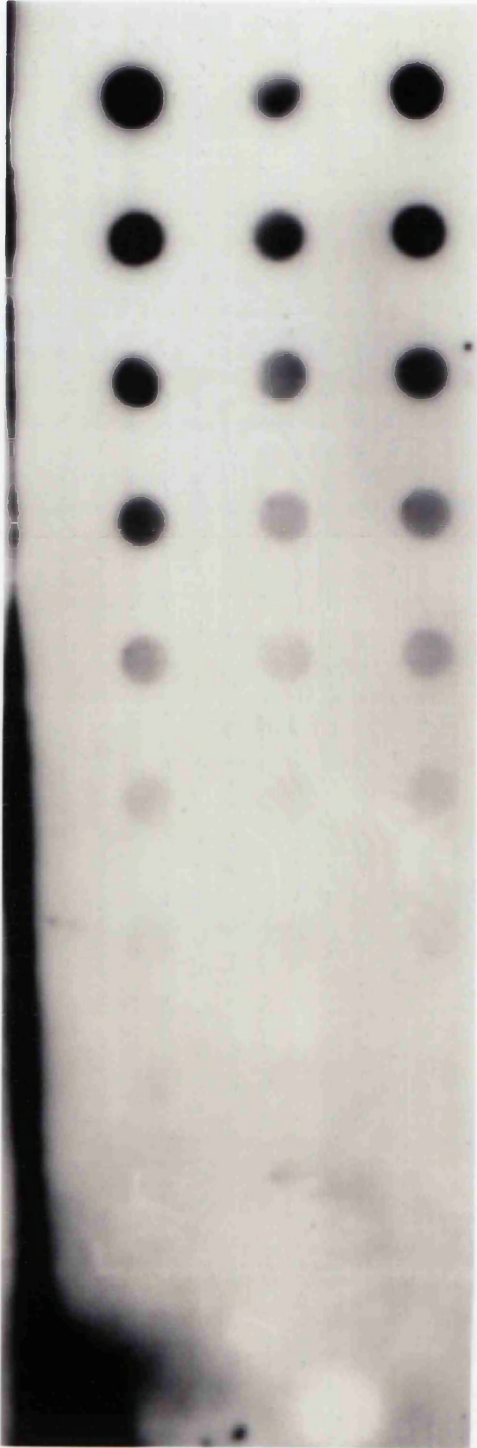
**Lane 1: L-DAN, Lane 2: CALU-3, Lane 3: SK-MES-1**

The first dot at the top of the filter corresponds to 50 $\mu$ g of sample. Successive dilutions of sample were then performed down to a protein concentration of 0.39 $\mu$ g.

Panel (a) shows the results when the dot blot filter was incubated with a mouse monoclonal primary antibody against the topoisomerase II beta enzyme. Panel (b) shows an identical filter strip which was exposed only to the secondary antibody.

Thus, expression of topoisomerase II $\beta$  was observed in all three cell lines, down to a protein concentration of approximately 0.78 $\mu$ g. L-DAN (lane 1) and SK-MES-1 (lane 3) show very similar amounts of topoisomerase II $\beta$  expression, whereas CALU-3 (lane 2) appears to express slightly less. Very little background was observed on the control filter.

a



1 2 3

b



1 2 3

## **Figure 5.2**

### **Detection of topoisomerase II $\beta$ using Western analysis.**

**Lane 1: L-DAN, Lane 2: CALU-3, Lane 3: SK-MES-1**

**Lane 4: L-DAN, Lane 5: CALU-3, Lane 6: SK-MES-1**

Lysate from  $10^5$  cells was loaded per lane for each cell line.

Topoisomerase II $\alpha$  (170kD) was detected using a rabbit polyclonal from Cambridge Research Biologicals.

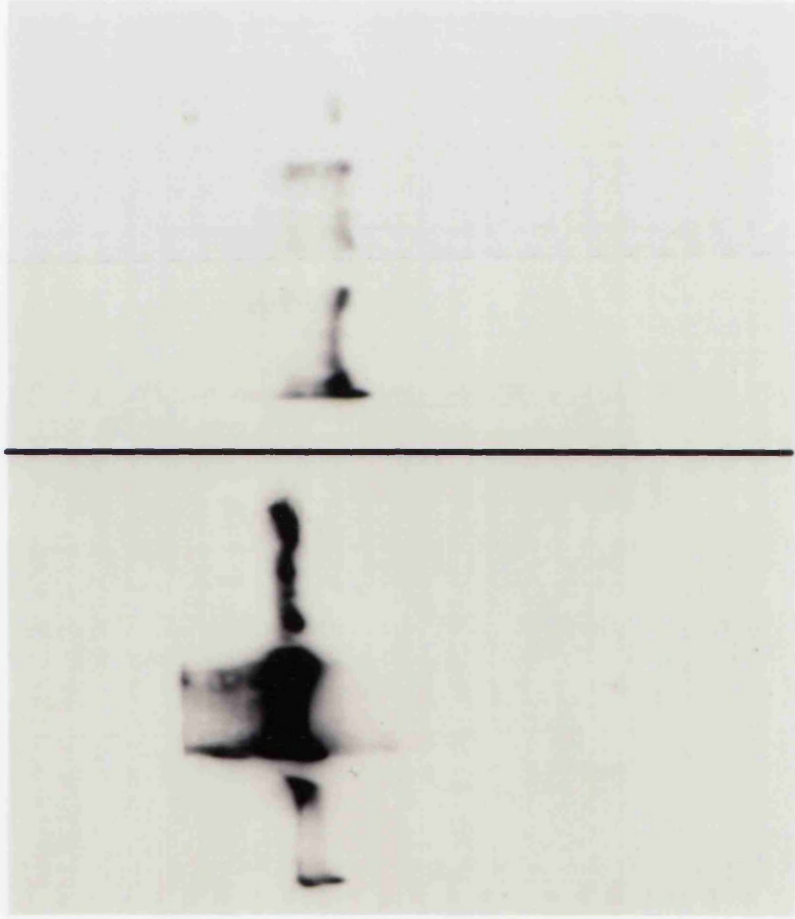
Topoisomerase II $\beta$  (180/150kD) was detected using 8F8.

Incubation with antibody against topoisomerase II $\alpha$  shows the same results as observed previously, with very high expression of the 170kD protein being seen in CALU-3 (lane 2).

Incubation with the anti-topoisomerase II $\beta$  antibody detects a smaller band of approximately 150kD in size. Expression of this protein appears to be highest in L-DAN (lane 4).

Topo II $\alpha$

Topo II $\beta$



- 170kD

- 150kD

1 2 3 4 5 6

compared to L-DAN (lane 1) and SK-MES-1 (lane 3), as was previously shown in Section 4.2. Incubation with the topoisomerase II $\beta$  antibody resulted in the detection of a 150kD band in all three cell lines (right hand panel, lanes 4, 5 and 6). This was assumed to be the degradation product from the topoisomerase II $\beta$  enzyme which is commonly observed in Western analysis of cell extracts (see section 5.1), unless extracts are handled extremely quickly following preparation. In lanes 4 and 5 (L-DAN and CALU-3, respectively) a faint band can be seen at approximately 170-180kD which could be the intact topoisomerase II $\beta$  protein. Signal in lane 6 (SK-MES-1) is very weak, thus making it difficult to compare expression in the three cell lines.

### **Band Depletion Assay**

Using cell lysates prepared for Western analysis, which may have been freeze-thawed once or twice previously, only the 150kD degradation product of the topoisomerase II $\beta$  enzyme could be detected. For this reason it was decided to incubate a filter from a band depletion assay with the topoisomerase II $\beta$  antibody. In this technique, the cell lysates are prepared directly from cells growing in culture (some of which have been drug treated) and these are immediately loaded onto a Western gel using a microsyringe (see Section 2.2.10.3 and 4.2). Therefore, handling of the extracts is extremely quick which may be beneficial when attempting to detect the topoisomerase II $\beta$  protein.

Figure 5.3 shows the autoradiographs resulting from topoisomerase II $\alpha$  (lower panel) and topoisomerase II $\beta$  (upper panel) detection of a band depletion assay filter. Results of the topoisomerase II $\alpha$  blot have been presented in more detail in Chapter 4. The topoisomerase II $\beta$  signal detected in CALU-3 (upper panel, lanes 5-8) appears to mimic that seen with topoisomerase II $\alpha$  in as much as at the highest concentration of VP16 there is a depletion in the amount of topoisomerase II $\beta$ . However, this is the only lane in CALU-3 where this effect is observed and it is not seen in either L-DAN (upper panel, lanes 1-4) or SK-MES-1 (upper panel, lanes 9-12). Since the two isozymes are very similar in protein sequence (see Chapter 1) there is the possibility that the signal observed in the topoisomerase II $\beta$  autoradiograph could be caused by anti-beta antibody cross-reaction with the alpha isozyme. This is unlikely, however, since the relative band intensities between the two autoradiographs are different. For example, of the

### **Figure 5.3**

#### **Band depletion assay of topoisomerase II $\beta$ using whole cell lysates, analysed by Western blot.**

Cells were incubated with decreasing amounts of VP16 for 2 hours at 37°C and then lysed in protein lysis buffer. Samples were resolved on a 6% polyacrylamide gel (see Section 2.2.10.3).

**Lanes 1-4: L-DAN, Lanes 5-8: CALU-3,  
Lanes 9-12: SK-MES-1**

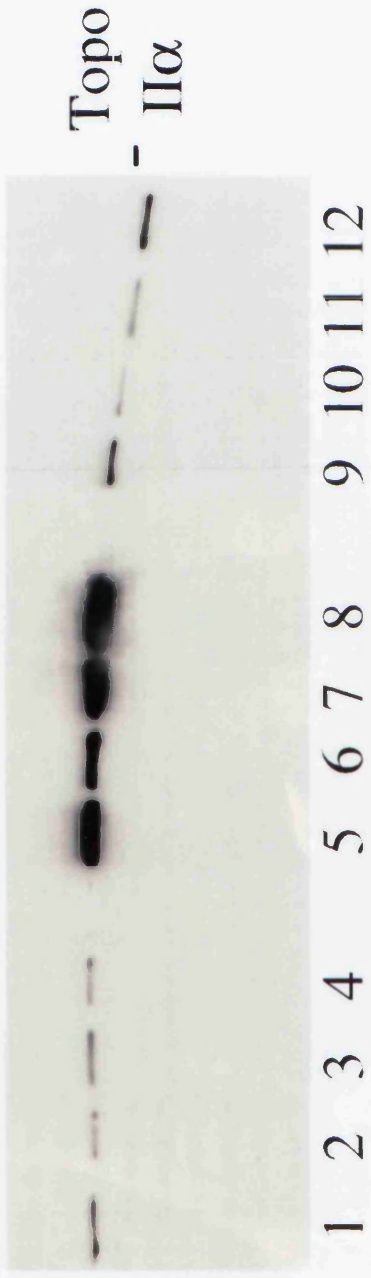
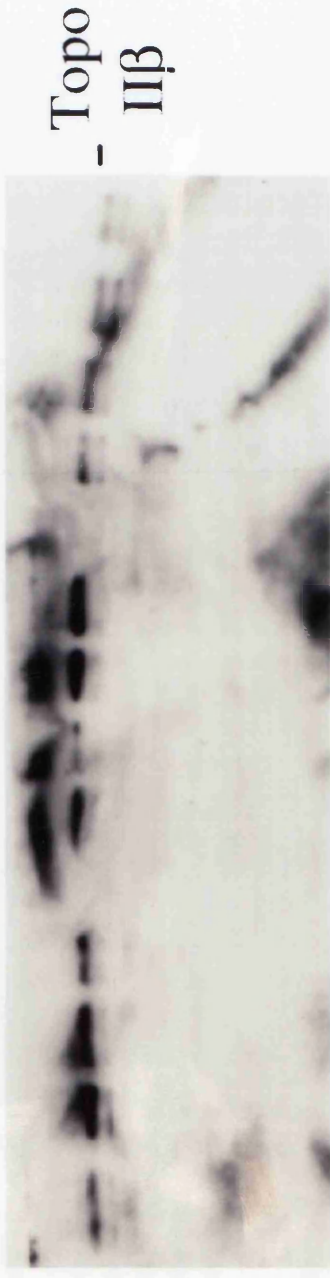
Cells in lanes 1,5 and 9 were not treated with drug, those in lanes 2,6 and 10 were treated with  $5 \times 10^{-4}$ M VP16, those in lanes 3,7 and 11 were treated with  $5 \times 10^{-5}$ M VP16 and those in lanes 4, 8 and 12 were treated with  $5 \times 10^{-6}$ M VP16.

The mouse monoclonal antibody 8F8 was used to detect topoisomerase II $\beta$ . A rabbit polyclonal from Cambridge Research Biologicals was used to detect topoisomerase II $\alpha$ .

This figure shows a re-probing of the band depletion Western from Figure 4.7 (also shown here) with the topoisomerase II $\beta$  antibody.

L-DAN and CALU-3 show similar levels of topoisomerase II $\beta$  expression with SK-MES-1 appearing to have a slightly lower level. Incubation of the cells with VP16 does not appear to have an effect on the topoisomerase II $\beta$  levels, unlike the results shown for topoisomerase II $\alpha$  (see Chapter 4).

L-DAN CALU-3 SK-MES-1



1 2 3 4 5 6 7 8 9 10 11 12

SK-MES-1 samples, lanes 10 and 11 in the topoisomerase II $\beta$  results appear more intense than either lanes 9 or 12. This is clearly different to the results from the topoisomerase II $\alpha$  band depletion since the strongest signals in this case are observed in lanes 9 and 12. The smaller band visible just below the main topoisomerase II $\beta$  band in the upper panel is assumed to be the 150kD degradation product, previously observed in Western analysis (see Figure 5.2). Therefore, the data presented here shows the presence of intact topoisomerase II $\beta$  protein in all three cell lines, but does not show any convincing evidence to suggest that the II $\beta$  isozyme is a target for VP16-directed topoisomerase inhibition.

### **Immunofluorescence Analysis of TOPO II $\beta$ Expression**

Immunofluorescence analysis was performed using 8F8 in order to see the cell to cell distribution and subcellular localisation of the topoisomerase II $\beta$  protein. Figure 5.4 shows the results of immunofluorescence analysis with L-DAN (a), CALU-3 (b) and SK-MES-1 (c). Topoisomerase II beta expression (yellow signal) was observed in every cell in all three cell lines. Beta expression has previously been reported to be largely confined to the nucleolus (Negri *et al.*, 1992), and the data presented in Figure 5.4 confirms this. Immunofluorescence is only semi-quantitative and due to the intense localised fluorescence pattern obtained when analysing expression of the topoisomerase II $\beta$  protein, any difference in expression levels between the three cell lines is difficult to assess. Therefore, expression of topoisomerase II $\beta$  differs from topoisomerase II $\alpha$  expression in that beta expression appears to be common to every cell in a population and also appears to be localised within a specific nuclear compartment. Again, it is not possible to distinguish whether or not the protein detected using this technique is the 180- or 150 kD form.

In order to confirm the localisation of topoisomerase II $\beta$  to the nucleolus, an anti-nucleolar antibody was obtained from ImmunoConcepts (see Section 2.1.6). Figure 5.5 shows the results of a co-localisation experiment with the nucleolar control antibody shown in green and topoisomerase II beta expression shown in red. Co-localisation of these signals is apparent where the two colours overlap, creating a yellow signal. This result was observed in L-DAN (a), CALU-3 (b) and SK-MES-1 (c). Therefore, topoisomerase II $\beta$  expression appears to co-localise with nucleolar proteins.

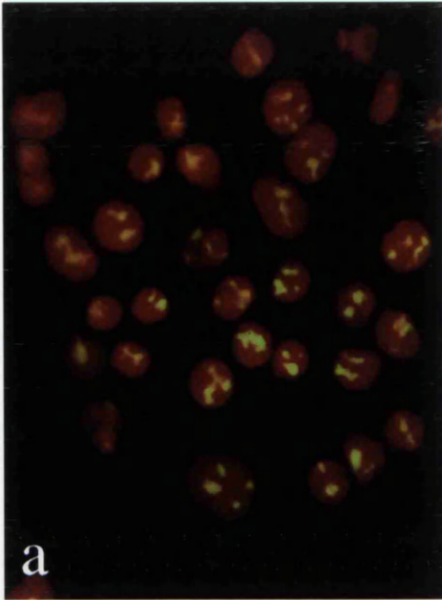
## **Figure 5.4**

### **Detection of TOPO II $\beta$ gene expression by immunofluorescence.**

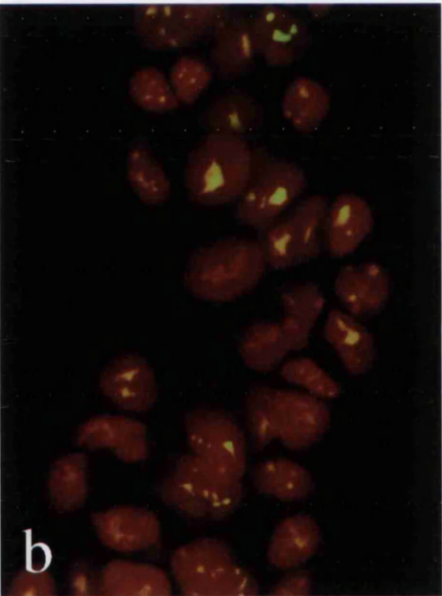
**(a): L-DAN, (b): CALU-3, (c): SK-MES-1**

Nuclei are counterstained with propidium iodide (pseudocoloured red), topoisomerase II $\beta$  detected with FITC (pseudocoloured green). The mouse monoclonal antibody 8F8 was used to detect topoisomerase II $\beta$ .

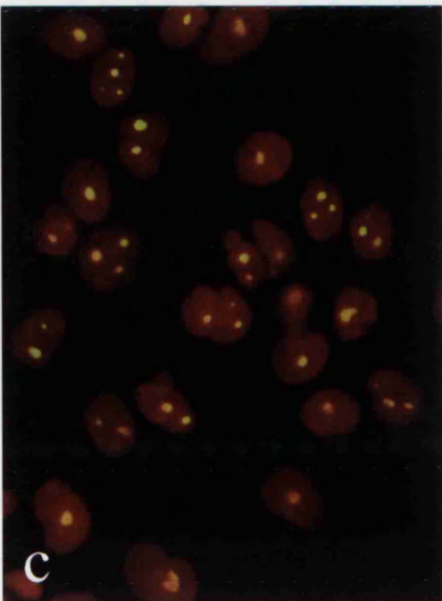
Topoisomerase II $\beta$  was observed in every cell of the population in all three cell lines. Expression of this enzyme appears to be restricted to the nucleoli.



L-DAN



CALU-3



SK-MES-1

## **Figure 5.5**

### **Co-localisation of topoisomerase II $\beta$ with a nucleolar control antibody.**

**(a): L-DAN, (b): CALU-3, (c): SK-MES-1**

Nuclei are counterstained with propidium iodide (pseudocoloured blue), topoisomerase II $\beta$  was detected with Cy<sup>5</sup> (pseudocoloured red), nucleolar control was detected with FITC (pseudocoloured green).

The mouse monoclonal antibody 8F8 was used to detect topoisomerase II $\beta$  and an anti-human nucleolus antibody from ImmunoConcepts (c/o Alpha Laboratories) was used to detect nucleoli.

Topoisomerase II $\beta$  expression was again observed in every cell of the population in all three cell lines, as was the nucleolar signal. Co-localisation of the two signals is apparent when a yellow signal is seen, caused by overlap of the green and red colours used for visualisation.

### **5.3 Discussion**

The data presented in this chapter show the expression of topoisomerase II $\beta$  in L-DAN, CALU-3 and SK-MES-1. Various techniques of both protein isolation and detection were used in an attempt to detect the intact 180kD topoisomerase II $\beta$  enzyme. The major problem in isolating this protein is that it appears to be extremely unstable, degrading very quickly following extraction to produce a 150kD protein (Drake *et al.*, 1989; Negri *et al.*, 1993). The antibody used for all the analyses was 8F8, a mouse monoclonal antibody kindly supplied by Dr. Astaldi Ricotti, Pavia, Italy. This antibody was one of six anti-topoisomerase II $\beta$  monoclonal antibodies produced by this group and was first reported in 1992 in a paper by Negri *et al.* (Negri *et al.*, 1992). This antibody has previously been shown in Western analysis to detect a single band in extracts from both human and bovine cells, and has also been shown not to cross-react with purified topoisomerase II $\alpha$  protein (Negri *et al.*, 1993).

Due to the problems often encountered in the detection of the intact topoisomerase II $\beta$  it was decided to use dot blotting as the initial method of detection. Although this technique does not give any idea of specificity of the antibody, since the size of any protein detected is not known, it does enable one to see that the antibody being used is recognising a protein. The autoradiograph in Figure 5.1 shows that 8F8 is recognising a protein in all three cell lines, and its' detection is linked to protein concentration. The blot incubated with secondary antibody alone shows that there was minimal background in this experiment, and the signal obtained in the first panel was as a result of incubation with the anti-topoisomerase II $\beta$  antibody.

To ensure that the anti-topoisomerase II $\beta$  antibody was detecting the topoisomerase II $\beta$  protein, a Western was run of L-DAN, CALU-3 and SK-MES-1 whole cell extracts. One half of this Western blot was incubated with anti-topoisomerase II $\alpha$  antibody, and the other with anti-topoisomerase II $\beta$  antibody. The results shown in Figure 5.2 clearly show a different signal is obtained in the topoisomerase II $\beta$  detected filter (lanes 4, 5 and 6) as opposed to the II $\alpha$  filter (lanes 1, 2 and 3), thus there does not appear to be any cross-reaction of the anti-topoisomerase II $\beta$  antibody with topoisomerase II $\alpha$ . Unfortunately in this Western, only the 150kD degradation product of topoisomerase II $\beta$  has been detected, which has also been reported on a number of occasions (Negri *et al.*, 1992; Zini *et al.*, 1992). It is difficult to compare levels of topoisomerase II $\beta$  expression by the levels of this 150kD protein since the beta isozyme may have different stabilities in

the different cell lines. The level of the 150kD protein in lane 6 (SK-MES-1) is very low. This may be a result of interference in either primary antibody incubation or detection by air bubbles which may block the signal. In lanes 4 and 5, (L-DAN and CALU-3, respectively), a very faint band can be seen above the 150kD band. This may be the intact topoisomerase II $\beta$  protein. There may be various reasons for the degradation of the topoisomerase II $\beta$  protein. Cells from 6-well plates were lysed directly into Western loading buffer and extracts were usually prepared in advance and kept at -20°C until required. It is not known what effect the storage at -20°C might have on this protein. Also, if Western gels were run overnight at room temperature this may affect the 180kD protein.

Therefore, to have some chance of detecting the beta enzyme, it appears that the cell extracts must be prepared very quickly and immediately loaded onto the Western gel. One technique which was already being used in which these criteria were met was the band depletion assay (previously described in Chapter 4). In this assay there is a very quick turn-around from cells in culture to lysates and on to the gel. It was therefore decided to re-incubate a filter from such an assay with the 8F8 antibody. This experiment would also show any effects of VP16 treatment of cells on topoisomerase II $\beta$  levels, if it was successful. The resulting autoradiograph from the topoisomerase II $\beta$  experiment (upper panel) is shown in Figure 5.3, together with the original result of the topoisomerase II $\alpha$  experiment (lower panel). The anti-topoisomerase II $\beta$  antibody detected two bands on the filter. It was assumed that the larger protein detected here was the intact 180kD topoisomerase II $\beta$  protein and the smaller, fainter band was the 150kD degradation product. The relative signal intensities between the topoisomerase II $\alpha$  and topoisomerase II $\beta$  bands is obviously very different. In the beta detected filter, there appears to be little evidence for any effect of VP16 on the levels of topoisomerase II $\beta$  detected, unlike the results seen for topoisomerase II $\alpha$ . This result may have been expected since it was previously reported that the beta isozyme was less sensitive to topoisomerase II inhibitors (Drake *et al.*, 1989). However, there does appear to be a depletion in the amount of topoisomerase II beta in lane 6 (CALU-3), in which the cells were treated with the highest concentration of VP16. Since this effect is not seen in the other two cell lines, it could be that the topoisomerase II $\beta$  in CALU-3 is more sensitive to VP16 than that present in L-DAN or SK-MES-1. In order to prove this, more repetitions of this experiment would be required.

From the levels of the 180kD band detected in this experiment, there appears to be little difference in expression of topoisomerase II $\beta$  between L-DAN and CALU-3, with SK-MES-1 perhaps expressing slightly less. It could be proposed from this result that there is differing stability of the topoisomerase II $\beta$  protein in the different cell lines since varying amounts of degradation of the 180kD protein can be seen on this autoradiograph. More intense bands of the 150kD product can be seen in the L-DAN and SK-MES-1 samples than for CALU-3. This could, of course, also be due to treatment of cells before extracts were made. For example, CALU-3 may have been the first cells lysed, followed by L-DAN and then SK-MES-1.

Immunofluorescence analysis was used as a method of detecting the topoisomerase II $\beta$  protein without worrying about degradation since the treatment of cells for immunofluorescence preserves the protein. Data shown in Figures 5.4 and 5.5 show topoisomerase II $\beta$  expression to be localised strictly to the nucleolus, as has been shown previously for this antibody (Negri *et al.*, 1992; Zini *et al.*, 1992). However, there does appear to be some controversy around the localisation of the topoisomerase II $\beta$  enzyme since a recent study found it to be in the nucleoplasm as well as the nucleolus (Petrov *et al.*, 1993). One explanation for this difference could be the use of polyclonal antibodies which whilst being specific for each isozyme on a Western blot, may cross-react with the related protein when that protein is still in its natural state.

Expression of the beta isozyme appears very different to that of topoisomerase II $\alpha$ , since topoisomerase II $\beta$  is expressed in every cell in all three cell lines. Since the signal is so intense in the cells, it is very difficult to quantify this result, although the results of Western blotting do not appear to show any major differences between L-DAN, CALU-3 and SK-MES-1. From Figure 5.5 it can be seen that the beta enzyme co-localises with a nucleolar control antibody. The anti-nucleolar antibody has not yet been fully characterised, thus it is not known what its' protein target is.

The finding that topoisomerase II $\beta$  expression is localised to nucleoli, and appears to be differentially regulated to topoisomerase II $\alpha$  has led to suggestions that the two isozymes may perform different functions within the cell. It has been proposed that topoisomerase II $\alpha$  is more involved with DNA replication since its expression is upregulated during cell proliferation, whereas topoisomerase II $\beta$  is involved with DNA transcription, particularly of ribosomal genes, since its expression appears to be higher at the plateau stage of the cell cycle. As mentioned previously, it was discovered that topoisomerase II $\beta$  bound preferentially to G-C-rich regions of DNA

(Drake *et al.*, 1989). This is of interest since certain genes have been found to exhibit G-C-rich promoter regions (Kozasa *et al.*, 1988). It may be that topoisomerase II $\beta$  plays a role in the transcriptional regulation of these genes. There is also evidence that nucleolar DNA itself is G-C-rich, and may therefore lend itself to preferential binding of topoisomerase II $\beta$  (Willems *et al.*, 1968). The discovery of the second topoisomerase II could also be extremely useful for cancer therapy since, although it appears to be slightly more resistant to the effects of current topoisomerase II inhibitors, it could be a target for therapy in its own right where there is low expression of topoisomerase II $\alpha$ . This could be extremely valuable in cases of relapsed tumours where cells have become resistant by reducing expression of topoisomerase II $\alpha$ , or are expressing a mutant topoisomerase II $\alpha$ .

In order to quantify TOPO II $\beta$  expression levels in the three cell lines which have been studied, RNase protection assays could be performed, and the Northern analysis could be repeated. With respect to protein analysis of the topoisomerase II beta enzyme, it should be pointed out that much of the data which has so far been accumulated on this enzyme has been through the use of only a couple of different antibodies, one from the Italian group of Dr. Astaldi Riccotti, and the other from Dr. Fred Drake. Therefore, perhaps detection of the topoisomerase II $\beta$  protein would be easier and more reliable if there were more anti-topoisomerase II $\beta$  antibodies available.

## CHAPTER 6

# INVESTIGATION INTO THE VP16-RESISTANCE OF A CALU-3 CLONE.

### 6.1 Introduction

As mentioned in previous chapters, topoisomerase II is the target for a number of anti-tumour agents including mAMSA and VP16. In section 4.1, details were given as to how both changes in the expression of topoisomerase II and alterations in the molecule itself can lead to resistance or sensitivity of cells to topoisomerase II-targeting agents. Numerous studies, using both human and rodent cell lines, have found that a low or reduced level of topoisomerase II expression correlates with drug resistance (Davies *et al.*, 1988; de Jong *et al.*, 1993; Friche *et al.*, 1992; Lefevre *et al.*, 1991; Long *et al.*, 1991; Per *et al.*, 1987; Potmesil *et al.*, 1988; Ritke *et al.*, 1994; Tan *et al.*, 1989; Webb *et al.*, 1991; Zwelling *et al.*, 1990b). With the exception of the study of normal and leukaemic lymphocytes by Potmesil *et al.*, all the above analyses were performed using drug-resistant cell lines derived *in vitro*. Despite most of these drug resistant cell lines being selected with one drug (commonly mAMSA, doxorubicin, mitoxantrone, VP16 or VM26), a cross-resistance to one or other of these drugs, or other topoisomerase II inhibitors can also be found (Cole *et al.*, 1991; de Jong *et al.*, 1993; Lefevre *et al.*, 1991; Long *et al.*, 1991; Per *et al.*, 1987; Schneider *et al.*, 1994; Webb *et al.*, 1991). Cross-resistance to *Vinca* alkaloids, such as vincristine and vinblastine, has also been observed in topoisomerase II inhibitor-resistant cell lines (Gupta, 1983; Hill & Bellamy, 1984; Per *et al.*, 1987). Thus cells can be resistant to a number of different agents that are not necessarily related by structure or mechanism of action, which suggests that reduced topoisomerase II levels are not solely responsible for this drug resistance.

This kind of broad cross-resistance is termed multidrug resistance, or MDR. The commonest feature of cells which exhibit the MDR phenotype is amplification and overexpression of the gene encoding a 170kD plasma membrane protein known as P-glycoprotein, which is also associated with a decreased accumulation of drug within the cell. Overexpression of P-glycoprotein has also been found in conjunction with altered topoisomerase II levels (Kamath *et al.*, 1992). In humans, two MDR genes have been discovered, MDR1 and MDR3 (also known as MDR2) (Nooter & Herweijer,

1991; Schinkel *et al.*, 1991; Van der Bliek *et al.*, 1988). It appears, however, that only the MDR1 gene is involved in multidrug resistance (Gros *et al.*, 1986a; Ueda *et al.*, 1987; Van der Bliek *et al.*, 1988). The P-glycoprotein molecule was shown to have a strong homology with bacterial transport proteins (Chen *et al.*, 1986; Gerlach *et al.*, 1986; Gros *et al.*, 1986b). Structural analysis of the protein showed that it consisted of two homologous halves, each containing a hydrophobic domain with six transmembrane regions and a hydrophilic domain (Chen *et al.*, 1986; Gerlach *et al.*, 1986). It was also noted that each segment contained a consensus site for ATP-binding. It was therefore proposed that P-glycoprotein functioned as an energy-dependent drug efflux pump, with the transmembrane domains forming a channel in the cell membrane through which suitable substrates are actively pumped out of the cell. This model for P-glycoprotein function also accounted for the observed decrease in accumulation of drug that was observed in multidrug resistant cells (Endicott & Ling, 1989; Riehm & Biedler, 1972; Sirotiak *et al.*, 1986).

A somewhat controversial issue is whether expression of the MDR phenotype is of relevance in an *in vivo* situation. Numerous studies have been undertaken to analyse P-glycoprotein expression in both haematological and solid tumours (reviewed in Roninson, 1992). A study of P-glycoprotein expression in acute lymphoblastic leukaemia (ALL) showed that the remission rate for MDR-positive patients was approximately half of that for MDR-negative patients (Goasguen *et al.*, 1993). Also, of those MDR-positive patients that achieved a first remission, 81% relapsed compared to 37% of MDR-negative patients. Therefore, P-glycoprotein expression would appear to be prognostically significant in ALL. Increased transcription levels of the MDR1 gene have also been found in high-grade, poorly differentiated bladder cancers (Clifford *et al.*, 1994). In this study, an association was made between high MDR1 gene expression and poor survival. Various studies have shown a correlation between expression of the protein and poor response to chemotherapy, or shorter progression-free survival in breast tumours (Lonn *et al.*, 1993; Verrelle *et al.*, 1991). Studies of other kinds of tumours, however, have found no evidence for involvement of P-glycoprotein in drug resistance (Lai *et al.*, 1989; Shin *et al.*, 1992). It would therefore appear that the significance of P-glycoprotein in tumours depends on the type and origin of the tumour analysed, and also the technique used to analyse expression (Holmes & West, 1994; Schlaifer *et al.*, 1990).

Following the discovery of P-glycoprotein, a number of cell lines were described which appeared to have the MDR phenotype, but in

which no MDR gene expression could be detected (Baas *et al.*, 1990; Beck *et al.*, 1987; Cole *et al.*, 1989; Danks *et al.*, 1987; Mirski *et al.*, 1987; Zwelling *et al.*, 1990b). Such cell lines, lacking P-glycoprotein expression but still exhibiting resistance to a number of natural product antitumour drugs, except the *Vinca* alkaloids, were classified as "atypical" MDR cell lines. Included in this classification are drug resistant cell lines in which no decrease in drug accumulation is observed, but alterations in topoisomerase II are commonly found (Beck *et al.*, 1993a; Beck *et al.*, 1993b). A study of drug resistance associated membrane proteins in human leukaemic HL60-adriamycin resistant cells (HL60/Adr), lacking expression of MDR genes, discovered a 190kD, ATP-binding protein which was not present in either HL60-vincristine resistant or HL60-sensitive cells (McGrath *et al.*, 1989). In a further study of resistance associated membrane proteins in HL60/Adr (Marquardt *et al.*, 1990), numerous antisera were raised against synthetic peptides from different sequence domains of the P-glycoprotein molecule. All of the antisera reacted with P-glycoprotein (p170) in the vincristine resistant HL60 cell line, whereas in HL60/Adr only 1 antiserum reacted with a 190kD protein (p190). As observed previously, the protein was also found to be capable of binding ATP (Marquardt *et al.*, 1990). These results indicated that a minor sequence homology existed between the 190kD protein and P-glycoprotein.

Differential hybridisation of cDNA prepared from total mRNA from the previously characterised H69AR human lung cancer cell line (Cole *et al.*, 1989; Mirski *et al.*, 1987) and parental H69 cells, found one cDNA which was 100- to 200-fold overexpressed in H69AR cells (Cole *et al.*, 1992). This overexpression was found to be caused by gene amplification, with the amplification being lost in reverted drug resistant cells. A further association between the overexpressed gene and drug resistance was made when overexpression of the gene was discovered in a drug resistant HeLa cell line, which lacked P-glycoprotein expression (Cole *et al.*, 1992). The protein coded for by this gene was designated MRP (multidrug resistance-associated protein) and was found to be a member of the ATP-binding cassette superfamily of transport systems (Hyde *et al.*, 1990), which also includes P-glycoprotein. The gene for MRP was mapped to the short arm of chromosome 16 (Cole *et al.*, 1992). Fluorescence in situ hybridisation analysis of H69AR and HT1080/DT4 chromosomes, (HT1080/DT was previously characterised in Zwelling *et al.*, (1990b)), localised the amplified MRP gene to homogeneously staining regions on numerous chromosomes in both cell lines, with hybridisation of MRP also found on double minutes in

H69AR (Slovak *et al.*, 1993). Therefore, further evidence was provided for the involvement of MRP in drug resistance of certain tumour types.

Following the cloning of the gene for MRP, it was deduced that the gene encoded a 190kD membrane bound glycoprotein (Krishnamachary & Center, 1993) which confirmed the earlier reports of the p190 protein found in HL60/Adr cells (Marquardt *et al.*, 1990). Transfection studies using the complete coding sequence of the MRP gene showed that the level of drug resistance in transfected cells was proportional to the level of 190kD protein expressed (Grant *et al.*, 1994). Transfectants were also shown to be resistant to vincristine and VP16, as was previously seen in "atypical" MDR cell lines. Another study investigated MRP expression levels in doxorubicin resistant non-small cell lung cancer cell lines (Barrand *et al.*, 1994) and also found that the most resistant cells exhibited the highest levels of MRP protein expression, with loss of MRP expression in revertant cell lines. It is also of interest to note that the MRP phenotype can be found in conjunction with changes to topoisomerase II expression (Cole *et al.*, 1991; de Jong *et al.*, 1993; Friche *et al.*, 1992; Schneider *et al.*, 1994).

Very recent data, generated using stable MRP transfectants and immunohistochemistry, has shown that the multidrug resistance-associated protein is plasma membrane bound and is possibly a drug efflux pump (Flens *et al.*, 1994; Zaman *et al.*, 1994), similar to P-glycoprotein. It would therefore be assumed to act in a similar way to P-glycoprotein by actively pumping drugs out of the cell. Differences have been found, however, in the substrates which can interact with the two molecules, since MRP-transfected cells do not appear to be resistant to taxol, whereas MDR1-transfected cells are (Mickisch *et al.*, 1991; Zaman *et al.*, 1994). Also, cyclosporin A is seen to reverse P-glycoprotein mediated drug resistance but is not capable of reversing MRP mediated resistance (Zaman *et al.*, 1994). Very little data has been generated concerning the relevance of MRP expression in the clinic. One study performed to investigate MRP RNA expression levels in acute and chronic leukaemias (Burger *et al.*, 1994) found a high frequency of MRP overexpression in chronic lymphocytic leukaemia samples, but only occasional high expression in acute cases. No samples were found with amplification of the gene.

The work presented in the following section has involved the characterisation of a VP16-resistant cell line derived from a CALU-3 sensitive clone. The resistant cell line, CALU-3/10<sup>-5</sup>M VP16 was derived as outlined in section 2.2.1. The ID<sub>50</sub> values for parental CALU-3 clone 4 and CALU-3/10<sup>-5</sup>M VP16 are shown in the table below (from Dr. J. Plumb, Medical

Oncology, Glasgow). The table shows results from a representative experiment, where each cell line was tested in triplicate.

Cell Line	ID <sub>50</sub> (μM)			
	VP16	Doxorubicin	Vincristine	Cisplatin
CALU-3 Clone 4	0.26 ± 0.02	0.0062 ± 0.0004	0.0107 ± 0.004	0.40 ± 0.03
CALU-3 10 <sup>-5</sup> M VP16	2.1 ± 0.1 (8x)	0.52 ± 0.08 (84x)	0.69 ± 0.04 (65x)	0.58 ± 0.05 (1.5x)

Therefore, it can be seen that CALU-3/10<sup>-5</sup>M is resistant to VP16 and cross-resistant to doxorubicin and vincristine. As has been previously mentioned, there could be at least three possible causes for this drug resistance, these being alterations to topoisomerase II, overexpression of P-glycoprotein or overexpression of MRP. Investigations were therefore carried out to analyse each of these possibilities using both the parental CALU-3 clone 4 cell line and CALU-3/10<sup>-5</sup>M VP16 resistant cell line. Biochemical assays were performed to check topoisomerase II activity in the two cell lines. Flow cytometry was carried out for P-glycoprotein expression, and Western analysis was performed to analyse MRP expression levels.

## **6.2 Results**

This chapter has involved the use of various techniques in an attempt to discover the cause of drug resistance in a VP16-resistant CALU-3 clone. Three successively more VP16 resistant CALU-3 cell lines were derived from CALU-3 clone 4, a VP16 sensitive clone. The first, CALU-3/10<sup>-6</sup>M VP16 was resistant to 1μM VP16. The second, CALU-3/9x10<sup>-6</sup>M VP16 was resistant to 9μM VP16. The final cell line, CALU-3/10<sup>-5</sup>M VP16 was resistant to 10μM VP16. Investigations were performed to analyse the expression levels of topoisomerase II $\alpha$ , P-glycoprotein and the multidrug resistance-associated protein, MRP using the parental CALU-3 clone 4 cell line and the derived, drug resistant CALU-3/10<sup>-5</sup>M VP16 cell line.

### **Western Blotting Detection of Topoisomerase II $\alpha$**

It is known from the results shown in Chapter 4 that CALU-3 has high expression of the topoisomerase II $\alpha$  enzyme. Therefore, it was of interest to see if the levels of topoisomerase II $\alpha$  protein were reduced in the derived drug resistant cell line, CALU-3/10<sup>-5</sup>M VP16 since this is a known mechanism of resistance against topoisomerase II targeting agents. Figure 6.1 shows the result from a Western blot of CALU-3 clone 4 and CALU-3/10<sup>-5</sup>M VP16 crude protein extracts incubated with anti-topoisomerase II $\alpha$  antibody from CRB. From Figure 6.1 there does not appear to any major difference in topoisomerase II $\alpha$  protein levels between the CALU-3 clone 4 (lane 1) and CALU-3/10<sup>-5</sup>M VP16 (lane 2). The smaller band observed at around 130kD is presumed to be a degradation product from the topoisomerase II $\alpha$  protein.

### **Biochemical Assays for Topoisomerase II**

Even though there does not appear to be any difference in topoisomerase II $\alpha$  protein levels between the parental and drug-resistant CALU-3 cell lines, the VP16 resistance could be caused by a mutation of the topoisomerase II molecule (Bugg *et al.*, 1991; Per *et al.*, 1987). If this was the case, the topoisomerase II from CALU-3/10<sup>-5</sup>M VP16 may have altered catalytic activity, as was shown in the above studies. Biochemical assays were performed to test this theory using the same crude nuclear extracts as used for the Western in Figure 6.1 in the TopoGEN assay system, as detailed in section 2.2.11. The results of these assays are shown in Figure 6.2. Panel

**Figure 6.1**

**Detection of topoisomerase II $\alpha$  in CALU-3 clone 4 and CALU-3/10<sup>-5</sup>M VP16 using Western analysis.**

**Lane 1: CALU-3 clone 4, Lane 2: CALU-VP16**

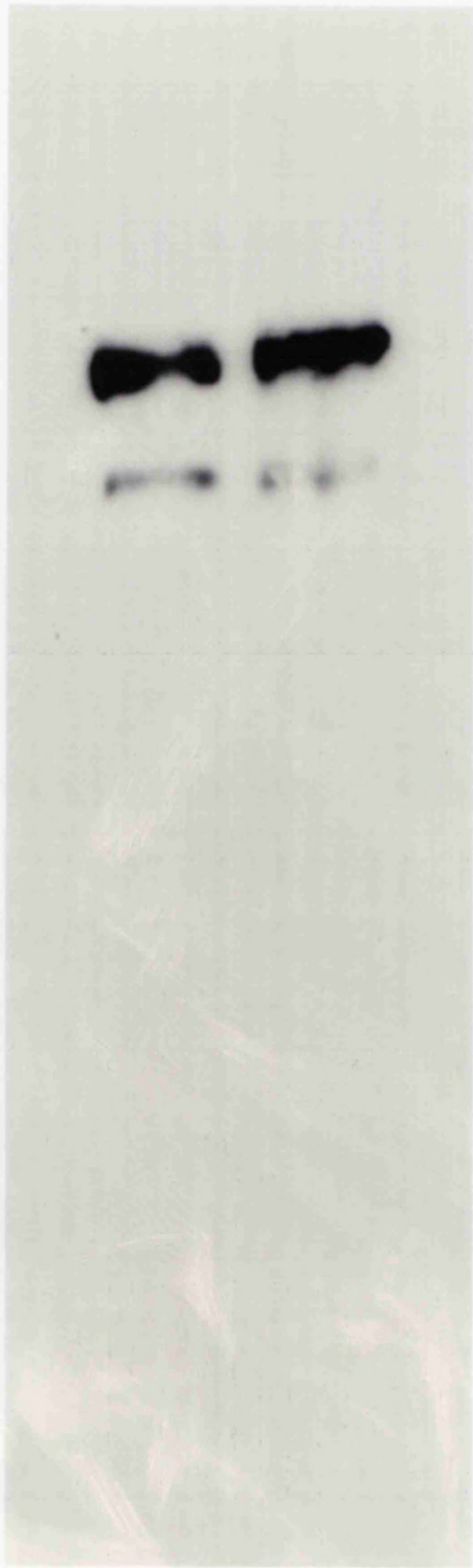
50 $\mu$ g of crude extract was loaded per lane for each cell line.

Topoisomerase II $\alpha$  (170kD) was detected using a rabbit polyclonal from Cambridge Research Biologicals.

Molecular mass standards are shown in kilodaltons on the right of the figure.

Incubation with antibody against topoisomerase II $\alpha$  shows approximately the same levels of topoisomerase II $\alpha$  are observed in the parental CALU-3 clone 4 cell line (lane 1) and CALU-3/10<sup>-5</sup>M VP16 line (lane 2).

The smaller band is a degradation product from the p170 protein.



— 206

← Topo IIα

— 110

— 70

— 43

1

2

## **Figure 6.2**

### **Decatenation of kinetoplast DNA by cellular extracts from A: CALU-3 clone 4, B: CALU-3/10<sup>-5</sup>M VP16.**

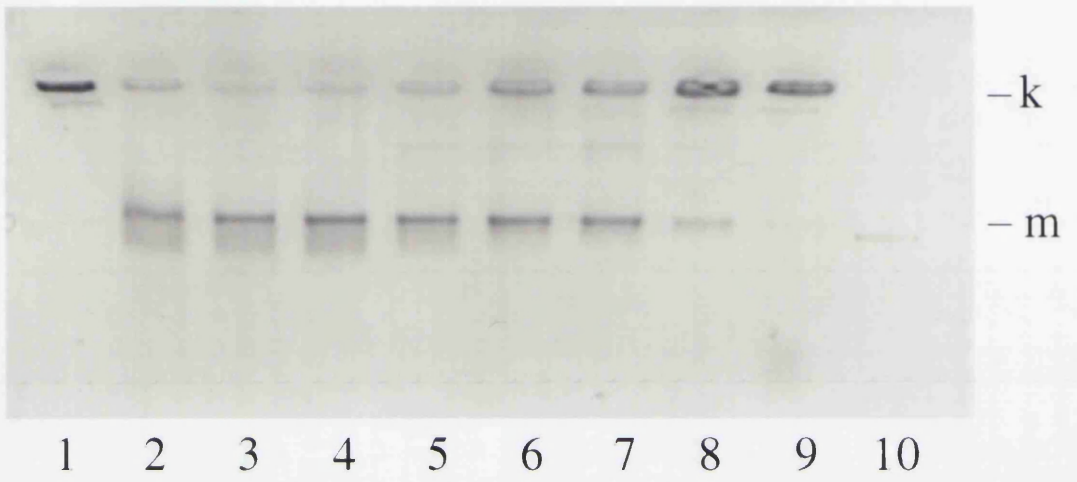
Serial dilutions of crude nuclear extracts were assayed for topoisomerase II activity:

**Lane 1: 0 $\mu$ g, Lane 2: 5 $\mu$ g, Lane 3: 2.5 $\mu$ g, Lane 4: 1.25 $\mu$ g,  
Lane 5: 0.625 $\mu$ g, Lane 6: 0.312 $\mu$ g, Lane 7: 0.156 $\mu$ g,  
Lane 8: 0.078 $\mu$ g, Lane 9: 0.039 $\mu$ g,  
Lane 10: Fully decatenated kinetoplast DNA**

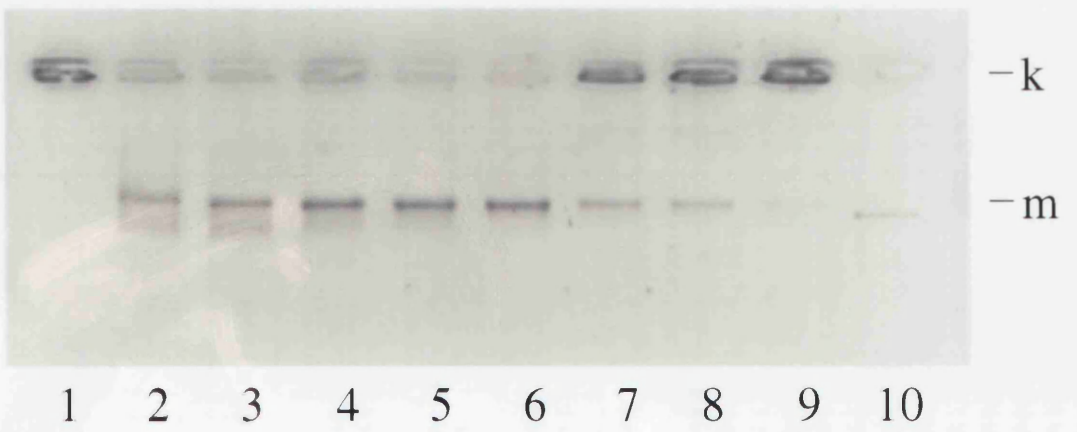
Topoisomerase II activity decatenates kinetoplast DNA to monomer minicircles (m). In the absence of cellular extract, kinetoplast DNA (k) remains in the well of the gel (Lane 1).

Topoisomerase II activity can be observed down to 0.039 $\mu$ g of protein in both CALU-3 clone 4 extract and CALU-3/10<sup>-5</sup>M VP16 extract. Therefore, there does not appear to be any difference in topoisomerase II activities between the parental and resistant cell lines.

A



B



A shows the catalytic activity in CALU-3 clone 4 and panel B shows the catalytic activity in the CALU-3/10<sup>-5</sup>M VP16 clone. In both the CALU-3 samples, topoisomerase II activity can be observed down to a protein concentration of 0.039µg (lane 9, panels A and B). Therefore there does not appear to be any difference in the catalytic activity of topoisomerase II between CALU-3 clone 4 and CALU-3/10<sup>-5</sup>M VP16.

Since there is no difference in topoisomerase II activity between the parental and resistant CALU-3 cell lines, the possibility of mutation of topoisomerase II was investigated which can also render a cell insensitive to topoisomerase II inhibitors (Takano *et al.*, 1992). This was achieved by attempting to inhibit the topoisomerase II activity in CALU-3/10<sup>-5</sup>M VP16 by the addition of VP16 to biochemical assay reactions. The same assay was shown in Chapter 4 with the three cell lines, CALU-3, L-DNA and SK-MES-1. Figure 6.3 shows the results of the inhibition assay with CALU-3/10<sup>-5</sup>M VP16. Formation of monomer minicircles, indicative of topoisomerase II catalytic activity, can be seen to be inhibited in reactions containing 100 and 200µM VP16 (lanes 4 and 5). A small amount of topoisomerase II activity remains, however, when cells are treated with 50µM VP16 (lane 3). Therefore, the topoisomerase II in the CALU-3/10<sup>-5</sup>M VP16 cell line is sensitive to inhibition by VP16, thus neither reduction in topoisomerase II expression nor alterations to the topoisomerase II molecule appear to be responsible for the VP16 drug resistance in CALU-3/10<sup>-5</sup>M VP16.

### **Flow Cytometry**

As mentioned in section 6.1, there are two major proteins which have been implicated in the development of drug resistance *in vitro*, these being P-glycoprotein and MRP. The level of P-glycoprotein was measured in both CALU-3 clone 4 and CALU-3/10<sup>-5</sup>M VP16. As a control, the A2780 and A2680/Adr cell lines were analysed since it is known that A2780/Adr overexpresses P-glycoprotein (Rogan *et al.*, 1984; Sugawara *et al.*, 1988; Van der Bliek *et al.*, 1988). Figure 6.4 shows the results of flow cytometry using A2780 and A2780/Adr with MRK16 and JSB1, independent anti-P-glycoprotein antibodies. Panels (A) and (B) show the results of incubation of A2780 cells with MRK16 and JSB1 antibodies, respectively. Panels (C) and (D) show results of incubation of A2780/Adr cells with MRK16 and JSB1 antibodies, respectively. Empty peaks correspond to isotype control samples, and coloured peaks correspond to incubation with

### **Figure 6.3**

#### **Inhibition of topoisomerase II activity by VP16**

Crude nuclear extract from the CALU-3/10<sup>-5</sup>M VP16 resistant cell line was assayed for decatenation activity in the presence of increasing concentrations of VP16.

**Lane 1:** no drug, no nuclear extract

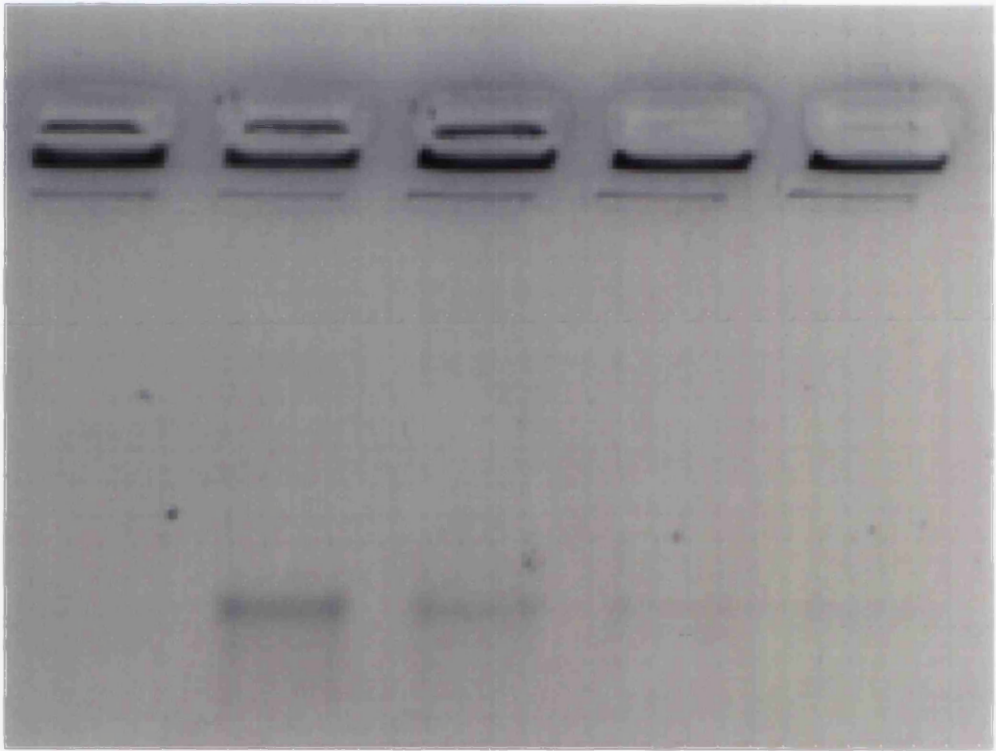
**Lane 2:** no drug, DMSO diluant control, **Lane 3:** 50 $\mu$ M VP16,

**Lane 4:** 100 $\mu$ M VP16, **Lane 5:** 200 $\mu$ M VP16

k=kinetoplast DNA, m=monomer minicircles

1.25 $\mu$ g of protein was used in each reaction

From this figure it can be seen that VP16 is capable of inhibiting topoisomerase II activity in CALU-3/10<sup>-5</sup>M VP16.



1

2

3

4

5

← k

← m

## **Figure 6.4**

### **Flow cytometry graphs of P-glycoprotein status in A & B: A2780, C & D: A2780/Adr**

Samples shown in plots A & C were analysed using the JSB1 antibody against P-glycoprotein

Samples shown in plots B & D were analysed using the MRK16 antibody against P-glycoprotein

Empty peaks indicate isotype control samples  
Coloured peaks indicate samples incubated with  
anti-P-glycoprotein primary antibody

X-axis: FITC fluorescence level

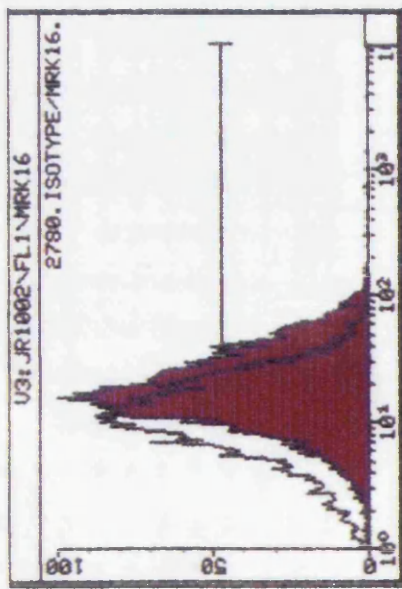
Y-axis: Cell number

Plots A and B (A2780) show that there is very little positivity for P-glycoprotein in this cell line since the coloured peak only shifts very slightly along the X-axis from the control peak, indicating low FITC fluorescence.

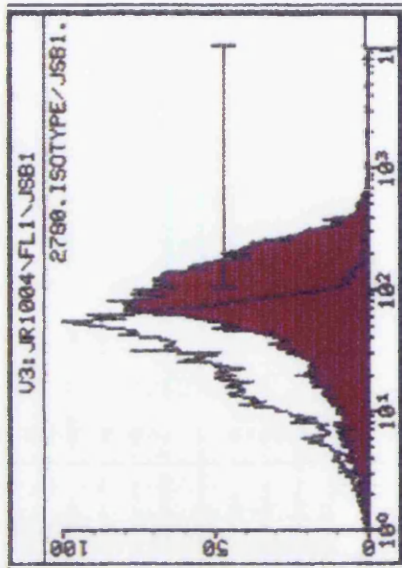
Plots C and D (A2780/Adr) show the high expression of P-glycoprotein which has previously been characterised in this cell line. This is shown by a large shift of the coloured peak along the X-axis from the control peak, indicating high levels of FITC fluorescence.

Therefore, P-glycoprotein expression is seen in the A2780/Adr resistant cell line using the two independent antibodies.

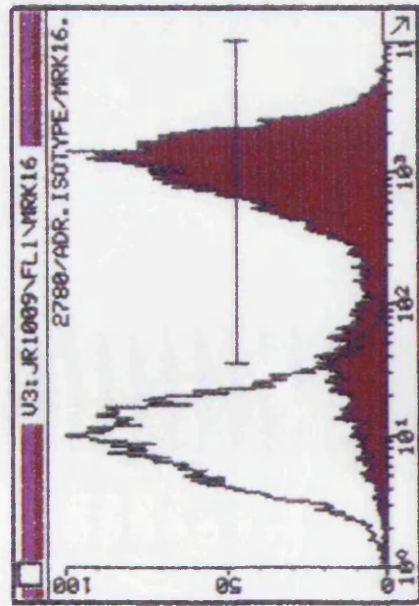
A



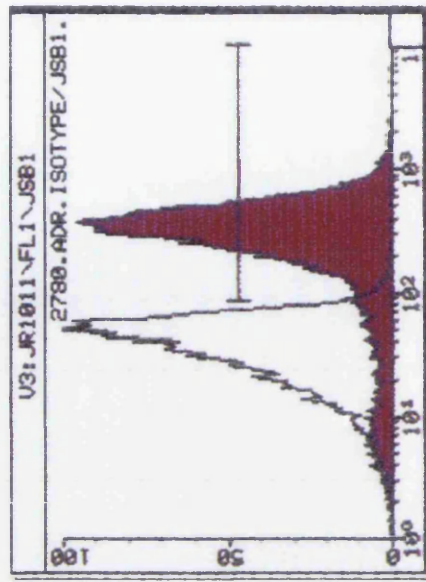
B



C



D



anti-P-glycoprotein antibodies. FITC fluorescence is shown along the x-axis in all four panels. With A2780 cells, the control peak and the MRK16/JSB1 peaks are almost super-imposed on one another, thus there is very little P-glycoprotein expression in this cell line. With A2780/Adr, however, there is a large shift of both the MRK16/JSB1 peaks to the right of the isotype control peaks. Thus, the levels of FITC fluorescence are much higher in this cell line, indicating a high level of P-glycoprotein expression.

Figure 6.5 shows the same experiment performed using CALU-3 clone 4 and CALU-3/10<sup>-5</sup>M VP16 cells. Panels (A) and (B) show results of JSB1 and MRK16 incubation of CALU-3 clone 4 cells. Again, empty peaks show isotype control samples and coloured peaks show results obtained with anti-P-glycoprotein antibodies. Therefore, the same results are seen with CALU-3 clone 4 cells as was seen with A2780 cells, indicating that there is little expression of P-glycoprotein in this cell line. Panels (C) and (D) show the results of incubation of CALU-3/10<sup>-5</sup>M VP16 cells with JSB1 and MRK16 antibodies. It would therefore appear from these results that, as observed in the parental clone 4 line, CALU-3/10<sup>-5</sup>M VP16 cells do not express P-glycoprotein.

### **Western Analysis for MRP**

Since from the above experiments it appeared that P-glycoprotein was not responsible for the drug resistance in CALU-3/10<sup>-5</sup>M VP16 it was decided to investigate the expression of the "atypical" drug resistance protein, MRP. Two independent experiments were performed to analyse MRP expression in the parental and drug resistant cell lines. One Western blot was incubated with the polyclonal rabbit antiserum against MRP, ASPKE, obtained from Dr. Melvin Center in Kansas. A different blot was sent to Dr. Susan Cole's laboratory in Canada and was incubated with their monoclonal antibody against MRP, QCRL-1. The results of this Western analysis are shown in Figure 6.6. Panel (A) shows the autoradiograph resulting from incubation of the Western blot with the ASPKE antibody. A band of approximately 190kD can clearly be seen in lanes 1 and 4, with a fainter band visible in lane 3. Protein samples from CALU-3 clone 4 and CALU-3/10<sup>-5</sup>M VP16 are present in lanes 3 and 4, respectively, of this Western blot. Therefore, it would appear that CALU-3/10<sup>-5</sup>M VP16 has increased expression of the MRP protein compared to the parental clone. Lane 1 contains a sample of protein extract from the NSCLC cell line, L-

## **Figure 6.5**

### **Flow cytometry graphs of P-glycoprotein status in A & B: CALU-3 clone 4, C & D: CALU-3/10<sup>-5</sup>M VP16**

Samples shown in plots A & C were analysed using the JSB1 antibody against P-glycoprotein

Samples shown in plots B & D were analysed using the MRK16 antibody against P-glycoprotein

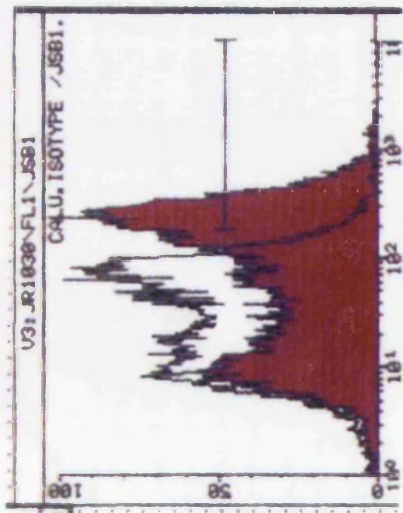
Empty peaks indicate isotype control samples  
Coloured peaks indicate samples incubated with  
anti-P-glycoprotein primary antibody

X-axis: FITC fluorescence level

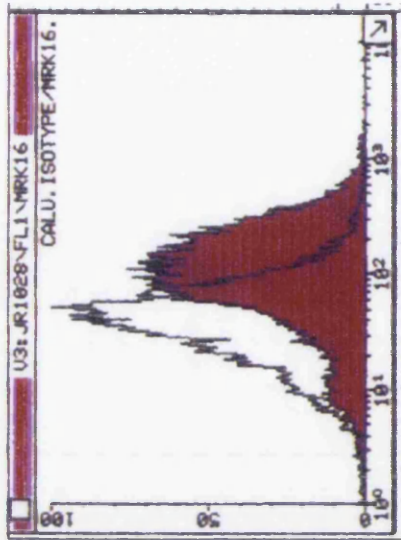
Y-axis: Cell number

These plots show that there is very little P-glycoprotein detectable in either CALU-3 (plots A and B) or the CALU-3/10<sup>-5</sup>M VP16 resistant cell line (plots C and D) since only a slight difference in X-axis position is observed between the two peaks.

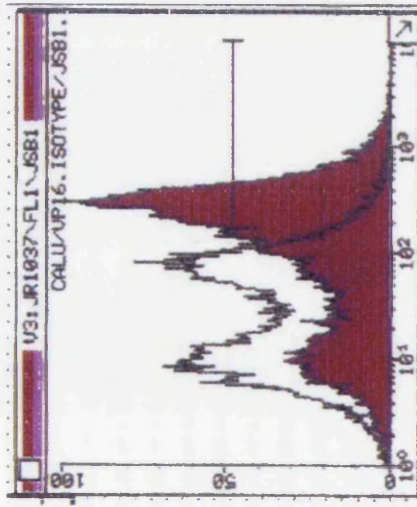
A



B



C



D

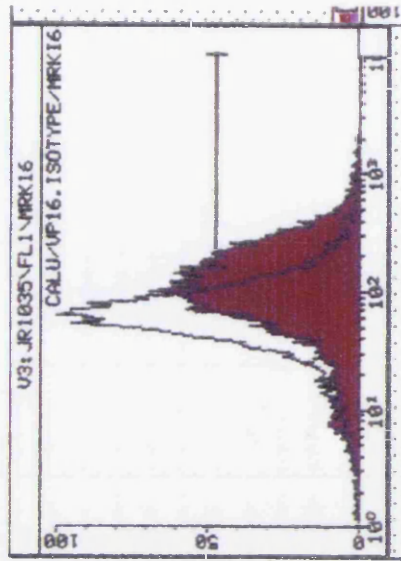


## **Figure 6.6**

### **Detection of MRP (p190) using Western analysis.**

**Blot A:** Incubated with ASPKE, polyclonal antiserum against MRP, kindly provided by Dr. Melvin Center.

**Lane 1:** L-DAN, **Lane 2:** SK-MES-1, **Lane 3:** CALU-3 clone 4,  
**Lane 4:** CALU-3/10<sup>-5</sup>M VP16

**Blot B:** Incubated with QCRL-1, a monoclonal antibody against MRP. Incubation kindly performed by Dr. Susan Cole.

**Lane 1:** L-DAN, **Lane 2:** SK-MES-1,  
**Lane 3:** CALU-3 (heterozygous population),  
**Lane 4:** CALU-3 clone 4, **Lane 5:** CALU-3/10<sup>-5</sup>M VP16

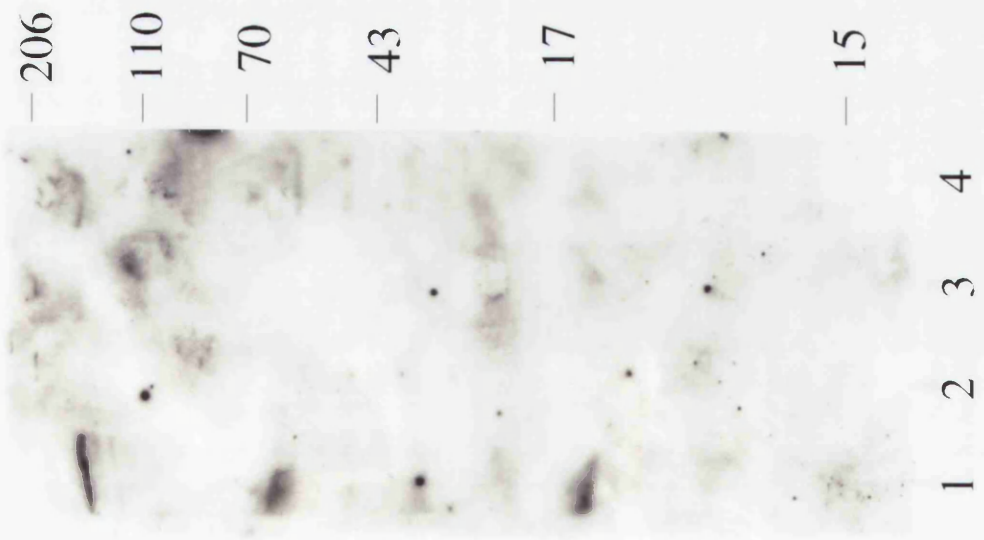
50 $\mu$ g of crude extract was loaded per lane for each cell line.

Molecular mass standards are shown in kilodaltons on the right of each panel

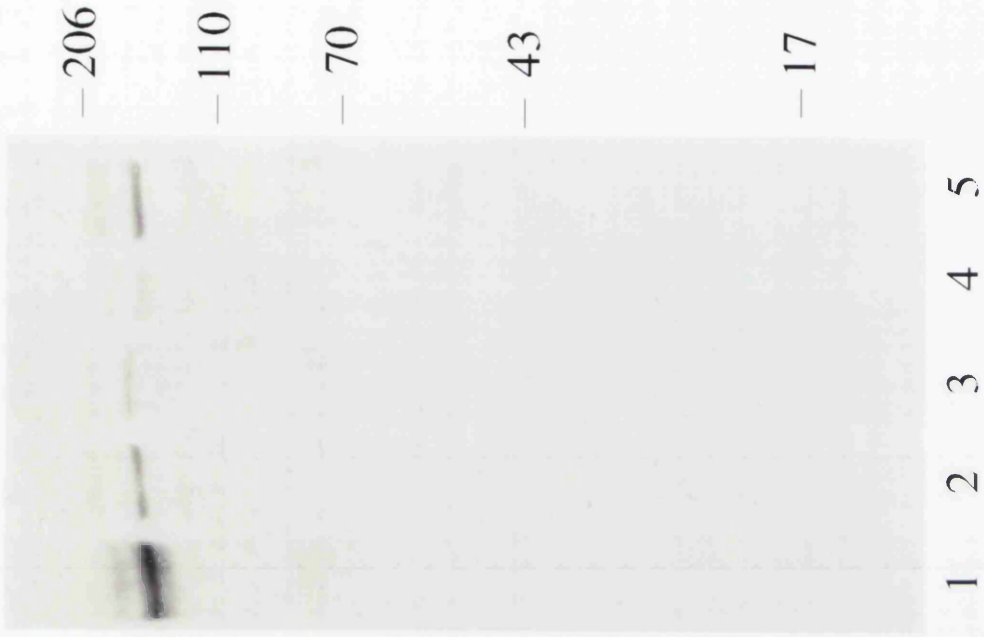
Blots A and B both show higher levels of MRP expression in CALU-3/10<sup>-5</sup>M VP16 (Blot A, lane 4 and Blot B, lane 5) than in the parental CALU-3 clone 4 cell line (Blot A, lane 3 and Blot B, lane 4). Therefore, high expression of this protein may be the cause of the drug resistance in CALU-3/10<sup>-5</sup>M VP16.

High expression of MRP is also seen in L-DAN (Lane 1 in both blots).

A



B



DAN, which also appears to have high levels of expression of MRP. No MRP expression is detectable in SK-MES-1 (lane 2).

The result of independent analysis of a different Western blot by Dr. Susan Cole with a monoclonal antibody against MRP is shown in Figure 6.6, panel (B). Using this antibody, a band of approximately 190kD can be seen in all lanes on the Western blot. Protein samples from CALU-3 clone 4 and CALU-3/10<sup>-5</sup>M VP16 are in lanes 4 and 5, respectively, on this blot. Lane 3 contains protein extract from the heterozygous CALU-3 population. Thus, low levels of MRP expression are seen in both the overall CALU-3 population, and in the CALU-3 clone 4 cells. The level of MRP expression in CALU-3/10<sup>-5</sup>M VP16 cell line appears to be higher than in either of the other two CALU-3 populations. Therefore, these results repeat the findings shown with the ASPKE antiserum. Interestingly, this blot again shows the high level of expression of MRP in L-DAN (lane 1) and MRP expression is also detectable in SK-MES-1 (lane 2).

### **6.3 Discussion**

There are several mechanisms of drug resistance in both cell lines and tumours, as previously described in section 6.1. The aim of this section of work has been to deduce the mechanism of drug resistance in a cell line, CALU-3/10<sup>-5</sup>M VP16, which displays an 8-fold resistance to VP16 when compared to the VP16-sensitive parental cell line, CALU-3 clone 4, as well as being highly cross resistant to doxorubicin and vincristine. The mechanisms of resistance that were analysed were possible alterations to topoisomerase II, with respect to genetic changes, expression levels and mutations to the molecule itself, overexpression of P-glycoprotein and overexpression of the multidrug resistance-associated protein, MRP.

The data presented in this chapter has revealed that the drug resistant, non-small cell lung adenocarcinoma cell line CALU-3/10<sup>-5</sup>M VP16 does not appear to have any change in expression of, or alteration to topoisomerase II when compared to the sensitive, parental CALU-3 clone 4. This has been shown by Western blotting (Figure 6.1) and biochemical assays (Figures 6.2 and 6.3). In the Western blotting data, however, only the topoisomerase II $\alpha$  isoform has been detected and by biochemical assay it is not possible to distinguish activity of the two topoisomerase II isoforms. Therefore, it should not be ruled out that changes may have occurred to topoisomerase II $\beta$ . The finding that topoisomerase II $\alpha$ , at least, does not appear to be affected in CALU-3/10<sup>-5</sup>M was quite a surprising result, as it was assumed that since the parental CALU-3 clone 4 cell line overexpressed topoisomerase II $\alpha$ , the favoured mechanism of creating a drug resistance when challenged with a topoisomerase II inhibitor would be to reduce the expression of topoisomerase II.

Following this finding, alternative mechanisms which can also result in topoisomerase II inhibitor drug resistance were investigated. The possibility that the drug resistance in CALU-3/10<sup>-5</sup>M VP16 was caused by overexpression of P-glycoprotein was ruled out by flow cytometry analysis performed using two independent monoclonal antibodies, JSB1 and MRK16 (Figure 6.5). These antibodies are truly independent as they each recognise different epitopes of the P-glycoprotein molecule (JSB1 recognises an internal epitope and MRK16 recognises an external epitope). Since a positive result was obtained with the control cell line, A2780/Adr, an adriamycin resistant ovarian carcinoma cell line which is known to overexpress P-glycoprotein (Rogan *et al.*, 1984; Sugawara *et al.*, 1988; Van der Blik *et al.*, 1988), this

proves that the experiment had worked and that the negative results observed with CALU-3 clone 4 and CALU-3/10<sup>-5</sup>M VP16 were true negatives.

Studies of P-glycoprotein expression in lung tumours and lung tumour cell lines have found no correlation between MDR1 gene expression and *in vitro* drug sensitivity of cells (Lai *et al.*, 1989; Shin *et al.*, 1992). Both of these papers showed a low level of MDR1 mRNA in all samples which were analysed, including any normal samples. Out of 114 lung tumours and cell lines analysed in both these studies, only 3 samples displayed low levels of MDR1 gene amplification (Shin *et al.*, 1992). Even clinical trials involving the use of modulators of P-glycoprotein mediated multidrug resistance show that very little effect of these agents is seen in solid tumour types (see Raderer & Scheithauer, 1993 for review). This leads one to propose that another mechanism may be responsible for the drug resistance seen in these tumours.

Since CALU-3/10<sup>-5</sup>M VP16 did not express P-glycoprotein, it was decided to analyse the multidrug resistance-associated protein (MRP) levels in this cell line. MRP has previously been found to be overexpressed in a number of lung tumour cell lines (Baas *et al.*, 1990; Cole *et al.*, 1992; Marquardt *et al.*, 1990; Mirski *et al.*, 1987) and so was a good candidate to be involved in the resistance of the CALU-3 line. Initial investigations into MRP expression were performed using the ASPKE polyclonal antiserum against the MRP protein from Dr. Melvin Center in Kansas (Figure 6.6, panel A). This was the first evidence that MRP was overexpressed in CALU-3/10<sup>-5</sup>M VP16 as compared to CALU-3 clone 4. Following this initial result, a protein blot was sent to Dr. Susan Cole, one of the first people to characterise an MRP-expressing cell line (Cole *et al.*, 1992; Cole *et al.*, 1991), where the blot was probed with a monoclonal antibody against MRP, QCRL-1 (Figure 6.6, panel B). This antibody, again, showed elevated levels of MRP in the VP16 resistant CALU-3 cell line when compared to CALU-3 clone 4. Therefore, it is proposed that overexpression of MRP plays a role in the drug resistance observed in CALU-3/10<sup>-5</sup>M VP16.

Further work remains to be performed with CALU-3/10<sup>-5</sup>M VP16 to investigate whether the MRP gene is amplified in this cell line. Various FISH studies could be carried out to confirm this, including whole chromosome 16 paint analysis (since the MRP gene has been located to chromosome 16p (Cole *et al.*, 1992)) and single copy gene analysis, providing a cosmid probe for MRP could be found. Initial FISH studies with a plasmid carrying a full length cDNA for MRP, pJ3-MRP (kindly provided by Drs. P.Borst and G. Zaman), have proved unsuccessful.

It should be noted that proteins other than MRP have also been found to be associated with drug resistance in studies using non-P-glycoprotein mediated multidrug resistant cell lines (Scheper *et al.*, 1993). This study found overexpression of a 110kD protein (p110) in a drug resistant cell line which was known not to express P-glycoprotein. Expression of p110 was reduced in revertants from the drug resistant cell line. Thus, there would appear to be the possibility that multidrug resistance, at least in *in vitro* derived cell lines, may be caused by a variety of proteins which could all be related.

## CHAPTER 7

### GENERAL DISCUSSION

The work presented in this thesis has involved the characterisation of an amplicon on chromosome 17 in the non-small cell lung adenocarcinoma cell line CALU-3. It has been shown that the TOPO II $\alpha$ , ERBB2, RAR $\alpha$  and G-CSF genes, and the cosmid C05123 from an unknown locus are all contained within an amplified region which is present on three separate chromosomes in CALU-3. The PKC $\alpha$ , NM23H1 and NF1 genes were also analysed and shown to be outside the region of amplification in CALU-3. Co-localisation studies demonstrated that the TOPO II $\alpha$ , ERBB2, RAR $\alpha$ , NM23H1, NF1 and C05123 gene cosmids all remained associated with chromosome 17-specific sequences. This is an important point since previous studies have observed that amplified sequences can remain at the original locus and can also be translocated to unrelated chromosomes (Roelofs *et al.*, 1992). These chromosomal translocation events are associated with the mechanism of amplification. In addition, both amplified and non-amplified genes were also found to co-localise to the same regions. Such co-localisation studies have also been important in providing structural detail of the amplicon. Much of the previous data concerning structural data of amplicons has been derived from *in vitro* selected drug resistant cell lines where the amplification of certain genes has been generated by exposure to particular drugs. This includes studies on amplified DHFR genes (Trask & Hamlin, 1989) and CAD gene amplification (Smith *et al.*, 1990). Both of these studies show a laddering effect of the amplified genes, indicative of amplification occurring via sister chromatid exchange, as discussed in Chapter 3. In comparison with these studies, the work presented in this thesis has involved the structural analysis of a "naturally" occurring amplicon, for which there has been no selective pressure applied. Therefore, it is interesting to note that small ladders of signal are detected for the amplified genes within the amplicon in CALU-3. This pattern of hybridisation of the single copy genes in CALU-3, together with the data showing association of the amplified genes with chromosome 17 centromere sequences, implies that the amplification in CALU-3 may have been brought about by initial sister chromatid exchange. The information gathered concerning the amplicon in CALU-3 is also extremely valuable since it is likely that such an amplicon exists in certain breast tumours (Keith *et al.*, 1993; Murphy *et al.*, in press; Smith *et al.*, 1993),

thus knowledge of the amplification of other genes from the 17q region may have an effect on the clinical treatment of these tumours.

In terms of analysing the structure of the amplicon in CALU-3, a recent technique has been developed which involves the micro-dissection of amplified regions and the production of microclone libraries (Guan *et al.*, 1992; Ray *et al.*, 1994; Zhang *et al.*, 1993). This approach would be useful for analysing the organisation of genes within the amplicon. For example, a recent study has successfully cloned and obtained a structure for amplified DNA sequences from double-minute chromosomes (Fakharzadeh *et al.*, 1993), with three genes found to be located on the circular double minute chromosome, arranged in two identical inverted repeats. Microdissection can also be used to generate probes for use in FISH. Recently, studies have used microdissected homogeneously staining regions in breast tumour cell lines as probes on normal metaphase chromosomes to deduce the origin of the amplified sequences (Guan *et al.*, 1994). Interestingly, microdissected probes generated from a single homogeneously staining region in a drug resistant cell line were found to hybridise to at least four different chromosomal locations on a normal metaphase spread (Ray *et al.*, 1994). This work emphasises the genuine complexity of gene amplification. Thus, if the 17q amplicon was microdissected from CALU-3 and hybridised back onto normal chromosomes, it would be interesting to see if all the sequences within the amplicon originate from chromosome 17q, and if they did, whether the genes amplified in CALU-3 were from a contiguous section of the chromosome.

The data presented in Chapter 3 indicates that ERBB2 is amplified to a greater extent than TOPO II $\alpha$ , which is in turn amplified more highly than RAR $\alpha$  and C05123. The exact copy numbers of these genes were not able to be calculated, however, a computer programme has now been made available to the department which will hopefully enable such data to be generated through ratioing of the fluorescent signals. Differences in the level of amplification of ERBB2 and TOPO II $\alpha$  have also been noted in breast tumour samples (Keith *et al.*, 1993; Smith *et al.*, 1993). The study by Smith *et al.* found ERBB2 amplification to be higher than TOPO II $\alpha$  amplification in three tumours which demonstrated co-amplification of these genes. In contrast, however, three tumours analysed by Keith *et al.* were found to have varying levels of ERBB2 and TOPO II $\alpha$  gene co-amplification, with two of these tumours exhibiting higher amplification of TOPO II $\alpha$  than ERBB2. Therefore, it may be that these variations in levels of gene amplification result from selective pressure in the tumours for the expression of particular genes. Thus, in different tumours there may be different selections applied. For there

to be any selective pressure, however, the respective genes must be expressed within the tumour.

Expression analyses carried out in Chapter 4 have demonstrated that amplification of both the TOPO II $\alpha$  and ERBB2 genes leads to high expression of their protein products. This is an important aspect of the CALU-3 amplicon since previous studies have shown that genes within other multi-locus amplicons can be amplified as "silent partners", with no expression of the genes detected. This has been observed in the case of INT2 and HSTF1 genes in the 11q amplicon (Fantl *et al.*, 1990; Lafage *et al.*, 1990; Tsuda *et al.*, 1989) and the ERBA1 gene, co-amplified with ERBB2 in certain breast tumours (van de Vijver *et al.*, 1987). Therefore, as suggested previously, it may be that expression of TOPO II $\alpha$  and ERBB2 genes was selected for during the process of tumour evolution of CALU-3. It was also noted that the topoisomerase II $\alpha$  encoded by CALU-3 is still capable of being stabilised in a drug/enzyme/DNA complex, and that the overall topoisomerase II content of CALU-3 has catalytic activity. Therefore, it appears that despite the high levels of amplification of the TOPO II $\alpha$  gene, there are no mutations of the enzyme. Flow cytometric analysis has revealed that although the topoisomerase II $\alpha$  protein is present at high levels in CALU-3, the expression of the enzyme still appears to be cell cycle regulated. This is interesting since it is not known what the result of constitutive topoisomerase II $\alpha$  expression would be on a mammalian cell. It may be that if expression of TOPO II $\alpha$  was deregulated that this would perhaps be toxic to the cell in some way.

Most of the work presented on topoisomerase II in this thesis has concentrated on the II $\alpha$  isoform. This is mainly due to the lack of reagents available for detection of the topoisomerase II $\beta$  isoform. Alternative methods could be used for the analysis of topoisomerase II $\beta$  expression, such as RNase protection assays (Jenkins *et al.*, 1992). This isozyme of topoisomerase II may well play a role in drug resistance as, interestingly, loss of the 3p region (the location of the TOPO II $\beta$  gene) has been noted in both tumours and derived drug-resistant cell lines (Patel & Fisher, 1993; Yokota *et al.*, 1987). Therefore, the approaches detailed in this thesis using molecular cytogenetic techniques would prove very valuable in investigations of possible loss of heterozygosity of the TOPO II $\beta$  locus in tumours and cell lines.

From the data presented in Chapter 6 it is clear that drug resistance can be produced by a variety of mechanisms, including the expression of certain drug efflux pumps and/or alterations to the topoisomerase II $\alpha$  molecule. The detection of MRP overexpression in the CALU-3/10<sup>-5</sup>M VP16 resistant line was unexpected. Since no alteration in

topoisomerase II $\alpha$  level was detected, this demonstrates that the phenotype of these cells is stable, even in the presence of topoisomerase II-targeting drugs. Therefore, it may be that in particular tumour types, upregulation of the MRP gene is the mechanism of choice when cells are challenged with certain anti-tumour agents. In fact, it appears that drug resistant lung tumour cell lines often express MRP (Barrand *et al.*, 1994; Cole *et al.*, 1992; Zaman *et al.*, 1993) and not P-glycoprotein. Since multidrug resistance usually appears to involve more than one mechanism, comparative genome hybridisation would be an extremely interesting approach to use with the sensitive parental and VP16-resistant CALU-3 cell lines described in Chapter 6. CGH is a powerful new molecular cytogenetic approach which involves the hybridisation of mixed tumour and normal DNA, each labelled with a different fluorochrome, to normal metaphase spreads. Gains or losses of sequences from the tumour can then be visualised by ratioing the different fluorochromes along each of the normal chromosomes. For example, a region of amplification would appear as an over-representation of the fluorochrome which the tumour DNA was labelled with. The opposite would obviously be seen in the case of gene deletions. This technique has been used for the analysis of genome-wide amplifications and deletions in a number of different tumour types (du Manoir *et al.*, 1993; Kallioniemi *et al.*, 1994; Kallioniemi *et al.*, 1992a; Suijkerbuijk *et al.*, 1994). The use of this technique would highlight any other, perhaps novel, regions of the genome in CALU-3/10<sup>-5</sup>M VP16 where genetic alteration may have resulted in an effect on drug resistance.

## REFERENCES

- Aaronson, S. (1991). Growth factors and cancer. *Science*, **254**, 1146-1153.
- Abel, K., Boehnke, M., Prahallad, M., Ho, P., Flejter, W., Watkins, M., Vanderstoep, J., Chandrasekharappa, S., Collins, F., Glover, T. & Weber, B. (1993). A radiation hybrid map of the *BRCA1* region of chromosome 17q12-21. *Genomics*, **17**, 632-641.
- Ackerman, P., Glover, C. & Osheroff, N. (1985). Phosphorylation of DNA topoisomerase II by casein kinase II: Modulation of eukaryotic topoisomerase II activity *in vitro*. *Proc. Natl. Acad. Sci. USA*, **82**, 3164-3168.
- Ackerman, P., Glover, C. & Osheroff, N. (1988). Phosphorylation of DNA topoisomerase *in vivo* and in total homogenates of *Drosophila* Kc cells. *J. Biol. Chem.*, **263**, 12653-12660.
- Adachi, Y., Kas, E. & Laemmli, U. (1989). Preferential, cooperative binding of DNA topoisomerase II to scaffold-associated regions. *EMBO J.*, **8**, 3997-4006.
- Adachi, Y., Luke, M. & Laemmli, U. (1991). Chromosome assembly *in vitro*: topoisomerase II is required for condensation. *Cell*, **64**, 137-148.
- Alvarez, L., Evans, J., Wilks, R., Lucas, J., Brown, M. & Giaccia, A. (1993). Chromosomal radiosensitivity at intrachromosomal telomeric sites. *Genes, Chromosomes & Cancer*, **8**, 8-14.
- Andersen, A., Christiansen, K., Zechiedrich, E., Jensen, P., Osheroff, N. & Westergaard, O. (1989). Strand specificity of the topoisomerase II mediated double-stranded DNA cleavage reaction. *Biochemistry*, **28**, 6237-6244.
- Anderson, L., Friedman, L., Osborne-Lawrence, S., Lynch, E., Weissenbach, J., Bowcock, A. & King, M.-C. (1993). High-density genetic map of the BRCA1 region of chromosome 17q12-21. *Genomics*, **17**, 618-623.

Antequera, F., Boyes, J. & Bird, A. (1990). High levels of de novo methylation and altered chromatin structure at CpG islands in cell lines. *Cell*, **62**, 503-514.

Arnoldus, E., Noordermeer, I., Peters, A., Voormolen, J., Bots, G., Raap, A., van der Ploeg, M. (1991). Interphase cytogenetics of brain tumours. *Genes, Chromosomes & Cancer*, **3**, 101-107.

Austin, C. & Fisher, L. (1990). Isolation and characterisation of a human cDNA clone encoding a novel DNA topoisomerase II homologue from HeLa cells. *FEBS Letters*, **266**, 115-117.

Austin, C., Sng, J.-H., Patel, S. & Fisher, L. (1993). Novel HeLa topoisomerase II is the II $\beta$  isoform: complete coding sequence and homology with other type II topoisomerases. *Biochimica et Biophysica Acta*, **1172**, 283-291.

Baas, F., Jongsma, A., Broxterman, H., Arceci, R., Housman, D., Scheffer, G., Riethorst, A., van Groenigen, M., Nieuwint, A. & Joenje, H. (1990). Non-P-glycoprotein mediated mechanism for multidrug resistance precedes P-glycoprotein expression during *in vitro* selection for doxorubicin resistance in a human lung cancer cell line. *Cancer Res.*, **50**, 5392-5398.

Bae, Y.-S., Kawasaki, I., Ikeda, H. & Liu, L. (1988). Illegitimate recombination mediated by calf thymus topoisomerase II *in vitro*. *Proc. Natl. Acad. Sci. USA*, **85**, 2076-2080.

Bar-Am, I., Mor, O., Yeger, H., Shiloh, Y., Avivi, L. (1992). Detection of amplified DNA sequences in human tumour cell lines by fluorescence *in situ* hybridisation. *Genes, Chromosomes & Cancer*, **3**, 314-320.

Barrand, M., Heppell-Parton, A., Wright, K., Rabbitts, P. & Twentyman, P. (1994). A 190-kilodalton protein overexpressed in non-P-glycoprotein-containing multidrug-resistant cells and its relationship to the MRP gene. *J. Natl. Cancer Inst.*, **86**, 110-117.

Baylin, S., Makos, M., Wu, J., Chiu Yen, R.-W., de Bustros, A., Vertino, P. & Nelkin, B. (1991). Abnormal patterns of DNA methylation in human

neoplasia: Potential consequences for tumour progression. *Cancer Cells*, **3**, 383-390.

Beck, W., Cirtain, M., Danks, M., Felsted, R., Safa, A., Wolverton, J., Suttle, D. & Trent, J. (1987). Pharmacological, molecular, and cytogenetic analysis of "atypical" multidrug-resistant human leukaemic cells. *Cancer Res.*, **47**, 5455-5460.

Beck, W., Danks, M., Wolverton, J., Granzen, B., Chen, M., Schimdt, C., Bugg, B., Friche, E. & Suttle, D. (1993a). Altered DNA topoisomerase II in multidrug resistance. *Cytotechnology*, **11**, 115-119.

Beck, W., Danks, M., Wolverton, J., Kim, R. & Chen, M. (1993b). Drug resistance associated with altered DNA topoisomerase II. *Advan. Enzyme Regul.*, **33**, 113-127.

Berchuck, A., Kamel, A., Whitaker, R., Kerns, B., Olt, G., Kinney, R., Soper, J., Dodge, R., Clarke-Pearson, D., Marks, P., McKenzie, S., Yin, S. & Bast Jr., R. (1990). Overexpression of *HER/neu* is associated with poor survival in advanced epithelial ovarian cancer. *Cancer Res.*, **50**, 4087-4091.

Bertrand, R., Kerrigan, D., Sarang, M. & Pommier, Y. (1991). Cell death induced by topoisomerase inhibitors. Role of calcium in mammalian cells. *Biochem. Pharmacol.*, **42**, 77-85.

Bojanowski, K., Filhol, O., Cochet, C., Chambaz, E. & Larsen, A. (1993). DNA topoisomerase II and casein kinase II associate in a molecular complex that is catalytically active. *J. Biol. Chem.*, **268**, 22920-22926.

Bollag, W. & Holdener, E. (1992). Retinoids in cancer prevention and therapy. *Annals of Oncology*, **3**, 513-526.

Botchan, M., Topp, W. & Sambrook, J. (1979). Studies on SV40 excision from cellular chromosomes. *Cold Spring Harbor Symp. Quant. Biol.*, **43**, 709-719.

Boy de la Tour, E. & Laemmli, U. (1988). The metaphase chromosome scaffold is helically folded: sister chromatids have predominantly opposite helical handedness. *Cell*, **55**, 937-944.

Brison, O. (1993). Gene amplification and tumour progression. *Biochimica et Biophysica Acta.*, **1155**, 25-41.

Bugg, B., Danks, M., Beck, W. & Suttle, D. (1991). Expression of a mutant DNA topoisomerase II in CCRF-CEM human leukemic cells selected for resistance to teniposide. *Proc. Natl. Acad. Sci. USA*, **88**, 7654-7658.

Burden, D., Goldsmith, L. & Sullivan, D. (1993). Cell-cycle-dependent phosphorylation and activity of Chinese-hamster ovary topoisomerase II. *Biochem. J.*, **293**, 297-304.

Burger, H., Nooter, K., Zaman, G., Sonneveld, P., van Wingerden, K., Oostrum, R. & Stoter, G. (1994). Expression of the multidrug resistance-associated protein (*MRP*) in acute and chronic leukaemias. *Leukemia*, **8**, 990-997.

Capranico, G., Kohn, K. & Pommier, Y. (1990). Local sequence requirements for DNA cleavage by mammalian topoisomerase II in the presence of doxorubicin. *Nuc. Acids Res.*, **18**, 6611-6619.

Capranico, G., Tinelli, S., Austin, C., Fisher, M. & Zunino, F. (1992). Different patterns of gene expression of topoisomerase II isoforms in differentiated tissues during murine development. *Biochimica et Biophysica Acta*, **1132**, 43-48.

Cardenas, M., Dang, Q., Glover, C. & Gasser, S. (1992). Casein kinase II phosphorylates the eukaryotic-specific C-terminal domain of topoisomerase II *in vivo*. *EMBO J.*, **11**, 1785-1796.

Cardenas, M. & Gasser, S. (1993). Regulation of topoisomerase II by phosphorylation: a role for casein kinase II. *J. Cell Sci.*, **104**, 219-225.

Cardenas, M., Walter, R., Hanna, D. & Gasser, S. (1993). Casein kinase II copurifies with yeast DNA topoisomerase II and re-activates the dephosphorylated enzyme. *J. Cell Sci.*, **104**, 533-543.

Carroll, S., DeRose, M., Gaudray, P., Moore, C., Needham-Vandevanter, D., Von Hoff, D. & Wahl, G. (1988). Double minute chromosomes can be

produced from precursors derived from a chromosomal deletion. *Mol. Cell. Biol.*, **8**, 1525-1533.

Carroll, S., DeRose, M., Kolman, J., Nonet, G., Kelly, R. & Wahl, G. (1993). Localisation of a bidirectional DNA replication origin in the native locus and in episomally amplified murine adenosine deaminase loci. *Mol. Cell. Biol.*, **13**, 2971-2981.

Carroll, S., Trotter, J. & Wahl, G. (1991). Replication timing control can be maintained in extrachromosomally amplified genes. *Mol. Cell Biol.*, **11**, 4779-4785.

Carter, N. (1994). Cytogenetic analysis by chromosome painting. *Cytometry (Communications in Clinical Cytometry)*, **18**, 2-10.

Castaigne, S., Chomienne, C., Daniel, M., Ballerini, P., Berger, R., Fenaux, P. & Degos, L. (1990). All-trans retinoic acid as a differentiation therapy for acute promyelocytic leukaemia. *Blood*, **76**, 1704-1709.

Cedar, H. (1988). DNA methylation and gene activity. *Cell*, **53**, 3-4.

Chang, K.-S., Trujillo, J., Ogura, T., Castiglione, C., Kidd, K., Zhao, S., Freireich, E. & Stass, S. (1991). Rearrangement of the retinoic acid receptor gene in acute promyelocytic leukaemia. *Leukemia*, **5**, 200-204.

Chen, C., Chin, J., Ueda, K., Clark, D., Pastan, I., Gottesman, M. & Roninson, I. (1986). Internal duplication and homology with bacterial transport proteins in the *mdr1* (P-glycoprotein) gene from multidrug-resistant human cells. *Cell*, **47**, 381-389.

Chung, T., Drake, F., Tan, K., Per, S., Crooke, S. & Mirabelli, C. (1989). Characterization and immunological identification of cDNA clones encoding two human DNA topoisomerase II isozymes. *Proc. Natl. Acad. Sci. USA*, **86**, 9431-9435.

Clifford, S., Thomas, D., Neal, D. & Lunec, J. (1994). Increased *mdr1* gene transcript levels in high-grade carcinoma of the bladder determined by quantitative PCR-based assay. *Br. J. Cancer*, **69**, 680-686.

Cockerill, P. & Garrard, W. (1986). Chromosomal loop anchorage of the kappa immunoglobulin gene occurs next to the enhancer in a region containing topoisomerase II sites. *Cell*, **44**, 273-282.

Cole, S., Bhardwaj, G., Gerlach, J., Mackie, J., Grant, C., Almquist, K., Stewart, A., Kurz, E., Duncan, A. & Deeley, R. (1992). Overexpression of a transporter gene in a multidrug-resistant human lung cancer cell line. *Science*, **258**, 1650-1654.

Cole, S., Chanda, E., Dicke, F., Gerlach, J. & Mirski, S. (1991). Non-P-glycoprotein multidrug resistance in a small cell lung cancer cell line: Evidence for decreased susceptibility to drug-induced DNA damage and reduced levels of topoisomerase II. *Cancer Res.*, **51**, 3345-3352.

Cole, S., Downes, H. & Slovak, M. (1989). Effect of calcium antagonists on the chemosensitivity of two multidrug-resistant human tumour cell lines which do not overexpress P-glycoprotein. *Br. J. Cancer*, **59**, 42-46.

Costa, A. (1993). Breast cancer chemoprevention. *Eur. J. Cancer*, **29A**, 589-592.

Coussens, L., Yang-Feng, T., Liao, Y.-C., Chen, E., Gray, A., McGrath, J., Seeburg, P., Libermann, T., Schlessinger, J., Francke, U., Levinson, A. & Ullrich, A. (1985). Tyrosine kinase receptor with extensive homology to EGF receptor shares chromosomal location with *neu* oncogene. *Science*, **230**, 1132-1139.

Coutts, J., Plumb, J., Brown, R. & Keith, W. (1993). Expression of topoisomerase II alpha and beta in an adenocarcinoma cell line carrying amplified topoisomerase II alpha and retinoic acid receptor alpha genes. *Br. J. Cancer*, **68**, 793-800.

Danks, M., Warmoth, M., Friche, E., Granzen, B., Bugg, B., Harker, W., Zwelling, L., Futscher, B., Suttle, D. & Beck, W. (1993). Single-strand conformational polymorphism analysis of the M<sub>r</sub> 170,000 isozyme of DNA topoisomerase II in human tumour cells. *Cancer Res.*, **53**, 1373-1379.

Danks, M., Yalowich, J. & Beck, W. (1987). Atypical multiple drug resistance in a human leukemic cell line selected for resistance to teniposide (VM-26). *Cancer Res.*, **47**, 1297-1301.

Davies, S., Jenkins, J. & Hickson, I. (1993). Human cells express two differentially spliced forms of topoisomerase II $\beta$  mRNA. *Nuc. Acids Res.*, **21**, 3719-3723.

Davies, S., Robson, C., Davies, S. & Hickson, I. (1988). Nuclear topoisomerase II levels correlate with the sensitivity of mammalian cells to intercalating agents and epipodophyllotoxins. *J. Biol. Chem.*, **263**, 17724-17729.

de Jong, S., Kooistra, A., de Vries, E., Mulder, N. & Zijlstra, J. (1993). Topoisomerase II as a target of VM-26 and 4'-(9-acridinylamino)methanesulfon-*m*-aniside in atypical multidrug resistant human small cell lung carcinoma cells. *Cancer Res.*, **53**, 1064-1071.

de The, H., Chomienne, C., Lanotte, M., Degos, L. & Dejean, A. (1990). The t(15;17) translocation of acute promyelocytic leukaemia fuses the retinoic acid receptor  $\alpha$  gene to a novel transcribed locus. *Nature*, **347**, 558-561.

Debatisse, M., Hyrien, O., Petit-Koskas, E., Robert de Saint-Vincent, B. & Buttin, G. (1986). Segregation and rearrangement of co-amplified genes in different lineages of mutant cells that overproduce adenylate deaminase. *Mol. Cell. Biol.*, **6**, 1776-1781.

Delidakis, C. & Kafatos, F. (1989). Amplification enhancers and replication origins in the autosomal chorion gene cluster of *Drosophila*. *EMBO J.*, **8**, 891-901.

Deville, P., Thierry, R., Kievits, T., Kolluri, R., Hopman, A., Willard, H., Pearson, P., Cornelisse, C. (1988). Detection of chromosome aneuploidy in interphase nuclei from human primary breast tumours using chromosome-specific repetitive DNA probes. *Cancer Res.*, **48**, 5825-5830.

DiNardo, S., Voelkel, K. & Sternglanz, R. (1984). DNA topoisomerase II mutant of *Saccharomyces cerevisiae*: Topoisomerase II is required for

segregation of daughter molecules at the termination of DNA replication. *Proc. Natl. Acad. Sci. USA.*, **81**, 2616-2620.

Dong, S., Geng, J.-P., Tong, J.-H., Wu, Y., Cai, J.-R., Sun, G.-L., Chen, S.-R., Wang, Z.-Y., Larsen, C.-J., Berger, R., Chen, S.-J. & Chen, Z. (1993). Breakpoint clusters of the *PML* gene in acute promyelocytic leukaemia: Primary structure of the reciprocal products of the *PML-RARA* gene in a patient with t(15;17). *Genes, Chromosomes & Cancer*, **6**, 133-139.

Drake, F., Hofmann, G., Bartus, H., Mattern, M., Crooke, S. & Mirabelli, C. (1989). Biochemical and pharmacological properties of p170 and p180 forms of topoisomerase II. *Biochemistry*, **28**, 8154-8160.

Drake, F., Zimmerman, J., McCabe, F., Bartus, H., Per, S., Sullivan, D., Ross, W., Mattern, M., Johnson, R., Crooke, S. & Mirabelli, C. (1987). Purification of topoisomerase II from amsacrine-resistant P388 leukemia cells. *J. Biol. Chem.*, **262**, 16739-16747.

du Manoir, S., Speicher, M., Joos, S., Schrock, E., Popp, S., Dohner, H., Kovacs, G., Robert-Nicoud, M., Lichter, P. & Cremer, T. (1993). Detection of complete and partial chromosome gains and losses by comparative genomic in situ hybridisation. *Human Genetics*, **90**, 590-610.

Earnshaw, W. & Heck, M. (1985). Localisation of topoisomerase II in mitotic chromosomes. *J. Cell Biol.*, **100**, 1716-1725.

Elder, J., Fisher, G., Zhang, Q.-Y., Eisen, D., Krust, A., Kastner, P., Chambon, P. & Voorhees, J. (1991). Retinoic acid receptor gene expression in human skin. *J. Invest. Dermatol.*, **96**, 425-433.

Endicott, J. & Ling, V. (1989). The biochemistry of P-glycoprotein-mediated multidrug resistance. *Annu. Rev. Biochem.*, **58**, 137-171.

Erickson, J., Finan, J., Nowell, P. & Croce, C. (1982). Translocation of immunoglobulin Vh genes in Burkitt lymphoma. *Proc. Natl. Acad. Sci. U.S.A.*, **79**, 5611-5615.

Fakharzadeh, S., Rosenblum-Vos, L., Murphy, M., Hoffman, E. & George, D. (1993). Structure and organisation of amplified DNA on double minutes containing the *mdm2* oncogene. *Genomics*, **15**, 283-290.

Fantl, V., Richards, M., Smith, R., Lammie, G., Johnstone, G., Allen, D., Gregory, W., Peters, G., Dickson, C. & Barnes, D. (1990). Gene amplification on chromosome band 11q13 and oestrogen receptor status in breast cancer. *Eur. J. Cancer*, **26**, 423-429.

Feinberg, A. & Vogelstein, B. (1983). Hypomethylation distinguishes genes of some human cancers from their normal counterparts. *Nature*, **301**, 89-92.

Fischer, D., Hock, R. & Scheer, U. (1994). DNA topoisomerase II is not detectable on lampbrush chromosomes but enriched in the amplified nucleoli of *Xenopus* oocytes. *Exp. Cell Res.*, **209**, 255-260.

Fleischmann, G., Pflugfelder, G., Steiner, E., Javaherian, K., Howard, G., Wang, J. & Elgin, S. (1984). *Drosophila* DNA topoisomerase I is associated with transcriptionally active regions of the genome. *Proc. Natl. Acad. Sci. USA*, **81**, 6958-6962.

Flejter, W., Barcroft, C., Guo, S.-W., Lynch, E., Boehnke, M., Chandrasekharappa, S., Hayes, S., Collins, F., Weber, B. & Glover, T. (1993). Multicolour FISH mapping with *Alu* -PCR-amplified YAC clone DNA determines the order of markers in the *BRCA1* region on chromosome 17q12-21. *Genomics*, **17**, 624-631.

Flens, M., Izquierdo, M., Scheffer, G., Fritz, J., Meijer, C., Scheper, R. & Zaman, G. (1994). Immunochemical detection of the multidrug resistance-associated protein MRP in human multidrug-resistant tumor cells by monoclonal antibodies. *Cancer Res.*, **54**, 4557-4563.

Flintoff, W., Livingston, E., Duff, C. & Worton, R. (1984). Moderate-level gene amplification in methotrexate-resistant chinese hamster ovary cells is accompanied by chromosomal translocations at or near the site of the amplified DHFR gene. *Mol. Cell. Biol.*, **4**, 69-76.

- Fosse, P., Rene, B., Le Bret, M., Paoletti, C. & Saucier, J.-M. (1991). Sequence requirements for mammalian topoisomerase II mediated DNA cleavage by an ellipticine derivative. *Nuc. Acids Res.*, **19**, 2861-2868.
- Freudenreich, C. & Kreuzer, K. (1993). Mutational analysis of a type II topoisomerase cleavage site: distinct requirements for enzyme and inhibitors. *EMBO J.*, **12**, 2085-2097.
- Friche, E., Danks, M. & Beck, W. (1992). Characterization of tumor cell resistance to 4'-deoxy-4'-iododoxorubicin developed in Ehrlich ascites cells *in vivo*. *Cancer Res.*, **52**, 5701-5706.
- Froelich-Ammon, S., Gale, K. & Osheroff, N. (1994). Site-specific cleavage of a DNA hairpin by topoisomerase II. DNA secondary structure as a determinant of enzyme recognition/cleavage. *J. Biol. Chem.*, **269**, 7719-7725.
- Fry, A., Chresta, C., Davies, S., Walker, M., Harris, A., Hartley, J., Masters, J. & Hickson, I. (1991). Relationship between topoisomerase II level and chemosensitivity in human tumour cell lines. *Cancer Res.*, **51**, 6592-6595.
- Fukushige, S.-I., Matsubara, K.-I., Yoshida, M., Sasaki, M., Suzuki, T., Semba, K., Toyoshima, K. & Yamamoto, T. (1986). Localisation of a novel *v-erb* B-related gene, *c-erb* B-2, on human chromosome 17 and its amplification in a gastric cancer cell line. *Molecular and Cellular Biology*, **6**, 955-958.
- Gasser, S. & Laemmli, U. (1986). The organisation of chromatin loops: characterisation of a scaffold attachment site. *EMBO J.*, **5**, 511-518.
- Gasser, S., Laroche, T., Falquet, J., Boy de la Tour, E. & Laemmli, U. (1986). Metaphase chromosome structure. Involvement of topoisomerase II. *J. Mol. Biol.*, **188**, 613-629.
- Gaub, M., Rochette-Egly, C., Lutz, Y., Ali, S., Matthes, H., Scheuer, I. & Chambon, P. (1992). Immunodetection of multiple species of retinoic acid receptor  $\alpha$ : Evidence for phosphorylation. *Exp. Cell Res.*, **201**, 335-346.
- Gerlach, J., Endicott, J., Juranka, P., Henderson, G., Sarangi, F., Deuchars, K. & Ling, V. (1986). Homology between P-glycoprotein and a bacterial

haemolysin transport protein suggests a model for multidrug resistance. *Nature*, **324**, 485-489.

Giaccone, G., Gazdar, A., Beck, H., Zunino, F. & Capranico, G. (1992). Multidrug sensitivity phenotype of human lung cancer cells associated with topoisomerase II expression. *Cancer Res.*, **52**, 1666-1674.

Gillard, E. & Solomon, E. (1993). Retinoic acid-induced remission. *Current Biology*, **3**, 185-187.

Gilles, A.-M., Presecan, E., Vonica, A. & Lascu, I. (1991). Nucleoside diphosphate kinase from human erythrocytes. *J. Biol. Chem.*, **266**, 8784-8789.

Goasguen, J., Dossot, J.-M., Fardel, O., Le Mee, F., Le Gall, E., Leblay, R., LePrise, P., Chaperon, J. & Fauchet, R. (1993). Expression of the multidrug resistance-associated P-glycoprotein (P-170) in 59 cases of de novo acute lymphoblastic leukemia: Prognostic implications. *Blood*, **81**, 2394-2398.

Goelz, S. & Vogelstein, B. (1985). Hypomethylation of DNA from benign and malignant human colon neoplasms. *Science*, **228**, 187-190.

Gosden, C., Davidson, C., Robertson, M. (1992) In *Human Cytogenetics A Practical Approach. Vol. 1 Constitutional Analysis*. 2<sup>nd</sup> Edition. Rooney, D., Czepulkowski, B. (ed) Chapter 2. IRL Press.

Grant, C., Valdimarsson, G., Hipfner, D., Almquist, K., Cole, S. & Deeley, R. (1994). Overexpression of multidrug resistance-associated protein (MRP) increases resistance to natural product drugs. *Cancer Res.*, **54**, 357-361.

Gros, P., Ben Neriah, Y., Croop, J. & Housman, D. (1986a). Isolation and expression of a complementary DNA that confers multidrug resistance. *Nature*, **323**, 728-731.

Gros, P., Croop, J. & Housman, D. (1986b). Mammalian multidrug resistance gene: Complete cDNA sequence indicates strong homology to bacterial transport proteins. *Cell*, **47**, 371-380.

Guan, X.-Y., Meltzer, P., Cao, J. & Trent, J. (1992). Rapid generation of region-specific genomic clones by chromosome microdissection: isolation of

DNA from a region frequently deleted in malignant melanoma. *Genomics*, **14**, 680-684.

Guan, X.-Y., Meltzer, P., Dalton, W. & Trent, J. (1994). Identification of cryptic sites of DNA sequence amplification in human breast cancer by chromosome microdissection. *Nature Genetics*, **8**, 155-161.

Gullick, W., Berger, M., Bennett, P., Rothbard, J. & Waterfield, M. (1987). Expression of the *c-erbB-2* protein in normal and transformed cells. *Int. J. Cancer*, **40**, 246-254.

Gullick, W., Love, S., Wright, C., Barnes, D., Gusterson, B., Harris, A. & Altman, D. (1991). *c-erbB-2* protein overexpression in breast cancer is a risk factor in patients with involved and uninvolved lymph nodes. *Br. J. Cancer*, **63**, 434-438.

Gupta, R. (1983). Genetic, biochemical, and cross-resistance studies with mutants of Chinese hamster ovary cells resistant to the anticancer drugs VM-26 and VP16-213. *Cancer Res.*, **43**, 1568-1574.

Haaf, T. & Willard, H (1992). Organisation, polymorphism, and molecular cytogenetics of chromosome-specific  $\alpha$ -satellite DNA from the centromere of chromosome 2. *Genomics*, **13**, 122-128.

Hahn, P. (1993). Molecular biology of double-minute chromosomes. *BioEssays*, **15**, 477-484.

Hahn, P., Kapp, L., Morgan, W. & Painter, R. (1986). Chromosomal changes without DNA overproduction in hydroxyurea-treated mammalian cells: Implications for gene amplification. *Cancer Res.*, **46**, 4607-4612.

Hastie, N., Dempster, M., Dunlop, M., Thompson, A., Green, D. & Allshire, R. (1990). Telomere reduction in human colorectal carcinoma and with ageing. *Nature*, **346**, 866-868.

Heck, M., Hittelman, W. & Earnshaw, W. (1988). Differential expression of DNA topoisomerases I and II during the eukaryotic cell cycle. *Proc. Natl. Acad. Sci. USA*, **85**, 1086-1090.

- Hennessey, C., Henry, J., May, F., Westley, B., Angus, B. & Lennard, T. (1991). Expression of the antimetastatic gene nm23 in human breast cancer: An association with good prognosis. *J. Natl. Cancer Inst.*, **83**, 281-285.
- Heppell-Parton, A., Albertson, D., Fishpool, R. & Rabbitts, P. (1994). Multicolour fluorescence in situ hybridisation to order small, single-copy probes on metaphase chromosomes. *Cytogenet. Cell Genet.*, **66**, 42-47.
- Hill, B. & Bellamy, A. (1984). Establishment of an etoposide-resistant human epithelial tumour cell line *in vitro*: Characterization of patterns of cross-resistance and drug sensitivities. *Int. J. Cancer*, **33**, 599-608.
- Hinds, M., Deisseroth, K., Mayes, J., Altschuler, E., Jansen, R., Ledley, F. & Zwelling, L. (1991). Identification of a point mutation in the topoisomerase II gene from a human leukemia cell line containing an amsacrine-resistant form of topoisomerase II. *Cancer Res.*, **51**, 4729-4731.
- Hochhauser, D., Stanway, C., Harris, A. & Hickson, I. (1992). Cloning and characterisation of the 5'-flanking region of the human topoisomerase II $\alpha$  gene. *J. Biol. Chem.*, **267**, 18961-18965.
- Holdener, E. & Bollag, W. (1993). Retinoids. *Current Opinion in Oncology*, **5**, 1059-1066.
- Holm, C., Stearns, T. & Botstein, D. (1989). DNA topoisomerase II must act at mitosis to prevent nondisjunction and chromosome breakage. *Mol. Cell. Biol.*, **9**, 159-168.
- Holmes, J. & West, R. (1994). The effect of *MDR-1* gene expression on outcome in acute myeloblastic leukaemia. *Br. J. Cancer*, **69**, 382-384.
- Holzmann, K., Blin, N., Welter, C., Zang, K., Seitz, G. & Henn, W. (1993). Telomeric associations and loss of telomeric DNA repeats in renal tumours. *Genes, Chromosomes & Cancer*, **6**, 178-181.
- Horowitz, J., Park, S.-H., Bogenmann, E., Cheng, J.-C., Yandell, D., Kaye, F., Minna, J., Dryja, T. & Weinberg, R. (1990). Frequent inactivation of the retinoblastoma anti-oncogene is restricted to a subset of human tumor cells. *Proc. Natl. Acad. Sci. USA*, **87**, 2775-2779.

Hsieh, T. & Brutlag, D. (1980). ATP-dependent DNA topoisomerase from *D. melanogaster* reversibly catenates duplex DNA rings. *Cell*, **21**, 115-125.

Hyde, S., Emsley, P., Hartshorn, M., Mimmack, M., Gileadi, U., Pearce, S., Gallagher, M., Gill, D., Hubbard, R. & Higgins, C. (1990). Structural model of ATP-binding proteins associated with cystic fibrosis, multidrug resistance and bacterial transport. *Nature*, **346**, 362-365.

Hynes, N. (1993). Amplification and overexpression of the *erb B2* gene in human tumours: its involvement in tumour development, significance as a prognostic factor, and potential as a target for cancer therapy. *Seminars in Cancer Biology*, **4**, 19-26.

Hyrien, O., Debatisse, M., Buttin, G. & Robert de Saint Vincent, B. (1988). The multicopy appearance of a large inverted duplication and the sequence at the inversion joint suggest a new model for gene amplification. *EMBO J.*, **7**, 407-417.

Igawa, M., Rukstalis, D., Tanabe, T. & Chodak, G. (1994). High levels of *nm23* expression are related to cell proliferation in human prostate cancer. *Cancer Res.*, **54**, 1313-1318.

Iglehart, J., Kraus, M., Langton, B., Huper, G., Kerns, B. & Marks, J. (1990). Increased *erb B2* gene copies and expression in multiple stages of breast cancer. *Cancer Res.*, **50**, 6701-6707.

Inazawa, J., Ariyama, T., Tokino, T., Tanigami, A., Nakamura, Y. & Abe, T. (1994). High resolution ordering of DNA markers by multi-color fluorescent in situ hybridisation of prophase chromosomes. *Cytogenet Cell Genet*, **65**, 130-135.

Ishida, R., Miki, T., Narita, T., Yui, R., Sato, M., Utsumi, K., Tanabe, K. & Andoh, T. (1991). Inhibition of intracellular topoisomerase II by anti-tumor bis(2,6-dioxopiperazine) derivatives: Mode of cell growth inhibition distinct from that of cleavable complex-forming type inhibitors. *Cancer Res.*, **51**, 4909-4916.

Jenkins, J., Ayton, P., Jones, T., Davies, S., Simmons, D., Harris, A., Sheer, D. & Hickson, I. (1992). Isolation of cDNA clones encoding the  $\beta$  isozyme of the human topoisomerase II and localisation of the gene to chromosome 3p24. *Nuc. Acids Res.*, **20**, 5587-5592.

Kafatos, F., Orr, W. & Delidakis, C. (1985). Developmentally regulated gene amplification. *Trends in Genetics*, **1**, 301-305.

Kallioniemi, A., Kallioniemi, O.-P., Piper, J., Tanner, M., Stokke, T., Chen, L., Smith, H., Pinkel, D., Gray, J. & Waldman, F. (1994). Detection and mapping of amplified DNA sequences in breast cancer by comparative genomic hybridisation. *Proc. Natl. Acad. Sci. USA*, **91**, 2156-2160.

Kallioniemi, A., Kallioniemi, O.-P., Sudar, D., Rutovitz, D., Gray, J., Waldman, F. & Pinkel, D. (1992a). Comparative genomic hybridisation for molecular cytogenetic analysis of solid tumors. *Science*, **258**, 818-821.

Kallioniemi, O.-P., Kallioniemi, A., Kurisu, W., Thor, A., Chen, L.-C., Smith, H., Waldman, F., Pinkel, W. & Gray, J. (1992b). *ERBB2* amplification in breast cancer analysed by fluorescence *in situ* hybridisation. *Proc. Natl. Acad. Sci. USA*, **89**, 5321-5325.

Kamath, N., Grabowski, D., Ford, J., Kerrigan, D., Pommier, Y. & Ganapathi, R. (1992). Overexpression of P-glycoprotein and alterations in topoisomerase II in P388 mouse leukemia cells selected *in vivo* for resistance to mitoxantrone. *Biochem. Pharmacol.*, **44**, 937-945.

Kas, E. & Laemmli, U. (1992). *In vivo* topoisomerase II cleavage of the *Drosophila* histone and satellite III repeats: DNA sequence and structural characteristics. *EMBO J.*, **11**, 705-716.

Kastan, M., Onyekwere, O., Sidransky, D., Vogelstein, B. & Craig, R. (1991). Participation of p53 protein in the cellular response to DNA damage. *Cancer Res.*, **51**, 6304-6311.

Kastner, P., Perez, A., Lutz, Y., Rochette-Egly, C., Gaub, M.-P., Durand, B., Lanotte, M., Berger, R. & Chambon, P. (1992). Structure, localisation and transcriptional properties of two classes of retinoic acid receptor  $\alpha$  fusion

proteins in acute promyelocytic leukemia (APL): structural similarities with a new family of oncoproteins. *EMBO J.*, **11**, 629-642.

Kaufman, R. & Schimke, R. (1981). Amplification and loss of dihydrofolate reductase genes in a chinese hamster ovary cell line. *Mol. Cell. Biol.*, **1**, 1069-1076.

Kaufmann, S., McLaughlin, S., Kastan, M., Liu, L., Karp, J. & Burke, P. (1991). Topoisomerase II levels during granulocytic maturation *in vitro* and *in vivo*. *Cancer Res.*, **51**, 3534-3543.

Keith, W., Douglas, F., Wishart, G., McCallum, H., George, W., Kaye, S. & Brown, R. (1993). Co-amplification of *erb B2*, topoisomerase II  $\alpha$  and retinoic acid receptor  $\alpha$  genes in breast cancer and allelic loss at topoisomerase I on chromosome 20. *Eur. J. Cancer*, **29A**, 1469-1475.

Keith, W., Tan, K. & Brown, R. (1992). Amplification of the topoisomerase II $\alpha$  gene in a non-small cell lung cancer cell line and characterisation of polymorphisms at the human topoisomerase II $\alpha$  and  $\beta$  loci in normal tissue. *Genes, Chromosomes & Cancer*, **4**, 169-175.

Kern, J., Schwartz, D., Nordberg, J., Weiner, D., Greene, M., Torney, L. & Robinson, R. (1990). p185<sup>neu</sup> expression in human lung adenocarcinomas predicts shortened survival. *Cancer Res.*, **50**, 5184-5191.

Kim, R. & Beck, W. (1994). Differences between drug-sensitive and -resistant human leukemic CEM cells in c-jun expression, AP-1 DNA-binding activity, and formation of Jun/Fos family dimers, and their association with internucleosomal DNA ladders after treatment with VM-26. *Cancer Res.*, **54**, 4958-4966.

Kim, R. & Wang, J. (1989). A subthreshold level of DNA topoisomerases leads to the excision of yeast rDNA as extrachromosomal rings. *Cell*, **57**, 975-985.

Kim, S., Lee, J., Ro, J., Gay, M., Hong, W. & Hittelman, W. (1993). Interphase cytogenetics in paraffin sections of lung tumors by non-isotopic *in situ* hybridisation. *Am. J. Pathol.*, **142**, 307-317.

- Kimura, K., Saijo, M., Ui, M. & Enomoto, T. (1994). Growth state- and cell cycle-dependent fluctuation in the expression of two forms of DNA topoisomerase II and possible specific modification of the higher molecular weight form in the M phase. *J. Biol. Chem.*, **269**, 1173-1176.
- King, R., Kraus, M. & Aaronson, S. (1985). Amplification of a novel v-*erbB*-related gene in a human mammary carcinoma. *Science*, **229**, 974-976.
- Knight, G., Gudas, J. & Pardee, A. (1987). Cell-cycle specific interaction of nuclear DNA binding proteins with a CCAAT sequence from the human thymidine kinase gene. *Proc. Natl. Acad. Sci. USA*, **84**, 8350-8354.
- Kozasa, T., Itoh, H., Tsukamoto, T. & Kaziro, Y. (1988). Isolation and characterisation of the human Gs $\alpha$  gene. *Proc. Natl. Acad. Sci. USA*, **85**, 2081-2085.
- Krishnamachary, N. & Center, M. (1993). The MRP gene associated with a non-P-glycoprotein multidrug resistance encodes a 190-kDa membrane bound glycoprotein. *Cancer Res.*, **53**, 3658-3661.
- Kunze, N., Klein, M., Richter, A. & Knippers, R. (1990). Structural characteristics of the human DNA topoisomerase I gene promoter. *Eur. J. Biochem.*, **194**, 323-330.
- Kunze, N., Yang, G., Dolberg, M., Sundarp, R., Knippers, R. & Richter, A. (1991). Structure of the human type I DNA topoisomerase gene. *J. Biol. Chem.*, **266**, 9610-9616.
- Kunze, N., Yang, G., Jiang, Z., Hameister, H., Adolph, S., Wiedorn, K., Richter, A. & Knippers, R. (1989). Localisation of the active type I DNA topoisomerase gene on human chromosome 20q11.2-13.1, and two pseudogenes on chromosomes 1q23-24 and 22q11.2-13.1. *Human Genetics*, **84**, 6-10.
- Lacombe, M.-L., Sastre-Garau, X., Lascu, I., Vonica, A., Wallet, V., Thiery, J. & Veron, M. (1991). Overexpression of nucleoside diphosphate kinase (Nm23) in solid tumours. *Eur. J. Cancer*, **27**, 1302-1307.

Lafage, M., Nguyen, C., Szeptowski, P., Pebusque, M.-J., Simonetti, J., Courtois, G., Gaudray, P., deLapeyriere, O., Jordan, B. & Birnbaum, D. (1990). The 11q13 amplicon of a mammary carcinoma cell line. *Genes, Chromosomes & Cancer*, **2**, 171-181.

Lai, S.-L., Goldstein, L., Gottesman, M., Pastan, I., Tsai, C.-M., Johnson, B., Mulshine, J., Ihde, D., Kayser, K. & Gazdar, A. (1989). MDR1 gene expression in lung cancer. *J. Natl. Inst. Cancer*, **81**, 1144-1150.

Lammie, G. & Peters, G. (1991). Chromosome 11q13 abnormalities in human cancer. *Cancer Cells*, **3**, 413-420.

Lazega, D., Schenker, E., Busso, N., Zelent, A., Chen, A. & Waxman, S. (1993). Down-regulation of retinoic acid receptor activity associated with decreased  $\alpha$  and  $\gamma$  isoforms expression in F9 embryonal carcinoma cells differentiated by retinoic acid. *J. Cell. Physiol.*, **157**, 90-96.

Lee, M., Sander, M. & Hsieh, T. (1989). Single strand DNA cleavage reaction of duplex DNA by *Drosophila* topoisomerase II. *J. Biol. Chem.*, **264**, 13510-13518.

Lee, M.-S., Wang, J. & Beran, M. (1992). Two independent amsacrine-resistant human myeloid leukemia cell lines share an identical point mutation in the 170 kDa form of human topoisomerase II. *J. Mol. Biol.*, **223**, 837-843.

Lefevre, D., Riou, J.-F., Ahomadegbe, J., Zhou, D., Benard, J. & Riou, G. (1991). Study of molecular markers of resistance to *m*-AMSA in a human breast cancer cell line. *Biochem. Pharmacol.*, **41**, 1967-1979.

Lehrach, H. (1990). In *Genome Analysis Volume 1: Genetic and Physical Mapping*, K. Davies & S. Tilghman (ed) p. 39-81 Cold Spring Harbor Laboratory Press: Cold Spring Harbor.

Leid, M., Kastner, P. & Chambon, P. (1992). Multiplicity generates diversity in the retinoic acid signalling pathways. *T.I.B.S.*, **17**, 427-433.

Leone, A., Flatow, U., VanHoutte, K. & Steeg, P. (1993a). Transfection of human *nm23-H1* into the human MDA-MB-435 breast carcinoma cell line:

effects on tumour metastatic potential, colonisation and enzymatic activity. *Oncogene*, **8**, 2325-2333.

Leone, A., Seeger, R., Hong, C., Hu, Y., Arboleda, M., Brodeur, G., Stram, D., Slamon, D. & Steeg, P. (1993b). Evidence for *nm23* RNA overexpression, DNA amplification and mutation in aggressive childhood neuroblastomas. *Oncogene*, **8**, 855-865.

Levine, A., Perry, M., Chang, A., Silver, A., Dittmer, D., Wu, M. & Welsh, D. (1994). The 1993 Walter Hubert Lecture: The role of the p53 tumour-suppressor gene in tumorigenesis. *Br. J. Cancer*, **64**, 409-416.

Liang, C., Spitzer, J., Smith, H. & Gerbi, S. (1993). Replication initiates at a confined region during DNA amplification in *Sciara* DNA puff II/9A. *Genes and Development*, **7**, 1072-1084.

Lichter, P., Cremer, T., Borden, J., Manuelidis, L. & Ward, D. (1988). Delineation of individual human chromosomes in metaphase and interphase cells by in situ suppression hybridisation using recombinant DNA libraries. *Hum. Genet.*, **80**, 224-234.

Lindsley, J. & Wang, J. (1991). Proteolysis patterns of epitopically labelled yeast DNA topoisomerase II suggest an allosteric transition in the enzyme induced by ATP binding. *Proc. Natl. Acad. Sci. USA*, **88**, 10485-10489.

Lindsley, J. & Wang, J. (1993). On the coupling between ATP usage and DNA transport by yeast DNA topoisomerase II. *J. Biol. Chem.*, **268**, 8096-8104.

Liotta, L. & Steeg, P. (1990). Clues to the function of Nm23 proteins and Awd proteins in development, signal transduction and tumor metastasis provided by studies of *Dictyostelium discoideum*. *J. Natl. Cancer Inst.*, **82**, 170-172.

Liu, E., Thor, A., He, M., Barcos, M., Ljung, B.-M. & Benz, C. (1992). The *HER2* (*c-erbB-2*) oncogene is frequently amplified in *in situ* carcinomas of the breast. *Oncogene*, **7**, 1027-1032.

Liu, L. (1989). DNA topoisomerase poisons as anti-tumor drugs. *Ann. Rev. Biochem.*, **58**, 351-375.

Liu, L., Liu, C.-C. & Alberts, B. (1980). Type II DNA topoisomerases: enzymes that can unknot a topologically knotted DNA molecule via a reversible double-strand break. *Cell*, **19**, 697-707.

Loflin, P., Hochhauser, D., Hickson, I., Morales, F. & Zwelling, L. (1994). Molecular analysis of a potentially phorbol-regulatable region of the human topoisomerase II-alpha gene promoter. *Biochemical and Biophysical Research Communications*, **200**, 489-496.

Long, B., Wang, L., Lorico, A., Wang, R., Brattain, M. & Casazza, A. (1991). Mechanisms of resistance to etoposide and teniposide in acquired resistant human colon and lung carcinoma cell lines. *Cancer Res.*, **51**, 5275-5284.

Lonn, U., Lonn, S. & Stenkvist, B. (1993). Appearance of amplified thymidylate synthase or dihydrofolate reductase genes in stage-IV breast-cancer patients receiving endocrine treatment. *Int. J. Cancer*, **54**, 237-242.

Lovekin, C., Ellis, I., Locker, A., Robertson, J., Bell, J., Nicholson, R., Gullick, W., Elston, C. & Blamey, R. (1991). c-erbB-2 oncoprotein expression in primary and advanced breast cancer. *Br. J. Cancer*, **63**, 439-443.

Lowe, S., Ruley, H., Jacks, T. & Housman, D. (1993). p53-dependent apoptosis modulates the cytotoxicity of anticancer agents. *Cell*, **74**, 957-967.

Ma, C., Martin, S., Trask, B. & Hamlin, J. (1993). Sister chromatid fusion initiates amplification of the dihydrofolate reductase gene in Chinese hamster cells. *Genes & Development*, **7**, 605-620.

Makos, M., Nelkin, B., Lerman, M., Latif, F., Zbar, B. & Baylin, S. (1992). Distinct hypermethylation patterns occur at altered chromosome loci in human lung and colon cancer. *Proc. Natl. Acad. Sci. USA*, **89**, 1929-1933.

Marquardt, D., McCrone, S. & Center, M. (1990). Mechanisms of multidrug resistance in HL60 cells: Detection of resistance-associated proteins with antibodies specific against synthetic peptides that correspond to the deduced sequence of P-glycoprotein. *Cancer Res.*, **50**, 1426-1430.

- Mattei, M., Petkovich, M., Mattei, J., Brand, N. & Chambon, P. (1988). Mapping of the human retinoic acid receptor to the q21 band of chromosome 17. *Hum. Genet.*, **80**, 186-188.
- McGrath, T., Latoud, C., Arnold, S., Safa, A., Felsted, R. & Center, M. (1989). Mechanisms of multidrug resistance in HL60 cells. Analysis of resistance associated membrane proteins and levels of *mdr* gene expression. *Biochem. Pharmacol.*, **38**, 3611-3619.
- Mehle, C., Ljungberg, B. & Roos, G. (1994). Telomere shortening in renal cell carcinoma. *Cancer Res.*, **54**, 236-241.
- Melzter, P., Guan, X.-Y. & Trent, J. (1993). Telomere capture stabilises chromosome breakage. *Nature Genetics*, **4**, 252-255.
- Meng-Er, H., Yu-Chen, Y., Shu-Rong, C., Jin-Ren, C., Jia-Xiang, L., Lin, Z., Long-Jun, G. & Zhen-Ji, W. (1988). Use of all-*trans* retinoic acid in the treatment of acute promyelocytic leukemia. *Blood*, **72**, 567-572.
- Merry, S., Courtney, E., Fetherston, C., Kaye, S. & Freshney, R. (1987). Circumvention of drug resistance in human non-small cell lung cancer *in vitro* by verapamil. *Br. J. Cancer*, **56**, 401-405.
- Mickisch, G., Merlino, G., Galski, H., Gottesman, M. & Pastan, I. (1991). Transgenic mice that express the human multidrug-resistance gene in bone marrow enable a rapid identification of agents that reverse drug resistance. *Proc. Natl. Acad. Sci. USA*, **88**, 547-551.
- Mirski, S., Evans, C., Almquist, K., Slovak, M. & Cole, S. (1993). Altered topoisomerase II $\alpha$  in a drug-resistant small cell lung cancer cell line selected in VP-16. *Cancer Res.*, **53**, 4866-4873.
- Mirski, S., Gerlach, J. & Cole, S. (1987). Multidrug resistance in a human small cell lung cancer cell line selected in adriamycin. *Cancer Res.*, **47**, 2594-2598.
- Moscow, J., Fairchild, C., Madden, M., Ransom, D., Wieand, H., O'Brien, E., Poplack, D., Cossman, J., Myers, C. & Cowan, K. (1989). Expression of

anionic glutathione-S-transferase and P-glycoprotein genes in human tissues and tumors. *Cancer Res.*, **49**, 1422-1428.

Motokura, T., Bloom, T., Kim, H., Juppner, H., Ruderman, J., Kronenberg, H. & Arnold, A. (1991). A novel cyclin encoded by a *bcl1* - linked candidate oncogene. *Nature*, **350**, 521-515.

Muller, M., Pfund, W., Mehta, V. & Trask, D. (1985). Eukaryotic type I topoisomerase is enriched in the nucleolus and catalytically active on ribosomal DNA. *EMBO J.*, **4**, 1237-1243.

Murphy, D., McHardy, P., Coutts, J., Mallen, E., George, W., Kaye, S., Brown, R. & Keith, W. Interphase cytogenetic analysis of ErbB2 and Topo II $\alpha$  co-amplification in invasive breast cancer and polysomy of chromosome 17 in ductal carcinoma *in situ*.. *Int. J. Cancer*, in press.

Muss, H., Thor, A., Berry, D., Kute, T., Liu, E., Koerner, F., Cirrincione, C., Budman, D., Wood, W., Barcos, M. & Henderson, I. (1994). *c-erbB-2* expression and response to adjuvant therapy in women with node-positive early breast cancer. *N. Engl. J. Med.*, **330**, 1260-1266.

Negri, C., Chiesa, R., Cerino, A., Bestagno, M., Sala, C., Zini, N., Maraldi, N. & Astaldi Ricotti, G. (1992). Monoclonal antibodies to human DNA topoisomerase I and the two isoforms of DNA topoisomerase II: 170- and 180-kDa isozymes. *Exp. Cell Res.*, **200**, 452-459.

Negri, C., Scovassi, A., Braghetti, A., Guano, F. & Astaldi Ricotti, G. (1993). DNA topoisomerase II $\beta$ : Stability and distribution in different animal cells in comparison to DNA topoisomerase I and II $\alpha$ . *Exp. Cell Res.*, **206**, 128-133.

Negrini, M., Felix, C., Martin, C., Lange, B., Nakamura, T., Canaani, E. & Croce, C. (1993). Potential topoisomerase II DNA-binding sites at the breakpoints of a t(9;11) chromosome translocation in acute myeloid leukemia. *Cancer Res.*, **53**, 4489-4492.

Newport, J. (1987). Nuclear reconstitution in vitro: Stages of assembly around protein-free DNA. *Cell*, **48**, 205-217.

Newport, J. & Spann, T. (1987). Disassembly of the nucleus in mitotic extracts: Membrane vesicularization, lamin disassembly, and chromosome condensation are independent processes. *Cell*, **48**, 219-230.

Nitiss, J., Liu, Y.-X., Harbury, P., Jannatipour, M., Wasserman, R. & Wang, J. (1992). Amsacrine and etoposide hypersensitivity of yeast cells overexpressing DNA topoisomerase II. *Cancer Res.*, **52**, 4467-4472.

Nooter, K. & Herweijer, H. (1991). Multidrug resistance (*mdr*) genes in human cancer. *Br. J. Cancer*, **63**, 663-669.

Oberhammer, F., Wilson, J., Dive, C., Morris, I., Hickman, J., Wakeling, A., Walker, P. & Silorska, M. (1993). Apoptotic death in epithelial cells: cleavage of DNA to 300 and/or 50kb fragments prior to or in the absence of internucleosomal fragmentation. *EMBO J.*, **12**, 3679-3684.

Osheroff, N. (1987). Role of the divalent cation in topoisomerase II mediated reactions. *Biochemistry*, **26**, 6402-6406.

Osheroff, N., Zechiedrich, E. & Gale, K. (1991). Catalytic function of DNA topoisomerase II. *BioEssays*, **13**, 269-275.

Pandolfi, P., Grignani, F., Alcalay, M., Mencarelli, A., Biondi, A., LoCoco, F., Grignani, F., Pelicci, P. (1991). Structure and origin of the acute promyelocytic leukemia *myl/RAR $\alpha$*  cDNA and characterisation of its retinoid-binding and transactivation properties. *Oncogene*, **6**, 1285-1292.

Park, J.-B., Rhim, J., Park, S.-C., Kimm, S.-W. & Kraus, M. (1989). Amplification, overexpression, and rearrangement of the *erbB-2* protooncogene in primary human stomach carcinomas. *Cancer Res.*, **49**, 6605-6609.

Parker, P., Coussens, L., Totty, N., Rhee, L., Young, S., Chen, E., Stable, S., Waterfield, M. & Uurich, A. (1986). The complete primary structure of protein kinase C-the major phorbol ester receptor. *Science*, **233**, 853-859

Parra, I. & Windle, B. (1993). High resolution visual mapping of stretched DNA by fluorescent hybridisation. *Nature Genetics*, **5**, 17-21.

Patel, S. & Fisher, L. (1993). Novel selection and genetic characterisation of an etoposide-resistant human leukemic CCRF-CEM cell line. *Br. J. Cancer*, **67**, 456-462.

Pearson, B., Nasheuer, H.-P. & Wang, T.-F. (1991). Human polymerase  $\alpha$  gene: Sequences controlling expression in cycling and serum-stimulated cells. *Mol. Cell. Biol.*, **11**, 2081-2095.

Per, S., Mattern, M., Mirabelli, C., Drake, F., Johnson, R. & Crooke, S. (1987). Characterisation of a subline of P388 leukemia resistant to amsacrine: Evidence of altered topoisomerase II function. *Mol. Pharmacol.*, **32**, 17-25.

Perren, T. (1991). *c-erb* B-2 oncogene as a prognostic marker in breast cancer. *Br. J. Cancer*, **63**, 328-332.

Persons, D., Hartmann, L., Herath, J., Borell, T., Cliby, W., Keeney, G. & Jenkins, R. (1993). Interphase molecular cytogenetic analysis of epithelial ovarian carcinomas. *Am. J. Pathol.*, **142**, 733-741.

Petrov, P., Drake, F., Loranger, A., Huang, W. & Hancock, R. (1993). Localisation of DNA topoisomerase II in chinese hamster fibroblasts by confocal and electron microscopy. *Exp. Cell Res.*, **204**, 73-81.

Pommier, Y., Capranico, G., Orr, A. & Kohn, K. (1991). Local base sequence preferences for DNA cleavage by mammalian topoisomerase II in the presence of amsacrine or teniposide. *Nuc. Acids Res.*, **19**, 5973-5980.

Pommier, Y., Kerrigan, D., Hartman, K. & Glazer, R. (1990). Phosphorylation of mammalian DNA topoisomerase I and activation by protein kinase C. *J. Biol. Chem.*, **265**, 9418-9422.

Potmesil, M., Hsiang, Y.-H., Liu, L., Bank, B., Grossberg, H., Kirschenbaum, S., Forlenzar, T., Penziner, A., Kanganis, D., Knowles, D., Traganos, F. & Silber, R. (1988). Resistance of human leukemic and normal lymphocytes to drug-induced DNA cleavage and low levels of DNA topoisomerase II. *Cancer Res.*, **48**, 3537-3543.

Press, M., Pike, M., Chazin, V., Hung, G., Udove, J., Markowicz, M., Danyluk, J., Godolphin, W., Sliwkowski, M., Akita, R., Paterson, M. &

Slamon, D. (1993). Her-2/*neu* expression in node-negative breast cancer: Direct tissue quantification by computerised image analysis and association of overexpression with increased risk of recurrent disease. *Cancer Res.*, **53**, 4960-4970.

Prosperi, E., Negri, C., Marchese, G. & Astaldi Ricotti, G. (1994). Expression of the 170-kDa and 180-kDa isoforms of DNA topoisomerase II in resting and proliferating human lymphocytes. *Cell Prolif.*, **27**, 257-267.

Prosperi, E., Sala, E., Negri, C., Oliani, C., Ricotti, R.-G. & Bottiroli, G. (1992). Topoisomerase II  $\alpha$  and  $\beta$  in human tumor cells grown *in vitro* and *in vivo*. *Anticancer Res.*, **12**, 2093-2100.

Pui, C.-H., Ribeiro, R., Hancock, M., Riveria, G., Evans, W., Raimondi, S., Head, D., Behm, F., Mahmoud, M., Sandlund, J. & Crist, W. (1991). Acute myeloid leukemia in children treated with epipodophyllotoxins for acute lymphoblastic leukemia. *N. Engl. J. Med.*, **325**, 1682-1687.

Raderer, M. & Scheithauer, W. (1993). Clinical trials of agents that reverse multidrug resistance. *Cancer*, **72**, 3553-3563.

Ramachandra, S., Machin, L., Ashley, S., Monaghan, P. & Gusterson, B. (1990). Immunohistochemical distribution of c-erbB-2 in *in situ* breast carcinoma-a detailed morphological analysis. *J. Pathol.*, **161**, 7-14.

Ray, M., Guan, X.-Y., Slovak, M., Trent, J. & Meltzer, P. (1994). Rapid detection, cloning and molecular cytogenetic characterisation of sequences from and *MRP*-encoding amplicon by chromosome microdissection. *Br. J. Cancer*, 85-90.

Riehm, H. & Biedler, J. (1972). Potentiation of drug effect by Tween 80 in Chinese hamster cells resistant to actinomycin D and daunomycin. *Cancer Res.*, **32**, 1195-1200.

Ritke, M., Roberts, D., Allan, W., Raymond, J., Bergoltz, V. & Yalowich, J. (1994). Altered stability of etoposide-induced topoisomerase II-DNA complexes in resistant human leukaemia K562 cells. *Br. J. Cancer*, **69**, 687-697.

Roberts, J., Buck, L. & Axel, R. (1983). A structure for amplified DNA. *Cell*, **33**, 53-63.

Robinson, M. & Osheroff, N. (1991). Effects of antineoplastic drugs on the post-strand-passage DNA cleavage/religation equilibrium of topoisomerase II. *Biochemistry*, **30**, 1807-1813.

Roca, J. & Wang, J. (1992). The capture of a DNA double helix by an ATP-dependent protein clamp: A key step in DNA transport by type II DNA topoisomerases. *Cell*, **71**, 833-840.

Roca, J. & Wang, J. (1994). DNA transport by a type II DNA topoisomerase: Evidence in favour of a two-gate mechanism. *Cell*, **77**, 609-616.

Roelofs, H., Nederlof, P., Tasseront-de-Jong, J., van de Putte, P. & Giphart-Gassler, M. (1992). Gene amplification in human cells may involve interchromosomal transposition and persistence of the original DNA region. *The New Biologist*, **4**, 75-86.

Rogan, A., Hamilton, T., Young, R., Klecker Jr., R. & Ozols, R. (1984). Reversal of adriamycin resistance by verapamil in human ovarian cancer. *Science*, **224**, 994-996.

Roninson, I. (1992). The role of the *MDR1* (P-glycoprotein) gene in multidrug resistance *in vitro* and *in vivo*. *Biochem. Pharmacol.*, **43**, 95-102.

Rottmann, M., Schroder, H., Gramzow, M., Renneisen, K., Kurelec, B., Dorn, A., Friese, U. & Muller, W. (1987). Specific phosphorylation of proteins in pore complex-laminae from the sponge *Geodia cynodium* by the homologous aggregation factor and phorbol ester. Role of protein kinase C in the phosphorylation of DNA topoisomerase II. *EMBO J.*, **6**, 3939-3944.

Sahyoun, N., Wolf, M., Besterman, J., Hsieh, T., Sander, M., LeVine III, H., Chang, K.-J. & Cuatrecasas, P. (1986). Protein kinase C phosphorylates topoisomerase II: Topoisomerase activation and its possible role in phorbol ester-induced differentiation of HL-60 cells. *Proc. Natl. Acad. Sci. USA*, **83**, 1603-1607.

Saint-Ruf, C., Malfoy, B., Scholl, S., Zafrani, B. & Dutrillaux, B. (1991). GST $\pi$  gene is frequently coamplified with INT2 and HSTF1 proto-oncogenes in human breast cancers. *Oncogene*, **6**, 403-406.

Saitoh, Y. & Laemmli, U. (1994). Metaphase chromosome structure: bands arise from a differential folding path of the highly AT-rich scaffold. *Cell*, **76**, 609-622.

Sambrook, J., Fritsch, E. & Maniatis, T. (1989). *Molecular Cloning: A laboratory manual*. Cold Spring Harbor Laboratory Press. Volume 2.

Sander, M. & Hsieh, T. (1985). *Drosophila* topoisomerase II double-strand DNA cleavage: analysis of DNA sequence homology at the cleavage site. *Nuc. Acids Res.*, **13**, 1057-1072.

Sawyer, J., Sammartino, G., Husain, M., Lewis, J., Anderson, B. & Boop, F. (1993). Ring chromosome 12 resulting from nonrandom telomeric associations with the short arm of chromosome 15 in a cerebellar astrocytoma. *Genes, Chromosomes & Cancer*, **8**, 69-73.

Schechter, A., Stern, D., Vaidyanathan, L., Decker, S., Drebin, J., Greene, M. & Weinberg, R. (1984). The *neu* oncogene: an *erb-B*-related gene encoding a 185,000-Mr tumour antigen. *Nature*, **312**, 513-516.

Scheper, R., Broxterman, H., Scheffer, G., Kaaijk, P., Dalton, W., van Heijningen, T., van Kalken, C., Slovak, M., de Vries, E., van der Valk, P., Meijer, C. & Pinedo, H. (1993). Overexpression of a Mr 110,000 vesicular protein in non-P-glycoprotein-mediated multidrug resistance. *Cancer Res.*, **53**, 1475-1479.

Schimke, R., Sherwood, S., Hill, A., Johnston, R. (1986). Overreplication and recombination of DNA in higher eukaryotes: Potential consequences and biological implications. *Proc. Natl. Acad. Sci. USA.*, **83**, 2157-2161.

Schinkel, A., Roelofs, M. & Borst, P. (1991). Characterisation of the human *MDR 3* P-glycoprotein and its recognition by P-glycoprotein-specific monoclonal antibodies. *Cancer Res.*, **51**, 2628-2635.

Schlaifer, D., Laurent, G., Chittal, S., Tsuruo, T., Soues, S., Muller, C., Charcosset, J., Alard, C., Brousset, P., Mazerrolles, C. & Delsol, G. (1990). Immunohistochemical detection of multidrug resistance associated P-glycoprotein in tumour and stromal cells of human cancers. *Br. J. Cancer*, **62**, 177-182.

Schneider, E., Horton, J., Yang, C.-H., Nakagawa, M. & Cowan, K. (1994). Multidrug resistance-associated protein gene overexpression and reduced drug sensitivity of topoisomerase II in a human breast carcinoma MCF7 cell line selected for etoposide resistance. *Cancer Res.*, **54**, 152-158.

Schneider, P., Hung, M.-C., Chiocca, S., Manning, J., Zhao, X., Fang, K. & Roth, J. (1989). Differential expression of the *c-erbB-2* gene in small cell and non-small cell lung cancer. *Cancer Res.*, **49**, 4968-4971.

Schneider, S., Hiemstra, J., Zehnauer, B., Taillon-Miller, P., Le Paslier, D., Vogelstein, B. & Brodeur, G. (1992). Isolation and structural analysis of a 1.2-megabase *N-myc* amplicon from a human neuroblastoma. *Mol. Cell. Biol.*, **12**, 5563-5570.

Schoenlein, P., Shen, D.-W., Barrett, J., Pastan, I. & Gottesman, M. (1992). Double minute chromosomes carrying the human multidrug resistance 1 and 2 genes are generated from the dimerisation of submicroscopic circular DNAs in colchicine-selected KB carcinoma cells. *Mol. Biol. Cell*, **3**, 507-520.

Schuuring, E., Verhoeven, E., Litvinov, S. & Michalides, R. (1993). The product of the *EMS1* gene, amplified and overexpressed in human carcinomas, is homologous to a *v-src* substrate and is located in cell-substratum contact sites. *Mol. Cell. Biol.*, **13**, 2891-2898.

Schuuring, E., Verhoeven, E., Mooi, W. & Michalides, R. (1992). Identification and cloning of two overexpressed genes, U21B31/*PRAD 1* and *EMS 1*, within the amplified chromosome 11q13 region in human carcinomas. *Oncogene*, **7**, 355-361.

Schwab, M. & Amler, L. (1990). Amplification of cellular oncogenes: A predictor of clinical outcome in human cancer. *Genes, Chromosomes & Cancer*, **1**, 181-193.

Semba, K., Kamata, N., Toyoshima, K. & Yamamoto, T. (1985). A *v-erbB*-related protooncogene, *c-erbB-2*, is distinct from the *c-erbB-1*/epidermal growth factor-receptor gene and is amplified in a human salivary gland adenocarcinoma. *Proc. Natl. Acad. Sci. USA*, **82**, 6497-6501.

Shi, D., He, G., Cao, S., Pan, W., Zhang, H.-Z., Yu, D. & Hung, M.-C. (1992). Overexpression of the *c-erbB-2/neu*-encoded p185 protein in primary lung cancer. *Mol. Carcinogenesis*, **5**, 213-218.

Shin, H., Lee, J., Hong, W. & Shin, D. (1992). Study of multidrug resistance (*mdr1*) gene in non-small cell lung cancer. *Anti-Cancer Res.*, **12**, 367-370.

Simpson, J., O'Malley, F., Dupont, W. & Page, D. (1994). Heterogeneous expression of nm23 gene product in noninvasive breast carcinoma. *Cancer*, **73**, 2352-2358.

Sirotnak, F., Yang, C.-H., Mines, L., Oribe, E. & Biedler, J. (1986). Markedly altered membrane transport and intracellular binding of vincristine in multidrug-resistant Chinese hamster cells selected for resistance to Vinca alkaloids. *J. Cell. Physiol.*, **126**, 266-274.

Slamon, D., Clark, G., Wong, S., Levin, W., Ullrich, A. & McGuire, W. (1987). Human breast cancer: Correlation of relapse and survival with amplification of the *HER-2/neu* oncogene. *Science*, **235**, 177-182.

Slamon, D., Godolphin, W., Jones, L., Holt, J., Wong, S., Keith, D., Levin, W., Stuart, S., Udove, J., Ullrich, A. & Press, M. (1989). Studies of the *HER-2/neu* proto-oncogene in human breast and ovarian cancer. *Science*, **244**, 707-712.

Slovak, M., Ho, J., Bhardwaj, G., Kurz, E., Deeley, R. & Cole, S. (1993). Localisation of a novel multidrug resistance-associated gene in the HT1080/DR4 and H69AR human tumour cell lines. *Cancer Res.*, **53**, 3221-3225.

Slovak, M., Ho, J., Pettenati, M., Khan, A., Douer, D., Lal, S. & Traweek, S. (1994). Localization of amplified *MYC* gene sequences to double minute chromosomes in acute myelogenous leukaemia. *Genes, Chromosomes & Cancer*, **9**, 62-67.

Smith, K., Gorman, P., Stark, M., Groves, R. & Stark, G. (1990). Distinctive chromosomal structures are formed very early in the amplification of *CAD* genes in Syrian hamster cells. *Cell*, **63**, 1219-1227.

Smith, K., Houlbrook, S., Greenall, M., Carmichael, J. & Harris, A. (1993). Topoisomerase II $\alpha$  co-amplification with *erbB2* in human primary breast cancer and breast cancer cell lines: relationship to *m*-AMSA and mitoxantrone sensitivity. *Oncogene*, **8**, 933-938.

Smith, K., Stark, M., Gorman, P. & Stark, G. (1992). Fusions near telomeres occur very early in the amplification of *CAD* genes in Syrian hamster cells. *Proc. Natl. Acad. Sci. USA*, **89**, 5427-5431.

Smith, P. (1990). DNA topoisomerase dysfunction: A new goal for antitumour chemotherapy. *BioEssays*, **12**, 167-172.

Solary, E., Bertrand, R., Kohn, K. & Pommier, Y. (1993). Differential induction of apoptosis in undifferentiated and differentiated HL-60 cells by DNA topoisomerase I and II inhibitors. *Blood*, **81**, 1359-1368.

Sperry, A., Blasquez, V. & Garrard, W. (1989). Dysfunction of chromosomal loop attachment sites: Illegitimate recombination linked to matrix association regions and topoisomerase II. *Proc. Natl. Acad. Sci. USA*, **86**, 5497-5501.

Stahl, J., Leone, A., Rosengard, A., Porter, L., King, C. & Steeg, P. (1991). Identification of a second human *nm23* gene, *nm23-H2*. *Cancer Res.*, **51**, 445-449.

Stark, G. (1993). Regulation and mechanisms of mammalian gene amplification. *Advances in Cancer Res.*, **61**, 87-113.

Stark, G., Debatisse, M., Giulotto, E. & Wahl, G. (1989). Recent progress in understanding mechanisms of mammalian DNA amplification. *Cell*, **57**, 901-908.

Steeg, P., Bevilacqua, G., Kopper, L., Thorgeirsson, U., Talmadge, J., Liotta, L. & Sobel, M. (1988a). Evidence for a novel gene associated with low tumour metastatic potential. *J. Natl. Cancer Inst.*, **80**, 200-204.

Steeg, P., Bevilacqua, G., Pozzatti, R., Liotta, L. & Sobel, M. (1988b). Altered expression of *NM23*, a gene associated with low tumour metastatic potential, during adenovirus 2 *Ela* inhibition of experimental metastasis. *Cancer Res.*, **48**, 6550-6554.

Stock, C., Ambros, I., Mann, G., Gadner, H., Amann, G. & Ambros, P. (1993). Detection of 1p36 in paraffin sections of neuroblastoma tissues. *Genes, Chromosomes & Cancer*, **6**, 1-9.

Sugawara, I., Kataoka, I., Morishita, Y., Hamada, H., Tsuruo, T. & Itoyama, M., S (1988). Tissue distribution of P-glycoprotein encoded by a multidrug-resistant gene as revealed by a monoclonal antibody, MRK16. *Cancer Res.*, **48**, 1926-1929.

Suijkerbuijk, R., Olde Weghuis, D., Van Den Berg, M., Pedeutour, F., Forus, A., Mykleborst, O., Glier, C., Turc-Carel, C. & van Kessel, A. (1994). Comparative genomic hybridisation as a tool to define two distinct chromosome 12-derived amplification units in well-differentiated liposarcomas. *Genes, Chromosomes & Cancer*, **9**, 292-295.

Sunde, L., Kjeldsen, E., Andoh, T., Keene, J. & Bolund, L. (1989). A three allele TaqI polymorphism at TOP1 gene. *Nuc. Acids Res.*, **18**, 5919.

Takano, H., Kohno, K., Matsuo, K., Matsuda, T. & Kuwano, M. (1992). DNA topoisomerase-targeting antitumour agents and drug resistance. *Anti-Cancer Drugs*, **3**, 323-330.

Tan, K., Dorman, T., Falls, K., Chung, T., Mirabelli, C., Crooke, S. & Mao, J. (1992). Topoisomerase II $\alpha$  and topoisomerase II $\beta$  genes: Characterisation and mapping to human chromosomes 17 and 3, respectively. *Cancer Res.*, **52**, 231-234.

Tan, K., Mattern, M., Eng, W.-K., McCabe, F. & Johnson, R. (1989). Nonproductive rearrangement of DNA topoisomerase I and II genes: Correlation with resistance to topoisomerase II inhibitors. *J. Natl. Cancer Inst.*, **81**, 1732-1735.

- Tan, K., Per, S., Boyce, R., Mirabelli, C. & Crooke, S. (1988). Altered expression and transcription of the topoisomerase II gene in nitrogen mustard-resistant human cells. *Biochem. Pharmacol.*, **37**, 4413-4416.
- Tanabe, K., Ikegami, Y., Ishida, R. & Andoh, T. (1991). Inhibition of topoisomerase II by antitumor agents bis(2,6-dioxopiperazine) derivatives. *Cancer Res.*, **51**, 4903-4908.
- Tanigami, A., Tokino, T., Takita, K., Ueda, M., Kasumi, F. & Nakamura, Y. (1992). Detailed analysis of an amplified region at chromosome 11q13 in malignant tumors. *Genomics*, **13**, 21-24.
- Tanner, M., Tirkkonen, M., Kallioniemi, A., Collins, C., Stokke, T., Karhu, R., Kowbel, D., Shadravan, F., Hintz, M., Kuo, W.-L., Waldman, F., Isola, J., Gray, J. & Kallioniemi, O.-P. (1994). Increased copy number at 20q13 in breast cancer: Defining the critical region and exclusion of candidate genes. *Cancer Res.*, **54**, 4257-4260.
- Tazi, J. & Bird, A. (1990). Alternative chromatin structure at CpG islands. *Cell*, **60**, 909-920.
- Tetu, B. & Brisson, J. (1994). Prognostic significance of HER-2/*neu* oncoprotein expression in node-positive breast cancer. *Cancer*, **73**, 2359-2365.
- Tew, K. (1994). Glutathione-associated enzymes in anticancer drug resistance. *Cancer Res.*, **54**, 4313-4320.
- Thomsen, B., Bendixen, C., Lund, K., Anderson, A., Sorensen, B. & Westergaard, O. (1990). Characterisation of the interaction between topoisomerase II and DNA by transcriptional footprinting. *J. Mol. Biol.*, **215**, 237-244.
- Toledo, F., Le Roscouet, D., Buttin, G. & Debatisse, M. (1992). Co-amplified markers alternate in megabase long chromosomal inverted repeats and cluster independently in interphase nuclei at early steps of mammalian gene amplification. *EMBO J.*, **11**, 2665-2673.

Trask, B. & Hamlin, J. (1989). Early dihydrofolate reductase gene amplification events in CHO cells usually occur on the same chromosome arm as the original locus. *Genes and Development*, **3**, 1913-1925.

Trent, J., Thompson, F. & Meyskens, F. (1989). Identification of a recurring translocation site involving chromosome 6 in human malignant melanoma. *Cancer Res.*, **49**, 420-423.

Tsai-Plugfelder, M., Liu, L., Liu, A., Tewey, K., Whang-Peng, J., Knutsen, T., Huebner, K., Croce, C. & Wang, J. (1988). Cloning and sequencing of cDNA encoding human DNA topoisomerase II and localisation of the gene to chromosome region 17q21-22. *Proc. Nat. Acad. Sci., USA*, **85**, 7177-7181.

Tsuda, T., Tahara, E., Kajiyama, g., Sakamoto, H., Terada, M. & Sugimura, T. (1989). High incidence of coamplification of *hst-1* and *int-2* genes in human esophageal carcinomas. *Cancer Res.*, **49**, 5505-5508.

Ueda, K., Cardarelli, C., Gottesman, M. & Pastan, I. (1987). Expression of a full-length cDNA for the human "MDR1" gene confers resistance to colchicine, doxorubicin, and vinblastine. *Proc. Natl. Acad. Sci. USA*, **84**, 3004-3008.

Uemura, T., Ohkura, H., Adachi, Y., Morino, K., Shiozaki, K. & Yanagida, M. (1987). DNA topoisomerase II is required for condensation and separation of mitotic chromosomes in *S. pombe*. *Cell*, **50**, 917-925.

van de Vijver, M., van de Bersselaar, R., Devilee, P., Cornelisse, C., Peterse, J. & Nusse, R. (1987). Amplification of the *neu* (*c-erbB-2*) oncogene in human mammary tumours is relatively frequent and is often accompanied by amplification of the linked *c-erbA* oncogene. *Mol. Cell. Biol.*, **7**, 2019-2023.

van der Zee, A., Holloma, H., de Jong, S., Boonstra, H., Gouw, A., Willemse, P., Zijlstra, J., de Vries, E. (1991). P-glycoprotein expression and DNA topoisomerase I and II activity in benign tumours of the ovary and in malignant tumours of the ovary, before and after platinum/cyclophosphamide chemotherapy. *Cancer Res.*, **51**, 5915-5920.

Van der Blik, A., Baas, F., Van der Velde-Koerts, T., Biedler, J., Meyers, M., Ozols, R., Hamilton, T., Joenje, H. & Borst, P. (1988). Genes amplified and

overexpressed in human multidrug-resistant cell lines. *Cancer Res.*, **48**, 5927-5932.

Varesco, L., Caligo, M., Simi, P., Black, D., Nardini, V., Casarino, L., Rocchi, M., Ferrara, G., Solomon, E. & Bevilacqua, G. (1992). The *nm 23* gene maps to human chromosome band 17q22 and shows a restriction fragment length polymorphism with *Bgl* II. *Genes, Chromosomes and Cancer*, **4**, 84-88.

Varley, J., Swallow, J., Brammar, W., Whittaker, J. & Walker, R. (1987). Alterations to either *c-erbB-2 (neu)* or *c-myc* proto-oncogenes in breast carcinomas correlate with poor short-term prognosis. *Oncogene*, **1**, 423-430.

Varshavsky, A. (1981). On the possibility of metabolic control of replicon "misfiring": Relationship to emergence of malignant phenotypes in mammalian cell lineages. *Proc. Natl. Acad. Sci. USA*, **78**, 3673-3677.

Verrelle, P., Meissonier, F., Fonck, C., Kwiatkowski, F., Plagne, R. & Chassagne, J. (1991). Clinical relevance of immunohistochemical detection of multidrug resistance P-glycoprotein in breast carcinoma. *J. Natl. Cancer Inst.*, **83**, 111-116.

Vogelstein, B. & Kinzler, K. (1993). The multistep nature of cancer. *Trends in Genetics*, **9**, 138-141.

Wahl, G. (1989). The importance of circular DNA in mammalian gene amplification. *Cancer Res.*, **49**, 1333-1340.

Wallet, V., Mutzel, R., Troll, H., Barzu, O., Wurster, B., Veron, M. & Lacombe, M.-L. (1990). *Dictyostelium* nucleoside diphosphate kinase highly homologous to nm23 and Awd proteins involved in mammalian tumour metastasis and *Drosophila* development. *J. Natl. Cancer Inst.*, **82**, 1199-1202.

Wang, J. (1985). DNA topoisomerases. *Ann. Rev. Biochem.*, **54**, 665-697.

Wang, J. (1991). DNA topoisomerases: Why so many? *J. Biol. Chem.*, **266**, 6659-6662.

Wang, L., Patel, U., Ghosh, L., Chen, H.-C. & Banerjee, S. (1993). Mutation in the *nm23* gene is associated with metastasis in colorectal cancer. *Cancer Res.*, **53**, 717-720.

Warrell, R., Frankel, S., Miller, W., Scheinberg, D., Itri, L., Hittelman, W., Vyas, R., Andreeff, M., Tafuri, A., Jakubowski, A., Gabrielove, J., Gordon, M. & Dmitrovsky, E. (1991). Differentiation therapy of acute promyelocytic leukemia with tretinoin (all-*trans*-retinoic acid). *N. Engl. J. Med.*, **324**, 1385-1393.

Webb, C., Latham, M., Lock, R. & Sullivan, D. (1991). Attenuated topoisomerase II content directly correlates with a low level of drug resistance in a chinese hamster ovary cell line. *Cancer Res.*, **51**, 6543-6549.

Weinberg, R. (1989). Oncogenes, anti-oncogenes, and the molecular bases of multistep carcinogenesis. *Cancer Res.*, **49**, 3713-3721.

Weinberg, R. (1991). Tumor suppressor genes. *Science*, **254**, 1138-1146.

Willard, H. (1990). Centromeres of mammalian chromosomes. *Trends in Genetics*, **6**, 410-416.

Willems, M., Wagner, E., Laing, R. & Penman, S. (1968). Base composition of ribosomal RNA precursors in the HeLa cell nucleolus: Further evidence of non-conservative processing. *J. Mol. Biol.*, **32**, 211-220.

Williams, G. & Smith, C. (1993). Molecular regulation of apoptosis: Genetic controls on cell death. *Cell*, **74**, 777-779.

Windle, B., Draper, B., Yin, Y., O'Gorman, S. & Wahl, G. (1991). A central role for chromosome breakage in gene amplification, deletion formation, and amplicon integration. *Genes & Development*, **5**, 160-174.

Winstanley, J., Cooke, T., Murray, G., Platt-Higgins, A., George, W., Holt, S., Myskov, M., Spedding, A., Barraclough, B. & Rudland, P. (1991). The long term prognostic significance of *c-erbB-2* in primary breast cancer. *Br. J. Cancer*, **63**, 447-450.

Wintersberger, E. (1994). DNA amplification. *Chromosoma*, **103**, 73-81.

Woessner, R., Mattern, M., Mirabelli, C., Johnson, R. & Drake, F. (1991). Proliferation- and cell cycle-dependent differences in expression of the 170 kilodalton and 180 kilodalton forms of topoisomerase II in NIH-3T3 cells. *Cell Growth and Differentiation*, **2**, 209-214.

Wood, E. & Earnshaw, W. (1990). Mitotic chromatin condensation in vitro using somatic cell extracts and nuclei with variable levels of endogenous topoisomerase II. *J. Cell. Biol.*, **111**, 2839-2850.

Wright, C., Nicholson, S., Angus, B., Sainsbury, J., Farndon, J., Carins, J., Harris, A. & Horne, C. (1992). Relationship between c-erbB-2 protein product expression and response to endocrine therapy in advanced breast cancer. *Br. J. Cancer*, **65**, 118-121.

Xiong, Y., Connolly, T., Futcher, B. & Beach, D. (1991). Human D-type cyclin. *Cell*, **65**, 691-699.

Yamaguchi, A., Urano, T., Goi, T., Takeuchi, K., Niimoto, S., Nakagawara, G., Furukawa, K. & Shiku, H. (1994). Expression of human *nm23-H1* and *nm23-H2* proteins in hepatocellular carcinoma. *Cancer*, **73**, 2280-2284.

Yamamoto, T., Ikawa, S., Akiyama, T., Semba, K., Nomura, N., Miyajima, N., Saito, T. & Toyoshima, K. (1986). Similarity of the protein encoded by the *c-erb-B-2* gene to epidermal growth factor receptor. *Nature*, **319**, 230-234.

Yokota, J., Wada, M., Shimosata, Y., Terada, M. & Sugimura, T. (1987). Loss of heterozygosity on chromosomes 3, 13, and 17 in small-cell carcinoma and on chromosome 3 in adenocarcinoma of the lung. *Proc. Natl. Acad. Sci. USA*, **84**, 9252-9256.

Zaman, G., Flens, M., van Leusden, M., de Haas, M., Mulder, H., Lankelma, J., Pinedo, H., Scheper, R., Baas, F., Broxterman, H. & Borst, P. (1994). The human multidrug resistance-associated protein MRP is a plasma membrane drug-efflux pump. *Proc. Natl. Acad. Sci. USA*, **91**, 8822-8826.

Zaman, G., Versantvoort, C., Smit, J., Eijdem, E., de Haas, M., Smith, A., Broxterman, H., Mulder, N., de Vries, E., Baas, F. & Borst, P. (1993). Analysis of the expression of *MRP*, the gene for a new putative

transmembrane drug transporter, in human multidrug resistant lung cancer cell lines. *Cancer Res.*, **53**, 1747-1750.

Zechiedrich, E., Christiansen, K., Andersen, A., Westergaard, O. & Osheroff, N. (1989). Double-stranded DNA cleavage/religation reaction of eukaryotic topoisomerase II: evidence for a nicked DNA intermediate. *Biochemistry*, **28**, 6229-6236.

Zechiedrich, E. & Osheroff, N. (1990). Eukaryotic topoisomerases recognise nucleic acid topology by preferentially interacting with DNA crossovers. *EMBO J.*, **9**, 4555-4562.

Zelent, A., Krust, A., Petkovich, M., Kastner, P. & Chambon, P. (1989). Cloning of murine  $\alpha$  and  $\beta$  retinoic acid receptors and a novel receptor  $\gamma$  predominantly expressed in skin. *Nature*, **339**, 714-717.

Zhang, H., D'Arpa, P. & Liu, L. (1990). A model for tumor cell killing by topoisomerase poisons. *Cancer Cells*, **2**, 23-27.

Zhang, Z., Trent, J. & Meltzer, P. (1993). Rapid isolation and characterisation of amplified DNA by chromosome microdissection: identification of IGF1R amplification in malignant melanoma. *Oncogene*, **8**, 2827-2831.

Zheng, J., Robinson, W., Ehlen, T., Yu, M. & Dubeau, L. (1991). Distinction of low grade from high grade human ovarian carcinomas on the basis of losses of heterozygosity on chromosomes 3, 6, and 11 and HER-2/*neu* gene amplification. *Cancer Res.*, **51**, 4045-4051.

Zini, N., Martelli, A., Sabatelli, P., Santi, S., Negri, C., Astaldi Ricotti, G. & Maraldi, N. (1992). The 180-kDa isoform of topoisomerase II is localised in the nucleolus and belongs to the structural elements of the nucleolar remnant. *Exp. Cell Res.*, **200**, 460-466.

Zwelling, L., Chan, D., Hinds, M., Mayes, J., Silberman, L. & Blick, M. (1988). Effect of phorbol ester treatment on drug-induced, topoisomerase II-mediated DNA cleavage in human leukemia cells. *Cancer Res.*, **48**, 6625-6633.

Zwelling, L., Hinds, M., Chan, D., Mayes, J., Lan Sie, K., Parker, E., Silberman, L., Radcliffe, A., Beran, M., Blick, M. (1989). Characterisation of an amsacrine-resistant line of human leukaemia cells: Evidence for a drug-resistant form of topoisomerase II. *J. Biol. Chem.*, **264**, 16411-16420.

Zwelling, L., Hinds, M., Chan, D., Altschuler, E., Mayes, J. & Zipf, T. (1990a). Phorbol ester effects on topoisomerase II activity and gene expression in HL-60 human leukaemia cells with different proclivities towards monocytoid differentiation. *Cancer Res.*, **50**, 7116-7122.

Zwelling, L., Slovak, M., Doroshaw, J., Hinds, M., Chan, D., Parker, E., Mayes, J., Lan Sie, K., Meltzer, P. & Trent, J. (1990b). HT1080/DR4: A p-glycoprotein-negative human fibrosarcoma cell line exhibiting resistance to topoisomerase II-reactive drugs despite the presence of a drug-sensitive topoisomerase II. *J. Natl. Cancer Inst.*, **82**, 1553-1561.